Neurodegeneration studies in Rat Brain Aging and Rotenone Induced Parkinson's Disease Model: Chronomics of Serotonin metabolism, Protein profile and Clock gene expression

A thesis submitted to the University of Hyderabad for the award of a Ph.D. degree in Animal Sciences

By

Mattam Ushodaya

Department of Animal Sciences
School of Life Sciences
University of Hyderabad
Hyderabad - 500 046
INDIA

Enrollment No: 07LAPH09
June, 2013

UNIVERSITY OF HYDERABAD

(A Central University Established in 1974 By An Act Of Parliament)

HYDERABAD - 500 046, INDIA

DECLARATION

I, Mattam Ushodaya, hereby declare that this thesis entitled "Neurodegeneration studies in Rat Brain Aging and Rotenone Induced Parkinson's Disease Model: Chronomics of Serotonin metabolism, Protein profile and Clock gene expression" submitted by me under the guidance and supervision of Dr. Anita Jagota, is an original and independent research work. I also declare that it has not been submitted previously in part or in full to this University or any other University or Institution for the award of any degree or diploma.

Date:

Name: Mattam Ushodaya

Signature:

Reg. No: 07LAPH09

UNIVERSITY OF HYDERABAD

(A Central University established in 1974 By The Act Of Parliament)

HYDERABAD – 500 046, INDIA

CERTIFICATE

This is to certify that this thesis entitled "Neurodegeneration studies in Rat Brain Aging and Rotenone Induced Parkinson's Disease Model: Chronomics of Serotonin metabolism, Protein profile and Clock gene expression" is a record of bonafide work done by Ms. Mattam Ushodaya, a research scholar for Ph.D. programme in Animal Sciences, School of Life Sciences, University of Hyderabad under my guidance and supervision.

The thesis has not been submitted previously in part or in full to this or any other University or Institution for the award of any degree or diploma.

Dr. Anita Jagota

Supervisor
Associate Professor
Dept. of Animal Sciences

Head
Department of Animal Sciences

Dean
School of Life Sciences

Acknowledgements

I express my deep sense of gratitude to my supervisor, **Dr. Anita Jagota** for giving me an opportunity to work under her guidance and for the constant support and scientific discussions throughout my work.

I am grateful to Head, Dept. of Animal Sciences Prof. B. Senthil Kumaran, and former Heads, Prof. Manjula Sritharan and Prof. S. Dayananda for allowing me to use the Department facilities.

I am thankful to Dean, School of Life Sciences, Prof. R. P. Sharma and former Deans, Prof. Aparna Dutta Gupta, Prof. M. Ramanadham and Prof. S. Raghavendra for allowing me to use school facilities.

I am grateful to my Doctoral Committee members Prof. K. V. A. Ramaiah and Prof. P. Prakash Babu for their critical assessment, discussions and advice during my research work.

I thank faculty members of School of Life Sciences for their timely and useful suggestions.

I thank all the non-teaching staff, Dept. of Animal Sciences and School of Life Sciences for timely help.

I thank all my lab mates: Dr. Kalyani, Dr. Pavan, Dr. Kapil, Dr. Yallamanda reddy, Dr. Anumodh, Dileep, Lakshmi, Vinod, Varsha, Aditya, Kunal, Neelesh and Kowshik for their timely help.

I thank my seniors, School of Life Sciences, Dr. Srinivas, Dr. Swapna, Dr. Rasheeda, Dr. Prasad, Dr. Usha Garapati and Dr. Sridevi for their timely help during my research work.

It’s my pleasure to thank all my friends Ramu, Lakshmi, Raji, Swarup, Vinod, Chiru, Siva, Jyothsna, Pandey, Ancy, Swarupa, Sujatha, Barnali for their friendly nature and help during my research work.

I thank Mr. Gopal Krishna Pradhan, Mr. Mallesh, Mr. Satish and Mr. Balakrishna for technical help in the lab.

I thank staff of Animal House for their help.

I would also like to thank all the Research Scholars in School of Life Sciences for their cooperation and help.

I thank DST, CSIR, ILS, UPE-I and II, CREA, DST, DST-Nano, ICMR, UGC, CWC and DBT for funding to the lab.

I thank DBT, DBT-CREBB, CSIR, DST, INSA, DST-FIST, UGC-SAP for funding to Department and School.

I thank UGC-SAP for fellowship.

I thank my husband **Noble** for his support and patience.

I am grateful to my **teachers, parents, sister** and other **family members** for their support.

Mattam Ushodaya

CONTENTS

Introduction and review of literature …….. 1-36

Objectives ……. 37-38

Materials and Methods ……... 39-52

Results …… 53-157

Discussion ……. 158-168

Summary and Conclusion …… 169-171

References ……..…… 172-186

List of Tables …… Appendix-I

List of Figures ……. Appendix-II

Abbreviations ……. Appendix-III

Introduction
and
Review of Literature

Contents

Circadian rhythms…….…….. 3

Biological clock in mammals……3

Suprachiasmatic Nucleus ……..... 4

Input or afferent pathways ……..…..… 5

Serotonin……... 7

Output or efferent pathways …….. 9

SCN-Pineal neural regulation……... 10

Melatonin……. 11

Indole metabolism……..……. 17

Molecular components and mechanisms of mammalian circadian clock….. 19

Aging…… 21

Aging and Biological clock…….. 21

Parkinson's disease……... 22

Types of PD…….. 23

Causes for neurodegeneration in PD…… 24

Biological clock and PD……..... 26

Substantia nigra……. 27

Biological clock and Substantia nigra……... 28

Experimental models of PD…….. 29

Rotenone……... 31

Rotenone mechanism of action……. 31

Melatonin in Aging and PD…… 32

Circadian rhythms

Biological rhythms are ubiquitous and are seen in wide range of organisms from unicellular prokaryotes to higher mammals (Dunlap, 1999). Biological rhythm that persists under constant conditions and has a period of approximately one day (24 hours (h)) is called circadian rhythm (for about-a day in Latin). Many physical, mental, and behavioral changes in living organisms follow a circadian pattern. Five features should be shown by a pattern to consider it as circadian, such as 1) the ability to become entrained (synchronized), 2) the persistence of the cycle after the removal of external cue, 3) the ability to shift the phase of the rhythm, 4) a period of around 24 hours, and 5) the ability to maintain its period independent of temperature (reviewed in Wilking *et al*., 2013). Such rhythms persist in the absence of external cues, for example in a deep cave or during the dark winter months near the Poles (Granados-Fuentes and Herzog, 2013). These have evolved as an adaptation to the oscillations found in the environment and to get entrained by them, notably to the day-night cycle (Jagota, 2006). Environmental cues (zeitgeber) that include photic, such as daily light-dark cycle, and non-photic, such as availability of food, water, temperature, etc., play an important role in entraining these rhythms in the organisms. When these zeitgebers are used under laboratory conditions then the time period is referred as Zeitgeber time (ZT). When the organisms are isolated from environmental time cues then also they show persistence of circadian rhythms. Under such constant conditions the rhythms progressively deviates from clock or real time and thus free-runs with a period either a little longer or shorter than 24 hours. Free running rhythms are independent of real time and under constant conditions are called circadian time (CT). The rhythms are generated in two ways - exogenous and endogenous. Rhythms which are driven directly by the environment or another external influence (direct effect) are exogenous and rhythms which are driven by internal biological clocks and are maintained even when environmental cues are removed are endogenous (Klein *et al*., 1991).

Biological clock in mammals

Circadian rhythms are regulated by biological clock consisting of three components: (i) the input or afferent pathways that relay external cues to the (ii) master oscillator which

generates entrained daily rhythms that are conveyed through the, (iii) output or efferent pathways and are manifested in the physiology and behavior of the organism (reviewed in Jagota, 2006).

Suprachiasmatic nucleus (SCN)

Numerous reports in mammals confirm that the suprachiasmatic nuclei (SCN; Fig. 1) function as "master clocks" and it is a light entrained circadian clock situated in the anterior hypothalamus on either side of the third ventricle, immediately above the optic chiasm regulates neuronal, endocrine and behavioral rhythms (Welsh *et al*., 2010). It is a precise time keeper that controls and synchronizes the circadian period of many physiological and behavioral functions and entrains them to the 24 h light/dark cycle (Jagota *et al*., 2000; Mohawk *et al*., 2012). It consists of group of neurons which receive direct photic information from the retina via retinal ganglion cells and allows them to entrain with the environmental light/dark cycle. SCN cells are organized topographically with coupling mechanism between the cells which keep them synchronized and they also show circadian rhythm in neuronal firing frequency (Welsh *et al*., 2010). SCN neurons are the smallest neurons in the brain. Anatomically SCN is divided into two subdivisions: core and shell region. Among two, core region receives direct input from retina and sends information to shell region. Thus, the SCN synchronizes (entrains) organism to the environmental light/dark cycle and in turn synchronizes other cellular oscillators (Jagota, 2006; Welsh *et al*., 2010).

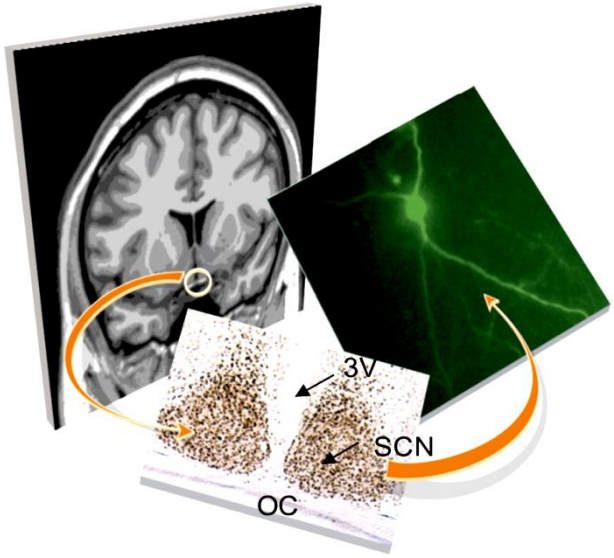

Fig. 1: Suprachiasmatic nucleus

Input or Afferent pathways of the SCN

To synchronize organism's physiology to the external environment, organism should receive the information from the environment, and then entrain the physiology. Three major pathways diverge from the retinal ganglion cells before they enter into the SCN such as retinohypothalamic tract (RHT), geniculohypothalamic tract (GHT) and retinoraphepathway (RRP) (Jagota, 2006) (Fig. 2).

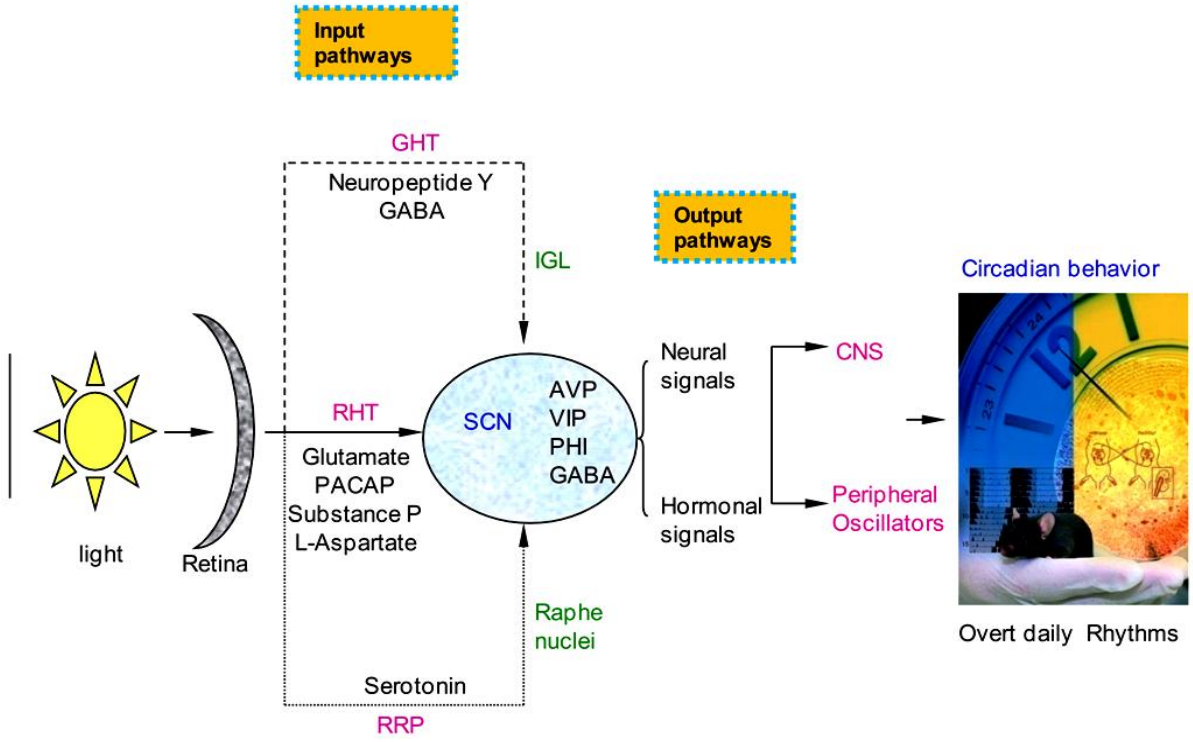

Fig. 2: Afferent and efferent pathways of the SCN. (i) Afferent to the SCN involves RHT - retinohypothalamic tract; GHT - geniculohypothalamic tract via intergeniculate nucleus (IGL); RRP -retino raphe pathway from median and dorsal raphe (ii) Efferent's of the SCN involves neural and humoral signals (Jagota, 2006).

Retinohypothalamic tract (RHT):

Retinohypothalamic tract (RHT) is the direct photic pathway which ends directly in the synaptic contacts of retinal ganglion cells with the SCN neurons. Major neurotransmitters involved in this pathway are glutamate, pituitary adenylylcyclase activating peptide (PACAP), L-aspartate and substance P. PACAP will enhance the effects of glutamate (reviewed in Jagota, 2006). Neurotransmitter release leads to the activation of several signaling pathways and induction of chromatin remodeling, expression of clock genes and immediate early genes

(Dibner *et al.*, 2010).Membrane depolarization by glutamate binding to N-methyl-D-aspartate (NMDA) receptors lead to calcium (Ca^{2+}) influx. Increased intracellular Ca^{2+} activates many kinases which ultimately phosphorylates cAMP response element binding protein (CREB). Phosphorylation of CREB is also attained by PACAP via activating PAC2 receptor. Activation of PAC2 leads to increase in cAMP levels and activation of Protein Kinase A (PKA) which phosphorylates CREB. Phosphorylated CREB activates transcription of many target genes which also include clock genes. Thus CREB mediated transcription is essential for light entrainment of the SCN (Fig. 3; Jagota, 2012).

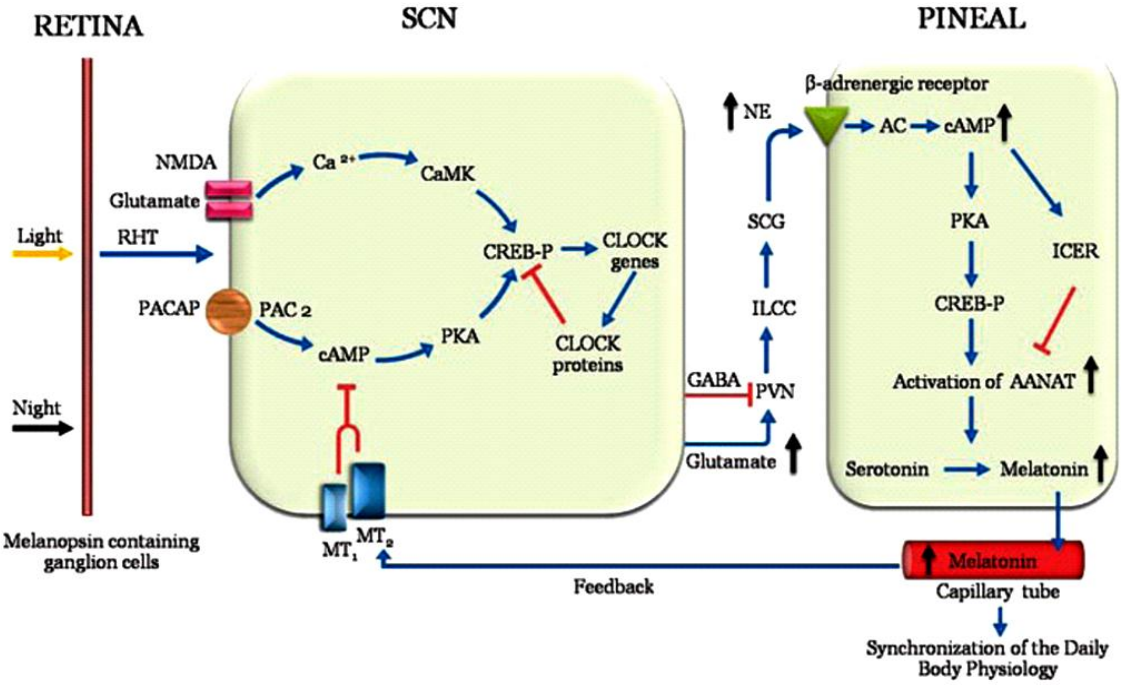

Fig. 3: Mammalian circadian timing system: Glutamate and PACAP which act on Cam K and PKA via NMDA and PAC2 receptors respectively to increase P-CREB thus entraining and regulating clock gene expression and clock proteins in SCN. The time information from SCN through GABA reaches PVN and then to SCG via ILCC. Then during the night the time information travels from SCG by NE to β-adrenergic receptors at pineal, stimulating AC resulting in increased cAMP which activate PKA and hence increased P-CREB activating AANAT resulting in melatonin synthesis. Both blood and CSF melatonin acts on SCN via MT1 and MT2 receptors for resetting the circadian pacemaker (Jagota, 2012).

Geniculohypothalamic tract (GHT):

To the SCN this is an indirect photic pathway from IGL. Retina conveys input signals to IGL via a separate branch of RHT that overlaps with the RHT terminals in the SCN. Photic as

well as non-photic responses such as motor activity necessary for entrainment of circadian rhythms are also mediated by this pathway (Jagota, 2006; Dibner *et al*., 2010). Neurotransmitters involved in this pathway which are transmitting the information to the SCN are NPY and GABA (Fig. 2; Jagota, 2006).

Retinoraphe pathway (RRP):

This is the third major input pathway to the SCN from the median and dorsal raphe nuclei. Neuronal fibers from raphe nuclei end in the core region of the SCN and Serotonin is the major neurotransmitter involved in this pathway. RRP participates in non photic regulation of the SCN and entrainment of the circadian clock (Jagota, 2006; Dibner *et al*., 2010).

Serotonin

Serotonin (5-hydroxytryptamine or 5-HT) is a biogenic amine synthesized from L-tryptophan and functions as both neurotransmitter and hormone (Fig. 4).

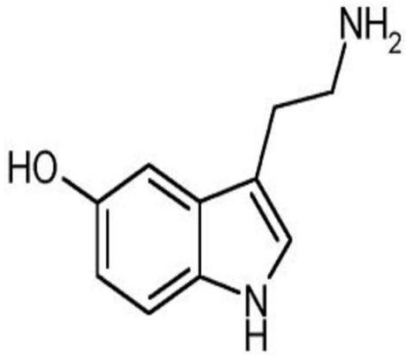

Fig. 4: Skeletal structure of Serotonin (5-Hydroxy tryptamine).

A wide variety of sensory, motor and cortical functions are regulated by 5-HT through its receptors (Julius, 1991). 5-HT receptors are classified into 7 types: 5-HT_1, 5-HT_2, 5-HT_3, 5-HT_4, 5-HT_5, 5-HT_6 and 5-HT_7. Each type of receptor is having further sub types. These receptors belongs to G protein (guanine nucleotide triphosphate (GTP)-binding protein)-coupled receptors (GPCRs) super family except 5-HT_3, which is ligand-gated ion channel (LGIC) found in the central and peripheral nervous systems (Saudou and Hen, 1994; Donaldson *et al*., 2013). Several types of G-proteins were found such as Gs (Stimulatory- Activates Ca^{2+} channels, activates adenylylcyclase (AC)), Gi (Inhibitory- Activates K^+ channels, inhibits AC), Gq (Activates phospholipase C (PLC)), Go (Inhibits Ca^{2+} channels).

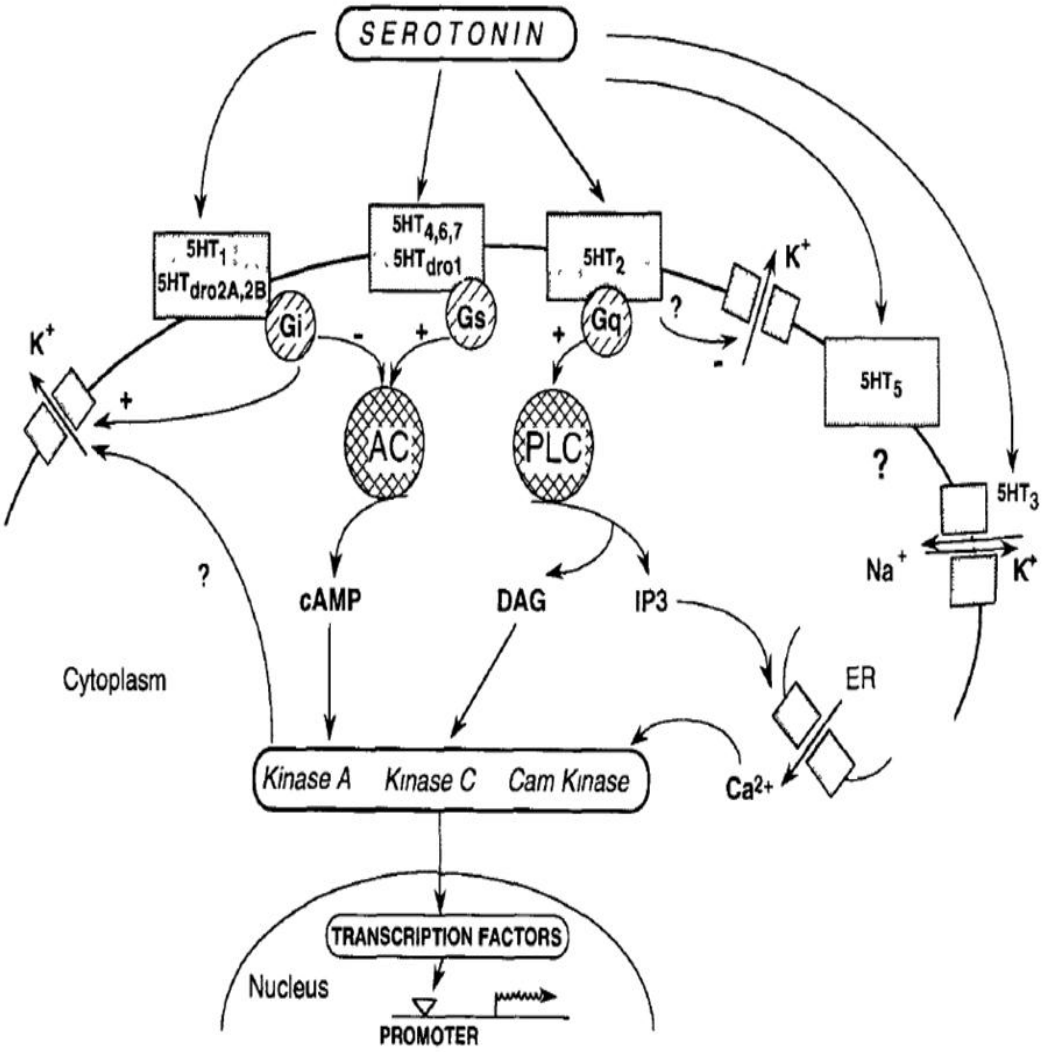

Fig. 5: Serotonin (5-HT) receptors and their effector systems. 5-HT1 receptor subtypes (5-HT1A, 5-HT1B, 5-HT1D, 5-HT1E and 5-HT1F) belongs to the family of Gi/o which is a pertusis toxin-sensitive G protein and inhibits Adenylylcyclase (AC), 5-HT2 receptor subtypes (5-HT2A, 5-HT2B and 5-HT2C) belongs to the family of Gq (pertusis toxin insensitive) activates phospholipase C (PLC), 5-HT3 is a Sodium (Na^+) – Potassium (K^+) ion channel and 5-HT4, 5-HT6 and 5-HT7 belongs to Gs (G stimulatory) and activates AC. cAMP. 3', 5'-adenosine monophosphate, DAG. 1, 2-diacylglycerol, IP3. inositol 1,4,5-triphosphate, ER. Endoplasmic reticulum (Saudou and Hen, 1994).

5-HT1 receptor subtypes includes 5-HT1A, 5-HT1B, 5-HT1D, 5-HT1E and 5-HT1F are Gi/o type receptors and inhibits AC, 5-HT2 receptor subtypes includes 5-HT2A, 5-HT2B and 5-HT2C are Gq type receptors activates PLC, 5-HT3 is a Sodium (Na^+) - Potassium (K^+) ion

channel and 5-HT4, 5-HT6 and 5-HT7 are Gs type receptors and activates AC (Fig. 5; Saudou and Hen, 1994).

In mammals serotonin is synthesized by two different types of Tryptophan hydroxylases TPH_1 and TPH_2. Synthesis of serotonin by TPH_1 occurs in pineal gland and enterochromaffin cells of the intestine whereas by TPH_2 in raphe nuclei and myenteric plexus. 90 % of the total serotonin is synthesized from the enterochromaffin cells and remaining comes from brain and pineal (Ruddick *et al*., 2006). It is a major neurotransmitter involved in the retino-raphe SCN pathway with dense serotonergic projection from midbrain raphe nuclei terminating predominantly in the retino-recipient region of the SCN (Moore *et al*., 1978) and thus serotonin neurotransmission is important in mammalian circadian clock functions (Mistlberger *et al*., 2000). Serotonin is precursor for melatonin (messenger of darkness) and involved in the regulation of circadian rhythms, sleep, mood (antidepressant action), temperature, appetite (appetite suppressant effect) by various types of receptors (Berger *et al.*, 2009). Serotonin also regulates the release of dopamine in Substantia nigra (SN) of the mid brain region neurons at the receptor level, 5-$HT_{2a/2b}$ receptors show excitatory and 5-HT_{2c} receptors show an inhibitory effect on dopamine release (Lucas *et al.*, 2000). Serotonin signaling in the brain decreases oxidative stress, which may be fundamental to aging and age related neurodegenerative diseases such as Parkinson's disease (Mattson *et al*., 2004).

Output or Efferent pathways from the SCN

The SCN mediates its circadian function by various neurotransmitters such as serotonin, glutamate, neuropeptides such as PACAP, vasoactive intestinal peptide (VIP), arginine vasopressin (AVP).

The communication within SCN neurons and between SCN and other brain regions is regulated through both neural and humoral signals.

Neural Pathway: The axonal projections from the SCN project to nearby hypothalamic regions, pineal gland and other brain regions (Saper *et al*., 2005). GABA, AVP, and VIP are the major neurotransmitters and neuropeptides involved in this pathway.

Humoral Pathway: This is a non-neural pathway which mediates the circadian signal via diffusible output from the SCN into the CSF and/or extracellular spaces. AVP, VIP, transforming growth factor α (TGF α), Prokinectin (PK2) are the major peptides that mediates the humoral

function. Locomotor activity will be under the control of humoral pathway (Reghunandanan and Reghunandanan, 2006).

SCN-Pineal neural regulation

The SCN regulates the rhythmic production and discharge of the serotonin derivative, melatonin (messenger of darkness) from pineal gland via multi synaptic efferent pathway on 24 h basis (Fig. 6; Reiter, 2010).

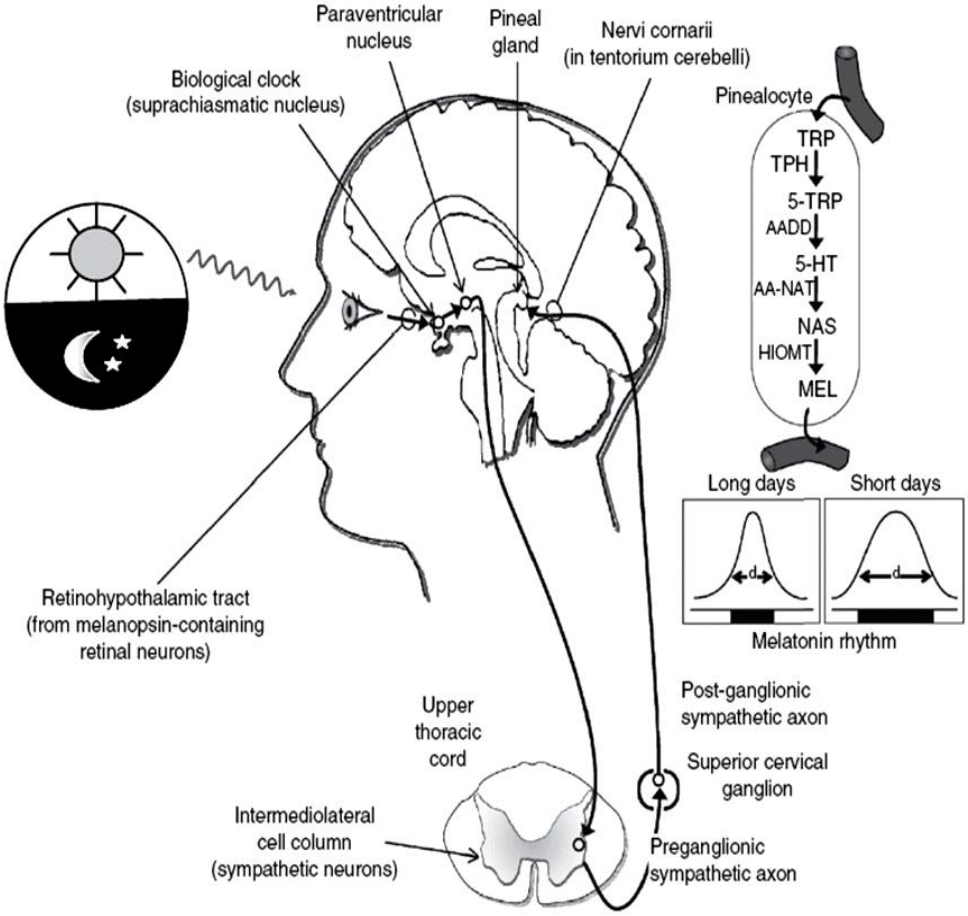

Fig. 6: Neural regulation of Pineal by SCN. Synthesis of Melatonin (MEL) from tryptophan (TRP) in pinealocyte. TPH - tryptophan hydroxylase; 5-TRP - 5-hydroxytryptophan; AADD - L-amino acid decarboxylase; 5-HT - serotonin, AANAT - arylalkylamine N-acetyltransferase; NAS - N-acetylserotonin; HlOMT - hydroxyindole-O-methyltransferase (Reiter *et al.*, 2010).

Neuronal cell projections from the SCN innervate into the cells of the PVN, which in turn send projections to intermediolateral cell column of the spinal cord. Then through sympathetic cells in the superior cervical ganglia (SCG), inferior carotid nerve and the nerviconarii projections leads

to pineal gland. Then stimulation of norepinephrine (NE) containing fibres in the perivascular space of pineal gland leads to its release which then diffuses to the surface of the pinealocyte. Released NE interacts with pinealocyte α- adrenoceptors, which then leads to an increase in pineal cAMP production and synthesis of melatonin. This pathway is actually activated during night without light stimuli (Fig. 3) (Jagota, 2006). Melatonin levels are high at night and low during the day and this rhythm is endogenous (Reiter, 2010; Jagota, 2012). Melatonin is one of the major clock output and its primary function is to transduce light and dark information to whole body physiology (Arendt, 2005).

Melatonin

Melatonin (N-acetyl-5-methoxytryptamine) is synthesized from serotonin produced primarily by the pineal gland, and the rate of its synthesis from serotonin is determined by 24-hour rhythms of arylalkylamine N-acetyl transferase (Fig. 7).

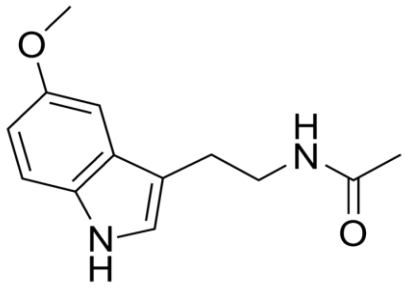

Fig. 7: Skeletal structure of Melatonin (*N*-[2-(5-methoxy-1*H*-indol-3-yl) ethyl] acetamide).

Melatonin regulates various physiological processes such as regulation of sleep (Cardinali *et al*., 2012), scavenger of free radical (Hardeland *et al*., 2011), tumor growth inhibition, seasonal reproduction, immune function, physiology of retina, regulation of blood pressure, circadian rhythms, mood and behavior (reviewed in Pandi-Perumal *et al*., 2013). Melatonin regulates many of the physiological processes by acting through its major receptors MT1 and MT2. These receptors are widely expressed in central nervous system and peripheral tissues. As MT1 and MT2 belongs to G-protein coupled receptor family, activation of these receptors by melatonin leads to the cascade of number of signal transduction pathways which finally result in specific physiological responses. Melatonin, depending on the specific cell and on the species, activates a variety of different second messenger cascades after its binding to membrane receptors.

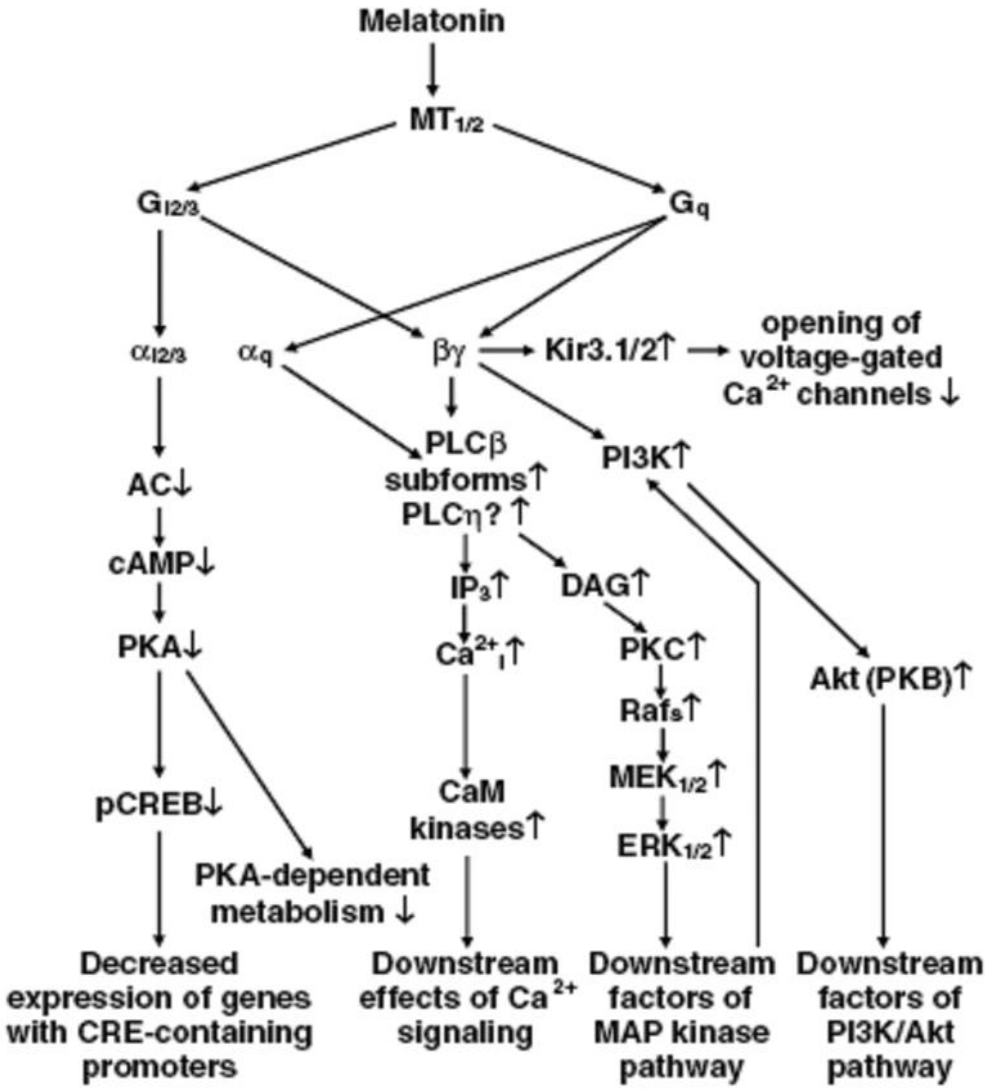

Fig. 8: Major signaling pathways of melatonin through membrane receptors MT1 and MT2. Diagrammatic representation of combined pathways. Every target cell may not have all these pathways collectively. Activation of MT1/MT2 leads to decrease in intracellular cAMP levels finally ends in decreased expression of gene with CRE-containing promoters. Another pathway which gets activated by MT1/MT2 is Cam Kinase and MAP kinase pathway. CaM-calmodulin, cAMP-cyclic adenosine monophosphate, DAG-diacyl glycerol, ERK-extracellular signal-regulated kinase, IP3-inositol 1,4,5-tris-phosphate, Kir3.1/2 subtypes 3. MAP-mitogen-activated protein kinase, MEK- MAP ERK kinase, pCREB- phosphorylated cAMP/Ca^{2+} Response element-binding protein, PI3K-phosphoinositide 3-kinase, PLC-phospholipase C, PK-protein kinase, Raf homolog of retroviral kinase, the product of oncogene v-raf, upregulation or rise, downregulation or decrease (Pandi-Perumal *et al*., 2013).

The MT1 and MT2 receptors regulate intracellular processes via an inhibition of AC, a reduction in intracellular cAMP levels which leads to decrease in PKA activity; this action involves a Gi

protein. Decreased activity of PKA leads to decreased phosphorylation of CREB which results into decreased expression of genes with CRE-containing promoters. Stimulation of both the MT1 and MT2 receptor activates phospholipase C-β which leads to increase of inositol-(1,4,5)-triphosphate (IP3) and 1,2-diacylglycerol (DAG). Increase in IP3 leads to elevation of intracellular calcium and activation of Calmodulin (CaM) kinases leading to downstream effects of calcium signaling. Increase in the levels of DAG leads to elevation of the phosphorylation of mitogen-activated protein kinase (MEK) 1/2 as well as extracellular signal-regulated kinase (ERK) 1/2 which leads to the activation of downstream factors of MAP kinase pathway. Activation of the MT1 receptor also leads to opening of voltage-gated calcium channels by activating potassium inwardly-rectifying channel, subfamily J, member 3 (Kir3 1/2), which finally leads to ATP mediated stimulation of the activity of protein kinase C (PKC) (Fig. 8; Reiter, 2010; Hardeland, 2012; Pandi-Perumal *et al*., 2013).

Through its binding to calmodulin (CaM) and other calcium binding proteins melatonin also affects cells directly. Melatonin is a potent antioxidant and shows receptor independent actions due to its direct scavenging ability of reactive oxygen species. (Reiter, 2010; Hardeland, 2012; Pandi-Perumal *et al*., 2013). Melatonin can directly neutralize many free radicals such as $OH^{\bullet}$, $ONOO^{-}$, $O_2^{\bullet-}$, H_2O_2, $^1O_2$, $NO^{\bullet}$, $LOO^{\bullet}$ and HClO (Reiter *et al*., 2009) and stimulate antioxidant enzymes. Oxygen (O_2) is precursor for variety of free radicals. Its chemical reduction gives rise to the majority of damaging radicals and related reactants. While radicals are generated throughout all cells, mitochondria are important contributors to free radical production. This results from the fact that as electrons are shunted between the complexes of the electron transport chain (ETC), some escape and reduce nearby O_2 molecules causing the formation of the $O_2^{\bullet-}$, goes on to form more toxic and damaging agents. Apart from detoxifying free radicals melatonin also activates many antioxidant enzymes and inhibiting pro-oxidant enzymes (Fig. 9; Reiter, 2010).

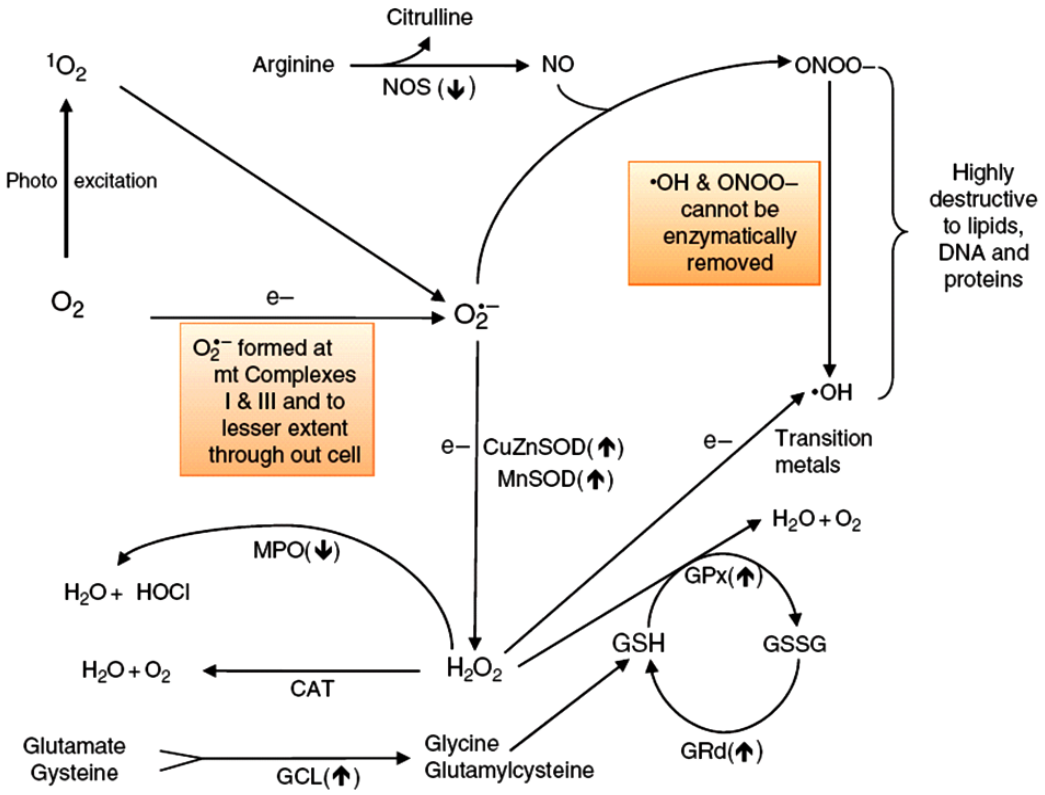

Fig. 9: Many free radicals are generated due to chemical reduction of molecular oxygen (O_2). Many of the free radicals are scavenged by melatonin. Apart from detoxifying free radicals melatonin activates many antioxidant enzymes (as indicated by ↑) and inhibiting pro-oxidant enzymes (as indicated by ↓). CAT, catalase; CuZnSOD, copper/zinc superoxide dismutase; MnSOD, magnesium superoxide dismutase; GCL, glutamylcysteine ligase; GPx, glutathione peroxidase; GRd, glutathione reductase; MPO, myeloperoxidase; $^1O_2$, singlet oxygen; $O^{2\bullet-}$, superoxide anion radical; H_2O_2, hydrogen peroxide, HOCl, hypochlorous acid; GSH, reduced glutathione; GSSG, oxidized glutathione; e^-, electron (Reiter, 2010).

Apart from melatonin, its precursor N-acetyl Serotonin (Lezoualc'h *et al*., 1998) and its metabolites that results from the interaction of melatonin with reactive oxygen species are equally efficient in scavenging free radicals (Fig. 7; Reiter, 2010). Like melatonin cyclic 3-hydroxymelatonin comes from melatonin functions as a radical scavenger and in the process is converted to *N*-acetyl-*N*-formyl-5-methoxykynuramine (AFMK).

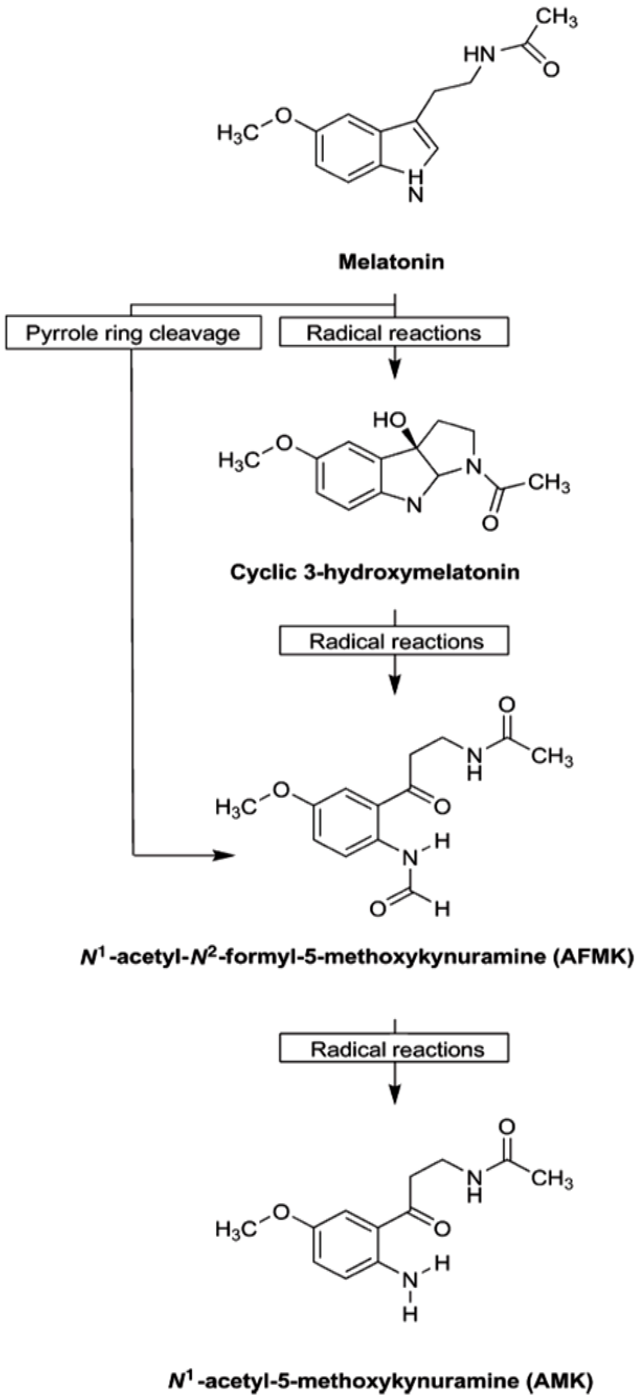

Fig. 10: Antioxidant cascade of melatonin occurs due to detoxification of free radicals by melatonin. Detoxification of $OH^{\bullet}$ by melatonin leads to the formation of cyclic 3-hydroxymelatonin, further cyclic 3-hydroxymelatonin also neutralizes free radicals and generates *N*-acetyl-*N*-formyl-5-methoxykynuramine (AFMK) or melatonin can directly forms AFMK by reacting with H_2O_2. AFMK also acts as free radical scavenger and generates *N*-acetyl-5-methoxykynuramine (AMK). As its precursors AMK also an antioxidant whose products are not yet identified (Reiter, 2010).

AFMK is also formed directly when melatonin interacts with H_2O_2. AFMK is also highly effective in scavenging toxic free radicals resulting in the generation of *N*-acetyl-5-methoxykynuramine (AMK). Further AMK also scavenges free radicals. These sequential reactions make melatonin highly efficient in reducing oxidative damage to sub-cellular organelles (Fig. 10; Reiter, 2010).

Melatonin shows two kinds of effects on SCN. One is neuronal firing suppression through MT1 and the other one is circadian phase resetting. This readjustment in circadian phase of SCN is mediated through MT2 (Hardeland, 2012). Melatonin has most prominent role as a regulator of sleep-wake cycle (Pandi-Perumal *et al*., 2008) and defining length of the night to SCN thus regulating phase of the circadian rhythms (reviewed in Pandi-Perumal *et al*., 2008). Melatonin also maintains circadian rhythms in peripheral oscillators such as adrenal cortex (Hardeland *et al*., 2012).

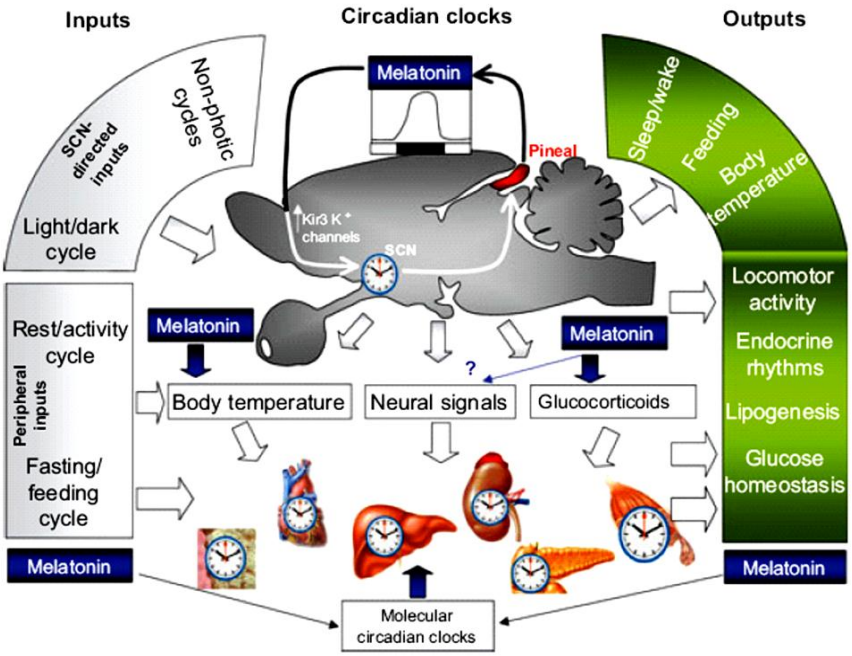

Fig. 11: Diagrammatic representation of role of melatonin in biological clock system (Hardeland *et al*., 2012).

Rhythmic melatonin secretion also has an important role in dopamine circadian rhythms and thus SCN indirectly regulate dopamine rhythms in the mid brain region (Khaldy *et al*., 2002). An overview of role of melatonin within central (SCN) and peripheral (liver, kidney, heart, intestine and muscle) oscillators and their connection to inputs (both SCN directed inputs and peripheral inputs) and outputs (sleep-wake, feeding, body temperature, glucose homeostasis, lipogenesis, endocrine rhythms and locomotor activity) is given in Fig. 11 (Hardeland *et al*., 2012).

Indole metabolism

Network of metabolite feedback pathways regulate transcription and translation. Alterations in the metabolome are the ultimate answer of an organism to genetic alterations, disease, or environmental influences (Weckwerth, 2003) (Fig. 12).

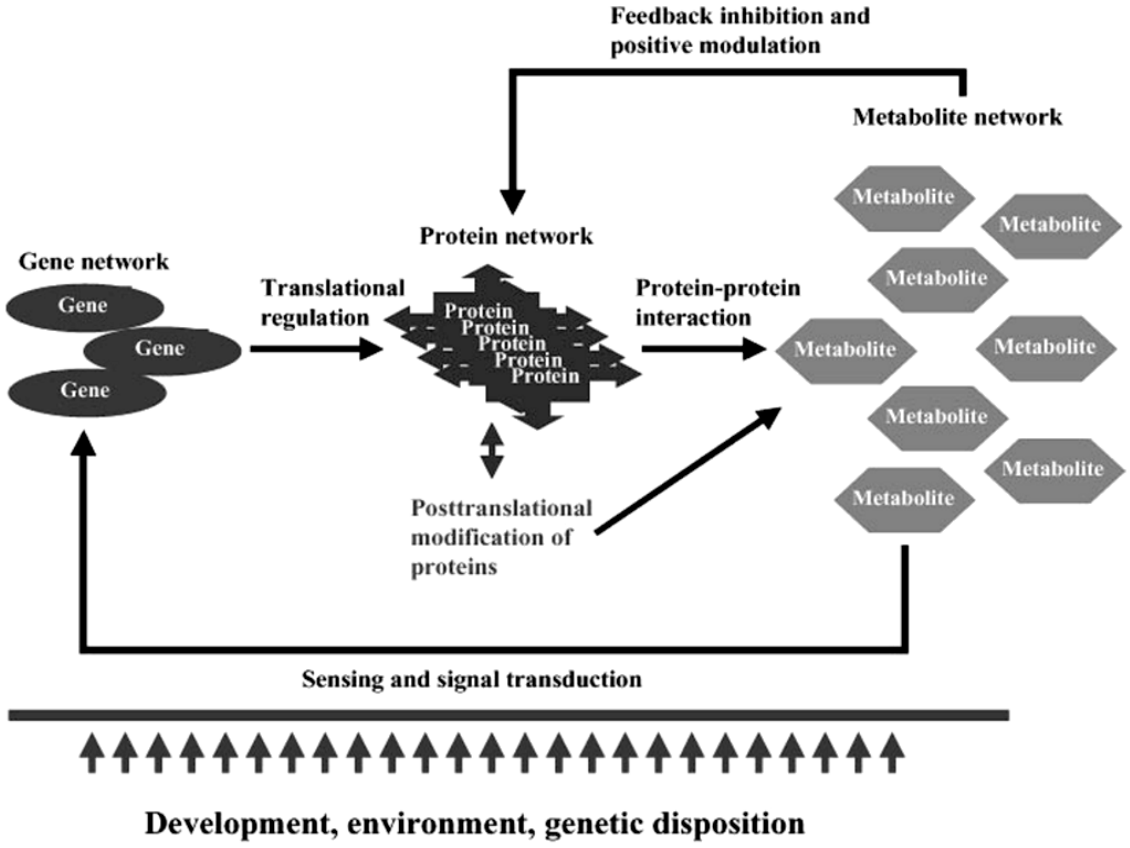

Fig. 12: Network of metabolite feedback pathways regulates transcription and translation. Alterations in the metabolome are the ultimate answer of an organism to genetic alterations, disease, or environmental influences (Weckwerth, 2003).

Hence, we have chosen 10 compounds of the indole pathway (Fig. 10), which include the precursors and the catabolites of serotonin, to study the daily rhythms in the chronomics of serotonin. Serotonin and melatonin are synthesized from essential amino acid L-tryptophan (TRP).

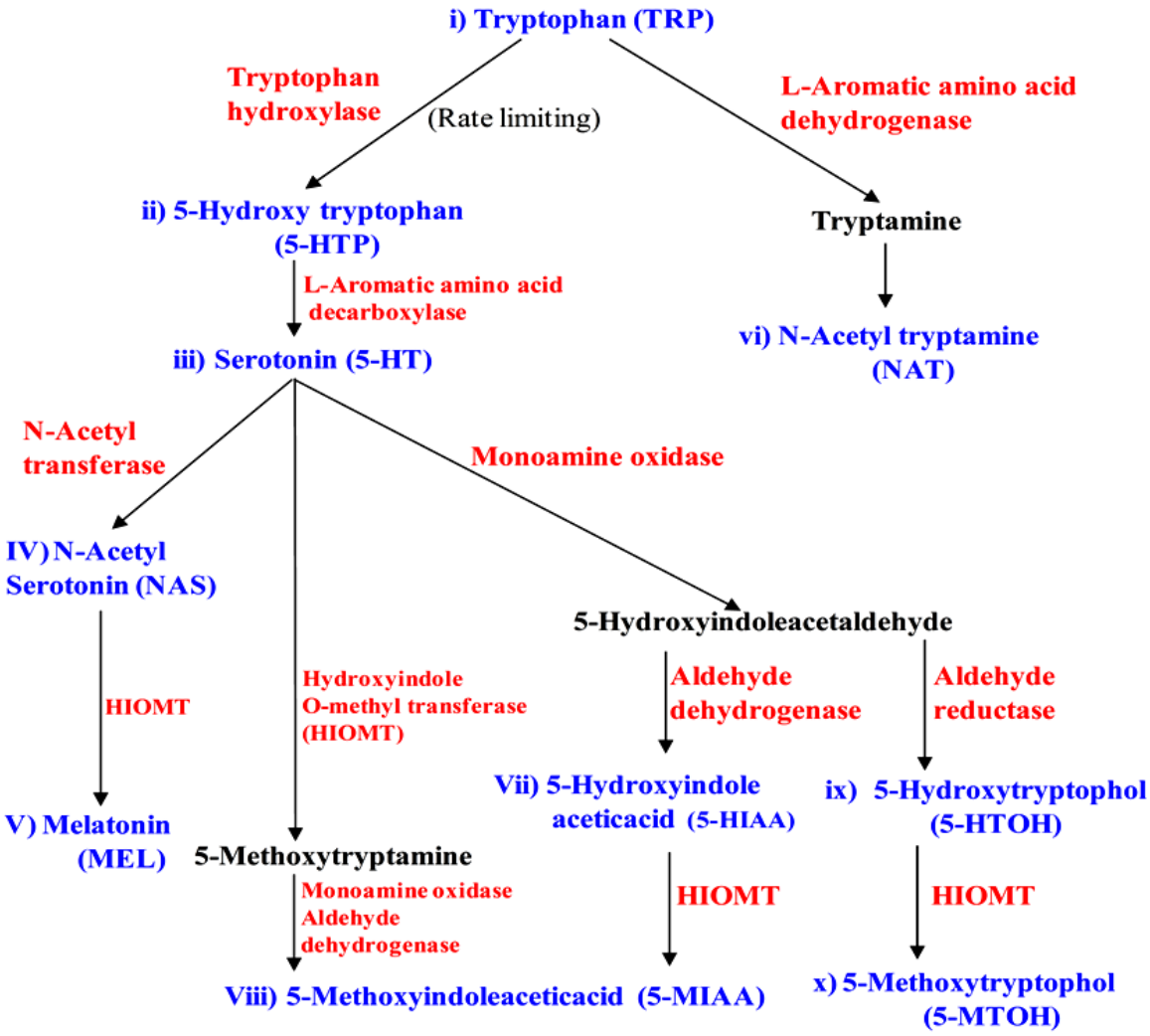

Fig. 13: Serotonin biosynthesis and catabolism. Tryptophan hydroxylase converts tryptophan (TRP) into to 5-hydroxytryptophan (5-HTP) and then 5-HTP is converted to serotonin (5-HT) by an enzyme L- aromatic amino acid decarboxylase. TRP is converted to N-acetyl tryptamine (NAT) by decarboxylase and acetylase enzymes respectively. 5-HT has two important pathways: (i) N-acetylase enzyme converts 5-HT into N-acetyl serotonin (NAS) and then to melatonin (MEL) by hydroxyl indole-O-methyl transferase (HIOMT) enzyme. (ii) Monoamine oxidase (MAO) converts 5-HT into 5-hydroxyindole acetaldehyde and then is converted to 5-hydroxyindoleacetic acid (5-HIAA) and 5-hydroxy tryptophol (5-HTOH) by aldehyde dehydrogenase and aldehyde reductase respectively. 5-HIAA is converted to 5- methoxyindole acetic acid (5-MIAA) and 5-HTOH is converted to 5-methoxy indole acetic acid (5-MTOH) by HIOMT enzyme (Garattini and Valzelli, 1965).

TRP is converted to 5-hydroxytryptophan (5-HTP) by the enzyme tryptophan hydroxylase. 5-HTP is then converted to serotonin (5-HT) by enzyme L- aromatic amino acid decarboxylase. Serotonin has two important pathways: (i) 5-HT is converted to N-acetyl serotonin (NAS) by N-acetylase enzyme which then is converted to melatonin (MEL) by hydroxy indole-O-methyl transferase (HIOMT) enzyme. (ii) 5-HT is converted to 5-hydroxyindole acetaldehyde by monoamine oxidase (MAO) which then is converted to 5-hydroxyindoleacetic acid (5-HIAA) and 5-hydroxy tryptophol (5-HTOH) by aldehyde dehydrogenase and aldehyde reductase respectively. 5-HIAA is converted to 5- methoxyindole acetic acid (5-MIAA) and 5-HTOH is converted to 5-methoxy indole acetic acid (5-MTOH) by HIOMT enzyme; TRP is converted to N-acetyl tryptamine (NAT) by decarboxylase and acetylase enzymes respectively (Fig. 13; Garattini and Valzelli, 1965).

Molecular components and mechanisms of mammalian circadian clock

The molecular machinery of circadian oscillator involves the coordinated expression of clock genes such as circadian locomotor output cycles kaput (*Clock*), Brain and muscle aryl hydrocarbon receptor nuclear translocator-like protein1 *(Bmal1), Period1 (Per1), Period2 (Per2), Period3 (Per3), Cryptochrome1 (Cry1), Cryptochrome2 (Cry2),* retinoic acid-related orphan nuclear receptors (*ROR), Rev-Erb* etc. In mammals the molecular machinery of biological clock is composed of two loops; a positive and a negative feedback loop which drives the coordinated expression of clock genes at transcriptional and translational levels. The positive loop includes members of the basic helix-loop-helix (bHLH)-PAS (Period-Arnt-Single-minded) transcription factor family CLOCK and BMAL1. CLOCK and BMAL1 heterodimerize and activate the transcription of target genes containing E-box elements in their promoter regions. These genes include *Per1*, *Per2*, *Per3, Cry1*, *Cry2*, Rev-erbα, Rorα and many other clock controlled genes (Ccg). This positive loop is regularly counterbalanced by a negative feedback loop formed by the proteins encoded by *Per1-3* and *Cry1-2* genes. PER and CRY proteins generate circadian rhythm by disrupting their own transcription. The stability of cytoplasmic PER and CRY proteins is regulated by the phosphorylation of PER by Casein Kinase I (CKI) and CRY by AMPK. Hyper phosphorylation of PER and CRY proteins targets them to ubiquitin-

proteasomal degradation. PER proteins that escape hyper phosphorylation and degradation, heterodimerise with the other negative elements such as CRY and translocate back into the nucleus, to repress the expression of Ccg's and their own transcription by acting on CLOCK: BMAL1 complex. Transcription of Rev-erbα and Rorα is a regulatory loop induced by CLOCK: BMAL1 heterodimers. Rev-erbα and Rorα subsequently compete to bind retinoic acid related orphan receptor response elements (ROREs) present in the promoter region of the *Bmal1*. ROR (α, β and γ) and REV-ERB (α and β) are able to regulate the expression of *Bmal1* through ROREs. Transcription of *Bmal1* is activated by ROR whereas repressed by REV-ERB's (Fig. 14; Ko and Takahashi, 2006; Toh, 2008; Mohawk *et al*., 2012).

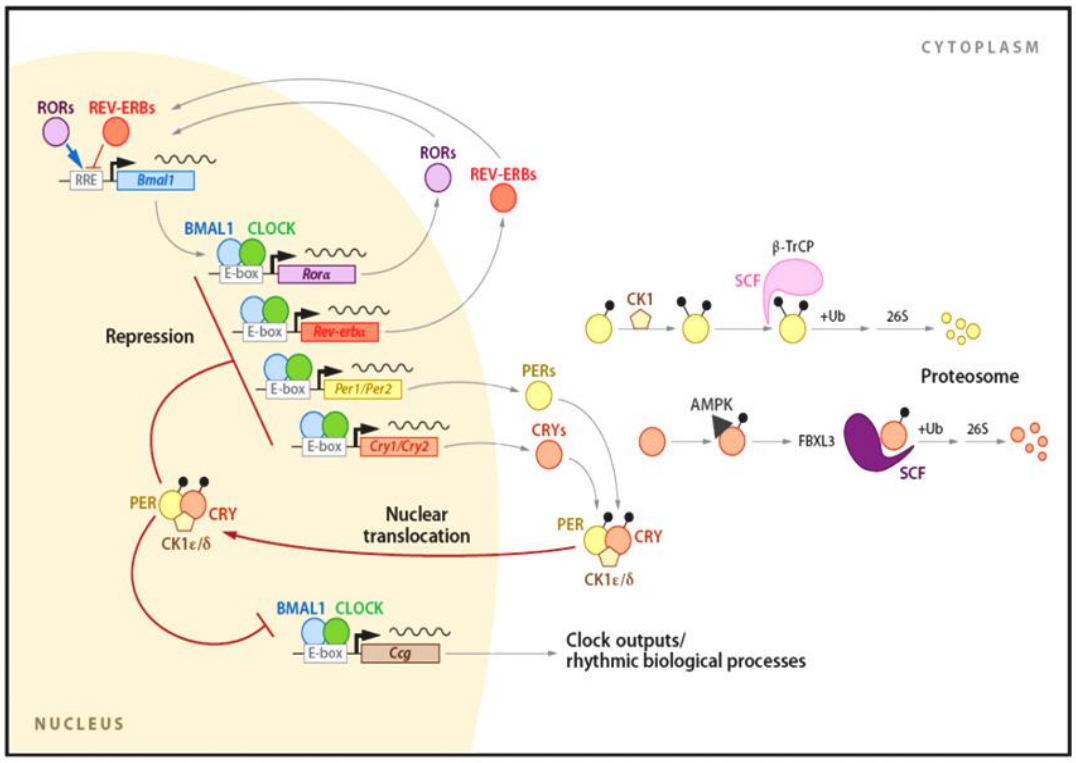

Fig. 14: Mammalian circadian clock molecular mechanism. SCN rhythmicity is regulated by the interactions of clock genes and their protein product characterized by feedback loops. C*lock*, *Bmal1* and *Rorα* are positive regulators. CLOCK and BMAL1 - forms heterodimers and promotes expression of *Per*, *Cry*, *Rorα, Rev-erb α* and *Ccg* genes. *Per*, *Cry* and *Rev-erbα* are negative regulators. PER/CRY complex inhibits the transcription of their own genes and as well as *Ccg's.* PER and CRY stability is determined by its phosphorylation states by CK1 and AMPK (Mohawk *et al*., 2012).

Aging

Aging is a complex process characterized by the slowing or alteration of cellular and bodily processes over time, resulting in reduced functionality of cells, increased susceptibility to disease, and ultimately the death of the organism. This is a process that happens naturally to all organisms, and can ultimately not be avoided. In the cell, indicators of aging can be seen in changes/damage to DNA, proteins, and other cellular components. One of the key factors that have been found to be involved in the aging process is oxidative stress. Aging leads to regional cell death in the brain which causes loss of function, behavioral changes and onset of age related diseases like Alzheimer's disease, Parkinson's disease etc. (Smith *et al*., 2005).

Aging and Biological clock

Aging is associated with a variety of alterations in circadian rhythms. Upon aging many biochemical and neurochemical changes occur in biological clock. Age related changes in the SCN have been addressed by many workers which may contribute to age related circadian dysfunction such as decline in circadian neural activity (Nakamura *et al*., 2011), decrease in the amplitude of the circadian body temperature rhythms (Weinert, 2010), altered serotonin rhythms in SCN (Jagota and Kalyani, 2010), neuropeptide content and GABAergic network of the SCN (Hofman and Swaab, 2006; Palomba *et al*., 2008) altered SCN sensitivity towards exogenous melatonin administration (Gall and Weaver, 2008; Jagota and Kalyani, 2010; Manikonda and Jagota, 2012). Upon aging circadian drinking behavior, locomotor activity rhythms and body temperature rhythms are reduced. Clock proteins BMAL-1 and PER are directly involved in regulation of free radical levels thus play role in regulating aging induced by the accumulation of free radicals (Kondratov *et al*., 2007). Disruption of *Per2* and *Bmal1* in mice has been reported by some workers with alterations in behavior rhythmicity and development of malignant tumors, metabolic syndrome (Kunieda *et al*., 2006) and premature aging (Kondrotov *et al*., 2009). Melatonin production, amplitude and its pulsatile pattern from pineal gland decreases upon aging (Miguez *et al*., 1998; Aujard *et al*., 2001). Disturbed circadian melatonin rhythm have profound effects on the health and well-being of the elderly subjects (Wu and Swaab, 2005; Poeggeler, 2005). 40% of elderly population show reduced amount and quality of sleep. Insufficient or decreased quality of sleep leads to the disruption of digestion, mood, alertness etc. (Fig. 15; Jagota, 2005).

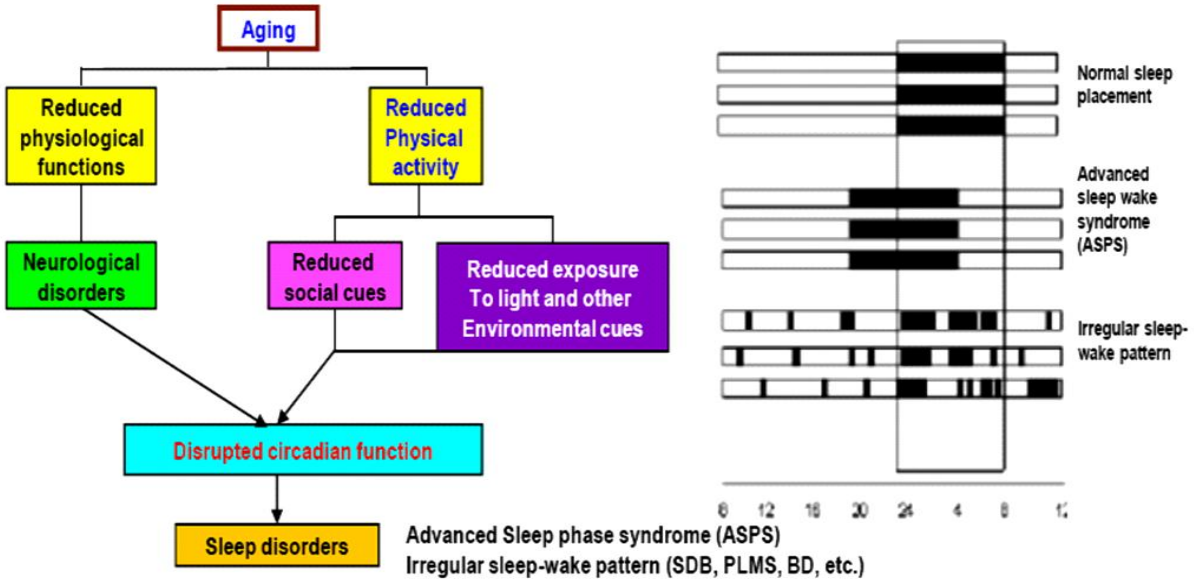

Fig.15: Schematic diagram showing various sleep disorders associated with disturbances of the circadian system. The open bars represent intervals during which wakefulness typically occurs, black bars correspond to usual sleep times in normal and pathological conditions and vertical rectangle represents desired sleep time. Individuals with advanced sleep phase syndrome (ASPS), sleep at earlier than desired time whereas individuals with irregular sleep-wake patterns such as sleep disordered breathing (SDB), periodic leg movements in sleep (PLMS) and rapid eye movement (REM) behavior disorder (RBD) etc. may have disturbed sleep at other than desired times also (Jagota, 2005).

Parkinson's disease

Parkinson's disease (PD) is the second most common age related neurodegenerative disorder (Beal, 2001), which is estimated to affect approximately 1% of the population older than 65 years of age (Jagota, 2005). Clinically patients with PD exhibit cardinal motor symptoms such as resting tremor on one or both sides of the body, bradykinesia (slowness of movement), rigidity (stiffness of limbs), and abnormal postural reflexes (gait or balance problems) (Uversky, 2004). Risk factors of PD include age, depression, cognitive impairment, environmental exposure: herbicide and pesticide exposure, life experiences (trauma, emotional stress etc.). Pathology of PD includes dopaminergic neurons present in the substantia nigra of mid brain region undergoes degeneration resulting in the deterioration of the neuronal connection between the substantia

nigra and the striatum (Fig. 16; nigrostriatal pathway) (Dauer and Przedborski, 2003) resulting in the decrease of dopamine levels.

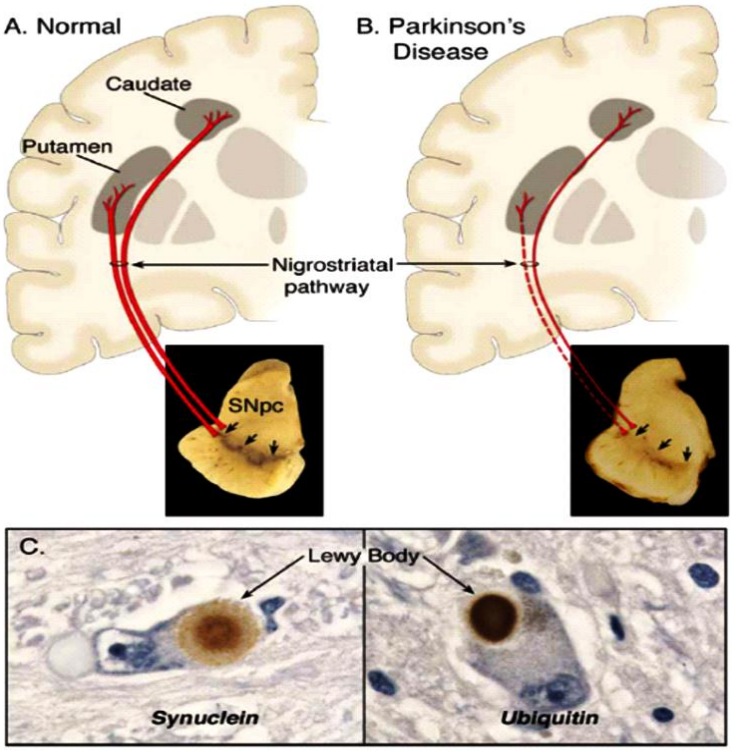

Fig. 16: Parkinson's disease neuropathology. (A) Schematic representation of the normal nigrostriatal pathway (in red). (B) Schematic representation of the nigrostriatal pathway in Parkinson's disease (in red). (C) Intraneuronal inclusions, termed Lewy bodies, in a SNpc dopaminergic neuron (Dauer and Przedborski, 2003).

Types of Parkinson's disease (PD):

Parkinson's disease can be divided into three subtypes according to their origin

1. Sporadic PD: It involves multiple neuronal systems and results from changes developing in a few susceptible types of nerve cells with an unknown cause.

2. Familial PD: Occurs due to mutation in some of the genes like α-synuclein (PARK 1), parkin (PARK 2) and ubiquitin-C-hydrolase-L1 (PARK 5).

3. Idiopathic PD: No precise cause. Some types include causes like head trauma, cerebral anoxia, drugs and induced by environmental toxins such as rotenone, MPTP, paraquat and maneb.

Causes for neurodegeneration in PD:

Activity of complex I of mitochondrial electron transport chain is reduced in brain, blood platelets and skeletal muscles of PD patients which lead to reduced ATP synthesis as well as increased ROS. The loss of dopaminergic neurons is caused by auto oxidation of dopamine due to relative high exposure of these neurons to free radicals. Dopamine has many functions in the brain and it plays a major role in behavior and cognition, motor activity, motivation and reward, inhibition of prolactin production (involved in lactation), sleep, mood, attention and learning (Uversky, 2004). In addition several other factors are responsible for neurodegeneration in PD, such as oxidative stress due to mitochondrial complex I deficiency (Betarbet *et al*., 2000; Yuan *et al*., 2007). Important pathological hallmark of PD is the presence of cytosolic filamentous inclusions known as Lewy bodies (LBs) and Lewy neurites (LNs; Forno, 1996) in some surviving nigral dopaminergic neurons. Major protein in these inclusions is α-synuclein which may play a role in the pathogenesis of disease (Spillantini *et al*., 1998; Di Monte, 2003). α-synuclein has been implicated in the environmental hypothesis of PD neurodegeneration, viz., direct interation between this protein and neurotoxicants might contribute to the development of PD (Di Monte, 2003).

PD pathology is also characterized by polymerization and development of altered conformation of soluble native neuronal protein, resulting in intracellular aggregation. Lewy bodies composed of α-synuclein made up of a number of neurofilament proteins together with proteins responsible for proteolysis (Davie, 2008). At native state α-synuclein is a soluble and unfolded protein. Its central hydrophobic region makes it highly favorable for aggregation and forms oligomer which ultimately forms insoluble fibrils (Giasson *et al*., 2001), which could be toxic through a variety of mechanisms. Ubiquitin Proteasomal System (UPS) maintains the intracellular proteolysis and viability of cells by removing the unwanted proteins that are no longer required by the cell. Discovery of mutations in genes coding for many UPS pathway proteins in PD reveals the link between UPS and PD. Role of UPS in PD is evidenced by the identification of genes such as PARKIN, UCHL-1 and LRRK2. The protein products of these genes play a major role in Ubiquitin Proteasomal degradation (Dauer and Przedborski, 2003). PARKIN gene codes for an E3-ubiquitin ligase which catalyzes the addition of ubiquitin chains to the target protein for degradation. Substrates for PARKIN include Synphilin-1, α-synuclein,

Cyclin E etc. (Cookson, 2005). Mutations in PARKIN results in the accumulation of its substrates (Kitada *et al*., 1998) thus leading to formation of inclusion bodies. Ubiquitin C-terminal hydrolase L-1 is coded by UCHL-1 convert's polyubiquitin chains back into monomeric ubiquitin. LRRK2 has a role in mediating neurodegeneration (Paisan *et al*., 2004).

Pathogenic genetic mutations may directly induce abnormal protein conformation or they may damage the ubiquitin-proteasome function to detect and degrade misfolded proteins. Oxidative damage linked to mitochondrial dysfunction and abnormal dopamine metabolism may also promote protein misfolding. Oxidative stress, energy depletion and activation of programmed cell death (PCD) are the major causes for death of the dopaminergic neurons in PD (Fig. 17; Dauer and Przedborski, 2003).

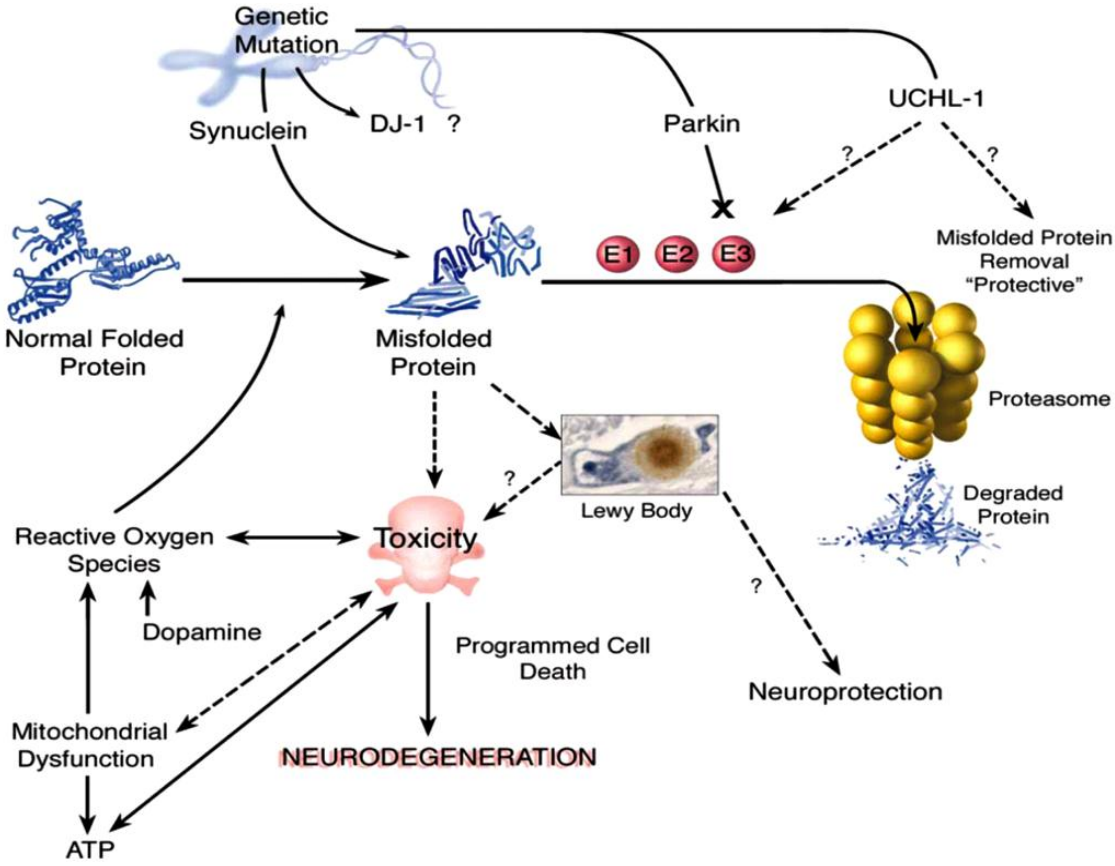

Fig. 17: Mechanisms of Neurodegeneration in Parkinson's disease. Accumulation of misfolded proteins, pathogenic mutations which lead to abnormal protein conformations, damage to cellular machinery which detect and degrade misfolded proteins. Oxidative damage resulting from mitochondrial dysfunction and abnormal dopamine metabolism plays a key role in PD neurodegeneration (Dauer and Przedborski, 2003).

Biological clock and Parkinson's disease

In PD there is a decreased level of dopamine leading to loss of regulation of motor activities. It is known that the SCN also controls locomotor activity rhythms. Environmental toxins, which cause Parkinson's disease, interrupt the electron transport chain (Dauer and Przedborski, 2003) leading to the accumulation of ROS, which is one of the reasons for aging. The role of circadian timing system in the ROS regulation is well established (Kondratov *et al*., 2006), which is a major cause for the neurodegeneration in Parkinson's disease. It has been reported from our laboratory that antioxidant enzymes, Pro-oxidant enzymes and lipid peroxidation levels daily rhythms in the rat liver (Manikonda and Jagota, 2012). It is reported that in case of PD along with the degeneration of dopaminergic neurons some other type of neurons such as serotonergic neurons also undergo degeneration leading to decrease in the serotonin level.

Along with the cardinal motor symptoms, non-motor symptoms like circadian disorders (Sleep dysfunction, insomnia, depression, sleep disordered breathing etc.) and autonomic dysfunction are commonly observed in all stages of PD, but they are frequently unrecognized by clinicians and remain untreated (Chaudhuri, 2006 and 2009). Circadian fluctuations are seen in motor and non-motor symptoms and as well as in the kinetics of drug treatment in PD patients. Sleep disturbances in PD also reveal alterations of circadian rhythms. Physiological day/night blood pressure profile, circadian heart rate variability is also altered in PD patients (Bruguerolle and Simon, 2002; Monge, 2004). Many circadian disorders observed in aging are also observed in PD which is more pronounced in case of latter (Chaudhuri, 2006 and 2009). One of the possible causes of circadian disorders observed in PD is degeneration in circadian clock regulating circuits in the SCN such as metabolism, antioxidant defense, melatonin, DNA repair and autophagy (Fig. 18; Kondratova and Kondratov, 2012).

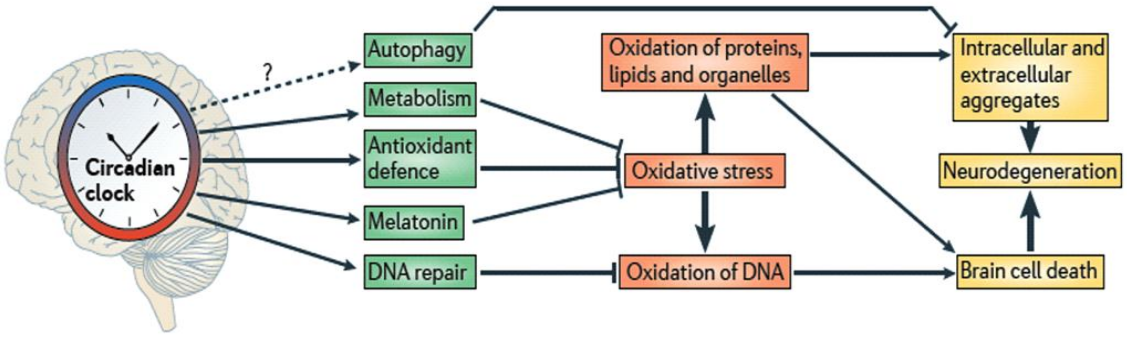

Fig. 18: Circadian clock-dependent regulation of neurodegeneration. Metabolism, reactive oxygen species (ROS) homeostasis, DNA repair and probably autophagy (systems and pathways controlled by the circadian clock are shown in green) are regulated by circadian clock. Compromise in the activities of these systems occurs with circadian disruption, which leads to oxidative stress (shown in red) and accumulation of intracellular and extracellular aggregates in the brain. This, in turn, leads to brain cell death and degeneration of brain structures (shown in yellow) (Kondratova and Kondratov, 2012).

Substantia nigra (SN):

It is a heterogenous region of the basal ganglia. Basal ganglia have Caudate, Putamen, Nucleus accumbens, Globus pallidus, SN (Fig. 19), Subthalamic nucleus. All these regions are involved in regulating locomotory activities. Any disturbances in these regions lead to movement disorders such as Huntington's disease and Parkinson's disease. Neuronal death in Caudate and Putamen lead to Huntington's disease characterized by unwanted movement and in SN leads to Parkinson's disease characterized by motor disability.

Classically SN is divided into two components:

1. Substantia nigra pars Compacta (SNpC) is composed of dopaminergic neurons.
2. Substantia nigra pars Reticulata (SNpR) is composed of GABAergic neurons.

In humans and rodents SNpC dopaminergic neurons look like a layer of cells with dark pigmentation due to presence of neuromelanin. All the neurons in SNpC send their axons through nigrostriatal pathway to the striatum where they release neurotransmitter dopamine. SN consists of 4,00,000 nerve cells at adult age in humans. The normal rate of nigral cell loss is about 2,500 nerve cells per year after reaching adult age. As the dopaminergic neurons decrease

with age, dopaminergic functions also decrease with age. Thus if any unaffected person lives long enough (>130 years), he or she would probably develop Parkinson's disease.

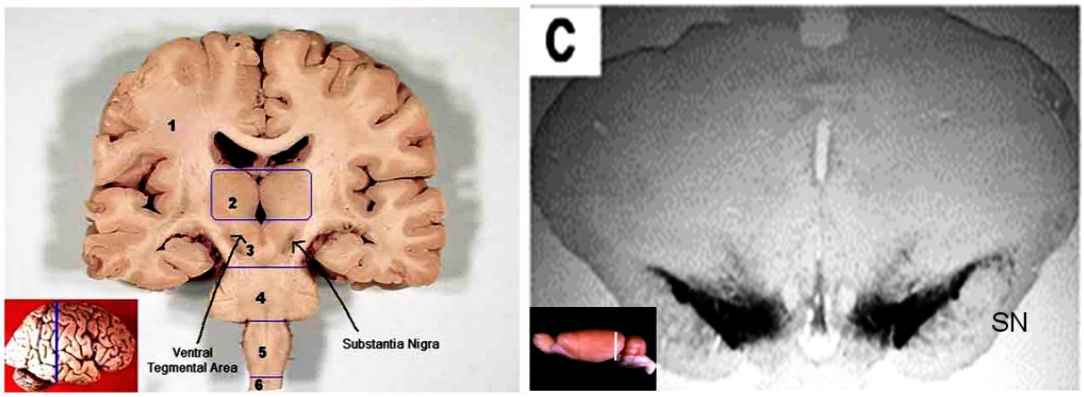

Human SN Rat SN

Fig. 19: Picture showing localization of human and rat substantia nigra (SN) in coronal sections of human and rat brain respectively.

Biological clock and SN:

Close interaction between the catecholamines and circadian timing system (CTS) have already been reported.

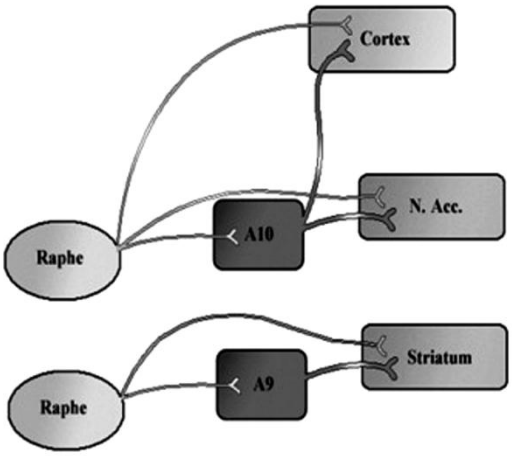

Fig. 20: Serotonin-dopamine interaction in the nigrostriatal dopaminergic system. Serotonin-containing cell bodies of the raphe nuclei send projections to dopaminergic cells in both the ventral tegmental area (VTA, A10) and the substantia nigra (SN, A9), and to their terminal fields in the nucleus accumbens, prefrontal cortex and striatum (Matteo *et al.*, 2008).

Striatal dopamine acts in a receptor dependent manner (Imbesi *et al*., 2009) to regulate the activity of BMAL1-CLOCK heterodimer (Yujnovsky, 2006). By the rhythmic expression of nigral tyrosine hydroxylase (TH) which is a rate limiting enzyme in dopamine biosynthesis, the production of this neurotransmitter is in turn under circadian regulation (Khaldy *et al*., 2002; Weber *et al*., 2004). Rhythmic melatonin secretion has an important role in dopamine circadian rhythms (Khaldy *et al*., 2002). Serotonin neuronal projections from raphe nuclei also regulates the release of dopamine in SN neurons (A9) and Ventral tagmental area (VTA; A10) at the receptor level (Fig. 20; Lucas *et al*., 2000).

Experimental models of PD:

The loss of dopaminergic system can be accelerated by an environmental insult that is acute exposure to neurotoxins and for direct relevance to humans an ideal model of PD should show the following characteristics:

1. The loss in dopaminergic neurons should exceed 50% and should be readily detectable using biochemistry and neuropathology.
2. Model should have easily detectable motor deficits, including cardinal symptoms of PD.
3. Model should show the development of characteristic Lewy bodies in some of the live dopaminergic neurons in SNpC (Beal, 2001).

Table 1: Characteristics of animal models of Parkinson's disease

Toxin	Animal	Dopamine neuron loss	α-synuclein	Motor deficits	Mode of administration
Rotenone	Rat Mice	+	+	+	Intra peritonial, Sub cutaneous and Stereotaxic way
MPTP	Rat Mice Primate	+	-	+	Intra peritonial and Stereotaxic way
6 hydroxy dopamine	Rat Mice	+	-	+	Stereotaxic way
Paraquat	Rat Mice	+	-	+	Stereotaxic way

Beal, 2001

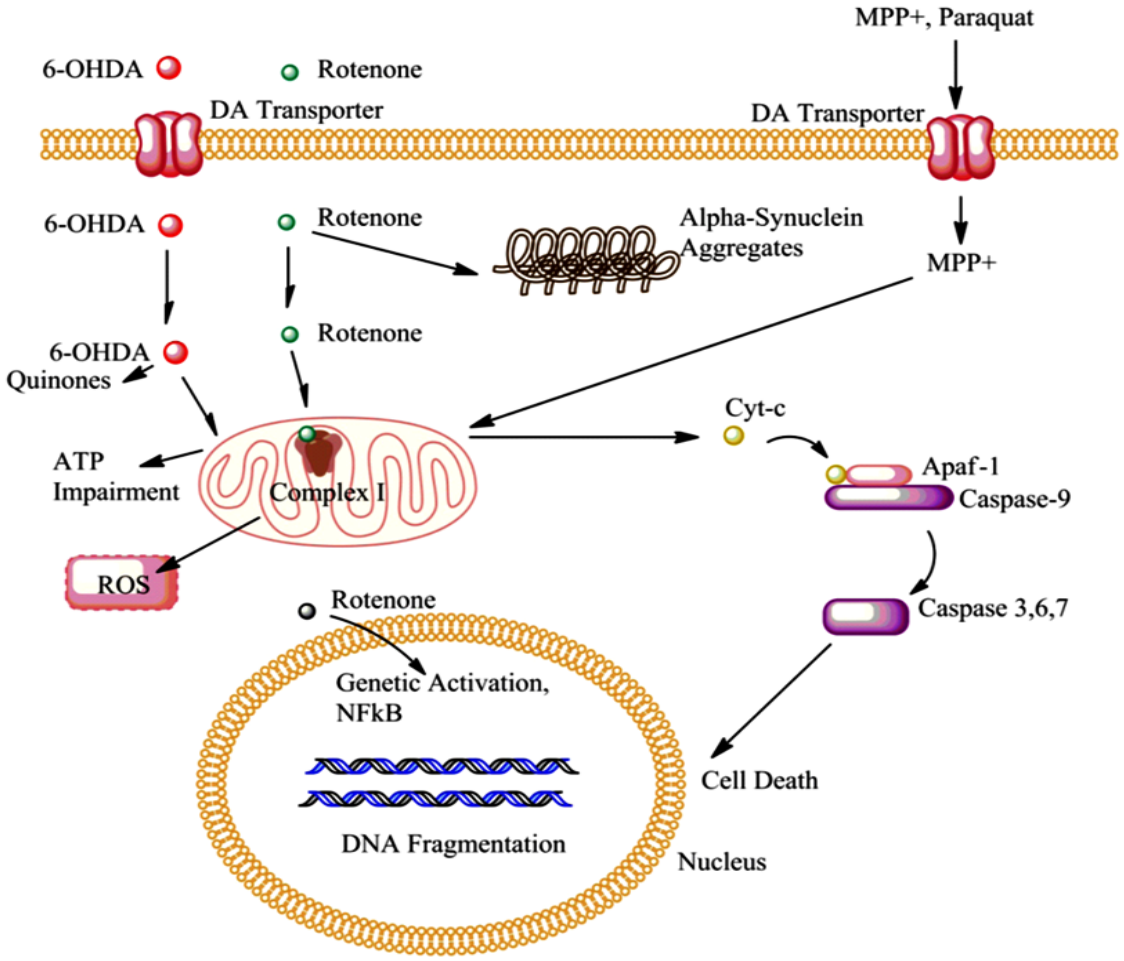

Fig. 21: Mode of action of various toxins used in the development of experimental models of Parkinson's disease. MPTP, 6-hydroxydopamine and paraquat gets entry into dopaminergic neurons through dopamine transporter whereas rotenone readily diffuses across the lipid bilayer and get enter into dopaminergic neurons. Pathology induced by these toxins is activation of programmed cell death via the release of cytochrome C and accumulation of misfolded proteins (Cabezas *et al*., 2013).

As dopaminergic neurons are more vulnerable to mitochondrial complex I inhibitors. Many toxins such as Rotenone (Betarbet *et al*., 2000), MPTP, 6-hydroxydopamine (Nicola *et al*., 2007), Maneb and Paraquat (Francesca *et al*., 2005) have been used in developing PD in rodents. The toxins such as MPTP, 6-hydroxydopamine and paraquat make use of dopamine transporter to get entry into dopaminergic neurons whereas rotenone doesn't need any transporter to get entry into dopaminergic neurons. These toxins activate release of cytochrome C and accumulation of misfolded proteins leading to programmed cell death (Table 1; Fig. 21).

Rotenone as a lipophilic molecule crosses blood brain barrier easily, leads to gradual loss of dopamine neurons, easily detectable motor deficits such as bradykinesia, postural instability and development of Lewy bodies (Beal, 2001; Betarbet *et al*., 2000; Alam and Schmidt, 2002). Other toxins such as 6-hydroxydopamine cannot cross the blood brain barrier, it must be administered by local stereotaxic injection into SN and Paraquat also does not easily penetrate blood brain barrier. 6-hydroxydopamine and MPTP cannot cause gradual loss of dopamine neurons and Lewy bodies formation even though they show motor symptoms of PD (Beal, 2001) (Table 1; Fig. 21; Cabezas *et al*., 2013).

Rotenone

Rotenone is a natural ketonic complex derived from the roots of *Lonchocarpus* species widely used as insecticide as well as pesticide (Caboni *et al*., 2004).

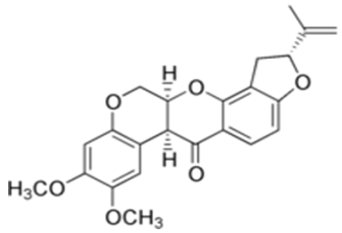

Fig. 22: Skeletal structure of Rotenone - (2*R*,6a*S*,12a*S*)-1,2,6,6a,12,12a-hexahydro-2-isopropenyl-8,9-dimethoxychromeno[3,4-*b*]furo(2,3-h)chromen-6-one

Mechanism of action

Rotenone is a high affinity inhibitor of complex I of electron transport chain (Fig. 23) and blocks the electron flow from complex I to Ubiquinone binding site in the mitochondria during oxidative phosphorylation (Grivennikova *et al*., 1997) which leads to increase in ROS (Wang *et al*., 2013). Rotenone acts as agonist and displaces the ubisemiquinone intermediate at the ubiquinone binding site (Esposti, 1998). State of complex I is altered by rotenone and lead to increase in superoxide production at ubiquinone binding site (Lambert and Brand, 2004). Rotenone also induces the formation of H_2O_2 in cell culture, resulting in altered mitochondrial membrane potential finally leading DNA fragmentation and apoptosis. Apoptotic intrinsic pathway is activated by rotenone via opening of transition pores in the outer membrane of the mitochondria (Oikawa *et al*., 2003). Thus increased oxidative stress due to rotenone leads to fast decrease in number of functional dopaminergic neurons, consequence is earlier onset of PD

(Betarbet *et al*., 2000). In addition, intra-peritoneal administration of rotenone has been related with dose dependent decrease in dopamine levels and TH activity associated with Parkinsonian symptoms (Alam and Schmidt, 2002; He *et al*., 2003). Thus rotenone is relevant toxin to induce PD in rat model.

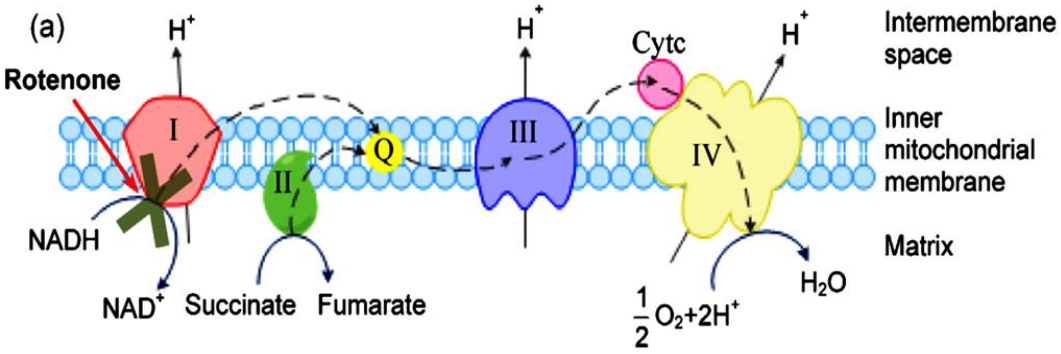

Fig. 23: Binding site of Rotenone to complex I of electron transport chain. This leads to inhibition of electron flow from complex I to ubiquinone binding site in the mitochondria during oxidative phosphorylation (Wang *et al*., 2013).

Melatonin in Aging and Parkinson's disease

Reduced melatonin synthesis and its secretion from pineal gland were reported upon aging (Fig. 24) and in Parkinson's disease (reviewed in Jagota, 2012). Modulation of mammalian circadian system by melatonin has been reported by many workers (Reiter, 2010; Jagota, 2012) with an entrainment effect on activity rhythms, phase shifts and synchronization of rhythmicity (Cassone *et al*., 1986; Sack *et al.*, 1998; Revell *et al*., 2006) as well as reversal of pinealectomy induced changes (Kolker *et al*., 2002) and suppression of behavioral phenotype of the CLOCK mutant (Shimomura *et al*., 2010), In addition it has been reported from our laboratory that the differential effects of melatonin in restoration of serotonin (Jagota and Reddy, 2007; Jagota and Kalyani, 2010), antioxidant enzymes and lipid peroxidation (Manikonda and Jagota, 2012) in aged rats.

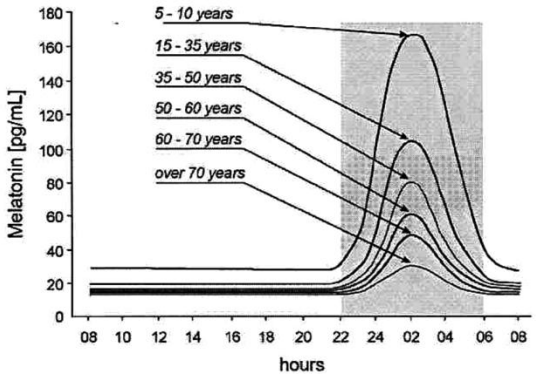

Fig. 24: Daily rhythmic profiles of serum melatonin concentrations at various age; grey area - darkness (Karasek, 2004).

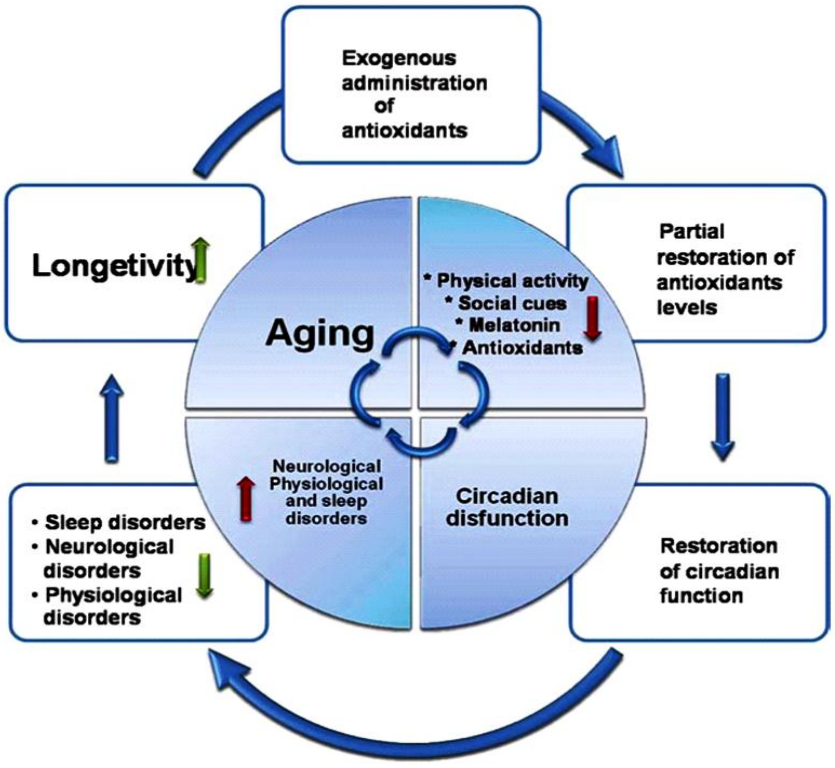

Fig. 25: Therapeutic effects of antioxidant melatonin in restoration of circadian functions. Exogenous administration of antioxidants leads to restoration of circadian function and decrease in the severity of neurological, physiological and sleep disorders which leads to increase in quality of life (Jagota, 2012).

Age induced decrease in physiological functions responsible for circadian dysfunction can be restored by melatonin which leads to longevity (Fig. 25). Various reports proved that

melatonin acts as an anti-aging agent. Positive effects of melatonin have been seen in reducing sleep disturbances in elderly population (reviewed in Jagota, 2012).

It is reported that mitochondrial oxidative damage which leads to oxidative stress in aging and other neurodegenerative diseases is prevented by melatonin by reducing apoptosis.

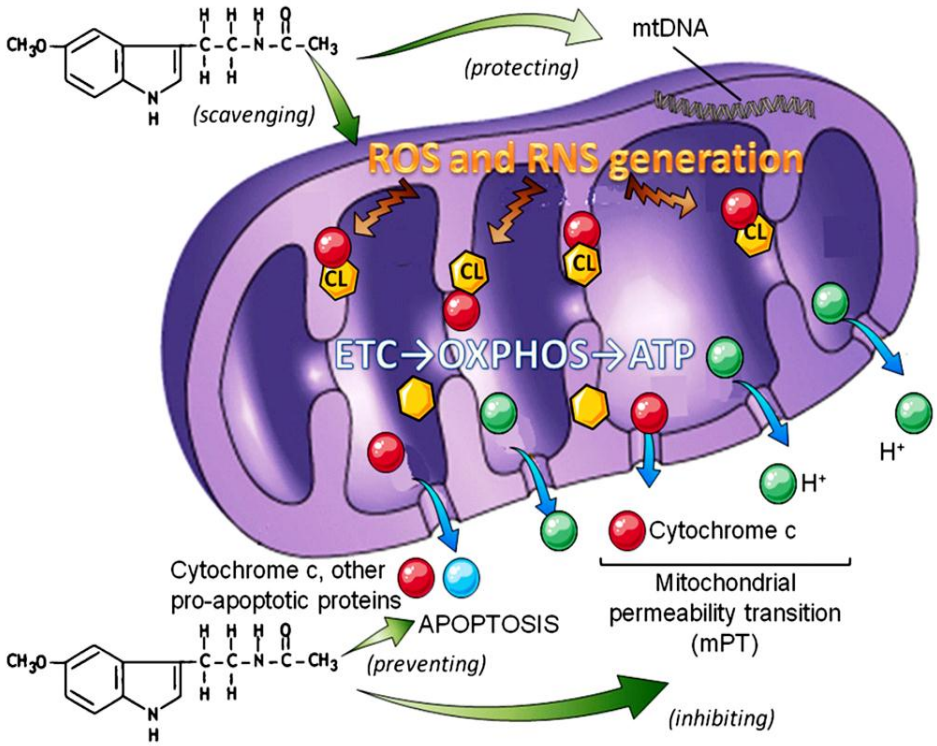

Fig. 26: Mitochondrial pathophysiology and Melatonin. Reactive oxygen species (ROS) production is mediated, partly via cardiolipin (CL) peroxidation which makes detachment of cytochrome c from the inner mitochondrial membrane and changes in mitochondrial permeability transition (mPT) leads to mitochondrial swelling and the release of cytochrome C and other pro-apoptotic proteins. Activation of caspase cascade in the cytoplasm results in apoptosis leading to cell death. Melatonin prevents this cascade by scavenging ROS and preventing apoptosis and inhibiting the change in mPT (Cardinali *et al*., 2013).

The mechanisms involved in electron transport chain dysfunction mainly depend on the generation of ROS which leads to oxidative stress and ATP depletion. This ROS production is mediated, partly via cardiolipin (CL) peroxidation which makes detachment of cytochrome C from the inner mitochondrial membrane and changes in mitochondrial permeability transition that leads to mitochondrial swelling and the release of cytochrome C and other pro-apoptotic proteins. Activation of caspase cascade in the cytoplasm results in apoptosis leading to cell

death. Melatonin and its metabolites (AFMK, AMK) prevent this cascade by acting at multiple sites in the mitochondria. Scavenging of ROS prevents free radical attack on electron transport chain complexes and mitochondrial DNA (Fig. 26; Cardinali *et al*., 2013).

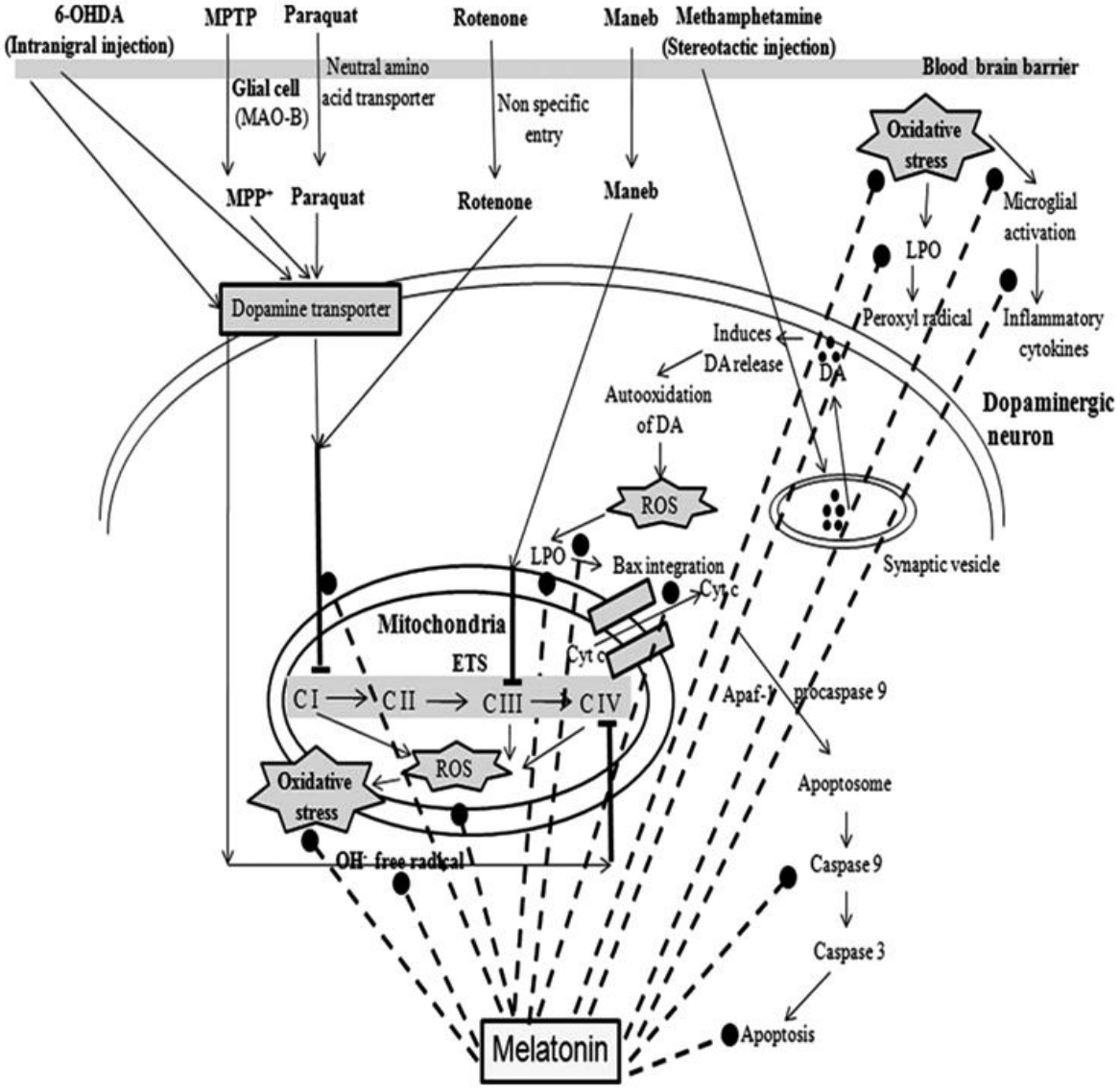

Fig. 27: Mode of neuroprotection by melatonin at various steps of toxin induced neurodegeneration. Melatonin inhibits oxidative stress, lipid peroxidation, microglial activation, inflammatory cytokines, caspase 9, apoptosis and decreases ROS (CI, CII, CIII and CIV - mitochondrial complexes I, II, III, and IV; ROS - reactive oxygen species; LPO - lipid peroxidation; DA - dopamine; Cyt - cytochrome; ETS - electron transport system; MAO-B monoamine oxidase-B enzyme) (Singhal *et al*., 2012).

Melatonin has been reported to show neuroprotective effects on dopaminergic neurons in rotenone induced PD rat model (Lin *et al*., 2008), MPTP induced PD model (Chen *et al*., 2002), 6-hydroxydopamine induced PD model (Willis and Robertson, 2004) and maneb induced PD model (Ishido, 2007). Although melatonin does not alter directly the rotenone induced inhibition of mitochondrial complex I, it is known to inhibit rotenone induced oxidative stress (Sousa and Castilho, 2005). Melatonin blocks fibril formation, stabilization, oligomerization and secondary structure transition of α-synuclein and further reduces cytotoxicity induced by α-synuclein (Ono *et al*., 2012). It offers neuroprotection against rotenone induced PD model by inhibiting the free radical generation, lipid peroxidation, microglial activation, inflammatory cytokines, caspase 9, and apoptosis, resisting TH-positive neuronal loss and restoration of the dopamine levels in the striatum (Fig. 27; Singhal *et al*., 2012).

Based on this literature background the following objectives were planned.

Objectives

Objectives:

1. Characterization of rotenone induced Parkinson's disease (RIPD) rat model.

2. Studies of Chronomics of Serotonin metabolism in SCN, Pineal and SN in RIPD rat model.

3. Studies of daily rhythms of protein profile in SCN, Pineal and SN upon aging and in RIPD rat model.

4. Studies of daily rhythms of various clock gene expression in SCN, Pineal and SN upon aging and in RIPD rat model.

5. Effect of melatonin administration on daily rhythms of various clock gene expressions in SCN, Pineal and SN upon aging and in RIPD rat model.

Materials and Methods

Chapter 2: Materials and Methods

Male wistar rats of different age groups (2, 3, 12 and 24 month (m)) were maintained at 23 ± 1°C with LD, 12:12 (lights on: 06:30 AM (Zeitgeber time (ZT)-0) and lights off: 6:30 PM (ZT-12)) for 2 weeks prior to experiment. All the animals were supplied food and water *ad libitum*. All rats were kept individually in polypropylene cages. Cage changing was done at random intervals**.** All experiments were performed as per Institutional Animal Ethics. The rats were separated into five groups.

Group 1A (n=64): 2 m animals received intraperitonially Rotenone dissolved in sunflower oil (2.5 mg/ml/kg body weight) once a day at ZT5 for 48 days (Alam and Schmidt, 2002). This group was further divided into four groups.

i. Characterization of rotenone induced Parkinson's disease (RIPD) rat model (objective1) n=6.
ii. Studies of chronomics of serotonin metabolism in SCN, Pineal and SN in RIPD rat model (objective 2) n=26.
iii. Studies of daily rhythms of protein profile in SCN, Pineal and SN upon aging and in RIPD rat model (objective 3) n=16.
iv. Studies of daily rhythms of various clock gene expression in SCN, Pineal and SN upon aging and in RIPD rat model (objective 4) n=16.

Group 1B (n=64): 2 m animals received sun flower oil intraperitonially (1ml/kg body weight) as vehicle once a day at ZT5 for 48 days (Alam and Schmidt, 2002). This group was further divided into four groups.

i. Characterization of rotenone induced Parkinson's disease (RIPD) rat model (objective1) n=6.
ii. Studies of chronomics of serotonin metabolism in SCN, Pineal and SN in RIPD rat model (objective 2) n=26.
iii. Studies of daily rhythms of protein profile in SCN, Pineal and SN upon aging and in RIPD rat model (objective 3) n=16.

iv. Studies of daily rhythms of various clock gene expression in SCN, Pineal and SN upon aging and in RIPD rat model (objective 4) n=16.

Group 2 (i) (n=16): 3 m animals received Melatonin (30 µg/Kg body weight) dissolved in 10% Ethanol in physiological saline subcutaneously once a day at ZT11 for 11 days (Jagota and Kalyani, 2010). This group is used for the study of effect of melatonin administration on daily rhythms of various clock gene expressions in SCN, Pineal and SN upon aging and in RIPD rat model (objective 5).

Group 2 (ii) (n=16): 3 m animals received 10% Ethanol in physiological saline as vehicle subcutaneously once a day at ZT11 for 11 days (Jagota and Kalyani, 2010). This group is used for objective 5. This group is used for the study of effect of melatonin administration on daily rhythms of various clock gene expressions in SCN, Pineal and SN upon aging and in RIPD rat model (objective 5).

Group 2 (iii) (n=32): This group consists of 3 m old animals. Among these 16 animals were used for the studies of daily rhythms of protein profile in SCN, Pineal and SN upon aging and in RIPD rat model (objective 3) and 16 animals were used for the studies of daily rhythms of various clock gene expressions in SCN, Pineal and SN upon aging and in RIPD rat model (objective 4).

Group 3 (i) (n=16): 12 m animals received Melatonin (30 µg/Kg body weight) dissolved in 10% Ethanol in physiological saline subcutaneously once a day at ZT11 for 11 days (Jagota and Kalyani, 2010). This group is used for the study of effect of melatonin administration on daily rhythms of various clock gene expressions in SCN, Pineal and SN upon aging and in RIPD rat model (objective 5).

Group 3 (ii) (n=16): 12 m animals received 10% Ethanol in physiological saline as vehicle subcutaneously once a day at ZT11 for 11 days (Jagota and Kalyani, 2010). This group is used for the study of effect of melatonin administration on daily rhythms of various clock gene expressions in SCN, Pineal and SN upon aging and in RIPD rat model (objective 5).

Group 3 (iii) (n=32): This group consists of 12 m old animals. Among these 16 animals were used for the studies of daily rhythms of protein profile in SCN, Pineal and SN upon aging and in RIPD rat model (objective 3) and 16 animals were used for the studies of daily rhythms of

various clock gene expression in SCN, Pineal and SN upon aging and in RIPD rat model (objective 4).

Group 4 (i) (n=16): 24 m animals received Melatonin (30 µg/Kg body weight) dissolved in 10% Ethanol in physiological saline subcutaneously once a day at ZT11 for 11 days (Jagota and Kalyani, 2010). This group is used for the study of effect of melatonin administration on daily rhythms of various clock gene expressions in SCN, Pineal and SN upon aging and in RIPD rat model (objective 5).

Group 4 (ii) (n=16): 24 m animals received 10% Ethanol in physiological saline as vehicle subcutaneously once a day at ZT11 for 11 days (Jagota and Kalyani, 2010). This group is used for the study of effect of melatonin administration on daily rhythms of various clock gene expressions in SCN, Pineal and SN upon aging and in RIPD rat model (objective 5).

Group 4 (iii) (n=32): This group consists of 24 m old animals. Among these 16 animals were used for the studies of daily rhythms of protein profile in SCN, Pineal and SN upon aging and in RIPD rat model (objective 3) and 16 animals were used for the studies of daily rhythms of various clock gene expression in SCN, Pineal and SN upon aging and in RIPD rat model (objective 4).

Group 5 (i) (n=16): 2 m animals received Rotenone intraperitonially (2.5 mg/ml/kg body weight) once a day at ZT5 for 48 days (Alam and Schmidt, 2002) and then Melatonin (30 µg/Kg body weight) dissolved in 10% Ethanol in physiological saline subcutaneously once a day at ZT11 for 11 days (Jagota and Kalyani, 2010). This group is used for the study of effect of melatonin administration on daily rhythms of various clock gene expressions in SCN, Pineal and SN upon aging and in RIPD rat model (objective 5).

Group 5 (ii) (n=16): 2 m animals received once a day Rotenone intraperitonially (2.5 mg/ml/kg body weight) at ZT5 and Melatonin subcutaneously at ZT11 (30 µg/Kg body weight) for 48 days.

This group is used for the study of effect of melatonin administration on daily rhythms of various clock gene expressions in SCN, Pineal and SN upon aging and in RIPD rat model (objective 5).

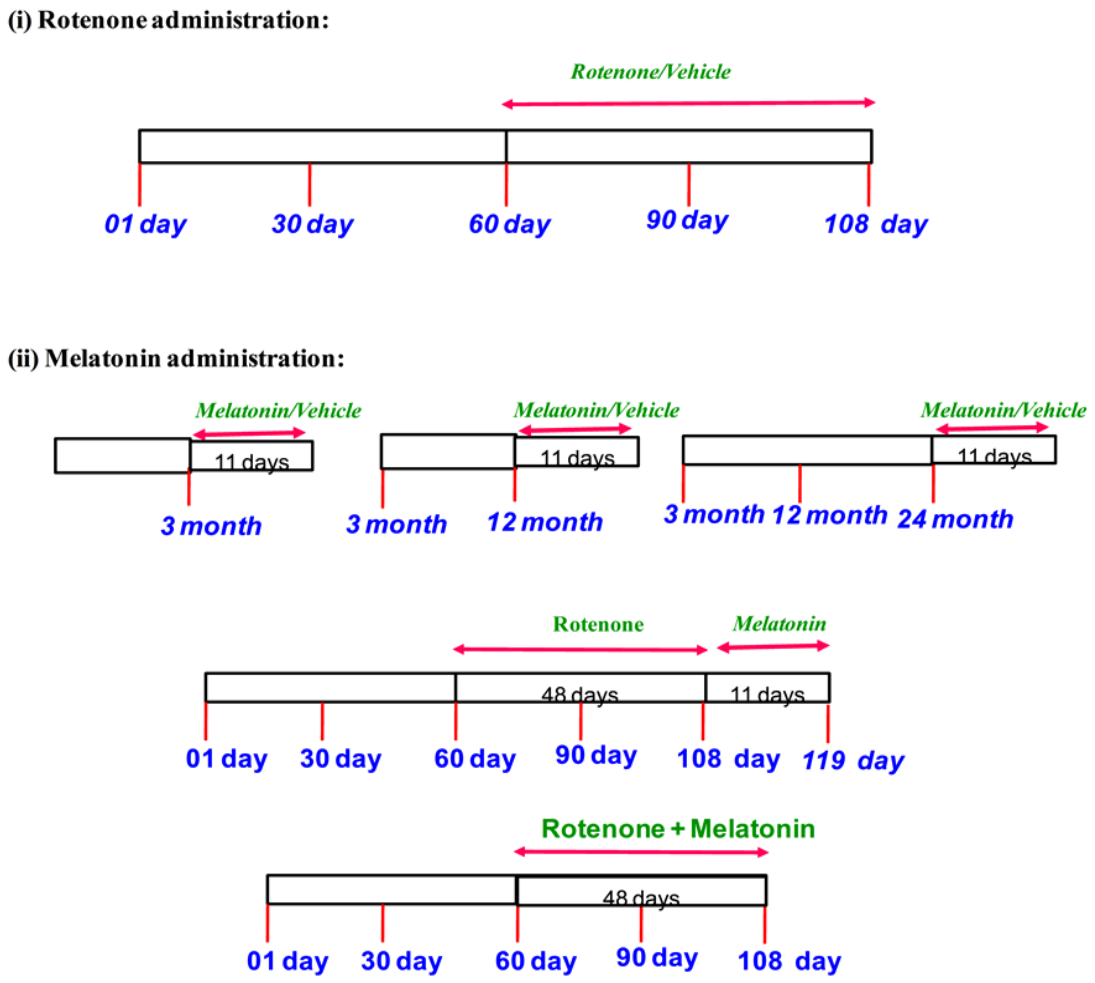

Fig. 28: Flow diagram showing plan of administration of (i) Rotenone and (ii) Melatonin.

SCN, Pineal and SN tissue preparation

Animals were sacrificed by decapitation and the brains were dissected out carefully at various time points such as Zeitgeber time (ZT) 0, ZT6, ZT12 and ZT18 for the studies of Chronomics of Serotonin metabolism in SCN, Pineal and SN in RIPD rat model (objective 2), studies of daily rhythms of various clock gene expressions in SCN, Pineal and SN upon aging and in RIPD rat model (objective 4) and effect of melatonin administration on daily rhythms of various clock gene expressions in SCN, Pineal and SN upon aging and in RIPD rat model (objective 5) and ZT6 and ZT18 for the studies of daily rhythms of protein profile in SCN, Pineal and SN upon aging and in RIPD rat model (objective 3). Pineal gland was separated. 500 μ brain slices were made using rat brain slicer (Zivic Instruments; Pittsburg USA) and the SCN was

carefully punched out with the help of a sharp scalpel (Jagota and Reddy, 2007). SN was removed according to Hefner *et al.*, 1980.

Tyrosine hydroxylase (TH) and α-synuclein assay

Protein estimation by Bradford's method:

Bovine serum albumin (BSA) was used as standard and standard graph was obtained by using a stock solution containing a concentration of 1 mg/ml, diluted to 10 folds prior to use with distilled water. 10 µl of sample was taken for assay and diluted to 100 µl with distilled water. 1ml of Bradford reagent was added to each sample and thoroughly mixed the contents by vortex mixture. The absorbance at 595 nm was measured after 2 minutes (min) and before 1 h against a reagent blank prepared from 0.1 ml of distilled water and 1 ml of Bradford reagent. The standard graph was prepared from 1µg to 10 µg. The protein concentration was estimated in sample by comparing the absorbance value with standard graph (Bradford, 1975).

Sample preparation:

After 48 days Rotenone treatment, Rotenone treated rat, Vehicle treated rat, control rat SN (7-10 mg) was separated and homogenized with 4 volumes of 50 mM Tris-HCl (pH 7.4) containing 1 mM EDTA and 0.1 mM PMSF. After centrifugation at 40,000 × g for 30 min, the supernatant was transferred to fresh tubes **(**Inden *et al.*, 2003). Protein concentration was estimated by Bradford's method.

Sodium dodecyl sulfate - Polyacrylamide gel electrophoresis (SDS-PAGE):

30 µg of protein from each sample was subjected to 12 % polyacrylamide gel in discontinuous gel and buffer system (Lamelli, 1970), i.e. 5% stacking gel (pH 6.8) and 12% resolving gel (pH 8.8). Prestained protein molecular mass markers were also loaded to assess the molecular weight of unknown protein band.

Western Blot of TH and α-Synuclein

Proteins from gel were transferred on nitrocellulose membrane by using towbin buffer (25mM Tris base, 250mM Glycine and 20 % methanol) for 8 h at 300 mA. Transfer was confirmed with the transfer of prestained protein molecular mass marker. After transferring the proteins from gel to nitrocellulose membrane, membrane was incubated for 30 min in blocking solution (5% non fat milk powder in Tris buffered saline (pH 7.4) containing 0.3 % Triton X (TBST)) at room temperature on shaker. Membrane was probed by incubating the membrane in

rabbit polyclonal antisera raised against TH or α-synuclein (1:1000 dilution, Santa Cruz Biotechnology, inc., Santa Cruz, CA). After washing five times (5 min each) in TBST, a further incubation with secondary antibody, goat anti-rabbit IgG, conjugated with Horse radish peroxidase (HRP) (1:2000 dilution, Santa Cruz Biotechnology, Inc.) were carried out. The membrane was washed further five times 5 min each in TBST. Then, the peroxidase reaction was developed by incubating membrane for 20 min in substrate solution containing 50 mg DAB in 100 ml of 50 mM phosphate buffer, pH 7.4, at room temperature (De Blas *et al*., 1983). The reaction was quenched by washing the membrane with water. Probing of β-tubulin was done as loading control. Densitometry analysis was performed by using Image J software. The α-synuclein, TH and β-tubulin were identified using the standard protein markers (Betarbet *et al*., 2000).

Immunohistochemistry (IHC) of TH

Sample preparation:

Animals were anesthetized and transcardial perfusion was performed with heparinized 0.9% saline followed by 4% paraformaldehyde in 0.1 M phosphate buffer (PB) (pH 7.4). The brains were rapidly removed and post-fixed in 4% paraformaldehyde 0.1 M PB (pH 7.4) for 2-4 hours and then stored in 20% sucrose in 0.1 M PB (pH 7.4) at 4°C for 24 h. 20 µ thick coronal sections of the brain were cut using Leica cryostat (CM 1850) and processed for IHC (Mammen and Jagota, 2011).

IHC:

Tyrosine hydroxylase-ir studies were performed with rabbit primary antisera generated against Tyrosine hydroxylase (sc-14007, Santa Cruz Biotechnology, Inc., Santa Cruz, CA) and detected using respective secondary antibodies, Goat anti-rabbit IgG-HRP (Bangalore Genei, India). After pre incubation at 25°C for 1-2 h with 1 % solution of normal goat serum in 0.01 M phosphate-buffered saline (pH 7.4) containing 0.3 % Triton X (PBS-T), sections were washed with PBS-T and incubated separately at 37°C for 1-2 h with primary antisera in PBS-T anti tyrosine hydroxylase (dilution 1:250) in blocking serum. The sections were then placed in the secondary antibody (dilution 1:250) for 1-2 h at 37°C and were subjected to 0.1% 3, 3-diaminobenzidine (DAB) containing 0.3 % H_2O_2 and incubated till color developed. Reaction

was stopped with water. All sections were photographed using DP-12 digital camera attached to Olympus microscope (BX-41) (Mammen and Jagota, 2011).

Measurement of various components of serotonin metabolism by reverse phase high performance liquid chromatography using electrochemical detector (RP HPLC-EC)

TRP, 5-HTP, 5-HT, 5-HIAA, NAS, MEL, 5-MIAA, 5-MTOH, 5-HTOH and NAT levels were assayed by using RP HPLC- EC method (Jagota and Reddy, 2007; Reddy, 2010).

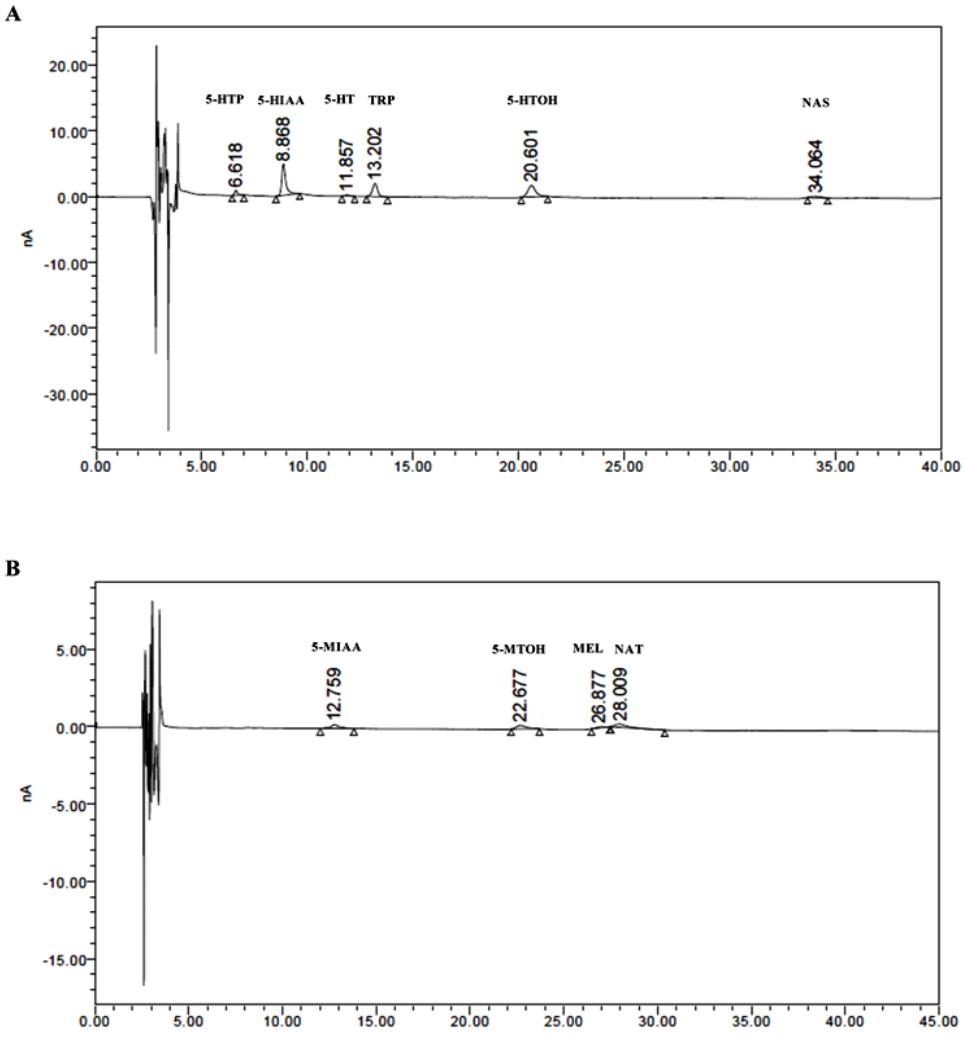

Fig. 29: Standard representative peaks of HPLC for Serotonin and its related compounds. (A) 10 % methanol; 0.1N sodium acetate; 0.1N citric acid, 50 mg/L EDTA was used for detection of compounds- 5-HTP, 5-HT, 5-HIAA, NAS, TRP and 5-HTOH. (B) 25 % methanol; 0.1N Sodium acetate; 0.1N citric acid, 50 mg/L EDTA was used for detection of compounds- 5-MIAA, 5-MTOH, MEL and NAT. nA refers to nano ampere (Unit of strength of electric current).

Standards:

Using known concentration (0.25ng-80ng) of TRP, 5-HTP, 5-HT, 5-HIAA, NAS, MEL, 5-MIAA, 5-MTOH, 5-HTOH and NAT dissolved in 0.1N perchloric acid standard graphs were prepared and linearity was established.

Sample preparation: Tissue sample was homogenized with 100 µl of 0.1N Perchloric acid (Qualigens) containing sodium bisulfate (1mM) (Sd-fine Chemicals). After homogenization the tissue sample was sonicated for approximately 5 seconds. The centrifugation was done at 12,800 x g for 10 min to remove tissue debris. The supernatant was filtered through 0.22 µm syringe filters (MDI membrane technologies).

HPLC analysis: 50 µl of filtered supernatant was applied to the chromatography system by using Eluant A (10 % methanol; 0.1M citric acid; 0.1M sodium acetate, 50 mg/L EDTA (pH-4.1)) to estimate TRP, 5-HTP, 5-HT, 5-HTOH, 5-HIAA and NAS and 50 µl by using Eluant B (25 % methanol ; 0.1 M citric acid , 0.1 M sodium acetate ; 50 mg/L EDTA; pH - 4.1) to estimate MEL, 5-MTOH, 5-MIAA and NAT.

Estimation: The amount of each compound in a sample was estimated by comparing the peak area to standard peak area generated by analyzing the known amounts of standard compounds (Fig. 29).

Gene expression studies by quantitative real time Polymerase Chain Reaction (qRT-PCR)

RNA extraction:

For 2-10 mg of SCN/ Pineal/ SN tissue, 250 µl of TRI reagent was added (Sigma) and homogenized. Samples were incubated for 5 min at room temperature. Then 0.1 ml of chloroform for each sample was added. Again incubated at room temperature for 5 min and then centrifuged for 15 min at 12,000 x g at 4˚C. Upper aqueous layer is transferred to a fresh tube and 125 µl of isopropyl alcohol was added to precipitate RNA. Mixed well and incubated at RT for 5 min. Centrifuged for 10 min at 12,000 x g at 4˚C. RNA was precipitated. Supernatant was discarded and RNA pellet was washed with 250µl of 75% ethanol. Mixed and centrifuged at 12,000 x g for 5 min at 4˚C. Washing was done for two times and RNA pellet was stored at -70˚C. Isolated RNA was then dissolved in 20 µl diethylpyrocarbonate (DEPC)-treated water for 5-10 min at 37˚C. The amount of extracted RNA was quantified by measuring the optical density

(OD) at 260 and 280 nm with Nano drop spectrophotometer (ThermoFischer) **(**Chomczynski and Sacchi, 2006).

Synthesis of cDNA:

The basic protocol involves the catalytic conversion of an RNA template to a single stranded cDNA by murine moloney leukemia virus (M-MLV) reverse transcriptase in the presence of primers approximately 1 mg/ml and dNTP's (each 5mM). A combination of oligo dT and random hexamers have been used for priming the RNA template. Extracted RNA (2 µg) was used for cDNA synthesis using Bio-Rad iScript cDNA synthesis kit in a total volume of 20 µl, containing 4 µl 5x iScript reaction mix , 1 µl iScript reverse transcriptase and final volume is obtained by adding RNase free water. The reverse transcription mixture was incubated: 5min at 25 °C, 30 min at 42°C and 5 min at 85°C. Assuming the 100 % reverse transcription, input RNA (2 µg) is equal to amount of cDNA synthesized. The cDNA was then diluted to 1:20 in RNase free water, and aliquots of 8 µl were used for the further analysis (Willem *et al.,* 2005).

Quantitative reverse transcriptase PCR (qRT-PCR):

Expression of clock genes *Per1, Per2, Cry1, Cry2* and *Bmal1* were analyzed by relative qRT-PCR by the SYBR Green detection method. 40ng of cDNA from each sample was used for qRT-PCR analysis. Successful reverse transcription was confirmed for all samples by performing PCR amplification of the internal control β-*actin*. Real-time specific primers for the entire clock genes studied as well as for internal control β-*actin* were selected as per Willem *et al*., 2005.

Primer sequence for *β-actin*: Forward- AGCCATGTACGTAGCCATCC
Reverse- CTCTCAGCTGTGGTGGTGAA

Per1: Forward- TCTGGTTCGGGATCCACGAA
Reverse- GAAGAGTCGATGCTGCCAAAG

Per2: Forward- CACCCTGAAAAGAAAGTGCGA
Reverse- CAACGCCAAGGAGCTCAAGT

Cry1: Forward- AAGTCATCGTGCGCATTTCA
Reverse- TCATCATGGTCGTCGGACAGA

Cry2: Forward- GGATAAGCACTTGGAACGGAA
Reverse- ACAAGTCCCACAGGCGGT

Bmal1: Forward- CCGATGACGAACTGAAACACCT
Reverse- TGCAGTGTCCGAGGAAGATAGC

PCR amplification was carried out using 2X power SYBR Green mastermix (Applied Biosystems) in the ABI-7500 real time PCR machine (Applied Biosystems). The PCR reaction setup includes 10 µl of 2X Power SYBR green PCR master mix (Applied Biosystems), 2 µl of 10 *p* mol primers, and 8 µl (40 ng) of cDNA in a total reaction volume of 20 µl.

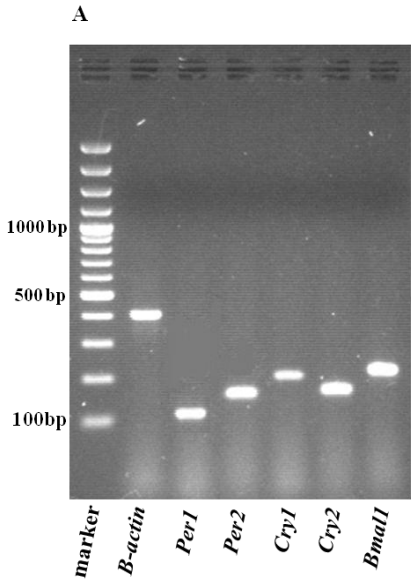

Size of the amplified product

β-actin	**400 bp**
Per1	**101 bp**
Per2	**148 bp**
Cry1	**196 bp**
Cry2	**155 bp**
Bmal1	**215 bp**

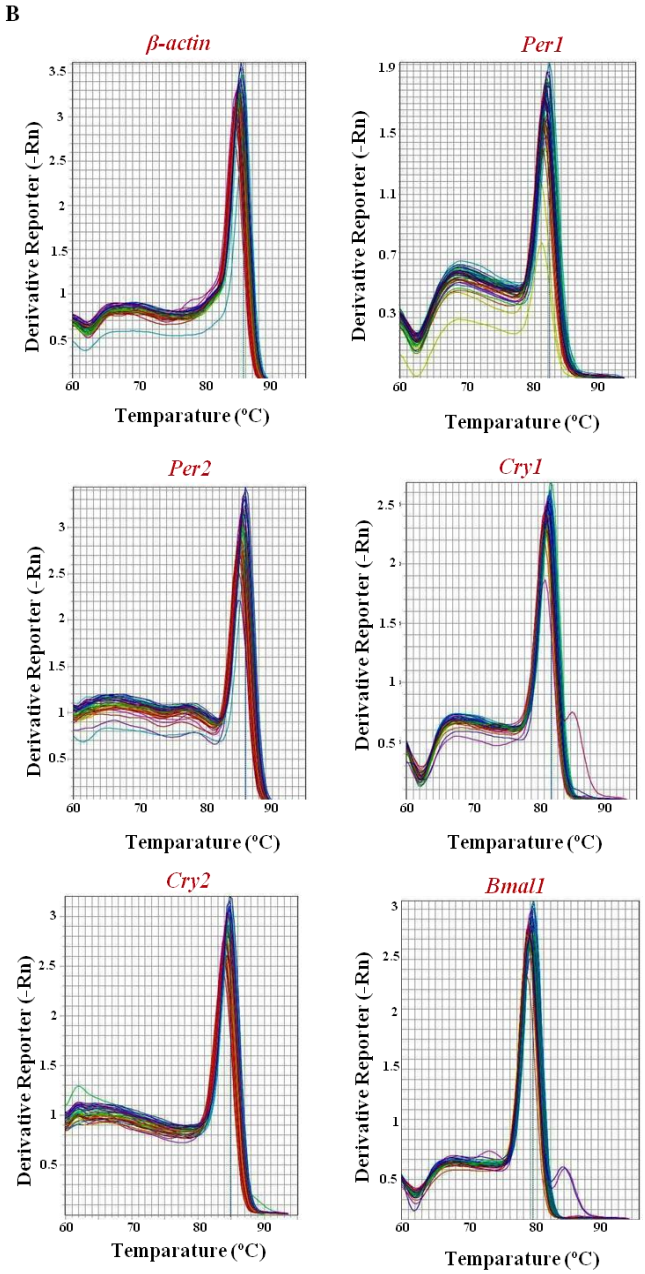

Fig. 30: (A) Agarose gel electrophoresis of PCR generated amplicons of various clock genes generated after 40 amplification cycle length of the PCR products in rat SCN. (B) Representative dissociation curves for *β-actin, Per1, Per2, Cry1, Cry2* and *Bmal1*genes.

The PCR conditions were as follows: denaturation for 3 min at 95°C, followed by 40 cycles of 30 seconds at 95°C, 20 seconds at 60°C, and 20 seconds at 72°C. All amplifications were carried out in duplicate. Dissociation curves showed a single amplified product and the absence of primer-dimer formation (Fig. 30). Cycle threshold (Ct) values were obtained from the exponential phase of PCR amplification. Comparative Ct method was used to analyze and the results were expressed as relative gene expression (Livak and Schmittgen, 2001).

Proteomic studies by 2-Dimensional electrophoresis

Preparation of protein samples for 2-Dimensional Electrophoresis:

20% homogenate of SCN, Pineal and SN is prepared with lysis buffer (7M Urea, 2M Thiourea, 2% CHAPS, 2% Ampholines, 20 mM DTT and 1mM PMSF). SCN and Pineal samples were prepared by pooling the tissues from four male wistar rats for each sample. Average weight of each SCN and Pineal was approximately 1 - 2 mg, SN was approximately 7-10 mg. Cells were disrupted by sonication for 2 min (45% amplitude, pulse on for 20 seconds and pulse off for 20 seconds) and centrifuged at 10,000 rpm for 5 min at 4°C. Clear supernatant is transferred to fresh tubes. 750 µl of Ice cold acetone was added to clear supernatant to precipitate proteins and kept at -20°C for 24 h. Acetone precipitated samples were dissolved in rehydration buffer (7M Urea, 2M Thiourea, 2% CHAPS, 2% Ampholines, 20 mM DTT).

Protein estimation by Amido Black method:

Amido Black method instead of bradford's method was used for estimating protein from tissue samples dissolved in rehydration buffer (7M Urea, 2M Thiourea, 2% CHAPS, 2% Ampholines, 20 mM DTT) due to presence of thiourea in the rehydration buffer which could react with Bradford's reagent (Bradford, 1975) giving false positive results. Standard graph for Bovine serum albumin (BSA) was obtained by using a stock solution containing a concentration of 1 mg BSA/ml of rehydration buffer, diluted with the same rehydration buffer to 10 folds prior to use. 2 µl of sample was taken for assay and spotted on nitrocellulose membrane and allowed to dry. Incubated the membrane in Amido Black solution (AB 50 mg; commercial name: Naphthol Blue Black 8 for electrophoresis; Acetic acid 5 ml; Methanol 22.5 ml; Water 22.5 ml; which was kept stirring overnight and used after 24 h) for 15 min. Destain the membrane with destaining solution (Methanol - 90%; Acetic acid - 2%) for 20 min and then allow the membrane to dry. Cut the blue color stained spots and place them in polypropylene tube and add 1 ml of

elution buffer (100% Ethanol – 25 ml; 25 µl - 10N NaOH; 4 ml- 250 mM EDTA). After adding elution buffer incubate the tubes at 40°C for 40 min and then measure OD at 630 nm with elution buffer as blank. The standard graph was prepared from 1 to 10 µg of BSA dissolved in rehydration buffer. The protein concentration was estimated in sample by comparing the absorbance value with standard graph (Schaffner and Weissmann, 1973).

2-Dimentional gel electrophoresis:

500µg of protein was loaded on each Iso Electro Focusing (IEF) strip (18 cm strip, pH 3-10 NL; GE Healthcare) and subjected to IEF for 60,000 V hours. Then the following program has been set.

The IEF was programmed as follows:

1. Step	500 V	for 1 h
2. Gradient	1000 V	for 6 h
3. Gradient	8000 V	for 4 h
4. Step	8000 V	for 2 h
5. Gradient	10000 V	for 5 h
6. Step	10000 V	for 60,000 V h
7. Step	500 V	(hold step to safeguard strip)

After IEF strips were equilibrated in 25 mM DTT and 50 mM Iodoacetamide. Strips were placed on the 12 % SDS PAGE gels and covered with 1% agarose dissolved in 0.1% bromophenol blue made in 1x SDS running buffer and subjected to electrophoresis.

Silver Staining Protocol:

After SDS-PAGE gels were kept in 300 ml of fixing solution (50% Methanol, 12% acetic acid, 0.0185% formaldehyde) for 8 h and then washed for 3 times 20 min each with 100 ml of 35% ethanol. Pretreatment was done for the gels for 2 min with 200 ml of 0.02% Sodium thoisulphate and then washed for 2 times 3 min each with 100 ml of distilled water. Gels were kept in 200 ml of silver nitrate solution (0.2% silver nitrate, 0.028% formaldehyde) for 20 min and then washed for 2 times 20 seconds each with 100 ml of distilled water. Staining was developed by treating the gels with 200 ml of developing solution (6% Sodium Carbonate, 0.0185% formaldehyde, 0.0004% Sodium thiosulphate) for 3 min and stopped the reaction with

200 ml of stopping solution (50% methanol, 12% acetic acid). After staining gels were preserved in 200 ml of 3% acetic acid solution at 4°C (Mortz *et al.*, 2001).

Analysis of 2-D gels and statistics:

Gels were scanned on high resolution scanner and saved as TIFF-files and transferred to the Image Master 2D Platinum software version 7 (GE Healthcare) on which the analysis was performed. All the gels (n=2) were matched and same spots on duplicate gels assigned the same match identity number (id). Spots were quantified and the volume percentage was obtained for all spots. Changes in expression between ZT6 and ZT18 were considered significant at *p* values less than 0.05 (ANOVA) given by software.

Data analysis

Statistical analysis: Data was analyzed using Jandel Scientific Sigma stat software by one way ANOVA followed by Post hoc Dunkan's test for multiple comparisons of all parameters determined at variable time points within an age group. Correlation analysis was done between various parameters using pair wise correlation (Manikonda and Jagota, 2012).

Results

OBJECTIVE - I

1. Characterization of rotenone induced Parkinson's disease (RIPD) rat model

Weight loss was observed in Rotenone treated (RT) rats as compared to Vehicle treated animals (Fig. 31 and 32).

Fig. 31: Representative picture of vehicle and rotenone treated rats.

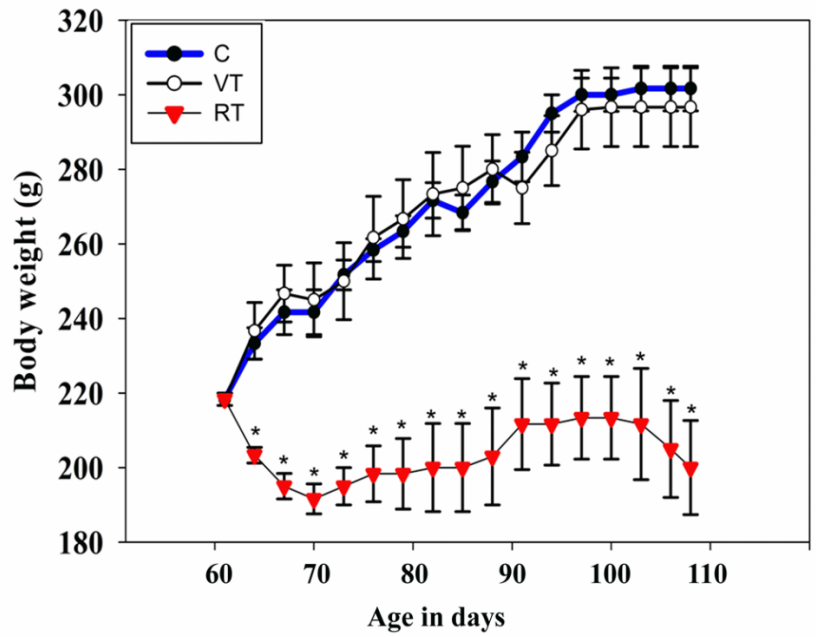

Fig. 32: Each value is mean ± SEM (n=10), $p \leq 0.05$ C - control, VT - Vehicle treated and RT - Rotenone treated. * refers to comparison between VT and RT.

In RT rats there was decrease in TH-immunoreactivity and increase in α-Synuclein-immunoreactivity when compared to vehicle treated and control (Fig. 33) which suggests PD like pathology in RT rats. Thus RIPD model (Alam and Schmidt, 2002) was successfully established in our laboratory.

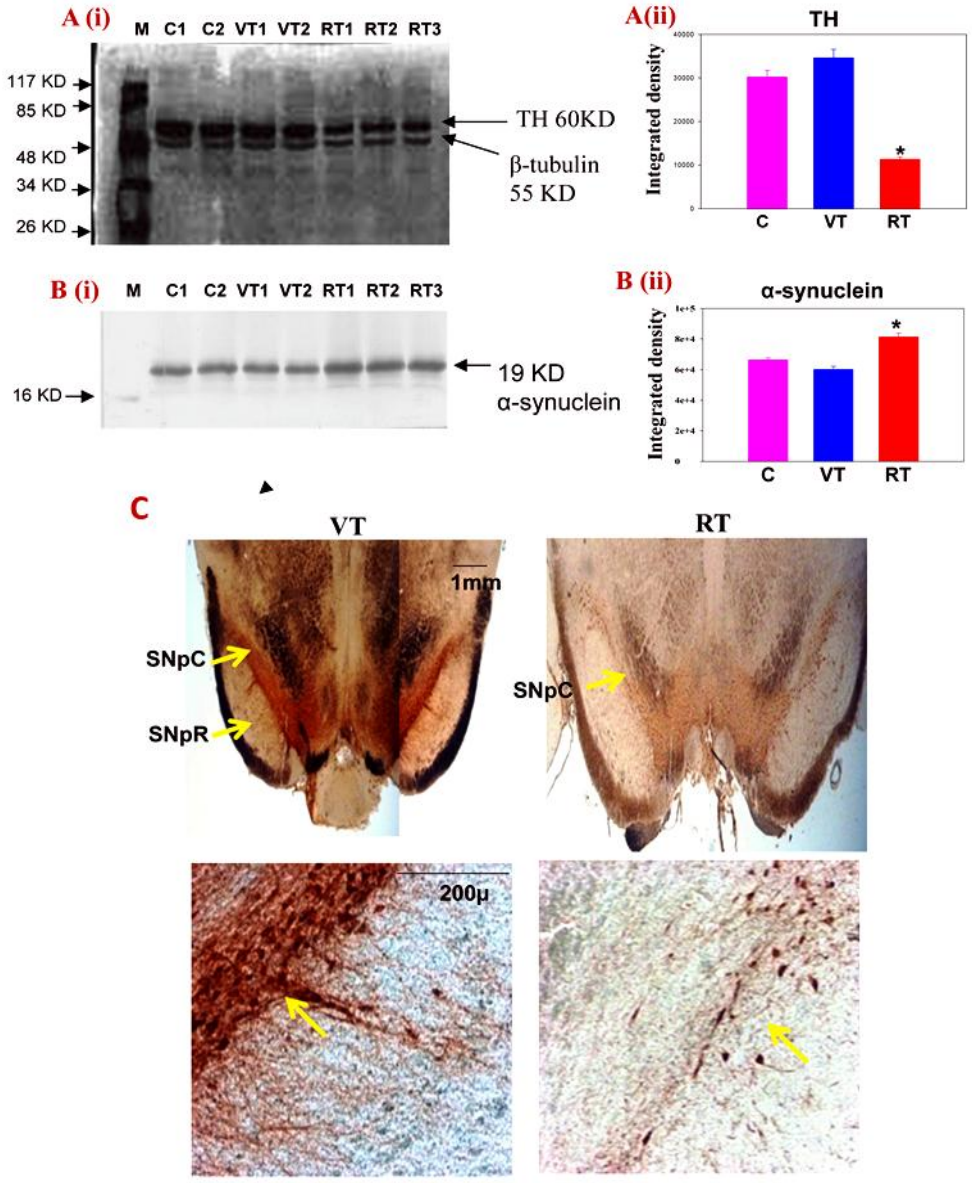

Fig. 33: Tyrosin hydroxylase (TH) and α- Synuclein immunoreactivity in Rat Substantia nigra (SN). A. (i and ii) TH immunoblot and densitometry analysis. B. (i and ii) α- Synuclein immunoblot and densitometry analysis. C. TH-immunoreactivity (TH-ir) in coronal SN brain sections of VT and RT. M- Molecular weight marker, C-Control, VT- Vehicle treated, RT-Rotenone treated, SNpC- Substantia nigra pars compacta, SNpR- Substantia nigra pars reticulata. Data were expressed as mean ± SE. $P \leq 0.05$. * refers to comparison between VT and RT.

OBJECTIVE – II

2. Studies of Chronomics of Serotonin metabolism in SCN, Pineal and SN in RIPD rat model

(a) Chronomics of Serotonin metabolism in the SCN of RIPD model:

No significant difference was found between the control and the vehicle control.
Daily rhythms were observed in 5-HT, 5-HIAA, NAS, MEL, TRP, 5-HTP, 5-MTOH, 5-HTOH, 5-MIAA and NAT levels (Fig. 34 and 35; Table 2; $p \leq 0.05$).

Pattern and daily rhythm of TRP were not altered in RIPD model compared to vehicle group and the levels at ZT0, 6, 12 and 18 were 0.09 ± 0.01, 1.05 ± 0.06, 0.076 ± 0.02 and 0.048 ± 0.011 µmol/g protein. TRP daily pulse was increased by 2.35 fold and mean level was decreased by 0.35 fold in RIPD model. Abolished daily rhythm was observed in case of MEL, 5-HTP and 5-MIAA in RIPD model. Daily pulse and mean levels of MEL were decreased by 0.04 and 0.25 fold respectively in RIPD model. 5-HTP daily pulse and mean levels were decreased by 0.68 and 0.48 folds respectively in RIPD model. Daily rhythm and pattern of 5-HT persisted in RIPD model and the levels were 1.72 ± 0.09, 3.15 ± 0.16, 0.38 ± 0.05 and 0.18 ± 0.12 µmol/g protein compared to vehicle. 5-HT daily pulse was increased by 8.14 fold and mean level was decreased by 0.35 fold in RIPD model compared to vehicle. In RIPD model 5-HIAA daily rhythm persisted with approximately 6h phase delay and levels were 22.78 ± 2.15, 7.85 ± 0.34, 9.16 ± 1.62 and 11.62 ± 1.78 µmol/g protein. 5-HIAA daily pulse was decreased by 0.63 fold in RIPD model; however mean 24 h levels were not altered. Persistence of daily rhythm with approximately 6h phase advance was observed in case of NAS in RIPD model and the levels were 0.52 ± 0.07, 3.37 ± 0.10, 0.30 ± 0.03 and 0.17 ± 0.04 µmol/g protein. NAS mean level was decreased by 0.23 fold and daily pulse was increased by 3.39 fold in RIPD model. Approximately 12 h of phase advance with persistence of daily rhythm was observed in case of 5-HTOH in RIPD model and the levels were 0.77 ± 0.09, 0.08 ± 0.01, 0.47 ± 0.06 and 0.38 ± 0.06 µmol/g protein. Daily pulse was decreased by 0.56 fold and mean level was increased by 2.7 fold in RIPD model where as in case of 5-MTOH approximately 12 h phase delay was observed in RIPD model and the levels were 0.015 ± 0.002, 0.004 ± 0.0004, 0.02 ± 0.002 and

0.02 ± 0.006 µmol/g protein. Increase in daily pulse and mean levels by 2.46 and 1.73 fold respectively was observed in RIPD model compared to vehicle. Daily rhythm and pattern of NAT in RIPD model persisted and the levels were 0.015 ± 0.002, 0.003 ± 0.0003, 0.008 ± 0.001 and 0.01 ± 0.001 µmol/g protein with increase in daily pulse and mean levels by 3 and 2.1 fold respectively compared to vehicle (Fig. 34, 35 and 36; Table 2; $p \leq 0.05$).

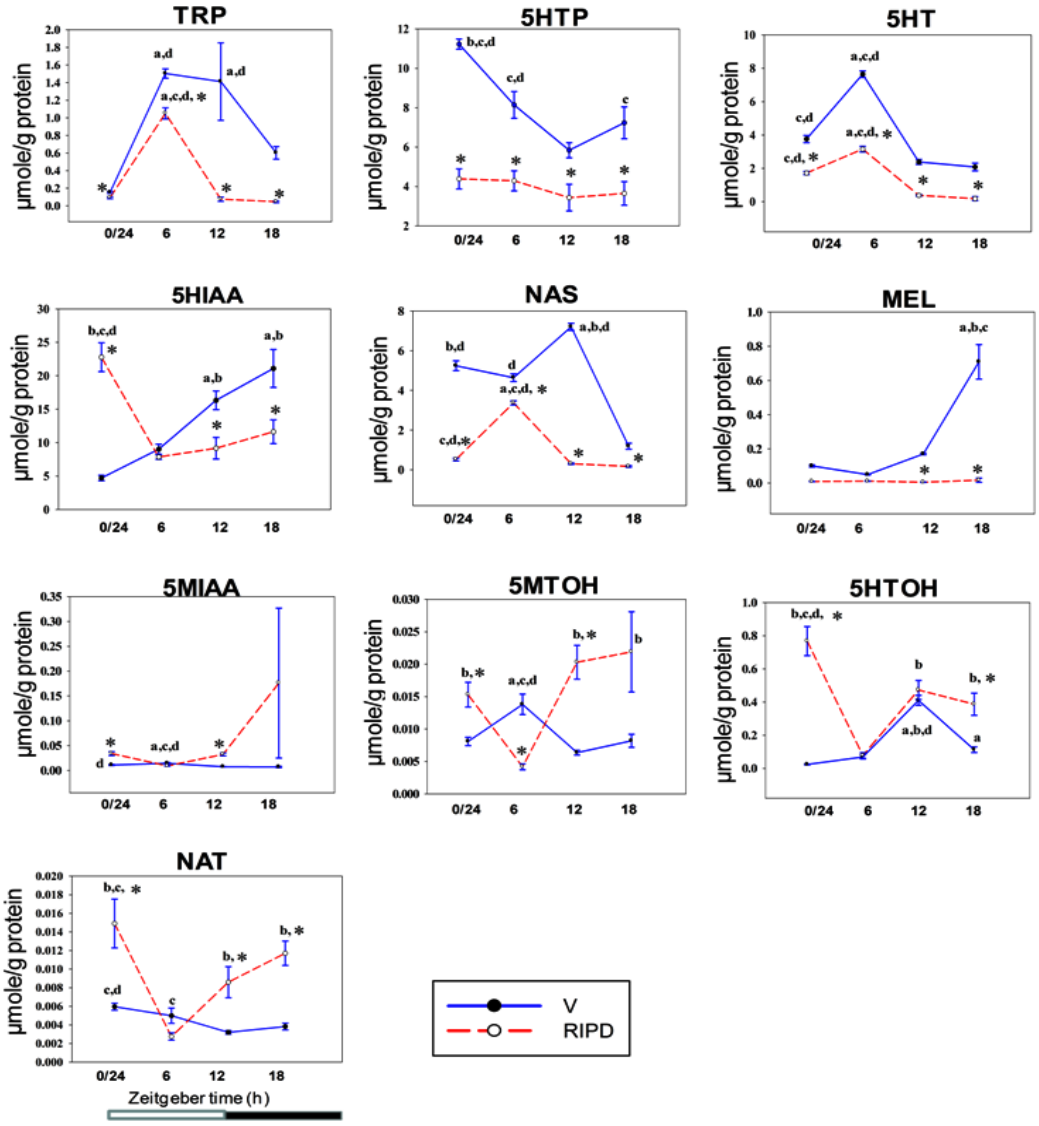

Fig. 34: Rhythmic alterations in the serotonin metabolism in the SCN of Rotenone induced Parkinson's disease (RIPD) rat model. Each value is mean ± SEM (n=6), p ≤ 0.05 and expressed in µmol/g protein. V - Vehicle. $p_a \leq 0.05$; $p_b \leq 0.05$, $p_c \leq 0.05$ and $p_d \leq 0.05$ (where a, b, c and d refers to comparison with ZT0, ZT6, ZT12 and ZT18 respectively within the group). * refers to comparison of levels at same time point in vehicle group.

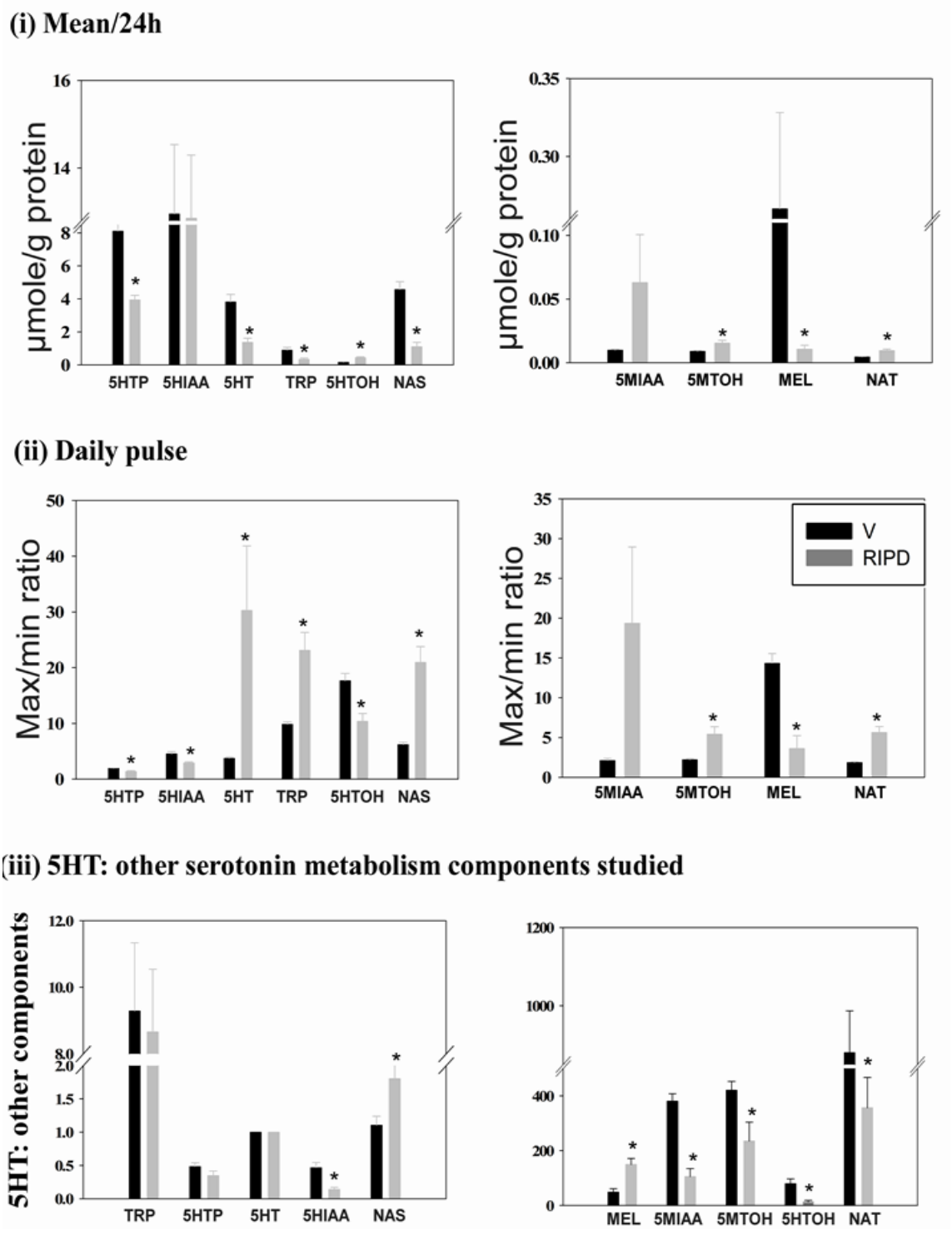

Fig. 35: Various parameters studied in serotonin metabolism components. (i) Mean 24h levels, (ii) Daily Pulse i.e. ratio between maximum and minimum and (iii) Ratio between 5-HT and other Serotonin metabolism components studied in SCN of Vehicle (V) and Rotenone induced PD rat model (RIPD). Each value is mean ± SEM; $p_* \leq 0.05$ (where * refers to comparison with vehicle group.

In RIPD model, ratio of 5-HT-5-HIAA; 5-HT-5-MIAA; 5-HT-5-MTOH; 5-HT-5-HTOH; 5-HT-NAT has been decreased and ratio between 5-HT-NAS; 5-HT-MEL has been increased compared to vehicle group (Fig. 35; Table 2; $p \leq 0.05$).

Pair wise correlation (Fig. 37) revealed vehicle group light phase positive correlation between 5-HT-5-MTOH and negative correlation between 5-HT-NAS; 5-HT-5-HTOH; 5-HT-MEL is absent in dark phase. There was no correlation between 5-HT-5-HTP; 5-HT-5-MIAA; 5-HT-NAT in the light phase whereas positive correlation between 5-HT-5-HTP; 5-HT-5-MIAA; 5-HT-NAT was observed in dark phase. In RIPD model there was no correlation between 5-HT-5-HIAA; 5-HT-NAT in light phase whereas this metabolites has shown positive correlation in dark phase and the negative correlation between 5-HT-5-HTOH in light phase has become positive in dark phase. The correlation observed between 5-HT-TRP; 5-HT-5-MIAA; 5-HT-5-MTOH; 5-HT-MEL in light phase is absent in dark phase (Fig. 37; $p \leq 0.05$).

In light phase there was no correlation between 5-HT-TRP; 5-HT-5-MIAA in vehicle group whereas in RIPD model we have observed positive and negative correlation between 5-HT-TRP; 5HT-5-MIAA respectively. Light phase vehicle group positive correlation between 5-HT-5-MTOH has become negative in RIPD model and vehicle group negative correlation between 5-HT-NAS; 5-HT-MEL has become positive in RIPD model. In dark phase there was no correlation between 5-HT-NAS; 5-HT-5-HTOH in vehicle group whereas in RIPD model we have observed positive correlation between 5-HTNAS; 5-HT-5-HTOH. Dark phase vehicle group positive correlation between 5-HT-5-HTP; 5-HT-5-MIAA has lost in RIPD model and vehicle group negative correlation between 5-HT-5-HIAA has become positive in RIPD model (Fig. 37; $p \leq 0.05$).

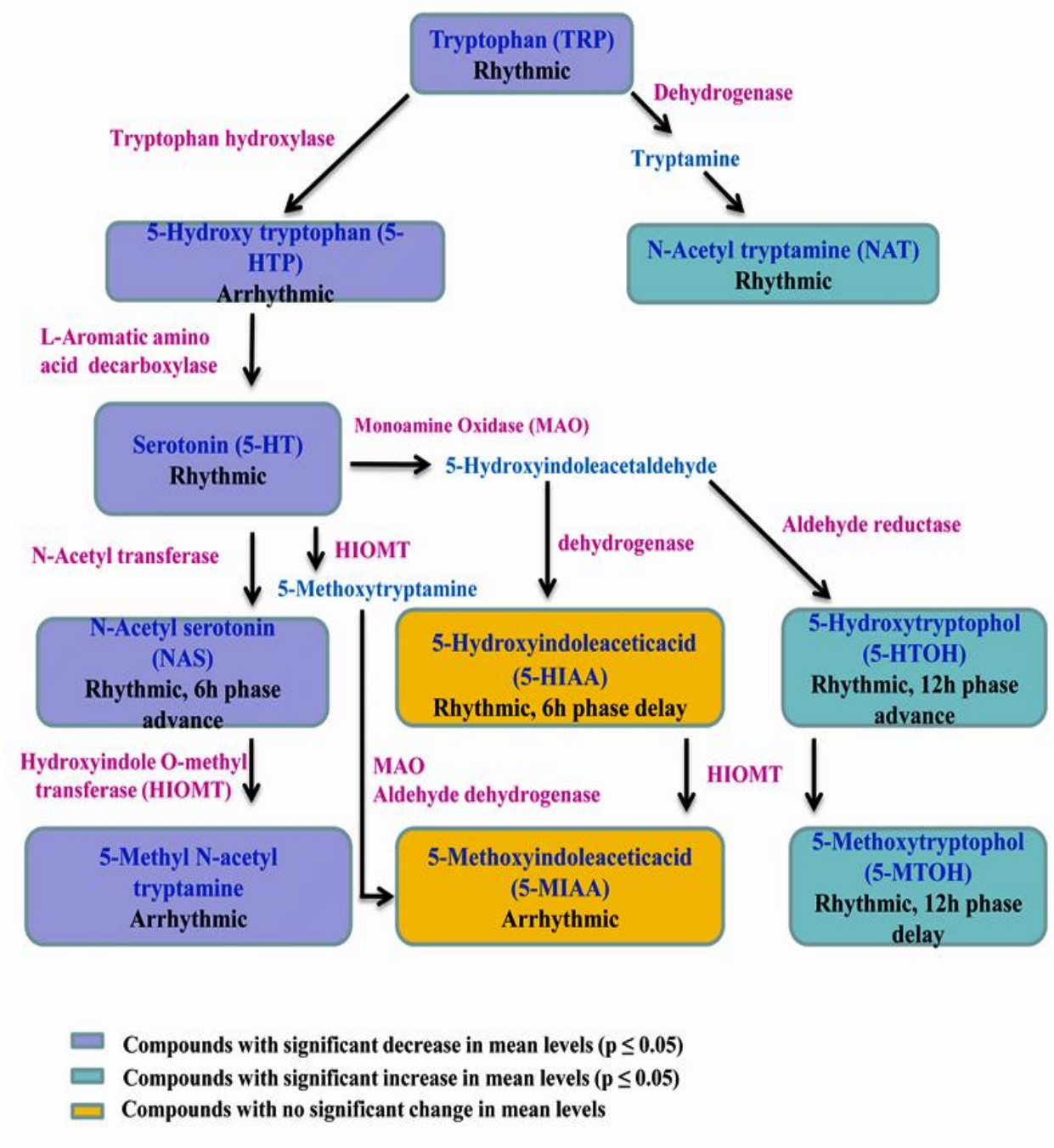

Fig. 36: Diagrammatic representation of mean 24 h alterations in the serotonin metabolism in the SCN of Rotenone induced Parkinson's disease (RIPD) rat model compared to vehicle.

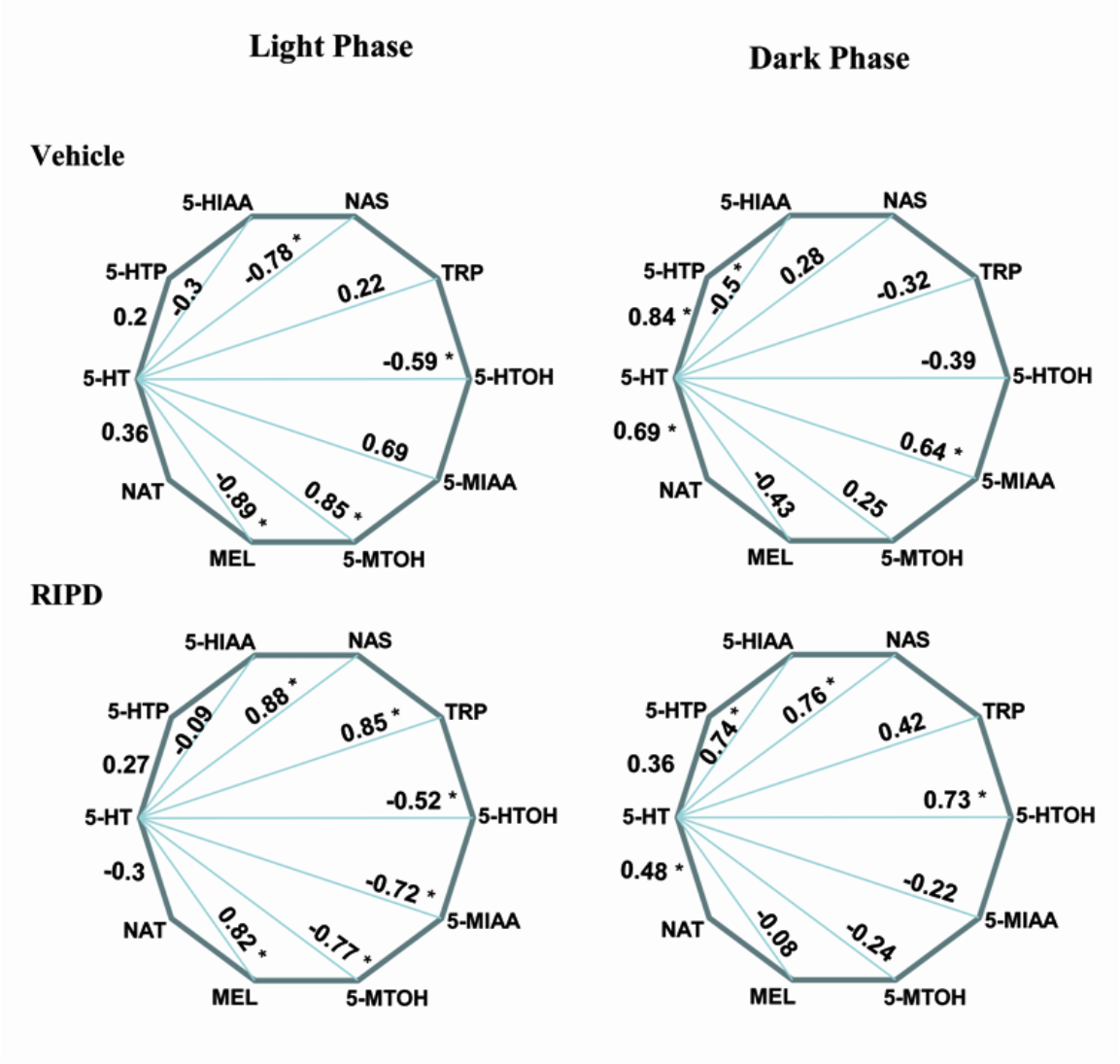

Fig. 37: Pair wise correlation between mean light (ZT 0, 6 and 12) and mean dark (ZT 12, 18 and 24/0) phase values of various components of serotonin metabolism in the SCN of vehicle (V) and Rotenone induced Parkinson's disease (RIPD) rat model. Each value is correlation coefficient between the parameters. * indicates statistically significant value between parameters ($p \leq 0.05$). Negative value indicates negative correlation between parameters.

Table 2: Rhythmic alterations in the serotonin metabolism in the SCN of Rotenone induced Parkinson's disease (RIPD) rat model.

Metabolite	Experimental Group	Maximum *	Minimum *	Ratio *	Mean** (24 h)	5HT: other components of Serotonin metabolism studied ***
TRP	V	1.50 ± 0.05	0.15 ± 0.01 ^{q}	9.83 ± 0.44	0.89± 0.16	9.28 ± 2.05
	RIPD	1.05 ± 0.06 ^{p}	0.04 ± 0.01 $^{p, q}$	23.09 ± 3.21 ^{p}	0.33 ± 0.09 ^{p}	8.65 ± 1.89
5-HTP	V	11.23 ± 0.26	5.84 ± 0.38 ^{q}	1.93± 0.078	8.11± 0.50	0.48± 0.06
	RIPD	4.39± 0.51 ^{p}	3.43± 0.67 ^{p}	1.33± 0.17 ^{p}	3.94± 0.28 ^{p}	0.35± 0.07
5-HT	V	7.64± 0.19	2.08± 0.23 ^{q}	3.71± 0.24	3.81±0.46	1
	RIPD	3.15± 0.16 ^{p}	0.18± 0.12 $^{p, q}$	30.25± 11.59 ^{p}	1.36± 0.25 ^{p}	1
5-HIAA	V	21.1± 2.83	4.71± 0.40 ^{q}	4.51± 0.41	12.95± 1.58	0.46± 0.078
	RIPD	22.78± 2.15	7.85± 0.34 $^{p, q}$	2.88± 0.19 ^{p}	12.85± 1.44	0.13± 0.03 ^{p}
NAS	V	7.20± 0.18	1.18± 0.15 ^{q}	6.17± 0.45	4.56± 0.48	1.10± 0.13
	RIPD	3.37± 0.10 ^{p}	0.17± 0.04 $^{p, q}$	20.94± 2.84 ^{p}	1.09± 0.28 ^{p}	1.80± 0.29 ^{p}
MEL	V	0.71± 0.10	0.05± 0.002^{q}	14.32± 1.23	0.26± 0.06	48.16± 12.47
	RIPD	0.017± 0.01 ^{p}	0.004± 0.001 ^{p}	3.61± 1.63 ^{p}	0.01± 0.003 ^{p}	149.29 ± 22 ^{p}
5-MIAA	V	0.01± 0.001	0.007± 0.001 ^{q}	2.11± 0.26	0.009± 0.0008	380.48 ± 26.66
	RIPD	0.17± 0.15	0.009± 0.0002	19.36± 9.59	0.06± 0.04	104.97± 29.54 ^{p}
5-MTOH	V	0.01± 0.001	0.006± 0.0003 ^{q}	2.2± 0.16	0.008± 0.0007	420.03 ± 32.42
	RIPD	0.02± 0.006	0.004± 0.0004 $^{p, q}$	5.40± 0.95 ^{p}	0.01± 0.002 ^{p}	235.04 ± 69.22 ^{p}
5-HTOH	V	0.41± 0.03	0.02± 0.002 ^{q}	17.64± 1.31	0.16± 0.03	79.56± 17.37
	RIPD	0.77± 0.09 ^{p}	0.08± 0.01 $^{p, q}$	10.34± 1.43 ^{p}	0.42± 0.06 ^{p}	13.21± 4.79 ^{p}
NAT	V	0.005± 0.0003	0.003± 0.0001 ^{q}	1.85± 0.09	0.004± 0.0003	879.89 ± 107.83
	RIPD	0.01± 0.002 ^{p}	0.002± 0.0003^{q}	5.63± 0.74 ^{p}	0.009± 0.001 ^{p}	356.82 ± 111.14 ^{p}

* Each value is mean ± S.E. (n=6); **each value is mean ± S.E., n=24, ***each value is mean ± SE of mean 24h ratio of 5HT with respective metabolites for Vehicle group (V) and Rotenone induced PD group (RIPD); $p \leq 0.05$; p refers to comparison between V and RIPD; q refers to comparison between maximum and minimum.

(b) Chronomics of Serotonin metabolism in the Pineal of RIPD model:

No significant difference was found between the control and the vehicle control. Daily rhythm has been shown by 5-HT, 5-HIAA, NAS, MEL, TRP, 5-HTP, 5-MTOH, 5-HTOH, 5-MIAA and NAT in vehicle group (Fig. 38 and 39; Table 3; $p \leq 0.05$).

In Pineal of RIPD model pattern and daily rhythm of TRP were not altered as seen in SCN of RIPD model compared to vehicle group and the levels were 0.3 ± 0.02, 9.96 ± 0.46, 0.12 ± 0.01 and 1.36 ± 0.17 µmol/g protein. TRP daily pulse was increased by 1.92 fold in RIPD model. Abolished daily rhythm was observed in case of 5-HTP in pineal as observed in SCN of RIPD model. 5-HTP daily pulse and mean levels were decreased by 0.18 and 0.06 fold respectively in RIPD model. Daily rhythm of 5-HT in RIPD model was persisted and has shown approximately 6 h phase advance and the levels were 276 ± 18.98, 182.04 ± 9.25, 214 ± 18.36 and 62.79 ± 3.14 µmol/g protein. 5-HT daily pulse was increased by 1.61 fold in RIPD model. In RIPD model 5-HIAA daily rhythm and pattern was persisted, levels were 0.18 ± 0.01, 36.76 ± 5.95, 14.82 ± 2.54 and 16.24 ± 1.37 µmol/g protein. 5-HIAA daily pulse was increased by 35.49 fold in RIPD model compared to vehicle. Persistence of daily rhythm with approximately 6h phase advance was observed in case of NAS in RIPD model and the levels were 0.11 ± 0.01, 0.41 ± 0.03, 0.42 ± 0.08 and 0.39 ± 0.03 µmol/g protein. NAS daily pulse was increased by 1.51 fold and mean level was decreased by 0.35 fold in RIPD model. Approximately 6 h of phase delay with persistence of daily rhythm was observed in case of MEL in RIPD model and the levels were 0.23 ± 0.05, 0.02 ± 0.004, 0.02 ± 0.004 and 0.02 ± 0.002 µmol/g protein. MEL daily pulse and mean levels were decreased by 0.2 and 0.12 fold respectively in RIPD model. Daily rhythm of 5-MIAA in RIPD model was persisted and levels were 0.07 ± 0.009, 0.003 ± 0.0002, 0.04 ± 0.006 and 0.02 ± 0.003 µmol/g protein. 5-MIAA daily pulse was increased by 3.18 fold and mean levels were decreased by 0.59 fold in RIPD model. In RIPD model 5-MTOH daily rhythm was persisted and levels were 0.1 ± 0.01, 0.007 ± 0.0001, 0.04 ± 0.003 and 0.009 ± 0.001 µmol/g protein. 5-MTOH daily pulse and mean levels were decreased by 0.11 and 0.1 folds respectively in RIPD model. Pattern and daily rhythm of 5-HTOH was persisted in RIPD model and the levels were 0.3 ± 0.02, 6.97 ± 0.49, 0.29 ± 0.06 and 2.91 ± 0.52 µmol/g protein. 5-HTOH daily pulse was increased by 2.08 fold in RIPD model. Daily rhythm of NAT was persisted in RIPD model and the levels were 0.03 ± 0.008, 0.002 ± 0.0001, 0.03 ± 0.002 and 0.038 ± 0.014

µmol/g protein. NAT daily pulse was decreased by 0.64 fold in RIPD model (Fig. 38, 39 and 40; Table 3; $p \leq 0.05$).

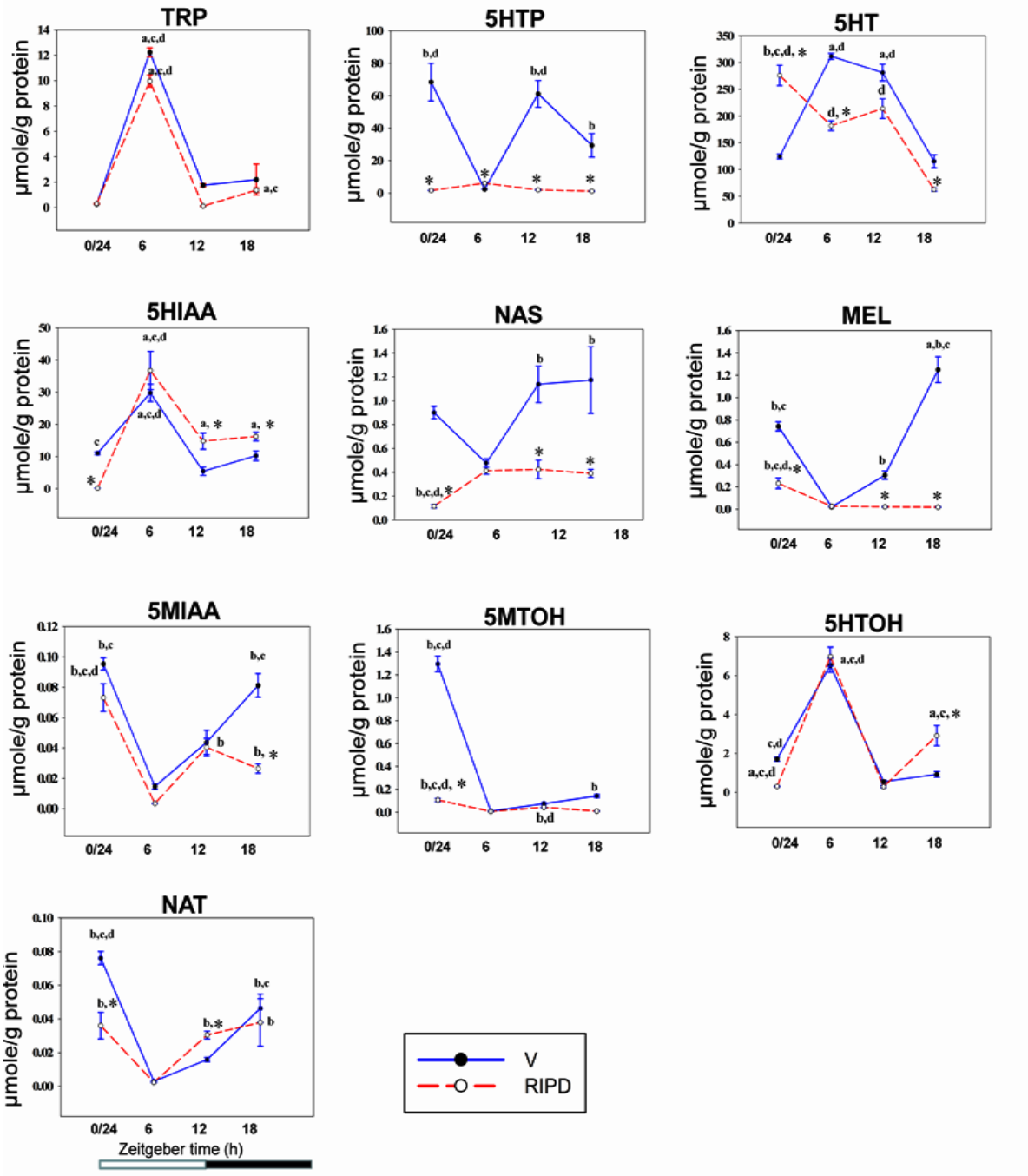

Fig. 38: Rhythmic alterations in the serotonin metabolism in the Pineal of Rotenone induced Parkinson's disease (RIPD) rat model. Each value is mean ± SEM (n=6), p ≤ 0.05 and expressed in µmol/g protein. V - Vehicle. $p_a \leq 0.05$; $p_b \leq 0.05$, $p_c \leq 0.05$ and $p_d \leq 0.05$ (where a, b, c and d refers to comparison with ZT0, ZT6, ZT12 and ZT18 respectively within the group). * refers to comparison of levels at same time point in vehicle group.

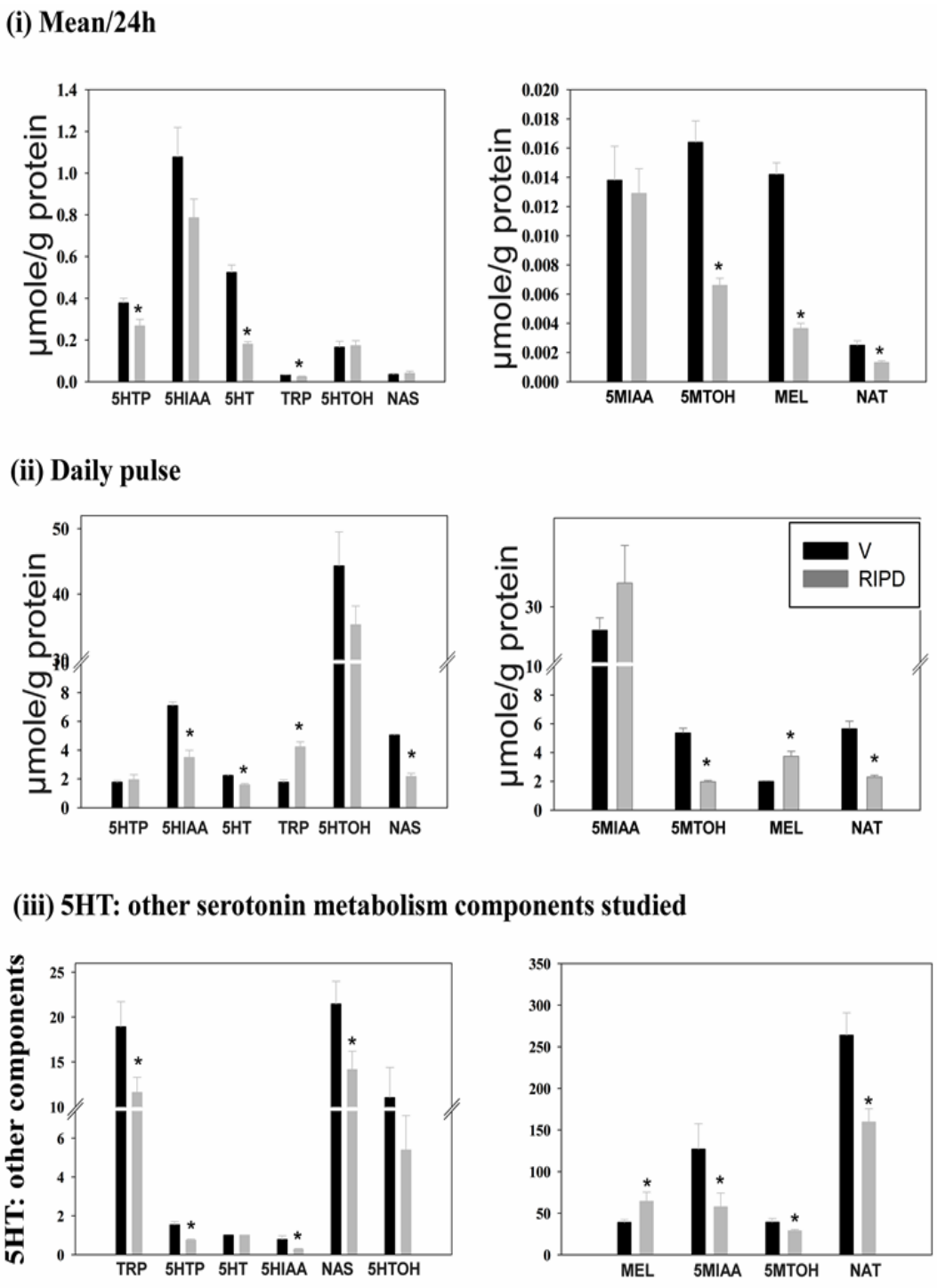

Fig. 39: Various parameters studied in serotonin metabolism components. (i) Mean 24h levels, (ii) Daily Pulse i.e. ratio between maximum and minimum and (iii) Ratio between 5-HT and other serotonin metabolism components studied in Pineal of Vehicle (V) and Rotenone induced PD rat model (RIPD). Each value is mean ± SEM; $p_* \leq 0.05$ (where * refers to comparison with vehicle group.

In RIPD model, ratio of 5-HT-TRP; 5-HT-5-MIAA; 5-HT-5-MTOH; 5-HT-5-HTOH; 5-HT-5HTP; 5-HT-MEL; 5-HT-NAS; 5-HT-HIAA has been increased and ratio between 5-HT-NAT has been decreased compared to vehicle group (Fig. 39; Table 3; $p \leq 0.05$).

Pair wise correlation (Fig. 41) revealed vehicle group light phase correlation between 5-HT-5-HTP; 5-HT-TRP is absent in dark phase whereas light phase positive correlation between 5-HT-5-HTOH has become negative in dark phase. In RIPD model there was no correlation between 5-HT-5-HTP in light phase whereas this metabolites has shown positive correlation in dark phase and the positive correlation between 5-HT-NAT in light phase is absent in dark phase (Fig. 41; $p \leq 0.05$).

In light phase there was no correlation between 5-HT-5-HIAA in vehicle group whereas in RIPD model we have observed negative correlation between 5-HT-5-HIAA. Light phase vehicle group negative correlation between 5-HT-5-HTP has lost and vehicle group positive correlation between 5-HT-TRP; 5-HT-5-HTOH has become negative whereas vehicle group negative correlation between 5-HT-5-MIAA; 5HT-5-MTOH; 5-HT-MEL; 5-HT-NAT has become positive in RIPD model. In dark phase there was no correlation between 5-HT-5-HTP; 5-HT-5-HIAA; 5-HT-TRP in vehicle group whereas in RIPD model we have observed positive correlation between 5-HT-5-HTP and negative correlation between 5-HT-5-HIAA; 5-HT-TRP. Dark phase vehicle group negative correlation between 5-HT-5-MIAA; 5-HT-5-MTOH; 5-HT-MEL has become positive whereas negative correlation between 5-HT-NAT has lost in RIPD model (Fig. 41; $p \leq 0.05$).

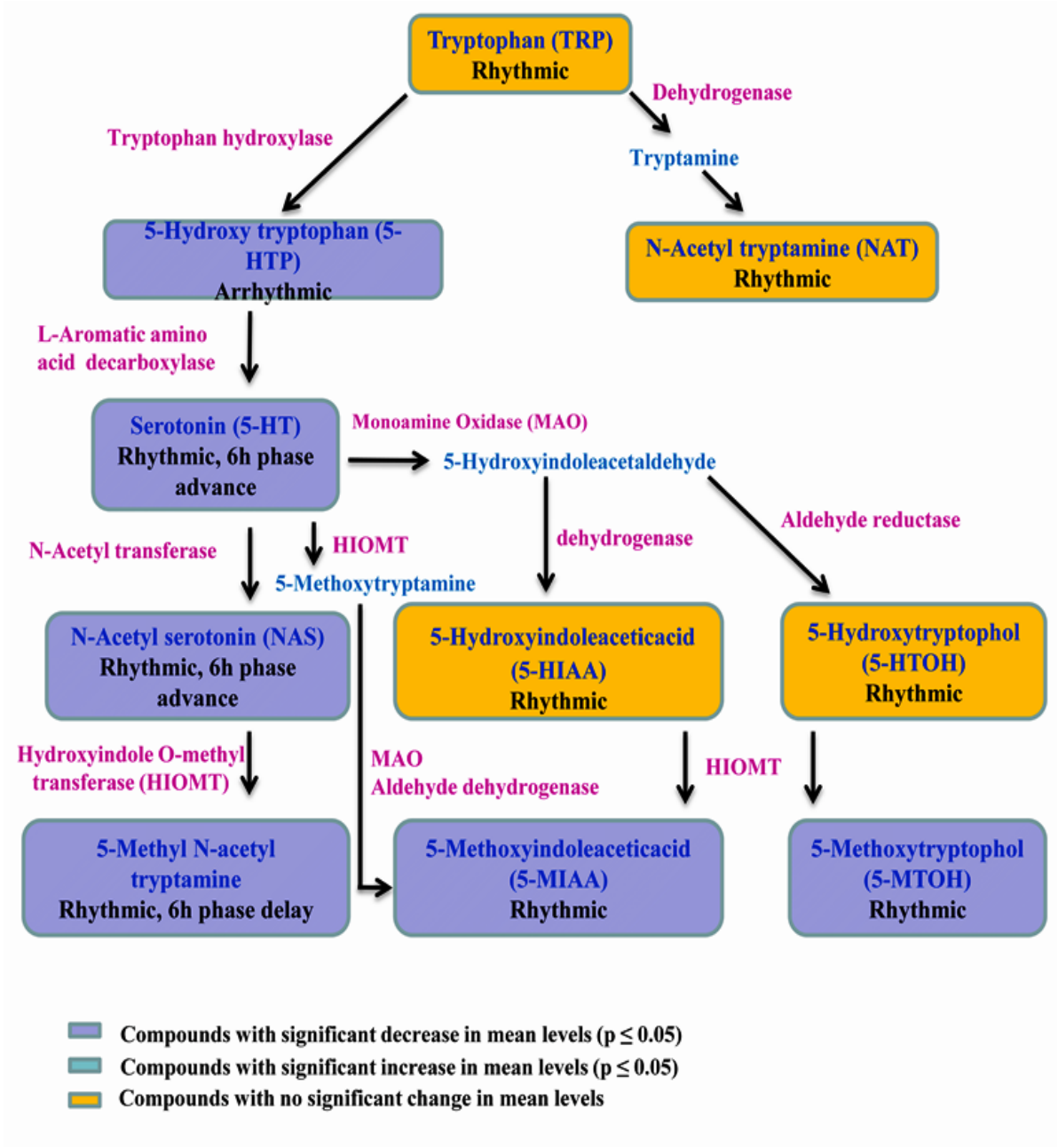

Fig. 40: Diagrammatic representation of mean 24 h alterations in the serotonin metabolism in the Pineal of Rotenone induced Parkinson's disease (RIPD) rat model compared to vehicle.

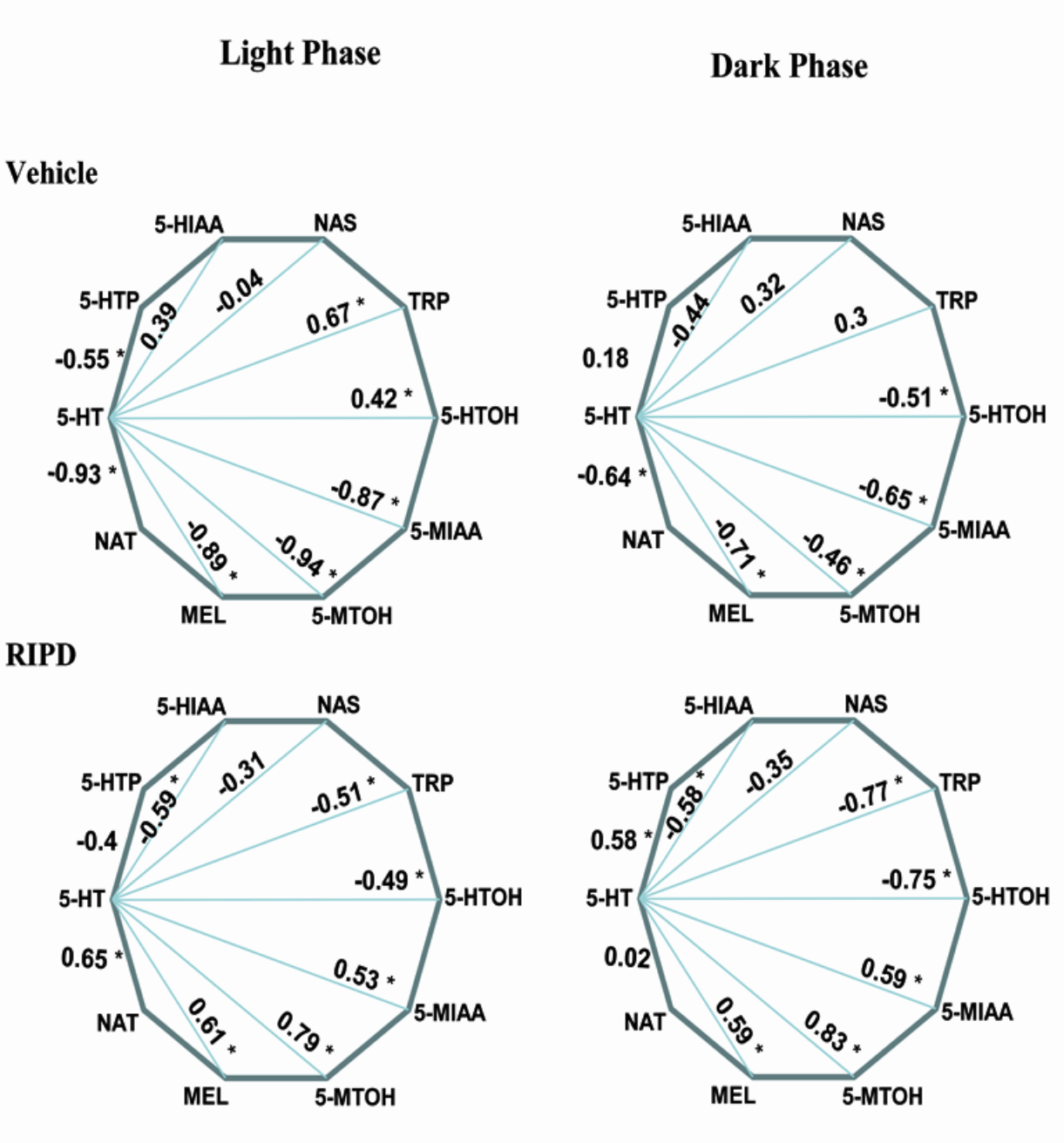

Fig. 41: Pair wise correlation between mean light (ZT 0, 6 and 12) and mean dark (ZT 12, 18 and 24/0) phase values of various components of serotonin metabolism in the Pineal of vehicle (V) and Rotenone induced Parkinson's disease (RIPD) rat model. Each value is correlation coefficient between the parameters. * indicates statistically significant value between parameters ($p \leq 0.05$). Negative value indicates negative correlation between parameters.

Table 3: Rhythmic alterations in the serotonin metabolism in the Pineal of Rotenone induced Parkinson's disease (RIPD) rat model.

Metabolite	Experimental Group	Maximum *	Minimum *	Ratio *	Mean** (24 h)	5HT: other components of Serotonin metabolism studied ***
TRP	V	12.23±0.35	0.27± 0.02 ^{q}	44.81±1.99	3.76±0.97	192.36±37.55
	RIPD	9.96±0.46 ^{p}	0.12±0.01 ^{p,q}	86.39±6.75 ^{p}	2.93±0.86	725.93±167.92 ^{p}
5-HTP	V	68.41±11.58	2.4±0.07 ^{q}	28.32±2.68	41.98±6.71	31.97±11.13
	RIPD	6.12±0.47 ^{p}	1.21±0.14 ^{p}	5.10±0.41 ^{p}	2.75±0.43 ^{p}	92.21±12.40 ^{p}
5-HT	V	311.87±5.57	115.53±12.38 ^{q}	2.73±0.17	203.82±19.47	1
	RIPD	276.11±18.98 ^{p}	62.78±3.14 ^{p,q}	4.41±0.21 ^{p}	183.74±17.46	1
5-HIAA	V	29.80±2.71	5.47±1.30 ^{q}	5.77±0.85	13.46±2.03	23.97±4.96
	RIPD	36.76±5.95 ^{p}	0.18±0.01 ^{q}	205 ±22.03 ^{p}	17 ±3.12	394.6±139.61 ^{p}
NAS	V	1.17±0.28	0.48±0.03 ^{q}	2.47±0.11	0.94±0.1	281.3±46.74
	RIPD	0.42±0.08 ^{p}	0.11±0.01 ^{p,q}	3.74±0.48 ^{p}	0.33±0.03 ^{p}	916.57±195.05 ^{p}
MEL	V	1.25±0.11	0.02±0.002 ^{q}	61.23±5.04	0.60±0.10	3772.91±1412.32
	RIPD	0.23±0.05 ^{p}	0.02±0.002 ^{q}	12.71±1.76 ^{p}	0.07±0.02^{p}	6134.16±968.62 ^{p}
5-MIAA	V	0.09±0.004	0.01±0.001 ^{q}	6.60±0.48	0.06±0.007	7552.52±1863.48
	RIPD	0.07±0.009 ^{p}	0.003±0.0002 ^{p,q}	21 ±1.75 ^{p}	0.03±0.005 ^{p}	16711.19±4683.71 ^{p}
5-MTOH	V	1.29±0.06	0.009±0.0006 ^{q}	143.56±7.43	0.39±0.11	8884.38±2983.88
	RIPD	0.10±0.01 ^{p}	0.006±0.001 ^{p,q}	16.97±2.78 ^{p}	0.04±0.009 ^{p}	13058.2±3755.27 ^{p}
5-HTOH	V	6.53±0.36	0.55±0.08 ^{q}	12.13±1.16	2.25±0.49	208.49±46.60
	RIPD	6.97±0.49	0.29±0.06 ^{p,q}	25.27±3.2 ^{p}	2.62±0.59	495.07±123.47 ^{p}
NAT	V	0.07±0.003	0.002±0.0003 ^{q}	26.36±1.96	0.03±0.006	30235.3±9641.68
	RIPD	0.04±0.01 ^{p}	0.002±0.0001 ^{p,q}	16.88±3.69 ^{p}	0.02±0.004	25261.17±7063.25 ^{p}

* Each value is mean ± S.E. (n=6); **each value is mean ± S.E., n=24, ***each value is mean ± SE of mean 24h ratio of 5HT with respective metabolites for Vehicle group (V) and Rotenone induced PD group (RIPD); $p \leq 0.05$; p refers to comparison between V and RIPD; q refers to comparison between maximum and minimum.

(c) Chronomics of Serotonin metabolism in the SN of RIPD model:

No significant difference was found between the control and the vehicle control. The metabolites such as 5-HT, 5-HIAA, NAS, MEL, TRP, 5-HTP, 5-MTOH, 5-HTOH, 5-MIAA and NAT have shown daily rhythmicity in vehicle group (Fig. 42 and 43; Table 4; $p \leq 0.05$).

Daily rhythm and its pattern of TRP was not altered in SN as observed in SCN and Pineal of RIPD model compared to vehicle group and the levels were 0.02 ± 0.002, 0.05 ± 0.002, 0.01 ± 0.001 and 0.014 ± 0.002 µmol/g protein. TRP daily pulse was increased by 2.38 fold and mean level was decreased by 0.72 fold in RIPD model. Abolished daily rhythm was observed in case of 5-HTP and 5-HT as observed in RIPD model. 5-HTP mean levels were decreased by 0.7 fold in RIPD model. 5-HT daily pulse and mean levels were decreased by 0.7 and 0.34 fold in RIPD model. 5-HIAA daily rhythm persisted with approximately 6h phase delay and levels were 1.27 ± 0.16, 0.34 ± 0.03, 0.68 ± 0.06 and 0.85 ± 0.16 µmol/g protein. 5-HIAA daily pulse was decreased by 0.49 fold in RIPD model. Persistence of daily rhythm was observed in case of NAS and the levels were 0.01 ± 0.001, 0.13 ± 0.004, 0.016 ± 0.001 and 0.007 ± 0.001 µmol/g protein. NAS daily pulse was decreased by 0.43 fold in RIPD model. Approximately 6 h of phase delay with persistence of daily rhythm was observed in case of MEL and the levels were 0.005 ± 0.0007, 0.003 ± 0.0002, 0.004 ± 0.0003 and 0.001 ± 0.0001 µmol/g protein. MEL daily pulse was increased by 1.88 fold and mean levels were decreased by 0.25 fold in RIPD model. Daily rhythm of 5-MIAA was persisted with approximately 6h phase delay and levels were 0.02 ± 0.001, 0.0008 ± 0.00005, 0.016 ± 0.001 and 0.01 ± 0.001 µmol/g protein in RIPD model. In RIPD model 5-MTOH daily rhythm persisted with approximately 6h phase delay and levels were 0.008 ± 0.001, 0.004 ± 0.0001, 0.008 ± 0.0006 and 0.006 ± 0.0007 µmol/g protein. 5-MTOH daily pulse and mean levels were decreased by 0.36 and 0.4 folds respectively in RIPD model. Daily rhythm of 5-HTOH was persisted and levels were 0.22 ± 0.02, 0.008 ± 0.0008, 0.29 ± 0.03 and 0.16 ± 0.02 µmol/g protein. No significant difference in daily pulse and mean levels were observed in RIPD model as compared to vehicle group. Daily rhythm of NAT in RIPD model was persisted with approximately 6 h phase delay and the levels were 0.0009 ± 0.00007, 0.002 ± 0.0001, 0.001 ± 0.0001 and 0.001 ± 0.0001 µmol/g protein. NAT daily pulse and mean levels were decreased by 0.4 and 0.52 folds respectively in the RIPD model (Fig. 42, 43 and 44; Table 4; $p \leq 0.05$).

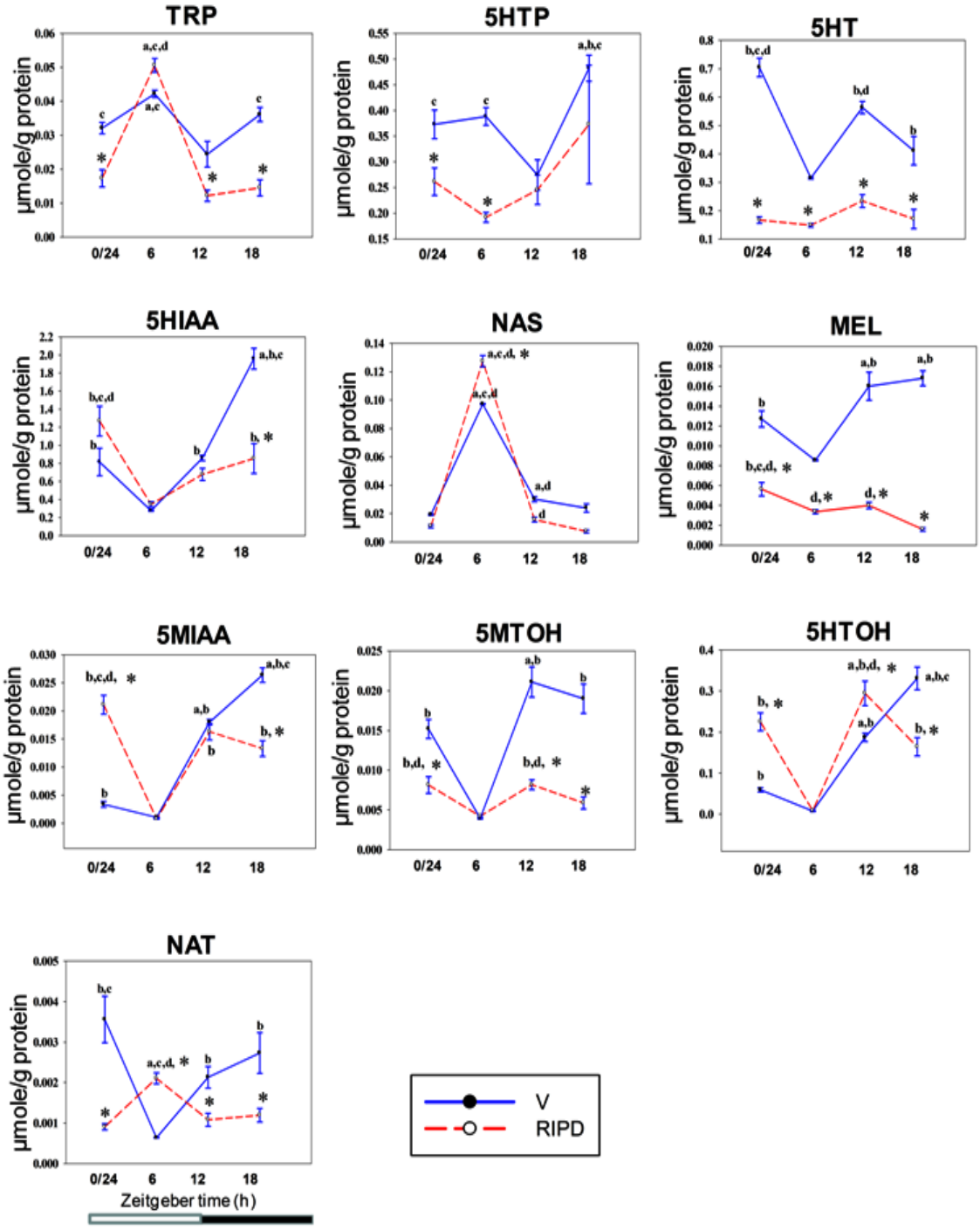

Fig. 42: Rhythmic alterations in the serotonin metabolism in the Substantia nigra of Rotenone induced Parkinson's disease (RIPD) rat model. Each value is mean ± SEM (n=6), $p \leq 0.05$ and expressed in µmol/g protein. V - Vehicle. $p_a \leq 0.05$; $p_b \leq 0.05$, $p_c \leq 0.05$ and $p_d \leq 0.05$ (where a, b, c and d refers to comparison with ZT0, ZT6, ZT12 and ZT18 respectively within the group). * refers to comparison of levels at same time point in vehicle group.

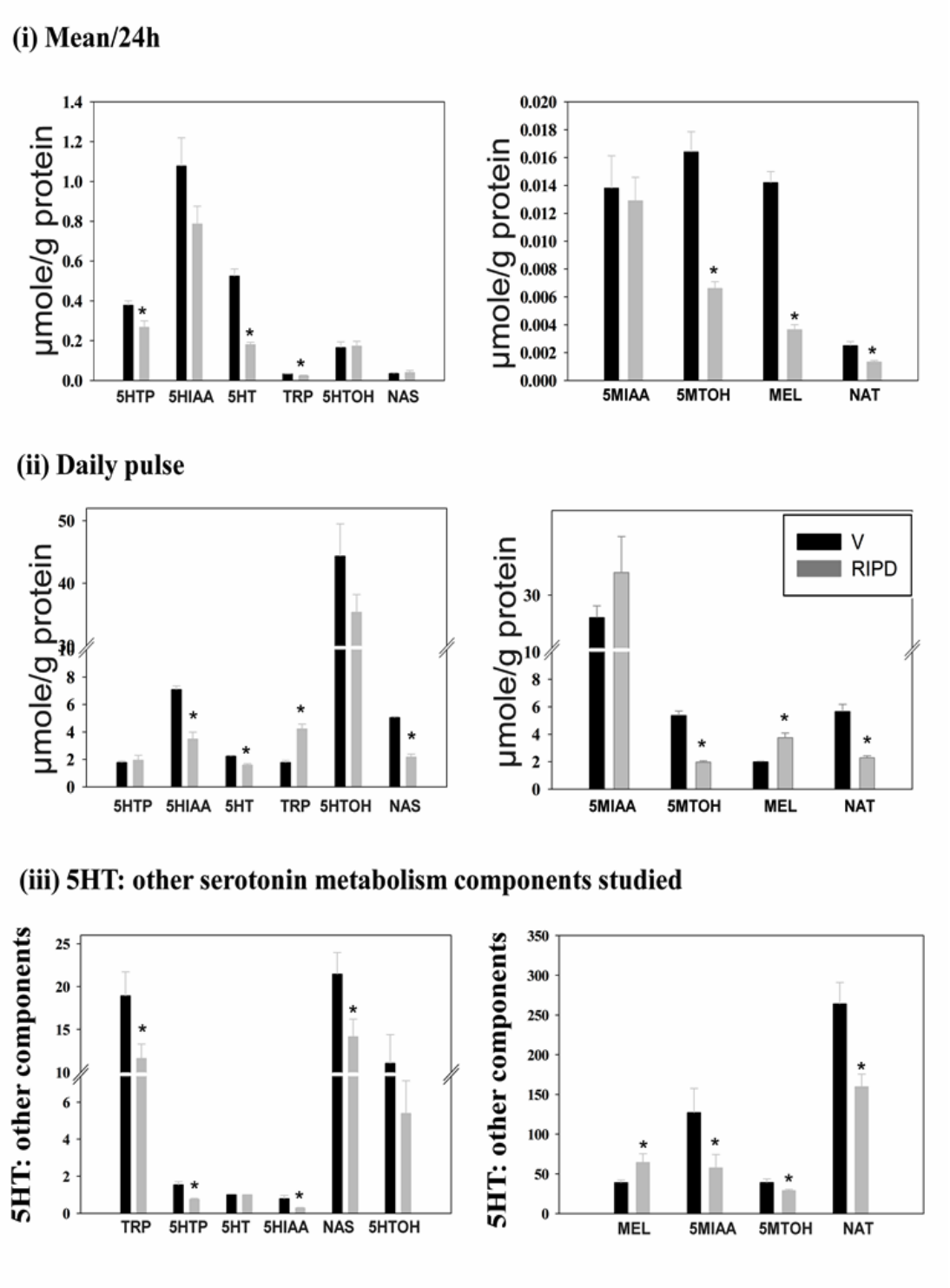

Fig. 43: Various parameters studied in serotonin metabolism components. (i) Mean 24h levels, (ii) Daily Pulse i.e. ratio between maximum and minimum and (iii) Ratio between 5-HT and other Serotonin metabolism components studied in SN of Vehicle (V) and Rotenone induced PD (RIPD) rat model. Each value is mean ± SEM; $p_* \leq 0.05$ (where * refers to comparison with vehicle group.

In RIPD model, ratio of 5-HT-TRP; 5-HT-5-HTP; 5-HT-5-HIAA; 5-HT-NAS; 5-HT-5-MIAA; 5-HT-5-MTOH; 5-HT-NAT has been decreased and ratio between 5-HT-MEL has been increased compared to vehicle group (Fig. 43;$p \leq 0.05$).

Pair wise correlation (Fig. 45) revealed vehicle group there was no correlation between 5-HT-5-HIAA; 5-HT-5-HTOH; 5-HT-5-MIAA in light phase whereas these metabolites has shown correlation in dark phase and correlation between 5-HT-NAS; 5-HT-NAT in light phase has not observed in dark phase. In RIPD model there was no correlation between 5-HT-5-HTP in light phase whereas this metabolites has shown correlation in dark phase (Fig. 45; $p \leq 0.05$).

In light phase there was no correlation between 5-HT-5-HTOH in vehicle group whereas in RIPD model we have observed positive correlation between 5-HT-5-HTOH. Light phase vehicle group negative correlation between 5-HT-NAS and positive correlation between 5-HT-NAT has lost in RIPD model. In dark phase there was no correlation between 5-HT-5-HTP in vehicle group whereas in RIPD model we have observed positive correlation between 5-HT-5-HTP. Dark phase vehicle group negative correlation between 5-HT-5-HIAA; 5-HT-5-MIAA has lost and negative correlation between 5-HT-5-HTOH in vehicle group has become positive in RIPD model (Fig. 45; $p \leq 0.05$).

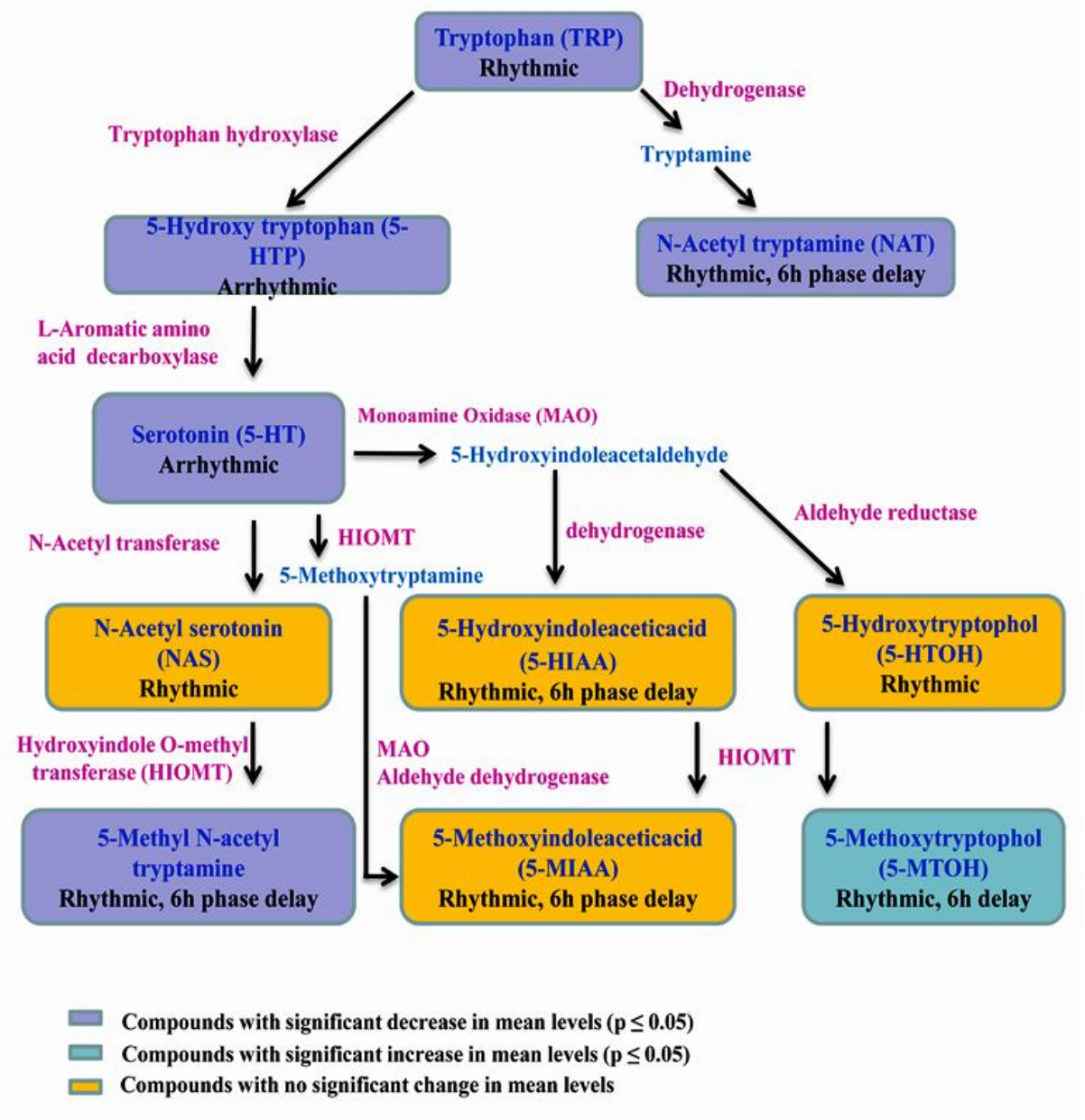

Fig. 44: Diagrammatic representation of mean 24 h alterations in the serotonin metabolism in the SN of Rotenone induced Parkinson's disease (RIPD) rat model compared to vehicle.

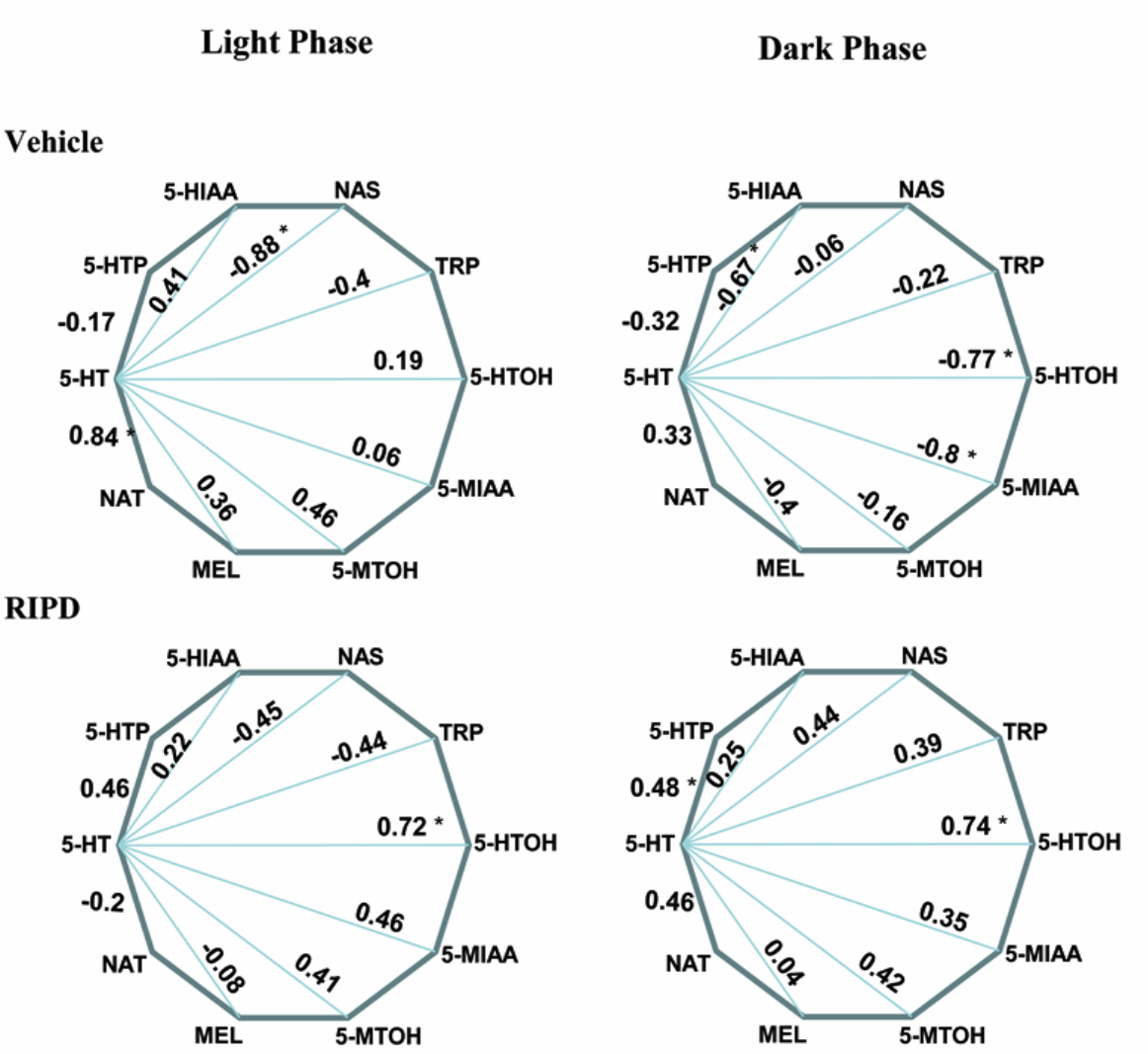

Fig. 45: Pair wise correlation between mean light (ZT 0, 6 and 12) and mean dark (ZT 12, 18 and 24/0) phase values of various components of serotonin metabolism in the SN of vehicle (V) and Rotenone induced Parkinson's disease (RIPD) rat model. Each value is correlation coefficient between the parameters. * indicates statistically significant value between parameters ($p \leq 0.05$). Negative value indicates negative correlation between parameters.

Table 4: Rhythmic alterations in the serotonin metabolism in the SN of Rotenone induced Parkinson's disease (RIPD) rat model.

Metabolite	Experimental Group	Maximum *	Minimum *	Ratio *	Mean** (24 h)	5HT: other components of Serotonin metabolism studied ***
TRP	V	0.04±0.001	0.02±0.003 ^{q}	1.77±0.16	0.03±0.001	18.93±2.80
	RIPD	0.05±0.002 ^{p}	0.01±0.001 $^{p, q}$	4.22±0.34 ^{p}	0.02±0.003	11.63±1.67 ^{p}
5-HTP	V	0.48±0.02	0.27±0.03 ^{q}	1.77±0.12	0.38±0.02	1.54±0.16
	RIPD	0.37±0.11	0.19±0.009	1.94±0.35	0.27±0.03	0.75±0.05 ^{p}
5-HT	V	0.70±0.03	0.31±0.003 ^{q}	2.23±0.06	0.52±0.03	1
	RIPD	0.23±0.02 ^{p}	0.15±0.005	1.58±0.09 ^{p}	0.18±0.01	1
5-HIAA	V	1.96±0.11	0.27±0.006 ^{q}	7.09±0.26	1.08±0.14	0.79±0.18
	RIPD	1.27±0.16 ^{p}	0.34±0.03 $^{p, q}$	3.49±0.49 ^{p}	0.78±0.09	0.28±0.02 ^{p}
NAS	V	0.1±0.0003	0.02±0.0005 ^{q}	5.05±0.08	0.03±0.005	21.47±2.52
	RIPD	0.13±0.003 ^{p}	0.007±0.001 ^{q}	2.17±0.21 ^{p}	0.04±0.01	14.15±2.05 ^{p}
MEL	V	0.01±0.0007	0.008±0.00004 ^{q}	1.99±0.05	0.01±0.0007	38.93±3.37
	RIPD	0.005±0.0006 ^{p}	0.001±0.0001 $^{p, q}$	3.74±0.34 ^{p}	0.003±0.0003	64.39±10.84 ^{p}
5-MIAA	V	0.02±0.001	0.001±0.00007 $^{p, q}$	27.86±1.12	0.014±0.002	127.17±30.27
	RIPD	0.02±0.001 ^{p}	0.0007±0.00004 ^{q}	32.13±3.40	0.01±0.001	57.57±16.70 ^{p}
5-MTOH	V	0.02±0.001	0.003±0.0001 ^{q}	5.36±0.33	0.01±0.001	39.14±4.54
	RIPD	0.008±0.0006 ^{p}	0.004±0.0001 ^{q}	1.96±0.10 ^{p}	0.006±0.0004	28.89±1.58 ^{p}
5-HTOH	V	0.33±0.03	0.007±0.001 ^{q}	44.34±5.17	0.16±0.03	11.04±3.35
	RIPD	0.29±0.03	0.008±0.0007 ^{q}	35.34±2.85	0.17±0.02	5.39±1.78
NAT	V	0.003±0.0005	0.0006±0.000008 ^{q}	5.65±0.52	0.002±0.0003	263.83±27.99
	RIPD	0.002±0.0001 ^{p}	0.0009±0.00007	2.29±0.14	0.001±0.0001 ^{p}	159.63±15.87 ^{p}

* Each value is mean ± S.E. (n=6); **each value is mean ± S.E., n=24, ***each value is mean ± SE of mean 24h ratio of 5HT with respective metabolites for Vehicle group (V) and Rotenone induced PD group (RIPD); $p \leq 0.05$; p refers to comparison between V and RIPD; q refers to comparison between maximum and minimum.

OBJECTIVE – III

3. Studies of daily rhythms of protein profile in SCN, Pineal and SN upon aging and in RIPD rat model

No significant difference was found between the control and the vehicle control.

(a) Studies of daily rhythms of protein profile in SCN upon aging and in RIPD rat model

In 3 m at ZT6 a total of 514 protein spots were matched between biological replicates with a correlation coefficient value of 0.99 whereas, at ZT18 we found 134 protein spots with a correlation coefficient of 0.7 between the replicates. In the 12 m category 425 protein spots were observed at ZT6 and 287 spots at ZT18; the correlation coefficient values between replicates were 0.99 and 0.79 respectively. At ZT6, in the 24 m group 181 protein spots were similar with a correlation coefficient value of 0.86 whereas at ZT18, 215 protein spots were matched with a correlation coefficient of 0.97. In the RIPD model a total of 306 protein spots were analyzed at ZT6 whereas 309 were found at ZT18. The correlation coefficient values between the respective biological replicates were 0.97 and 0.94. The number of protein spots which were showing daily rhythm is 35 in 3 m (Table 5; $p \leq 0.05$), whereas this number has been decreased to 22 in 12 m (Table 6; $p \leq 0.05$), 9 in 24 m (Table 7; $p \leq 0.05$; Fig. 46) and 10 in RIPD rat model (Fig. 49; $p \leq 0.05$). Of the 35 protein spots differentially expressed in 3m, 22 were up regulated at ZT6 and 13 were up regulated at ZT18. At 12m 22 protein spots were differentially expressed, out of which 19 were up regulated at ZT6 and 3 spots at ZT18. 6 spots were up regulated at ZT6 and 3 at ZT18 out of the 9 protein spots differentially expressed in the 24m. In RIPD model, of the 10 protein spots differentially expressed 5 were up regulated at ZT6 and 5 at ZT18. The number of protein spots that have shown daily pulse (maximum: minimum ratio) greater than 5 is 11 in 3 m, 2 in 12 m and 6 in 24 m. Differentially expressed protein spots between 3, 12 and 24 m at ZT6 are 34 and at ZT18 are 19 (Fig. 47; $p \leq 0.05$); between vehicle and RIPD rat model at ZT6 are 16and ZT18 are 28 (Fig. 50; $p \leq 0.05$). 12 protein spots were differentially expressed between all the 3, 12 and 24 m and within a day (Fig. 48; $p \leq 0.05$). 7 protein spots were differentially expressed between vehicle and RIPD rat model and within a day (Fig. 51; $p \leq 0.05$).

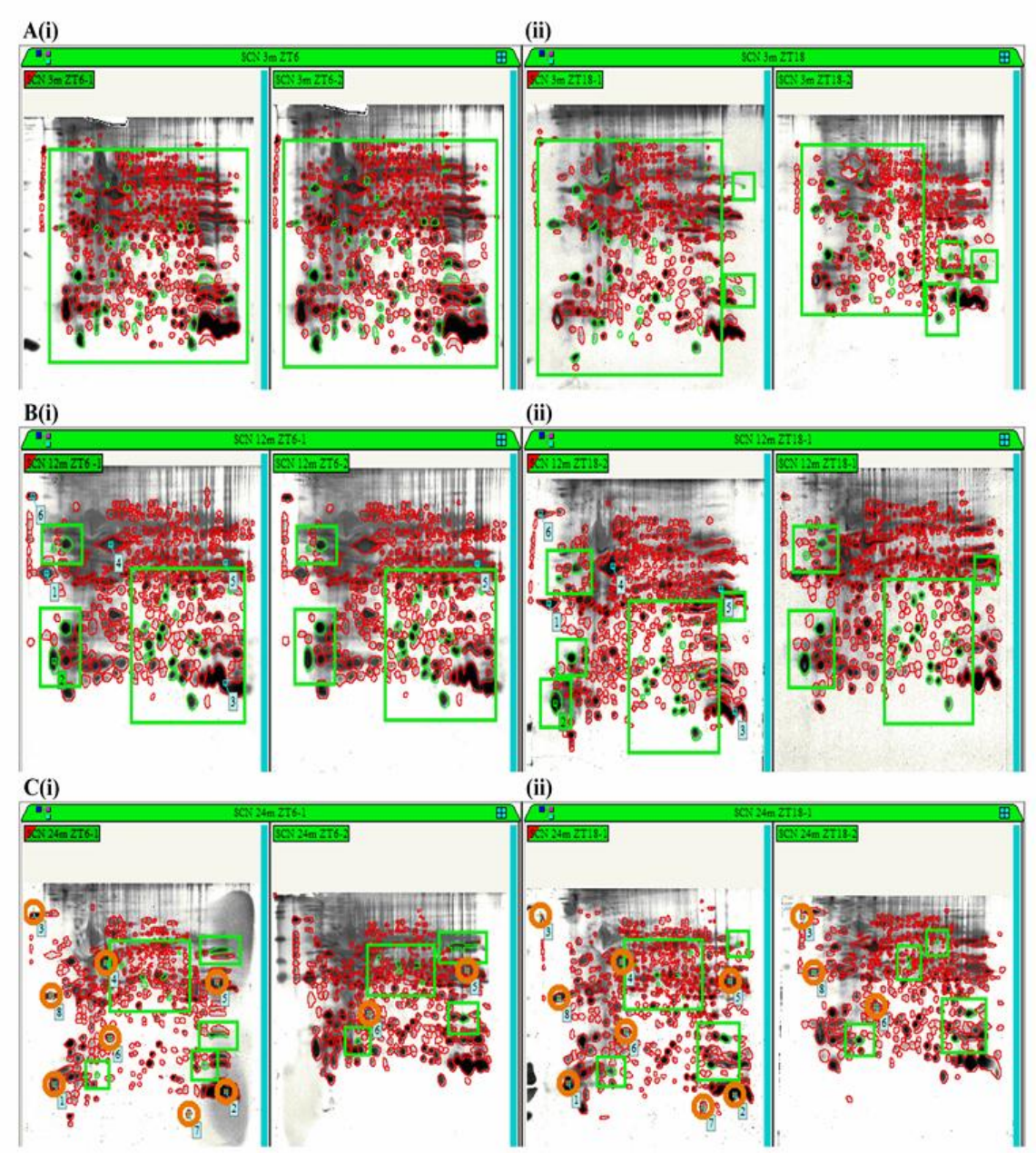

Fig. 46: Age induced alteration in protein profiles in variable age groups. (A) 3, (B) 12 and (C) 24 m SCN at (i) ZT6 and (ii) ZT18 with n=2. Protein spots which were differentially expressed between ZT6 and ZT18 of SCN are highlighted with green.

Table 5: Daily rhythms of protein profiles in 3 month SCN

S. No.	Match ID	ZT6	ZT18	Max / min ratio	Mean 24 h
1	1	0.11	0.0027	41.69	0.058
2	10	0.055	0.0082	6.78	0.032
3	21	0.044	0.16	3.68	0.10
4	24	0.058	0.58	9.95	0.32
5	38	0.018	0.18	9.64	0.098
6	47	0.016	0.12	7.21	0.068
7	55	0.091	0.017	5.44	0.054
8	63	0.056	0.013	4.11	0.034
9	84	0.97	0.27	3.57	0.62
10	86	0.18	0.043	4.20	0.11
11	88	0.25	0.15	1.71	0.2
12	90	0.67	0.15	4.46	0.41
13	96	0.64	0.29	2.14	0.47
14	101	0.26	0.14	1.86	0.19
15	110	1.11	0.33	3.34	0.72
16	112	0.47	1.17	2.45	0.82
17	118	0.37	0.14	2.56	0.25
18	126	0.11	0.0046	23.51	0.056
19	133	0.61	0.20	3.080	0.41
20	138	1.41	1.68	1.19	1.54
21	139	0.39	0.61	1.57	0.50
22	149	0.39	0.013	29.12	0.20
23	153	0.19	0.045	4.36	0.12
24	154	0.20	0.11	1.85	0.15
25	161	0.13	0.071	1.89	0.10
26	164	0.42	0.23	1.84	0.32
27	165	0.17	0.25	1.49	0.21
28	178	0.36	1.64	4.53	1.0050
29	181	0.24	0.010	22.62	0.13
30	182	0.27	0.066	4.065	0.17
31	202	0.051	0.16	3.073	0.10
32	210	0.48	1.20	2.51	0.84
33	213	0.18	0.028	6.58	0.10
34	216	0.022	0.12	5.60	0.074
35	222	0.053	0.12	2.24	0.087

Each value in column 2 refers to particular protein spot id given by software, column 3 and 4 refers to mean percent volume of particular spot (n=2) in ZT6 and ZT18, column 5 refers daily pulse (max / min ratio) and column 6 refers mean 24 h levels.

Table 6: Daily rhythms of Protein Profiles in 12 month SCN

S.No.	Match ID	ZT6	ZT18	Max / min ratio	Mean 24 h
1	0	12.053	7.84	1.54	9.94
2	4	0.075	0.39	5.17	0.23
3	22	1.38	0.77	1.77	1.078
4	23	0.72	0.43	1.65	0.57
5	24	0.69	0.34	2.028	0.52
6	31	0.87	0.58	1.50	0.73
7	33	0.15	0.078	1.96	0.11
8	34	0.44	0.29	1.53	0.37
9	36	2.78	3.086	1.10	2.93
10	42	1.074	0.34	3.18	0.70
11	43	0.15	0.081	1.89	0.12
12	46	0.38	0.26	1.44	0.32
13	49	0.76	0.48	1.58	0.62
14	54	0.74	0.59	1.23	0.67
15	55	0.39	0.27	1.46	0.33
16	57	1.77	1.28	1.38	1.52
17	69	0.48	0.31	1.53	0.39
18	72	0.47	0.097	4.87	0.28
19	74	0.32	0.069	4.68	0.19
20	76	0.23	0.024	9.86	0.13
21	86	0.11	0.28	2.41	0.19
22	87	1.010	0.76	1.32	0.89

Each value in column 2 refers to particular protein spot id given by software, column 3 and 4 refers to mean percent volume of particular spot (n=2) in ZT6 and ZT18, column 5 refers daily pulse (max / min ratio) and column 6 refers mean 24 h levels

Table 7: Daily rhythms of Protein Profiles in 24 month SCN

S. No.	Match ID	ZT6	ZT18	Max / min ratio	Mean 24 h
1	1	1.070	0.038	28.10	0.55
2	29	0.012	0.081	6.38	0.047
3	45	0.18	0.021	8.51	0.10
4	56	1.36	1.077	1.26	1.22
5	76	0.19	0.76	3.94	0.48
6	82	0.13	1.024	7.54	0.58
7	140	0.14	0.018	8.086	0.082
8	164	0.093	0.051	1.79	0.072
9	175	0.30	0.19	1.56	0.24
10	183	0.12	0.014	8.51	0.068

Each value in column 2 refers to particular protein spot id given by software, column 3 and 4 refers to mean percent volume of particular spot (n=2) in ZT6 and ZT18, column 5 refers daily pulse (max / min ratio) and column 6 refers mean 24 h levels.

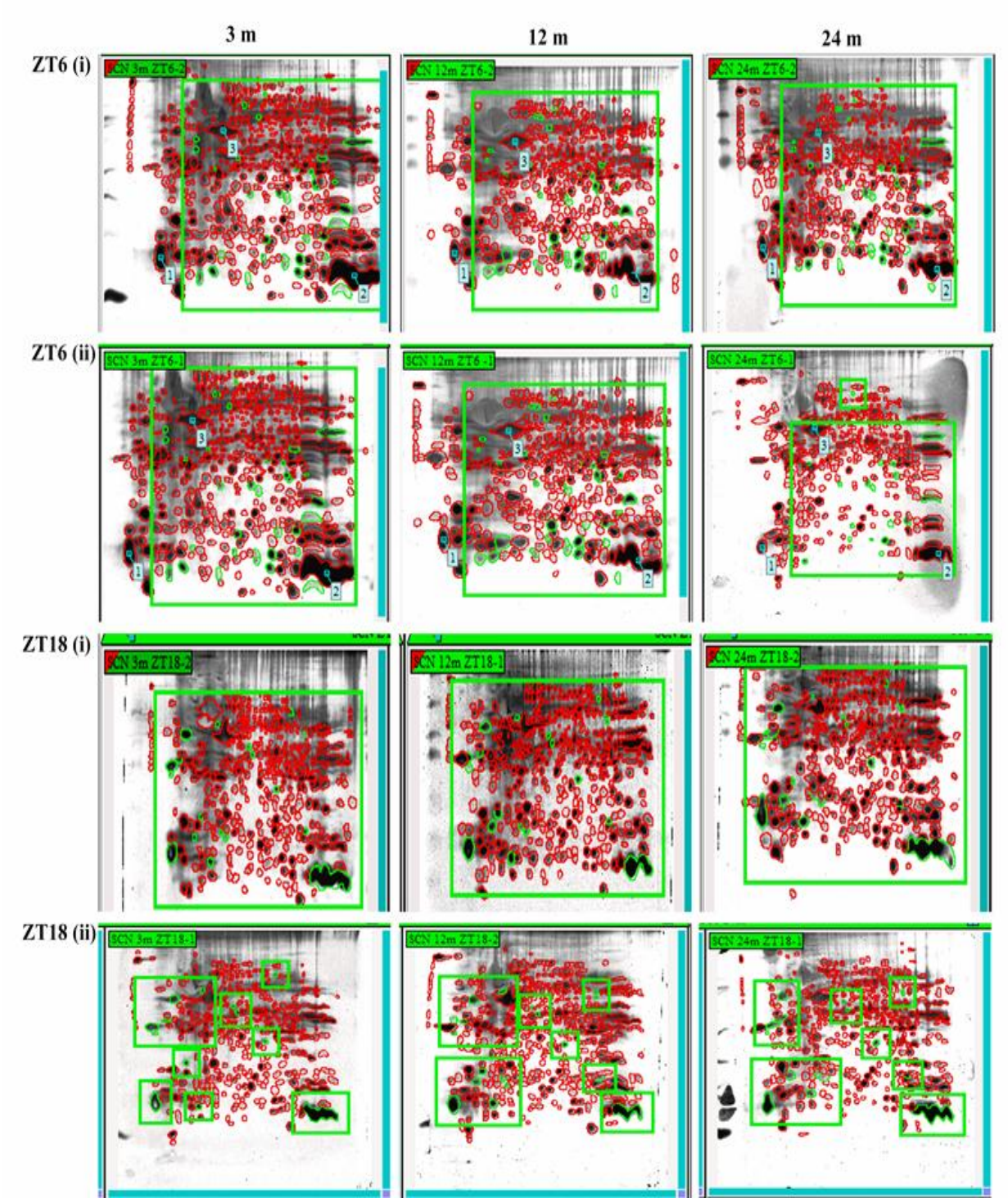

Fig. 47: Age induced alteration in protein profiles in SCN of variable age groups at ZT6 (i and ii) and ZT18 (i and ii) with n=2. Protein spots which were differentially expressed between 3, 12 and 24 m SCN at ZT6 and ZT18 were highlighted.

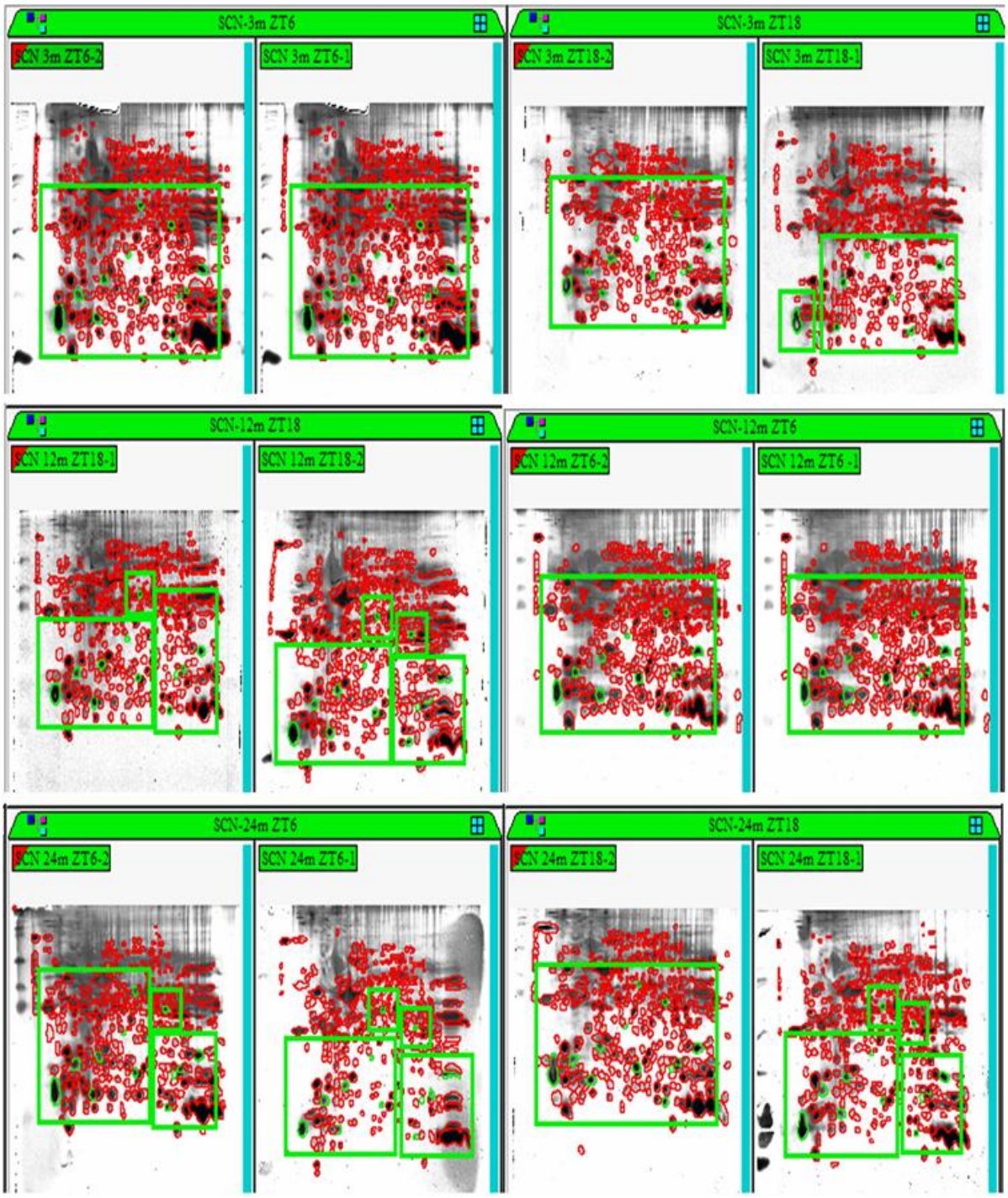

Fig. 48: Age induced alteration in protein profiles in variable age groups. Protein spots which were differentially expressed daily in 3, 12 and 24 m SCN were highlighted.

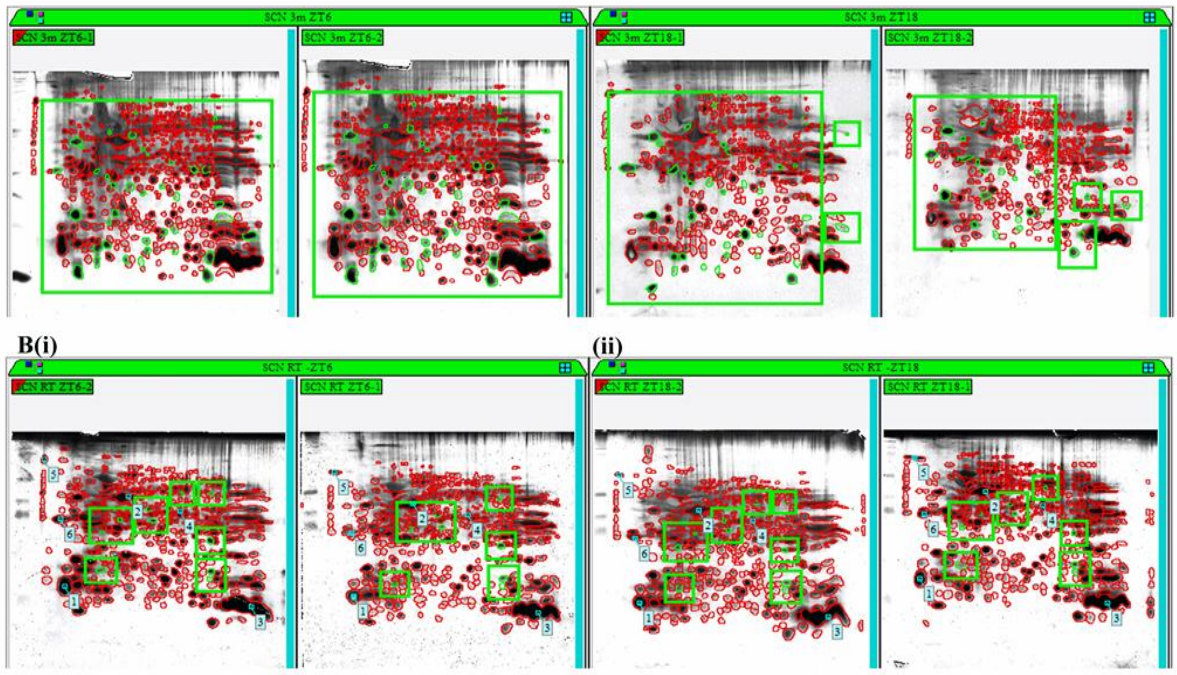

Fig. 49: Daily rhythms of Protein Profiles in SCN of Control and Rotenone induced Parkinson's disease (RIPD) rat model. Protein spots which were differentially expressed between ZT6 and ZT18 of control A (i) and (ii) and RIPD B (i) and (ii) were highlighted with green.

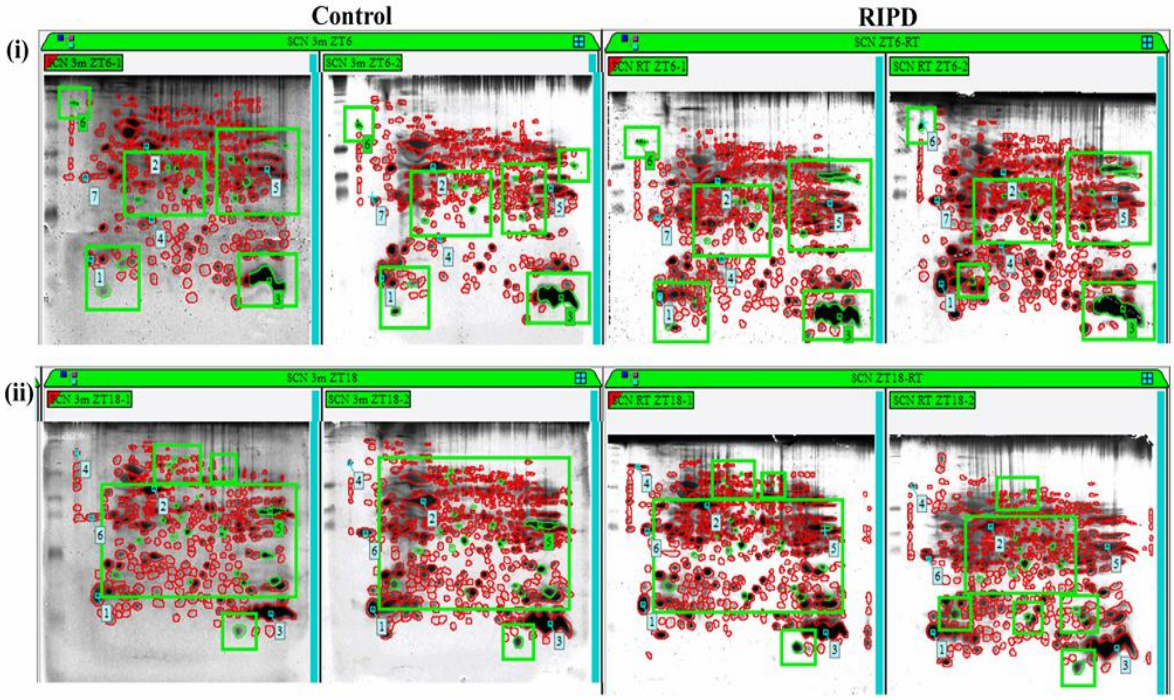

Fig. 50: Daily rhythms of Protein Profiles in SCN at ZT6 (i) and ZT18 (ii) of Control and Rotenone induced Parkinson's disease (RIPD) rat model.

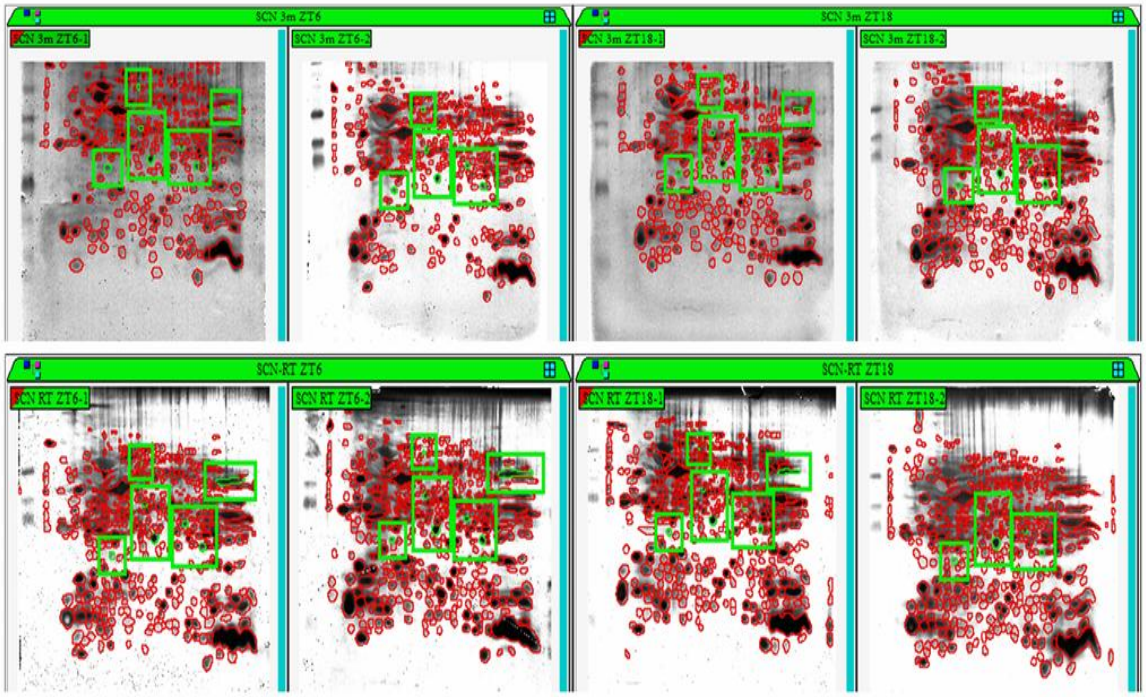

Fig. 51: Daily rhythms of Protein Profiles in SCN of Control and Rotenone induced Parkinson's disease (RIPD) rat model. Protein spots which were differentially expressed daily in SCN of control and RIPD rat model were highlighted.

(b) Studies of daily rhythms of protein profile in pineal upon aging and in RIPD rat model

In 3 m 306 protein spots were observed at ZT6 whereas at ZT18 we could find 460 spots. The correlation coefficient values between the biological replicates for the respective time points were 0.98 and 0.99. In 12 m at ZT6, a total of 239 protein spots were matched between replicates, 208 protein spots were detected at ZT18. In 24 m at ZT6 there were 238 protein spots and at ZT18, 541 spots. The correlation coefficient value between the biological replicates for ZT6 and ZT12 for both 12 and 24 m group was 0.99. Daily rhythm showing protein spots were 51 in 3 m (Table 8; $p \leq 0.05$), 22 in 12 m (Table 9; $p \leq 0.05$) and 61 in 24 m (Table 10 and 11; $p \leq 0.05$; Fig. 52). In 3 m, 51 protein spots were differentially expressed. 20 were up regulated at ZT6 and 31 were up regulated at ZT18. Of the 22 protein spots differentially expressed in 12 m, 12 were up regulated at ZT6 and 10 spots at ZT18. In the 24 m out of the 61 spots that were found to be differentially expressed 26 were up regulated at ZT6 and 35 at ZT18. The number of protein spots that have shown daily pulse (maximum: minimum ratio) greater than 5 is 21 in 3 m,

14 in 12 m and 30 in 24 m. Differentially expressed protein spots between 3, 12 and 24 m at ZT6 are 13 and at ZT18 are 28 (Fig. 53; $p \leq 0.05$). 18 protein spots were differentially expressed between all the 3, 12 and 24 m and within a day (Fig. 54; $p \leq 0.05$).

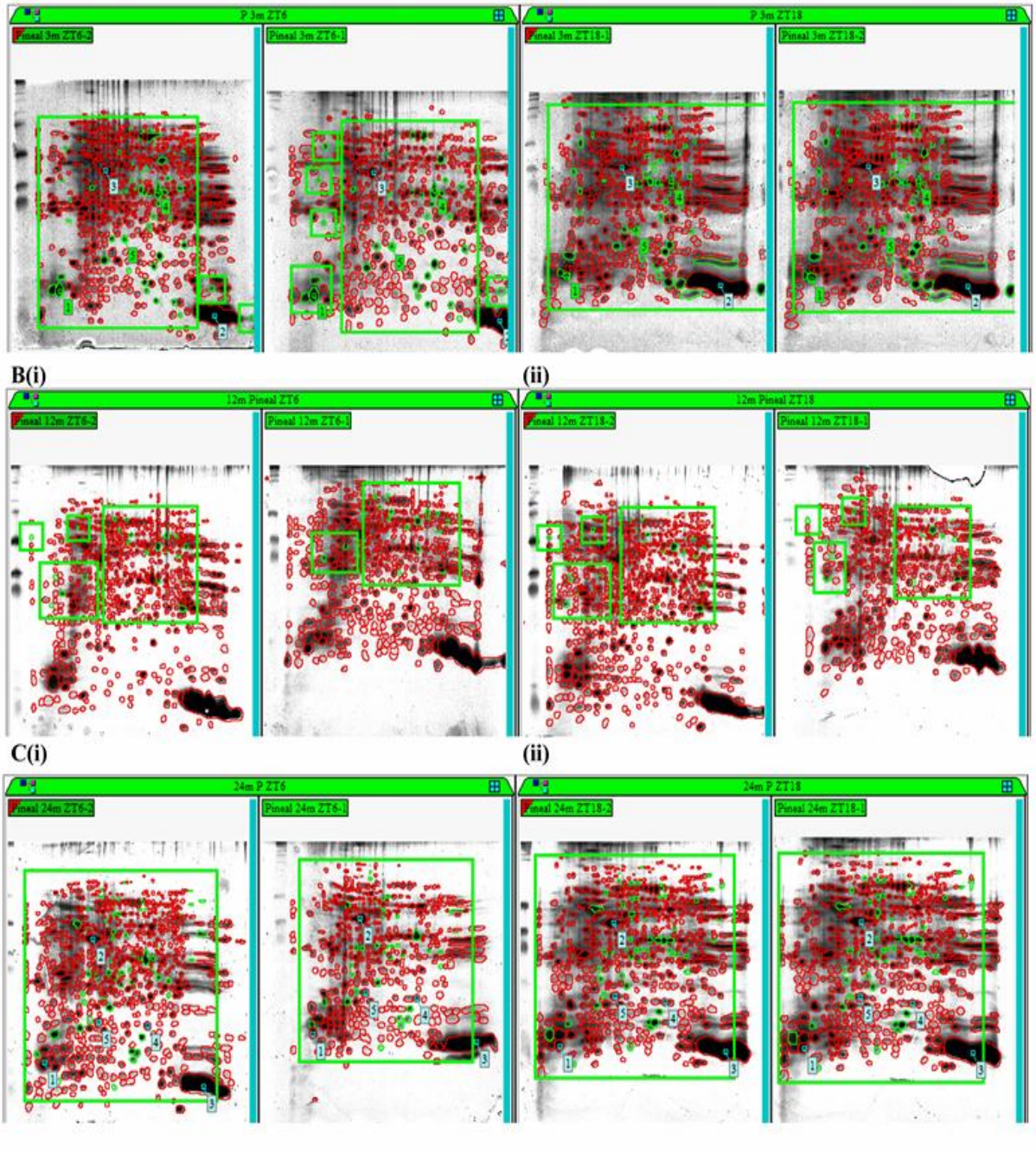

Fig. 52: Age induced alteration in protein profiles in variable age groups. (A) 3, (B) 12 and (C) 24 m Pineal at (i) ZT6 and (ii) ZT18 with n=2. Protein spots which were differentially expressed between ZT6 and ZT18 of Pineal are highlighted with green.

Table 8: Daily rhythms of Protein Profiles in 3 month Pineal

S. No.	Match ID	ZT6	ZT18	Max / min ratio	Mean 24 h
1	4	0.0056	0.047	8.31	0.026
2	8	0.0022	0.056	25.18	0.029
3	9	0.0042	0.089	21.38	0.047
4	10	0.0054	0.14	26.45	0.075
5	11	0.0062	0.083	13.36	0.045
6	18	0.0040	0.065	16.17	0.034
7	22	0.0052	0.028	5.37	0.016
8	23	0.0082	0.055	6.71	0.032
9	24	0.0051	0.050	9.92	0.028
10	30	0.0021	0.060	27.66	0.031
11	47	0.015	0.10	6.69	0.059
12	50	0.027	0.092	3.32	0.059
13	51	0.0059	0.15	25.40	0.079
14	52	0.0078	0.085	10.85	0.046
15	53	0.021	0.20	9.59	0.11
16	55	0.033	0.20	6.12	0.12
17	56	0.50	0.17	2.95	0.34
18	57	1.27	0.37	3.38	0.82
19	59	0.16	1.65	10.07	0.91
20	60	0.092	1.43	15.48	0.76
21	63	0.25	1.03	4.095	0.64
22	64	0.25	0.73	2.89	0.49
23	67	0.17	0.16	1.044	0.17
24	68	0.31	2.75	8.92	1.53
25	73	0.39	0.29	1.35	0.34
26	75	0.42	0.74	1.77	0.58
27	77	0.045	0.21	4.69	0.13
28	78	0.30	0.46	1.54	0.38
29	83	0.56	0.23	2.39	0.39
30	84	0.63	0.51	1.25	0.57
31	93	0.32	0.16	1.94	0.24
32	95	0.43	0.31	1.39	0.37
33	96	0.28	0.19	1.45	0.24
34	102	0.19	0.35	1.89	0.27
35	105	0.095	0.17	1.83	0.13
36	109	0.059	0.11	1.91	0.087
37	110	0.14	0.081	1.71	0.11
38	120	0.14	0.067	2.055	0.10
39	122	0.06	0.024	2.54	0.042
40	129	0.12	0.018	6.41	0.067
41	132	0.15	0.047	3.19	0.098
42	134	0.96	0.37	2.57	0.67
43	135	0.18	0.031	5.73	0.10
44	136	0.22	0.086	2.60	0.15
45	137	0.06	0.016	3.61	0.038
46	140	0.026	0.17	6.43	0.097
47	141	0.069	0.11	1.59	0.09
48	143	0.11	0.048	2.39	0.082

49	**161**	**0.51**	**0.32**	**1.57**	**0.41**
50	**165**	**0.063**	**0.013**	**4.98**	**0.038**
51	**171**	**0.12**	**0.24**	**1.95**	**0.18**
52	**182**	**0.23**	**0.12**	**1.96**	**0.17**
53	**185**	**0.75**	**0.19**	**3.75**	**0.47**

Each value in column 2 refers to particular protein spot id given by software, column 3 and 4 refers to mean percent volume of particular spot (n=2) in ZT6 and ZT18, column 5 refers daily pulse (max / min ratio) and column 6 refers mean 24 h levels.

Table 9: Daily rhythms of Protein Profiles in 12 month Pineal

S. No.	Match ID	ZT6	ZT18	Max / min ratio	Mean 24 h
1	**31**	**0.0046**	**0.10**	**23.39**	**0.056**
2	**38**	**0.0093**	**0.065**	**6.99**	**0.037**
3	**72**	**0.18**	**0.014**	**12.85**	**0.10**
4	**121**	**0.0065**	**0.098**	**14.93**	**0.052**
5	**247**	**0.075**	**0.11**	**1.48**	**0.094**
6	**258**	**0.014**	**0.34**	**23.41**	**0.18**
7	**294**	**0.19**	**0.016**	**11.71**	**0.10**
8	**318**	**0.18**	**0.0079**	**23.28**	**0.096**
9	**330**	**0.029**	**0.16**	**0.18**	**0.098**
10	**333**	**0.10**	**0.019**	**5.56**	**0.061**
11	**377**	**0.079**	**0.063**	**1.26**	**0.071**
12	**387**	**0.087**	**0.033**	**2.6**	**0.06**
13	**407**	**0.48**	**0.59**	**1.24**	**0.53**
14	**415**	**0.076**	**0.015**	**5.051**	**0.046**
15	**422**	**0.067**	**0.03**	**2.18**	**0.049**
16	**425**	**0.01**	**0.095**	**8.97**	**0.053**
17	**427**	**0.14**	**0.16**	**1.14**	**0.15**
18	**430**	**0.38**	**0.0055**	**69.69**	**0.19**
19	**435**	**0.070**	**0.0056**	**12.51**	**0.038**
20	**462**	**0.11**	**0.014**	**7.80**	**0.06**
21	**464**	**0.093**	**0.0054**	**17.086**	**0.049**

Each value in column 2 refers to particular protein spot id given by software, column 3 and 4 refers to mean percent volume of particular spot (n=2) in ZT6 and ZT18, column 5 refers daily pulse (max / min ratio) and column 6 refers mean 24 h levels.

Table 10: Daily rhythms of Protein Profiles in 24 month Pineal

S. No.	Match ID	ZT6	ZT18	Max / min ratio	Mean 24 h
1	1	0.31	0.46	1.51	0.38
2	3	0.0023	0.013	5.37	0.0075
3	7	0.035	0.083	2.35	0.059
4	10	0.022	0.0041	5.38	0.013
5	16	0.020	0.074	3.67	0.047
6	29	0.0038	0.067	17.43	0.035
7	32	0.014	0.078	5.33	0.046
8	43	0.0059	0.058	9.73	0.032
9	44	0.0083	0.053	6.34	0.031
10	48	0.032	0.19	6.27	0.11
11	50	0.0021	0.015	7.33	0.0088
12	65	0.011	0.092	8.32	0.051
13	66	0.014	0.098	7.026	0.056
14	69	0.37	0.080	4.67	0.23
15	70	0.051	0.10	2.068	0.078
16	73	0.0079	0.077	9.69	0.042
17	74	0.0082	0.049	5.96	0.028
18	77	0.0048	0.11	22.25	0.056
19	78	0.0045	0.063	13.97	0.034
20	79	0.0085	0.18	21.13	0.094
21	81	0.026	0.31	11.92	0.16
22	85	0.052	0.018	2.88	0.035
23	86	0.0037	0.026	6.91	0.015
24	88	0.032	0.11	3.42	0.072
25	94	0.019	0.12	6.23	0.071
26	99	0.075	0.22	2.95	0.15
27	102	0.031	0.27	8.75	0.15
28	115	0.23	0.14	1.70	0.18
29	124	0.24	0.67	2.81	0.45
30	125	0.39	0.68	1.73	0.54
31	126	0.36	0.22	1.61	0.29

Each value in column 2 refers to particular protein spot id given by software, column 3 and 4 refers to mean percent volume of particular spot (n=2) in ZT6 and ZT18, column 5 refers daily pulse (max / min ratio) and column 6 refers mean 24 h levels.

Table 11: Daily rhythms of Protein Profiles in 24 month Pineal

S. No.	Match ID	ZT6	ZT18	Max / min ratio	Mean 24 h
32	140	0.39	0.30	1.29	0.35
33	142	0.028	0.22	7.72	0.12
34	145	0.61	0.11	5.28	0.36
35	149	0.49	0.22	2.17	0.36
36	157	0.17	0.082	2.10	0.13
37	167	0.46	0.23	2.0025	0.35
38	178	0.10	0.16	1.50	0.13
39	182	0.061	0.11	1.85	0.088
40	184	0.088	0.12	1.44	0.10
41	197	0.079	0.13	1.61	0.10
42	200	0.15	0.029	5.085	0.090
43	202	0.11	0.0075	15.10	0.060
44	204	0.095	0.039	2.39	0.067
45	207	0.14	0.065	2.09	0.10
46	209	0.10	0.019	5.11	0.06
47	212	0.061	0.028	2.16	0.044
48	213	0.17	0.082	2.14	0.13
49	215	0.084	0.034	2.47	0.059
50	216	0.14	0.045	3.14	0.094
51	220	0.06	0.038	1.57	0.049
52	229	0.038	0.29	7.61	0.16
53	230	0.88	0.39	2.24	0.64
54	255	0.027	0.0043	6.18	0.015
55	265	0.05	0.13	2.52	0.089
56	282	0.014	0.084	5.81	0.049
57	283	0.12	0.049	2.41	0.083
58	286	0.11	0.052	2.078	0.08
59	289	0.16	0.058	2.72	0.11
60	296	0.013	0.076	5.60	0.045
61	301	0.015	0.11	7.11	0.063

Each value in column 2 refers to particular protein spot id given by software, column 3 and 4 refers to mean percent volume of particular spot (n=2) in ZT6 and ZT18, column 5 refers daily pulse (max / min ratio) and column 6 refers mean 24 h levels.

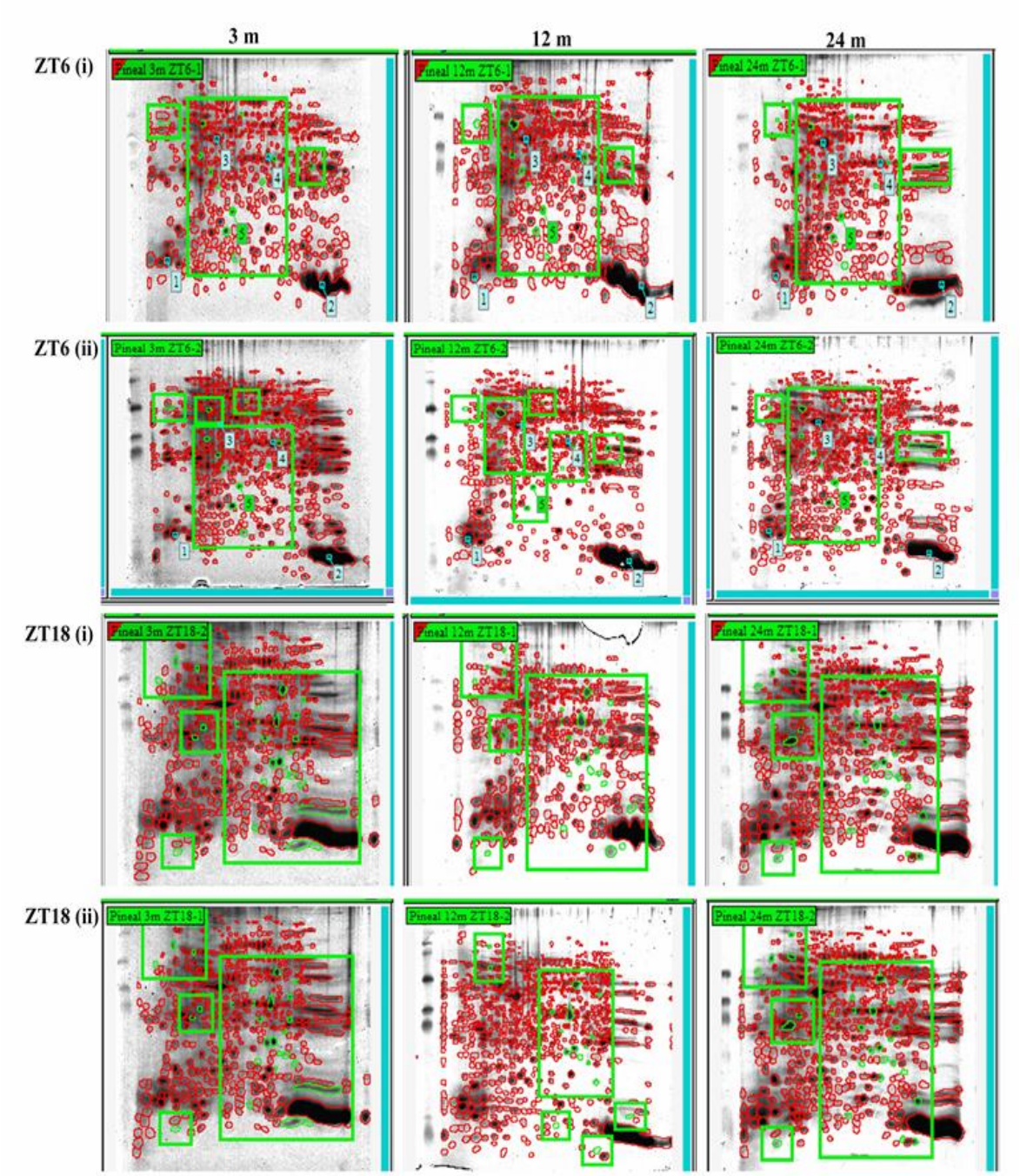

Fig. 53: Age induced alteration in protein profiles in pineal of variable age groups at ZT6 (i and ii) and ZT18 (i and ii) with n=2. Protein spots which were differentially expressed between 3, 12 and 24 m pineal at ZT6 and ZT18 were highlighted.

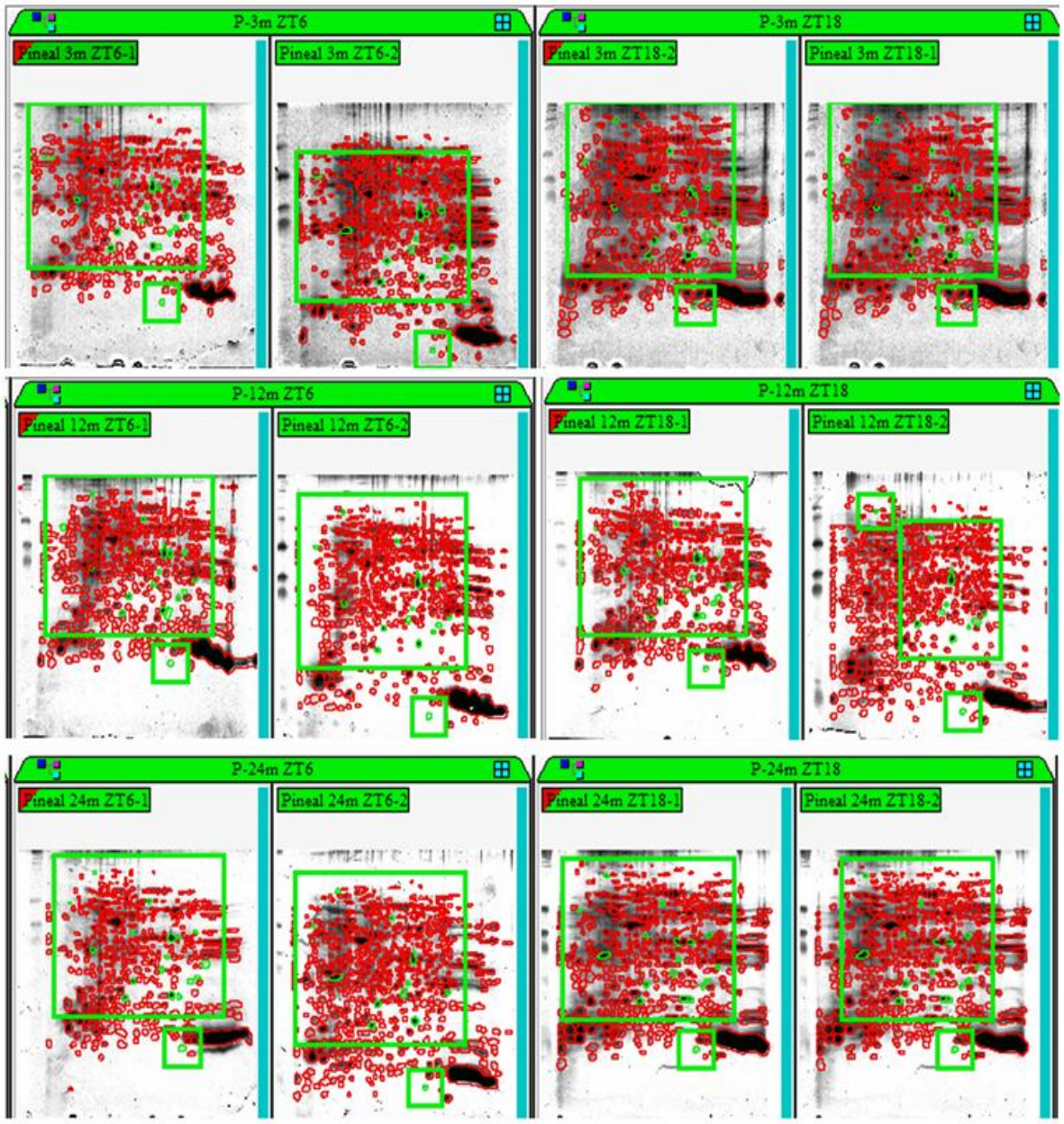

Fig. 54: Age induced alteration in protein profiles in variable age groups. Protein spots which were differentially expressed daily in 3, 12 and 24 m Pineal were highlighted.

(c) Studies of daily rhythms of protein profile in SN upon aging and in RIPD rat model

In 3 m at ZT6 and ZT18 the number of protein spots detected was 450 and 582, respectively. The correlation coefficient values between the biological replicates for the respective time points were 0.69 and 0.97. In 12 m at ZT6, 576 protein spots were matched; correlation coefficient value was 0.96. At ZT18 protein spots detected was 406 and the correlation coefficient value between replicates was 0.67. At ZT6, 348 protein spots were matched between replicates with correlation coefficient value of 0.78 in the 24 m group, whereas at ZT18 we found a total of 334 protein spots were matched with a correlation coefficient of 0.79. In the RIPD model 332 protein spots were detected at ZT6 and 342 at ZT18; the correlation coefficient values between the biological replicates of respective time points were 0.79 and 0.68. The number of protein spots which were showing daily rhythm is 60 in 3 m (Table 12; $p \leq 0.05$), whereas this number has been decreased to 31 in 12 m (Table 13; $p \leq 0.05$), 13 in 24 m (Table 14; $p \leq 0.05$; Fig. 55) and 12 in RIPD rat model (Fig. 58; $p \leq 0.05$). Of the 60 protein spots differentially expressed in 3 m, 10 were up regulated at ZT6 and 50 were at ZT18. In 12 m, 31 protein spots were differentially expressed, of these 24 were up regulated at ZT6 and 7 at ZT18. 13 protein spots differentially expressed in the 24 m of these 6 were up regulated at ZT6 and 7 were up regulated at ZT18. In the RIPD model 12 protein spots were differentially expressed, 5 were up regulated at ZT6 and 7 were up regulated at ZT18. The number of protein spots that have shown daily pulse (maximum: minimum ratio) greater than 5 is 24 in 3 m, 13 in 12 m and 4 in 24 m. Differentially expressed protein spots between 3, 12 and 24 m at ZT6 are 20 and at ZT18 are 24 (Fig. 56; $p \leq 0.05$); between vehicle and RIPD rat model at ZT6 are 10 and ZT18 are 6 (Fig. 59; $p \leq 0.05$). 19 protein spots were differentially expressed between all the 3, 12 and 24 m and within a day (Fig. 57; $p \leq 0.05$). 8 protein spots were differentially expressed between vehicle and RIPD rat model and within a day (Fig. 60; $p \leq 0.05$).

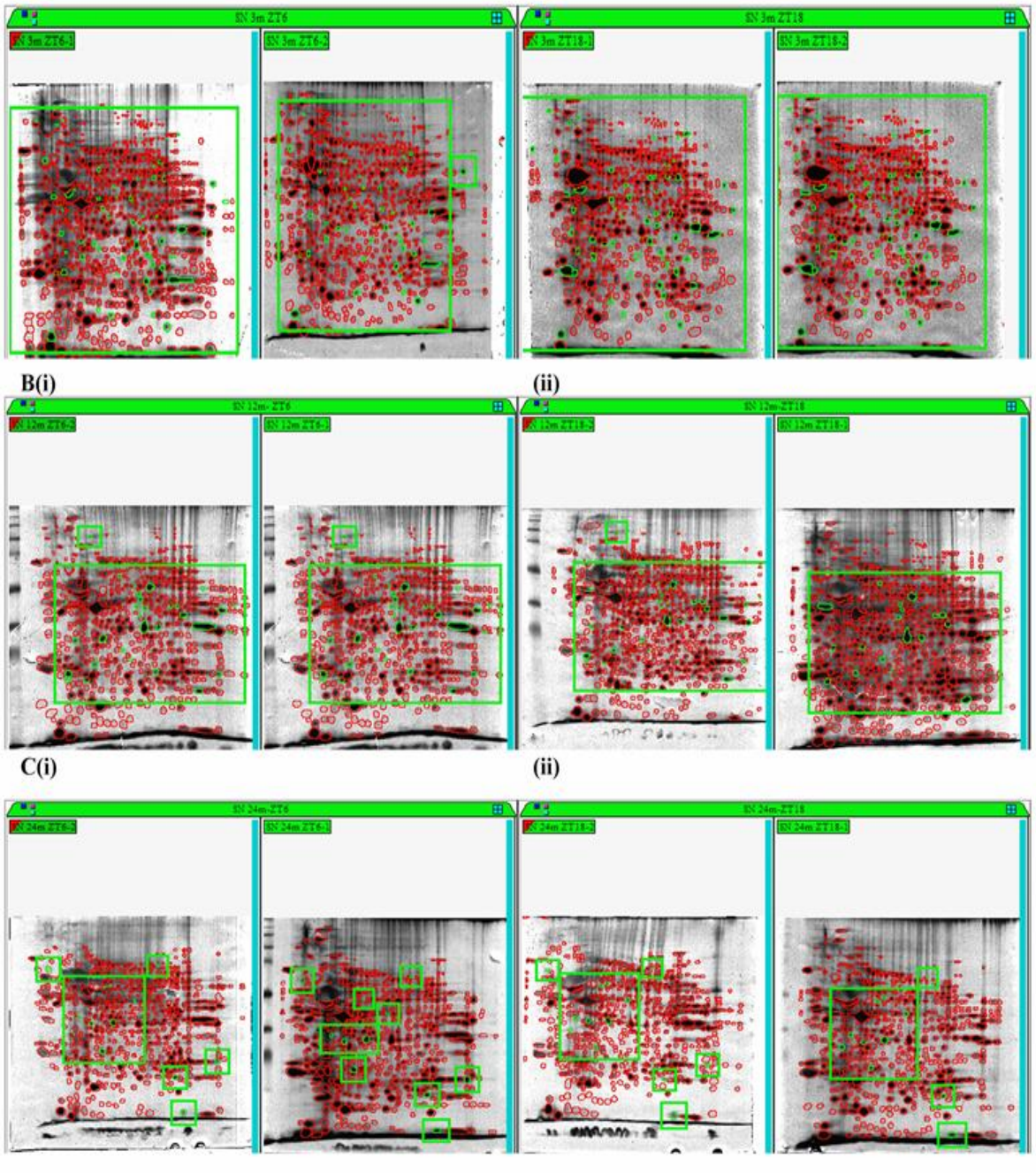

Fig. 55: Age induced alteration in protein profiles in variable age groups. (A) 3, (B) 12 and (C) 24 m SN at (i) ZT6 and (ii) ZT18 with n=2. Protein spots which were differentially expressed between ZT6 and ZT18 of SN are highlighted with green.

Table 12: Daily rhythms of Protein Profiles in 3 month SN

S. No.	Match ID	ZT6	ZT18	Max / min ratio	Mean 24 h
1	3	0.0044	0.052	11.75	0.028
2	6	0.0054	0.034	6.24	0.019
3	9	0.0050	0.032	6.38	0.018
4	37	0.015	0.18	12.34	0.098
5	39	0.0073	0.051	6.97	0.029
6	40	0.018	0.051	2.73	0.034
7	44	0.029	0.28	9.30	0.15
8	46	0.027	0.29	10.63	0.16
9	52	0.063	0.36	5.81	0.21
10	56	0.012	0.12	9.98	0.069
11	72	0.0097	0.062	6.40	0.036
12	75	0.039	0.11	2.95	0.077
13	80	0.0016	0.056	34.099	0.029
14	81	0.012	0.073	6.19	0.042
15	84	0.0025	0.064	25.27	0.033
16	102	0.06	1.026	16.97	0.54
17	105	0.50	1.18	2.34	0.84
18	107	0.015	0.10	6.82	0.058
19	110	0.026	0.053	2.040	0.039
20	112	0.022	0.14	6.15	0.08
21	113	0.0032	0.059	18.19	0.031
22	120	0.0039	0.082	20.91	0.043
23	125	0.0057	0.11	19.18	0.058
24	129	0.049	1.41	28.56	0.73
25	130	0.13	0.18	1.45	0.156
26	136	0.034	0.10	2.99	0.068
27	138	1.11	0.52	2.12	0.81
28	146	0.84	0.61	1.37	0.72
29	151	0.43	0.22	1.98	0.32
30	156	0.26	0.15	1.68	0.20
31	157	0.09	0.15	1.72	0.12
32	162	0.028	0.17	6.34	0.10
33	178	0.11	0.15	1.38	0.13
34	193	0.21	0.28	1.29	0.25
35	198	0.059	0.11	1.92	0.086
36	208	0.13	0.27	2.10	0.19
37	212	0.060	0.099	1.64	0.079
38	225	0.084	0.15	1.78	0.12
39	226	0.059	0.17	2.87	0.11
40	230	0.10	0.19	1.94	0.15
41	231	0.045	0.16	3.62	0.10
42	241	0.041	0.087	2.10	0.064
43	246	0.072	0.23	3.19	0.15
44	248	0.32	0.33	1.045	0.33
45	251	0.056	0.15	2.74	0.10
46	252	0.13	0.20	1.51	0.17
47	260	0.072	0.14	2.025	0.11
48	276	0.097	0.14	1.46	0.12
49	285	0.055	0.015	3.55	0.035
50	294	0.082	0.018	4.55	0.050
51	305	0.018	0.24	13.22	0.13
52	306	0.097	0.016	6.065	0.056
53	324	0.30	0.19	1.53	0.25
54	330	0.042	0.31	7.39	0.17

55	332	0.082	0.13	1.57	0.10
56	353	0.037	0.10	2.83	0.071
57	356	0.028	0.079	2.81	0.053
58	366	0.061	0.019	3.21	0.040
59	372	0.11	0.17	1.59	0.14
60	392	0.085	0.31	3.71	0.199731

Each value in column 2 refers to particular protein spot id given by software, column 3 and 4 refers to mean percent volume of particular spot (n=2) in ZT6 and ZT18, column 5 refers daily pulse (max / min ratio) and column 6 refers mean 24 h levels.

Table 13: Daily rhythms of Protein Profiles in 12 month SN

S. No.	Match ID	ZT6	ZT18	Max / min ratio	Mean 24 h
1	5	0.064	0.0092	7.0083	0.037
2	23	0.053	0.0076	6.96	0.030
3	33	0.019	0.40	20.85	0.21
4	55	2.050	0.24	8.37	1.14
5	83	0.29	0.67	2.24	0.48
6	93	0.31	0.025	12.79	0.17
7	94	0.20	0.012	17.044	0.11
8	99	0.26	0.031	8.43	0.15
9	101	0.68	0.40	1.67	0.54
10	108	0.21	0.0098	21.29	0.11
11	122	0.35	0.12	2.89	0.24
12	134	0.078	0.097	1.23	0.088
13	153	0.092	0.11	1.23	0.10
14	168	0.22	0.19	1.16	0.21
15	172	0.49	0.17	2.87	0.33
16	189	0.13	0.53	4.061	0.33
17	197	1.12	0.68	1.64	0.90
18	199	0.14	0.096	1.43	0.11
19	207	0.06	0.0057	10.61	0.033
20	208	0.38	0.18	2.073	0.28
21	220	0.56	0.096	5.89	0.33
22	222	0.11	0.0045	25.89	0.060
23	223	0.064	0.15	2.31	0.10
24	224	0.11	0.046	2.48	0.080
25	225	0.089	0.13	1.51	0.11
26	227	0.16	0.019	7.99	0.089
27	237	0.098	0.028	3.53	0.063
28	243	0.079	0.024	3.24	0.052
29	245	0.088	0.0084	10.34	0.048
30	252	0.47	0.39	1.19	0.43
31	274	0.070	0.039	1.76	0.055

Each value in column 2 refers to particular protein spot id given by software, column 3 and 4 refers to mean percent volume of particular spot (n=2) in ZT6 and ZT18, column 5 refers daily pulse (max / min ratio) and column 6 refers mean 24 h levels.

Table 14: Daily rhythms of Protein Profiles in 24 month SN

S. No.	Match ID	ZT6	ZT18	Max / min ratio	Mean 24 h
1	20	0.026	0.12	4.55	0.072
2	36	0.012	0.074	6.31	0.043
3	38	0.024	0.079	3.25	0.052
4	47	0.011	0.16	13.44	0.085
5	57	0.35	0.49	1.40	0.42
6	93	0.43	0.65	1.51	0.54
7	126	0.36	0.20	1.79	0.28
8	161	0.48	0.079	6.058	0.28
9	181	0.27	0.16	1.71	0.21
10	219	0.19	0.13	1.55	0.16
11	228	0.056	0.14	2.44	0.097
12	312	0.22	0.037	6.025	0.12
13	316	0.059	0.026	2.26	0.043

Each value in column 2 refers to particular protein spot id given by software, column 3 and 4 refers to mean percent volume of particular spot (n=2) in ZT6 and ZT18, column 5 refers daily pulse (max / min ratio) and column 6 refers mean 24 h levels.

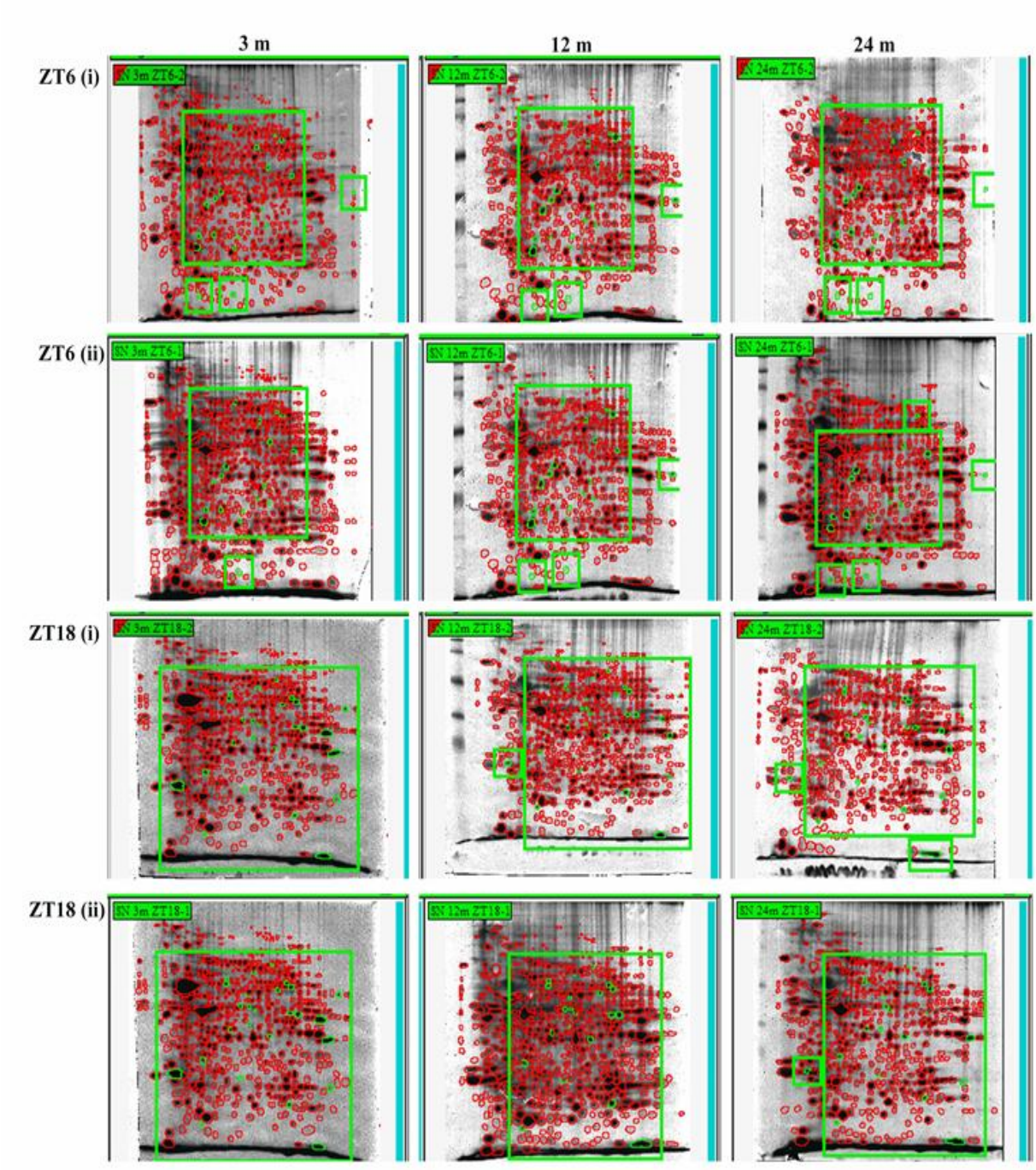

Fig. 56: Age induced alteration in protein profiles in SN of variable age groups at ZT6 (i and ii) and ZT18 (i and ii) with n=2. Protein spots which were differentially expressed between 3, 12 and 24 m SN at ZT6 and ZT18 were highlighted.

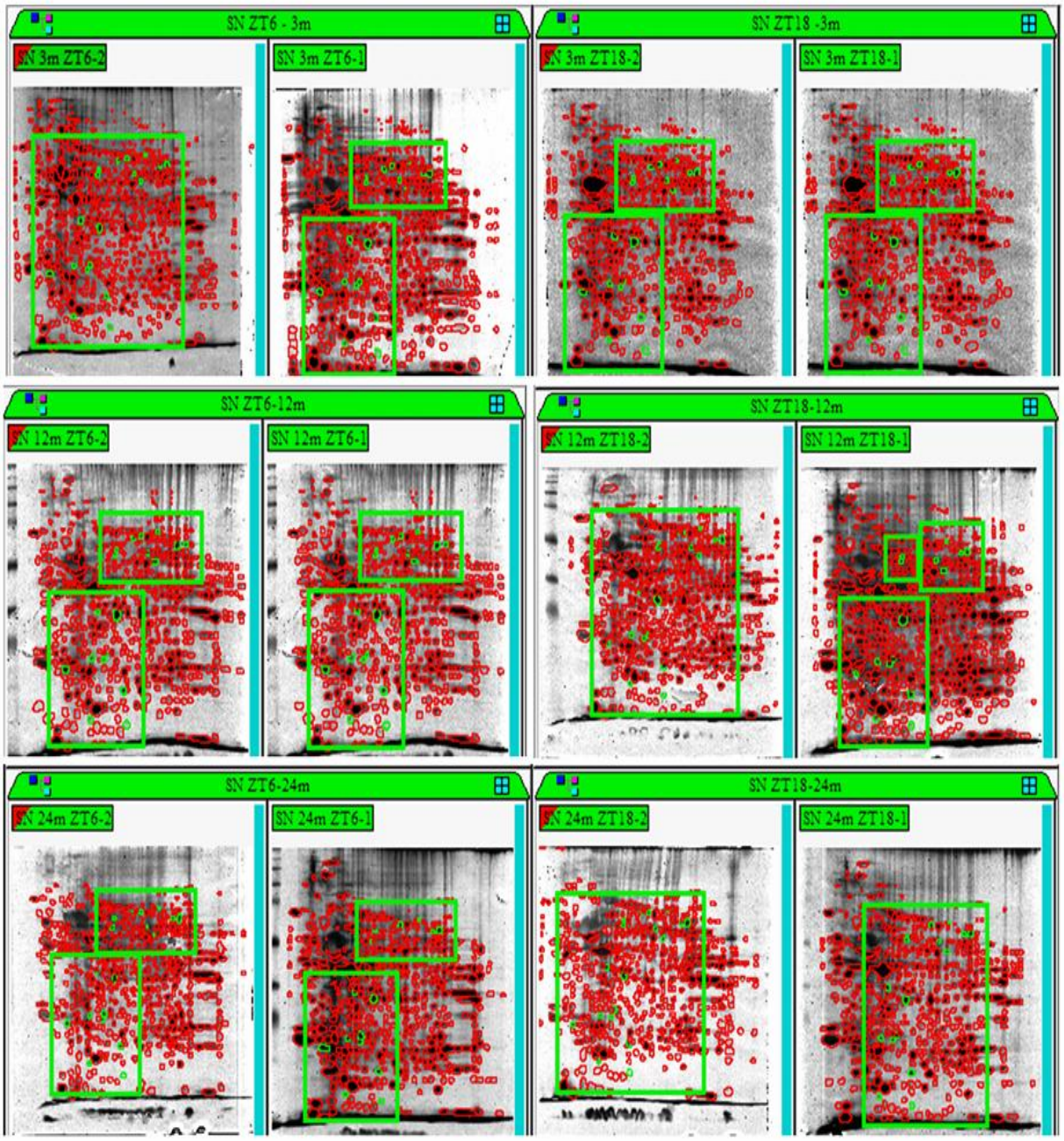

Fig. 57: Age induced alteration in protein profiles in variable age groups. Protein spots which were differentially expressed daily in 3, 12 and 24 m SN were highlighted.

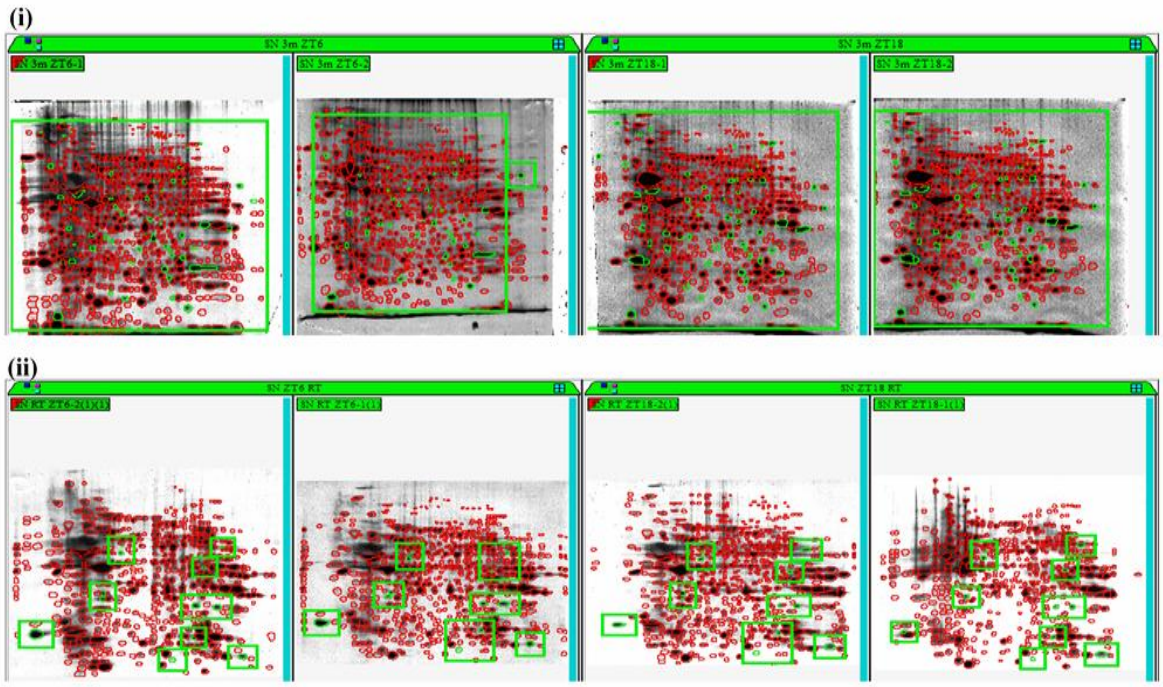

Fig. 58: Daily rhythms of Protein Profiles in SN of Control and Rotenone induced Parkinson's disease (RIPD) rat model. Protein spots which were differentially expressed between ZT6 and ZT18 of Control A(i) and (ii) and RIPD B(i) and (ii) were highlighted with green.

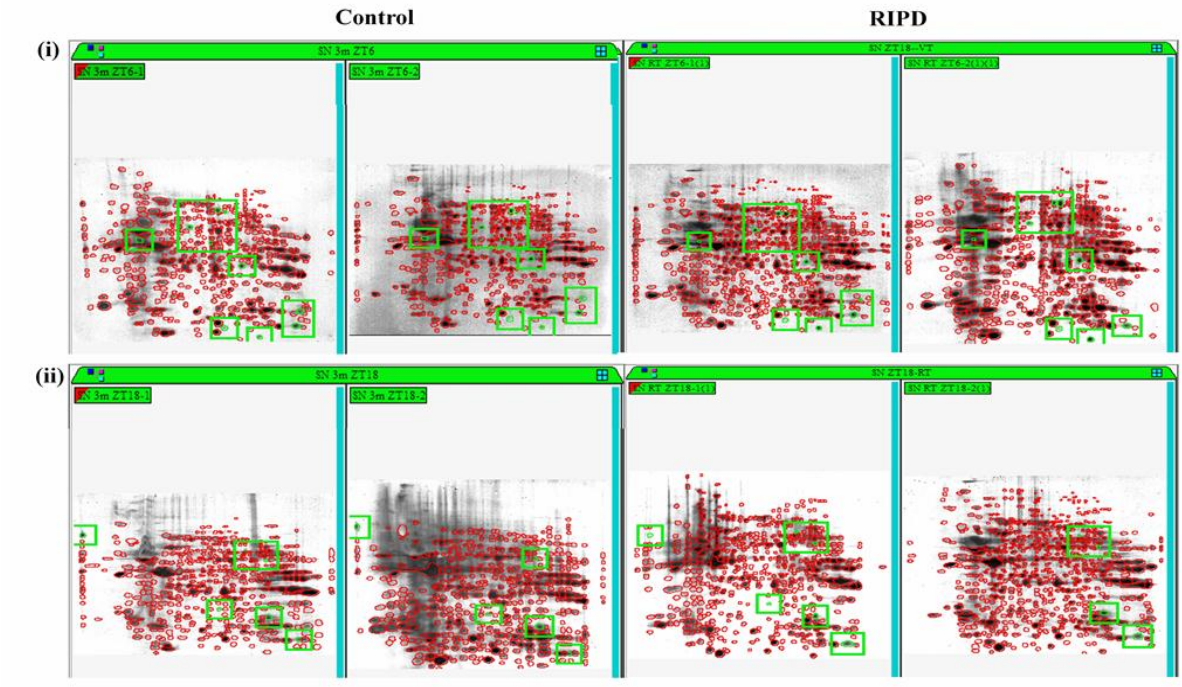

Fig. 59: Daily rhythms of Protein Profiles in SN at ZT6 (i) and ZT18 (ii) of Control and Rotenone induced Parkinson's disease (RIPD) rat model.

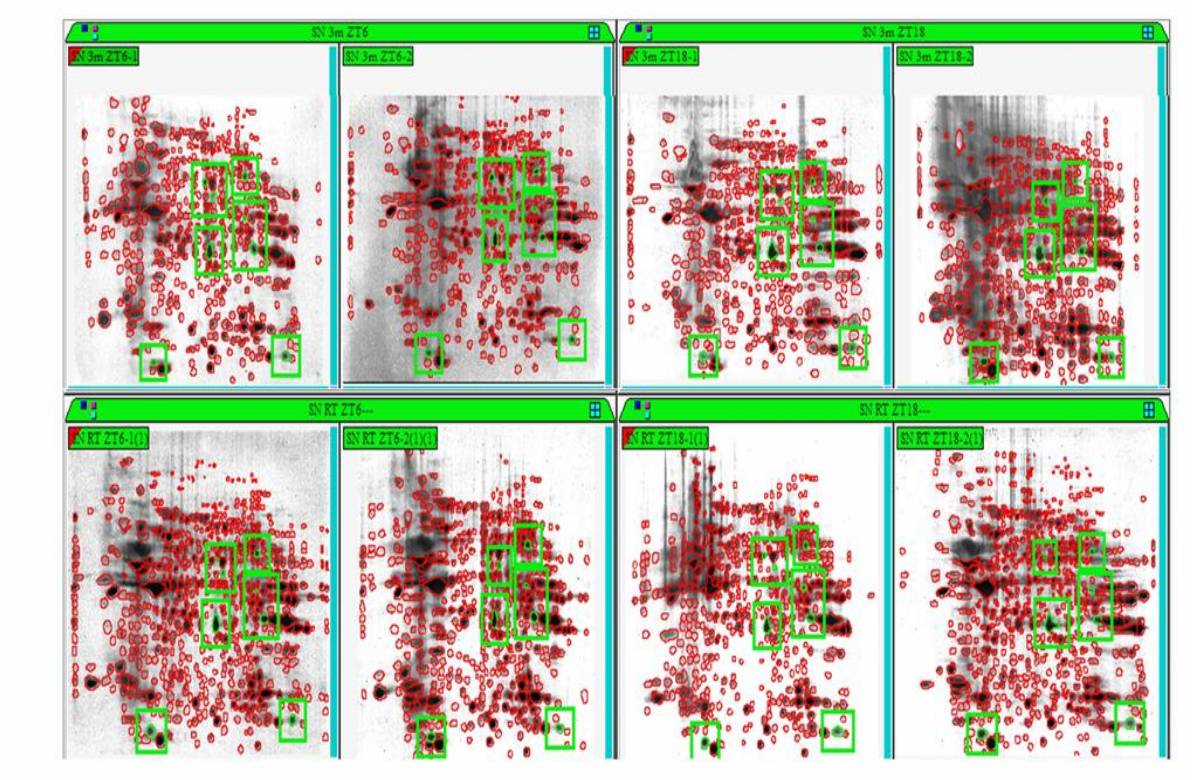

Fig. 60: Daily rhythms of Protein Profiles in SN of Control and Rotenone induced Parkinson's disease (RIPD) rat model. Protein spots which were differentially expressed daily in SN of control and RIPD rat model were highlighted.

Table 15: Daily rhythms of Protein Profiles in aging and RIPD rat model

Protein spots with daily rhythm				
Tissue	**Age in months (m)**			**RIPD**
	3 m	**12m**	**24 m**	
SCN	**35**	**22**	**9**	**10**
Pineal	**51**	**22**	**61**	**?**
SN	**60**	**31**	**13**	**12**

Each value refers to number of differentially expressed protein spots between ZT6 and ZT18 in SCN, Pineal and SN of RIPD rat model, 3, 12 and 24m.

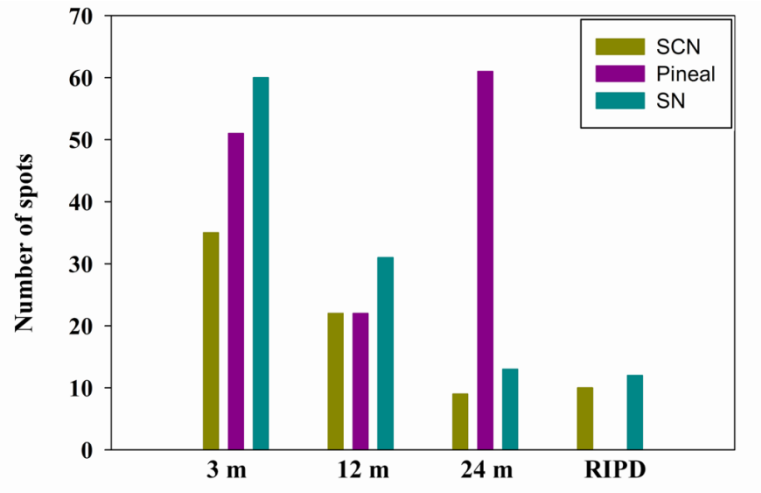

Fig. 61: Alterations in the number of protein spots which were differentially expressed daily in SCN, Pineal and SN. 3 month (m), 12 m, 24 m and rotenone induced Parkinson's disease (RIPD) rat model.

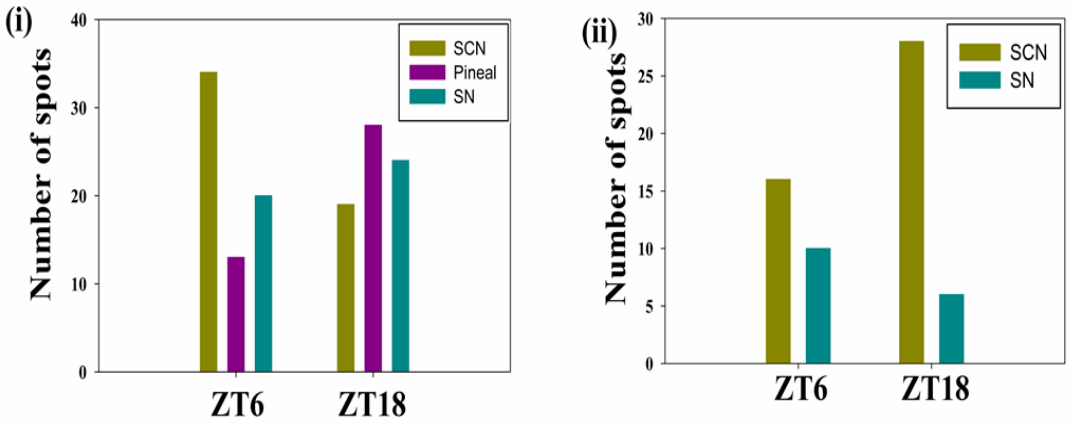

Fig. 62: Age induced alterations in the number of protein spots which were differentially expressed in (i) variable age groups and (ii) Rotenone induced Parkinson's disease (RIPD) rat model at ZT6 and ZT18.

OBJECTIVE – IV

4. Studies of daily rhythms of various clock gene expression in SCN, Pineal and SN upon aging and in RIPD rat model

(a) Age induced alterations in daily rhythms and levels of expression of various clock genes in the SCN:

Per1: Daily rhythm of *Per1* gene expression persisted in 3, 12 and 24 m. Maximum and minimum expression levels of this gene was observed to be at ZT6 and ZT0 respectively in the 3 m, at ZT18 and ZT6 in the12 m and ZT0 and ZT12 in the 24 m animals. When compared to the 3 m group the expression peek was delayed approximately by 12 h in the 12 m, whereas it was advanced approximately by 6 h in the 24 m group. The maximum expression levels were also delayed by approximately by 6 h in the 24 m in comparison to the 12 m animals (Fig. 63; $p \leq 0.05$). Mean 24 h levels were not altered significantly from 3 to 24 m, whereas daily pulse in 24 m has been increased by about 2.65 and 5.39 fold compared to 3 and 12 m respectively (Fig. 64, Table 16; $p \leq 0.05$).

Per2: In 3 m daily rhythm was observed with maximum levels at ZT12 and minimum at ZT18, in 12 m daily rhythm persisted and maximum levels were observed at ZT18 and minimum at ZT12 that means maximum levels in 12 m has shown approximately 6h delay compared to 3 m. In 24 m phase of the daily rhythm and the pattern was persisted and its maximum levels were observed at ZT12 and minimum at ZT0 (Fig. 63; $p \leq 0.05$). Mean 24 h levels in 24 m were decreased by 0.27 and 0.11 fold compared to 3 and 12 m respectively, whereas daily pulse in 12 m has been increased by about 2.78 and 1.86 fold compared to 3 and 24 m respectively (Fig. 64, Table 16; $p \leq 0.05$).

Cry1 and *2:* The rhythmic expression profile was persisted in both the 3 and 12 m old animals. In 24 m old animals, the expression of both *Cry1* and *2* could be detected only at ZT12. The maximum and minimum levels of expression were observed respectively at ZT12 and ZT0 in 3 m. In 12 m animals the expression peek was delayed approximately by 6 h at ZT18 and the 3 m of expression was at ZT12 (Fig. 63; $p \leq 0.05$). Mean 24 h levels of *Cry1* was increased in 12 m by about 5.95 fold compared to 3 m and then decreased in 24 m by about 0.28 fold compared to 12 m. Daily pulse of *Cry1* in 12 m has been decreased by about 0.02 fold compared to 3 m.

Mean 24 h levels of *Cry2* were increased in 12 m by about 6.54 fold compared to 3 m and then decreased in 24 m by about 0.35 fold compared to 12 m. Daily pulse of *Cry2* in 12 m has been decreased by about 0.07 fold compared to 3 m (Fig. 64, Table 16; $p \leq 0.05$).

Bmal1: Daily rhythm was observed in 3 m with maximum levels at ZT18 and minimum at ZT0**,**in 12 m daily rhythm persisted and maximum levels were observed at ZT6 and minimum at ZT12 that means maximum levels in 12 m has shown approximately 12h advance compared to 3 m. We could detect *Bmal1* levels at only ZT12 in 24 m but not at other time points (Fig. 63; $p \leq 0.05$). Mean 24 h levels were not altered significantly between 3 and 12 m, however decreased in 24 m by about 0.3 fold compared to 3 and 12 m respectively. Daily pulse in 12 m has been decreased by about 0.005 fold compared to 3 m (Fig. 64, Table 16; $p \leq 0.05$).

Table 16. Clock gene expression in 3, 12 and 24 m SCN

Genes	Age in Months (m)	Gene expression levels (relative gene expression)		Ratio	Mean levels
		maximum	minimum		
Per1	3	0.036 ± 0.002	0.0081 ± 0.0011 [q]	4.72 ± 0.76	0.019±0.0027
	12	0.02 ± 0.001 [x]	0.0098 ± 0.0008 [q]	2.32±0.28 [x]	0.016±0.001
	24	0.07 ± 0.006 [x, y]	0.0056 ± 0.0006 [q, y]	12.5±0.74 [x, y]	0.024±0.007
Per2	3	0.005 ± 0.0005	0.00037 ± 0.0001 [q]	3.5±0.63	0.0022±0.0004
	12	0.012±0.0005 [x]	0.0013±0.0001 [q, x]	9.75±0.58 [x]	0.0052±0.0011 [x]
	24	0.001±0.00009 [x, y]	0.00031±0.00009 [q, y]	5.23±2.09 [y]	0.0006±0.00009 [x, y]
Cry1	3	0.003±0.0002	0.000024±0.000003 [q]	132±15	0.0009±0.0003
	12	0.0104±0.0003 [x]	0.0011±0.00006 [q, x]	9.03±0.38 [x]	0.0053±0.0009 [x]
	24	0.0015±0.0001 [x, y]	?	?	0.0015±0.0001 [y]
Cry2	3	0.032±0.003	0.000003±0.0000003 [q]	147±72	0.0082±0.003
	12	0.106±0.006 [x]	0.0099±0.001 [q, x]	10.89±0.63 [x]	0.053±0.009 [x]
	24	0.019±0.0016 [x, y]	?	?	0.019±0.0016 [x, y]
Bmal1	3	0.44±0.008	0.00003±0.000001 [q]	1461±256	0.018±0.005
	12	0.031±0.003 [x]	0.004±0.0002 [q, x]	8.15±1.22 [x]	0.017±0.0027
	24	0.0051±0.0002 [x, y]	?	?	0.0051±0.0002 [x, y]

Each value is mean ± SEM (n=4), $p \leq 0.05$ and expressed in relative gene expression. $p_x \leq 0.05$, $p_y \leq 0.05$ and $p_z \leq 0.05$ (where x, y and z refers to comparison with 3, 12 and 24 m respectively and q refers to comparison between maximum and minimum within the group).

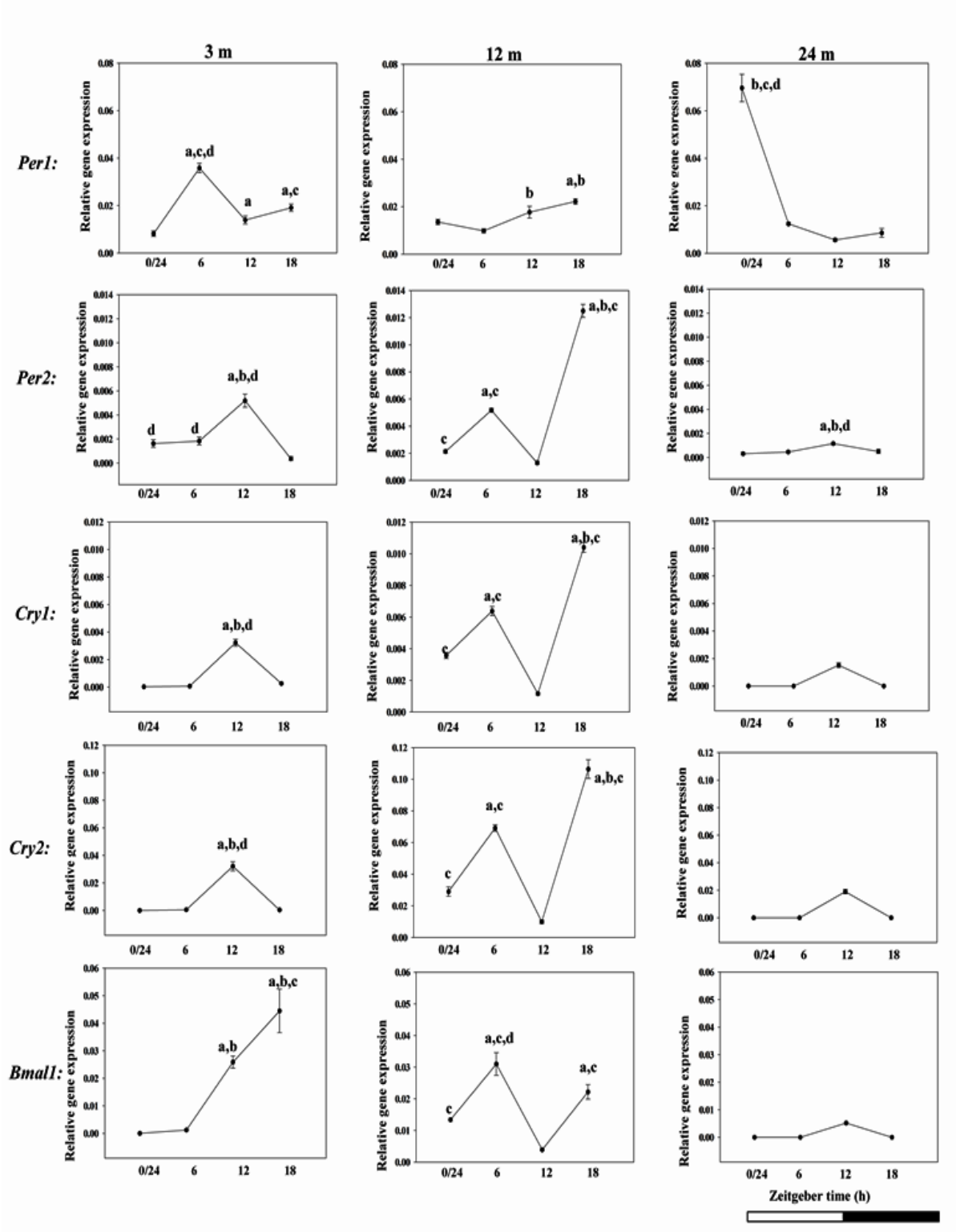

Fig. 63: Effect of aging on expression of *Per1*, *Per2*, *Cry1*, *Cry2* and *Bmal1* genes in the SCN of male wistar rat. Each value is mean ± SEM (n=4), $p \leq 0.05$ and expressed in relative gene expression. 3, 12 and 24 m. $p_a \leq 0.05$; $p_b \leq 0.05$, $p_c \leq 0.05$ and $p_d \leq 0.05$ (where a, b, c and d refers to comparison with ZT-0, ZT-6, ZT-12 and ZT-18 respectively within the group).

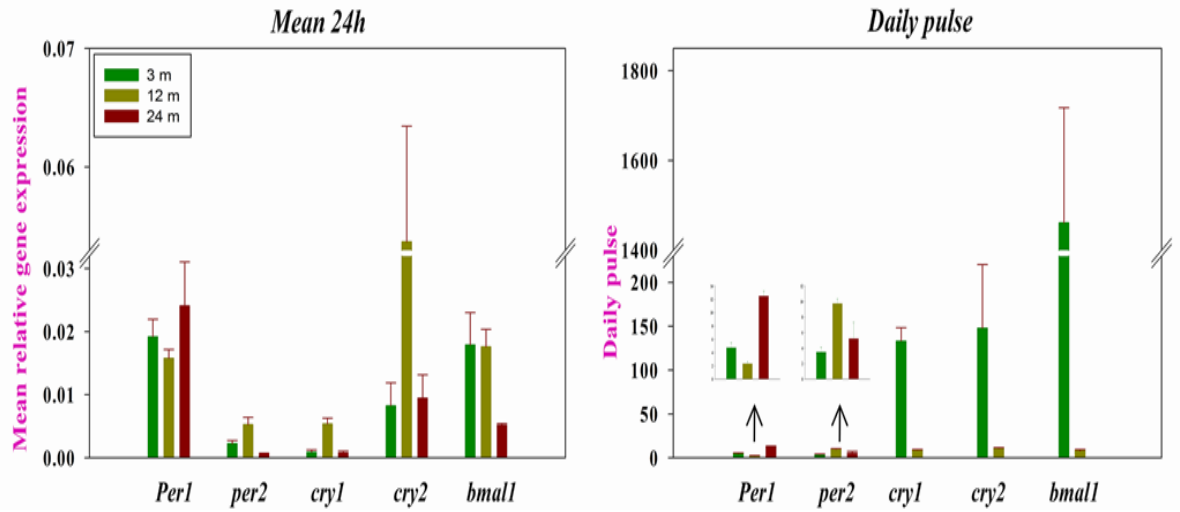

Fig. 64: Effect of aging on mean 24 h levels and daily pulse of various clock genes expression in SCN of male wistar rat.

(b) Effect of aging on various clock gene expression levels and its rhythmicity in the Pineal:

Per1: Daily rhythm persisted in 3, 12 and 24 m. The maximum and minimum expression levels were observed at ZT18 and ZT6 in 3 m, at ZT18 and ZT12 in 12 m and ZT0 and ZT6 in 24 m. Maximum levels in 24 m has shown approximately 6h delay when compared to both 3 and 12 m (Fig. 65; $p \leq 0.05$). Mean 24 h levels were increased by 2.27 fold in 12 m compared to 3 m and then decreased by about 0.78 fold in 24 m compared to 12 m whereas daily pulse in 24 m has been decreased by about 0.22 in 12 m compared to 3 m and then increased by about 4.43 fold in 24m compared to 12 m (Fig. 66, Table 17; $p \leq 0.05$).

Per2: Daily rhythm was observed in 3 m with maximum levels at ZT18 and minimum at ZT6, in 12 m daily rhythm persisted and maximum levels were observed at ZT6 and minimum at ZT0 that means maximum levels in 12 m has shown approximately 12h advance compared to 3 m. In 24 m phase of the daily rhythm persisted and its maximum levels were observed at ZT18 and minimum at ZT12 (Fig. 65; $p \leq 0.05$). Mean 24 h levels were not altered upon aging,

whereas daily pulse in 12 and 24 m were decreased by 0.03 and 0.034 fold respectively compared to 3 m (Fig. 66, Table 17; $p \leq 0.05$).

Cry1: In 3 m daily rhythm was observed with maximum levels at ZT18 and minimum at ZT0, in 12 m daily rhythm persisted and maximum levels were observed at ZT6 and minimum at ZT0 that means maximum levels in 12 m has shown approximately 12h advance compared to 3 m. In 24 m daily rhythm persisted and maximum levels were observed at ZT12 and minimum at ZT6 that means maximum levels in 24 m has shown approximately 6h advance compared to 3 m and approximately 6h delay compared to 12 m (Fig. 65; $p \leq 0.05$). Mean 24 h levels were increased by 1.54 fold in 12 m compared to 3 m and then decreased by about 0.1 fold in 24 m compared to 12 m whereas daily pulse in 12 and 24 m has been decreased by about 0.02 and 0.03 fold respectively compared to 3 m (Fig. 66, Table 17; $p \leq 0.05$).

Cry2: Daily rhythm was observed in 3 m with maximum levels at ZT18 and minimum at ZT0, in 12 m daily rhythm persisted and maximum levels were observed at ZT6 and minimum at ZT18 that means maximum levels in 12 m has shown approximately 12h advance compared to 3 m. In 24 m phase of the daily rhythm persisted and its maximum levels were observed at ZT18 and minimum at ZT0 (Fig. 65; $p \leq 0.05$). Mean 24 h levels were decreased in 24 m by about 0.09 and 0.05 fold compared to 3 and 12 m respectively. Daily pulse in 12 and 24 m has been decreased by about 0.005 and 0.0008 fold respectively compared to 3 m (Fig. 66, Table 17; $p \leq 0.05$).

Bmal1: The rhythmic pattern of gene expression has persisted in 3, 12 and 24 m. The maximum and minimum expression levels were observed to be respectively at ZT18 and ZT0 in 3 m, ZT6 and ZT18 in 12 m and ZT18 and ZT6 in 24 m. The gene expression has peaked with a 12 h phase advance in 12 m in comparison to the 3 m. (Fig. 65; $p \leq 0.05$). Mean 24 h levels were increased by 2.26 fold in 12 m compared to 3 m and then decreased by about 0.01 fold in 24 m compared to 12 m. Daily pulse were increased by 4.59 fold in 12 m compared to 3 m and then decreased by about 0.08 fold in 24 m compared to 12 m (Fig. 66, Table 17; $p \leq 0.05$).

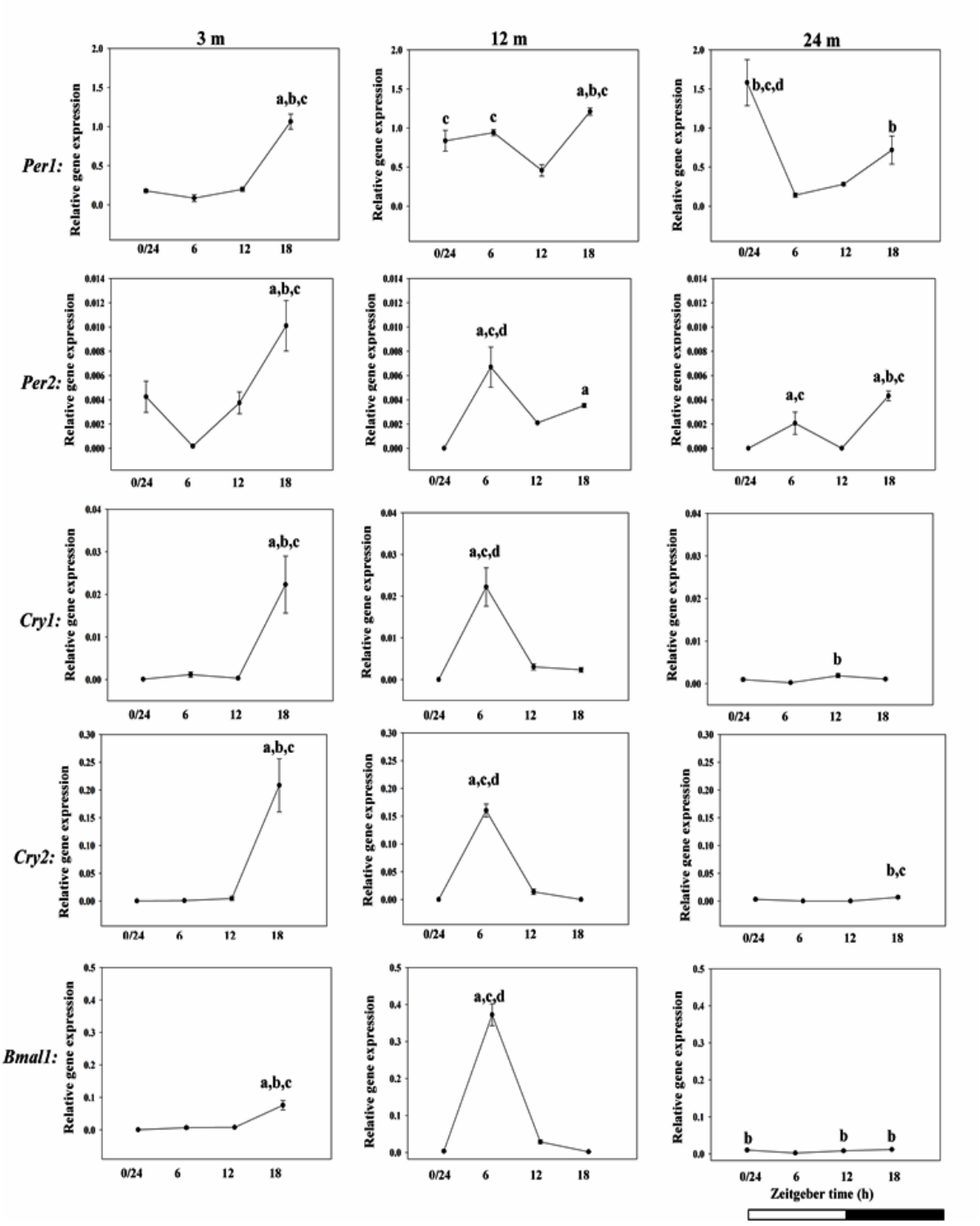

Fig. 65: Effect of aging on expression of *Per1*, *Per2*, *Cry1*, *Cry2* and *Bmal1* genes in the Pineal of male wistar rat. Each value is mean ± SEM (n=4), $p \leq 0.05$ and expressed in relative gene expression. 3, 12 and 24 m. $p_a \leq 0.05$; $p_b \leq 0.05$, $p_c \leq 0.05$ and $p_d \leq 0.05$ (where a, b, c and d refers to comparison with ZT0, ZT6, ZT12 and ZT18 respectively within the group).

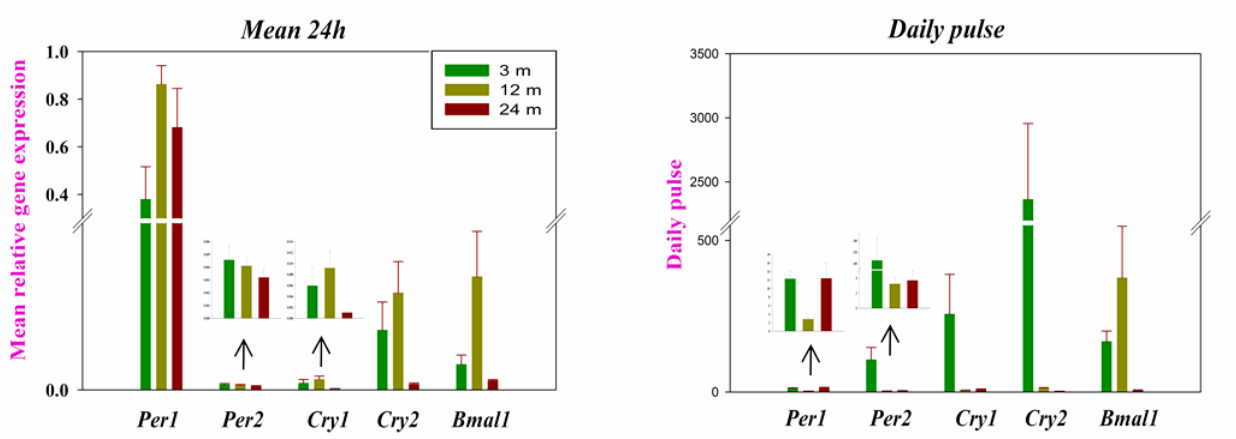

Fig. 66: Effect of aging on mean 24 h levels and daily pulse of various clock genes expression in Pineal of male wistar rat.

Table 17. Clock gene expression in 3, 12 and 24 m Pineal

Genes	Age in Months (m)	Gene expression levels (relative gene expression)		Ratio	Mean levels
		maximum	minimum		
Per1	3	1.06±0.09	0.08±0.044 ^{q}	12.29±1.8	0.38±0.14
	12	1.21±0.04	0.46±0.07 $^{q, x}$	2.79±0.33 ^{x}	0.86±0.079 ^{x}
	24	1.58±0.29 $^{x, y}$	0.14±0.026 $^{q, y}$	12.39±3.56 ^{y}	0.68±0.16 ^{x}
Per2	3	0.01±0.002	0.0002±0.00009 ^{q}	105±41	0.004±0.001
	12	0.006±0.001 ^{x}	0.002±0.00006 $^{x, q}$	3.23±0.84 ^{x}	0.004±0.0007
	24	0.0043±0.0004 ^{x}	0.002±0.0009 $^{x, q}$	3.68±1.28 ^{x}	0.003±0.0006
Cry1	3	0.023±0.0006	0.00008±0.000005 ^{q}	256±131	0.006±0.003
	12	0.022±0.004	0.0023±0.0005 $^{q, x}$	5.46±1.54 ^{x}	0.009±0.003 ^{x}
	24	0.0018±0.0004 $^{x, y}$	0.00022±0.000005 $^{q, y}$	8.32±2.08 ^{x}	0.001±0.0002 $^{x, y}$
Cry2	3	0.21±0.047	0.00009±0.000005 ^{q}	2362±593	0.053±0.02
	12	0.16±0.012	0.014±0.005 $^{q, x}$	12.48±2.33 ^{x}	0.087±0.028
	24	0.0068±0.002 $^{x, y}$	0.003±0.001 $^{q, y}$	1.97±0.82 ^{x}	0.005±0.001 ^{y}
Bmal1	3	0.076±0.014	0.0004±0.00002 ^{q}	166±35	0.023±0.008
	12	0.37±0.03 ^{x}	0.0016±0.0006 $^{x, q}$	376±170	0.1±0.04 ^{x}
	24	0.012±0.001 $^{x, y}$	0.0022±0.0006 $^{x, q}$	6.36±1.27 ^{x}	0.008±0.001 ^{y}

Each value is mean ± SEM (n=4), $p \leq 0.05$ and expressed in relative gene expression. $p_x \leq 0.05$, $p_y \leq 0.05$ and $p_z \leq 0.05$ (where x, y and z refers to comparison with 3, 12 and 24 m respectively and q refers to comparison between maximum and minimum within the group).

(c) Effect of aging on various clock gene expression levels and its rhythmicity in the SN:

Per1: The daily rhythm of gene expression persisted in 12 and 24 m as seen in 3 m. The peak and trough of gene expression levels were observed respectively at ZT18 and ZT6 in 3 m, ZT6 and ZT0 in 12 m and ZT0 and ZT12 in 24 m. Maximum expression levels showed phase advancement of 12 h in the 12 m group, whereas a 6 h phase delay in the 24 m group when compared to the 3 m old animals. 6 h phase advancement could also be observed in the 24 m in comparison to the 12 m group (Fig. 67; $p \leq 0.05$). Mean 24 h levels were increased in 12 and 24 m by about 10.31 and 8.75 fold respectively compared to 3 m whereas daily pulse in 12 and 24 m has been decreased by about 0.26 and 0.12 fold respectively compared to 3 m (Fig. 68, Table 18; $p \leq 0.05$).

Per2: Maximum and minimum expression levels were observed respectively at ZT12 and ZT6 in 3 m, ZT0 and ZT18 in 12 m and ZT12 and ZT0 in 24 m. The gene expression in 12 m peeked with an approximate 12 h phase advancement when compared to the 3 m. (Fig. 67; $p \leq 0.05$). Mean 24 h levels in 24 m were increased by 1.56 fold compared to 12 m, whereas daily pulse did not alter upon aging (Fig. 68, Table 18; $p \leq 0.05$).

Cry1: In 3 m daily rhythm was observed with maximum levels at ZT18 and minimum at ZT6, in 12 m daily rhythm persisted and maximum levels were observed at ZT0 and minimum at ZT18 that means maximum levels in 12 m has shown approximately 6h delay compared to 3 m. In 24 m daily rhythm persisted and maximum levels were observed at ZT12 and minimum at ZT6 that means maximum levels in 24 m has shown approximately 6h advance compared to 3 m. (Fig. 67; $p \leq 0.05$). Mean 24 h levels were not altered significantly where as daily pulse is increased in 12 m by 3.49 fold and then decreased in 24 m by 0.31 fold compared to 3m (Fig. 68, Table 18; $p \leq 0.05$).

Cry2: Daily rhythm was observed in 3 m with maximum levels at ZT12 and minimum at ZT0, in 12 m daily rhythm persisted and maximum levels were observed at ZT0 and minimum at ZT18 that means maximum levels in 12 m has shown approximately 12h advance compared to 3 m. In 24 m daily rhythm persisted and its maximum levels were observed at ZT18 and minimum at ZT0 that means maximum levels in 24 m has shown approximately 6h delay and approximately 6h advance compared to 3 and 12 m respectively (Fig. 67; $p \leq 0.05$). Mean 24 h levels were decreased in 12 m by about 0.58 fold compared to 3 m and then increased in 24 m by

about 1.96 fold compared to 12 m. Daily pulse were increased in 12 m by about 6.16 fold compared to 3 m and then decreased in 24 m by about 0.06 fold compared to 12 m (Fig. 68, Table 18; $p \leq 0.05$).

Bmal1: Daily rhythmicity was persisted in 3 and 12 m. The maximum and minimum levels of gene expression were observed at ZT18 and ZT6 in 3 m and ZT0 and ZT18 in 12 m. The daily rhythmicity in gene expression was found to be abolished in 24 m old animals (Fig. 67; $p \leq 0.05$). Mean 24 h levels were not altered significantly upon aging. Daily pulse was increased in 12 m by about 7.5 fold compared to 3 m and then decreased in 24 m by about 0.12 fold when compared to 12 m (Fig. 68, Table 18; $p \leq 0.05$).

Table 18. Clock gene expression in 3, 12 and 24 m SN

Genes	Age in Months (m)	Gene expression levels (relative gene expression)		Ratio	Mean levels
		maximum	minimum		
Per1	3	0.018±0.002	0.0006±0.0002 ^{q}	19 ±4.3	0.006±0.002
	12	0.12±0.007 ^{x}	0.023±0.001 $^{x, q}$	5.2±0.38 ^{x}	0.066±0.01 ^{x}
	24	0.075±0.002 $^{x, y}$	0.031±0.002 $^{x, y, q}$	2.41±0.14 ^{x}	0.056±0.0.005 ^{x}
Per2	3	0.009±0.0006	0.003±0.0003 ^{q}	3.17±0.45	0.006±0.0008
	12	0.006±0.001 ^{x}	0.002±0.0002 $^{x, q}$	2.64±0.66	0.004±0.0005 ^{x}
	24	0.009±0.0002 ^{y}	0.005±0.0002 $^{x, y, q}$	1.85±0.12	0.007±0.0006 ^{y}
Cry1	3	0.009±0.001	0.002±0.0001 ^{q}	4.55±0.68	0.005±0.00074
	12	0.007±0.0007	0.0005±0.00005 $^{x, q}$	15.89±1.09 ^{x}	0.003±0.0007 ^{x}
	24	0.004±0.0001 $^{x, y}$	0.003±0.0001 $^{x, y, q}$	1.44±0.08 $^{x, y}$	0.004±0.0002
Cry2	3	0.059±0.004	0.017±0.001 ^{q}	3.44±0.19	0.0367±0.005
	12	0.037±0.005 ^{x}	0.002±0.00007 $^{x, q}$	21.22±2.73 ^{x}	0.021±0.35 ^{x}
	24	0.047±0.003 $^{x, y}$	0.037±0.0009 $^{x, y, q}$	1.28±0.11 ^{y}	0.042±0.001 ^{y}
Bmal1	3	0.027±0.005	0.012±0.002 ^{q}	2.24±0.31	0.022±0.002
	12	0.033±0.004	0.002±0.0002 $^{x, q}$	16.6±3.09 ^{x}	0.014±0.003 ^{x}
	24	0.02±0.002 $^{x, y}$	0.013±0.00006 ^{y}	2.15±0.87 ^{y}	0.0±0.001 ^{x}

Each value is mean ± SEM (n=4), $p \leq 0.05$ and expressed in relative gene expression. $p_x \leq 0.05$, $p_y \leq 0.05$ and $p_z \leq 0.05$ (where x, y and z refers to comparison with 3, 12 and 24 m respectively and q refers to comparison between maximum and minimum within the group).

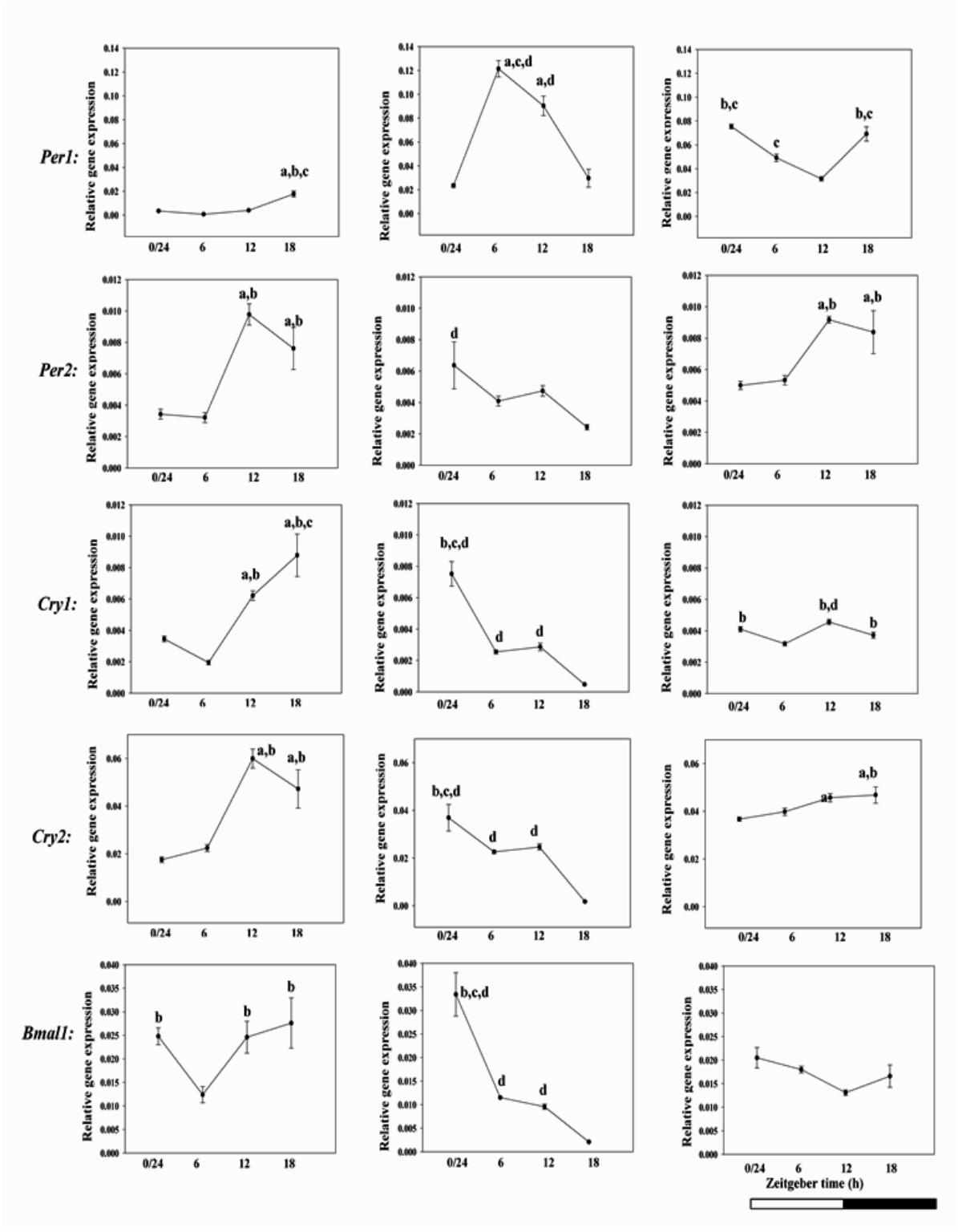

Fig. 67: Effect of aging on expression of *Per1*, *Per2*, *Cry1*, *Cry2* and *Bmal1* in the SN of male wistar rat. Each value is mean ± SEM (n=4), $p \leq 0.05$ and expressed in relative gene expression. 3, 12 and 24 m. $p_a \leq 0.05$; $p_b \leq 0.05$, $p_c \leq 0.05$ and $p_d \leq 0.05$ (where a, b, c and d refers to comparison with ZT0, ZT6, ZT12 and ZT18 respectively within the group).

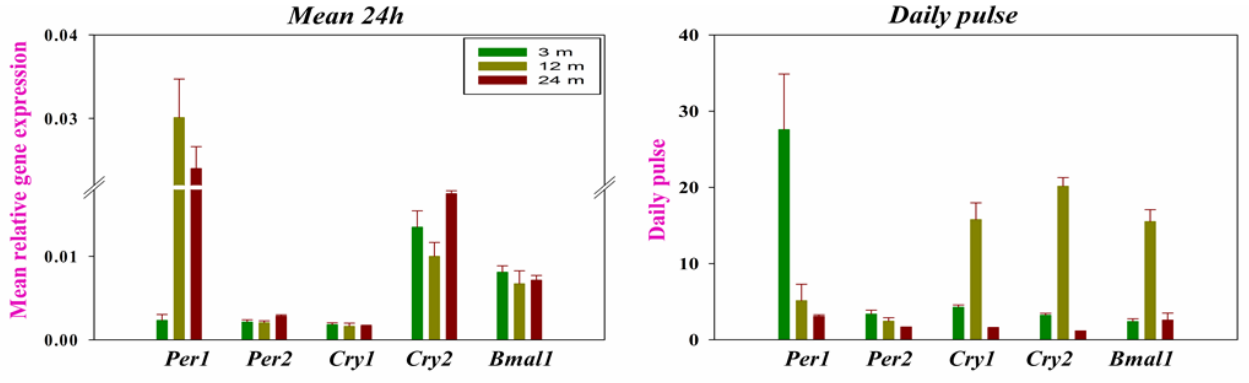

Fig. 68: Effect of aging on mean 24 h levels and daily pulse of various clock genes expression in Substantia nigra of male wistar rat.

(d) Expression of various clock genes in the SCN of rotenone induced PD model

No significant difference was found between 3 m control and vehicle group.

Per1: Daily rhythm was persisted in RIPD model and the maximum levels were observed at ZT12 and minimum at ZT18 whereas in control group maximum levels were observed at ZT6 and minimum at ZT18 that means we have observed approximately 6 h delay in RIPD group (Fig. 69; $p \leq 0.05$). Mean 24h levels and daily pulse was decreased by about 0.5 and 0.36 fold respectively in RIPD model compared to control (Fig. 70, Table 19; $p \leq 0.05$). The phase delay observed in RIPD model is not comparable with 24 m because we have observed approximately 6 h advance in 24 m compared to control.

Per2: In RIPD model daily rhythm and pattern was not altered compared to control. Maximum levels were observed at ZT12 and minimum at ZT18 in both control and RIPD model (Fig. 69; $p \leq 0.05$). Mean 24h levels were increased by about 1.7 fold whereas daily pulse was decreased by about 0.6 fold in RIPD model compared to control (Fig. 70, Table 19; $p \leq 0.05$).In

24 m also we have observed similar type of daily rhythm pattern with maximum levels at ZT12 which is comparable to RIPD model.

Cry1: Daily rhythm was persisted in RIPD model and the maximum levels were observed at ZT0 and minimum at ZT18 whereas in control group maximum levels were observed at ZT12 and minimum at ZT18 that means we have observed approximately 12 h advance in RIPD group (Fig. 69; $p \leq 0.05$). In RIPD group mean 24h levels and daily pulse were decreased by about 0.74 and 0.14 fold respectively compared to control (Fig. 70, Table 19; $p \leq 0.05$). The phase advance observed in RIPD model is not comparable with 24 m because we could detect the *Cry1* levels at ZT12 only in 24 m compared to control.

Cry2: In RIPD model daily rhythm and pattern was not altered compared to control. Maximum levels were observed at ZT12 and minimum at ZT18 in both control and RIPD model (Fig. 69; $p \leq 0.05$). Mean 24h levels were not altered in RIPD group whereas daily pulse was decreased by about 0.1 fold compared to vehicle (Fig. 70, Table 19; $p \leq 0.05$). Similar kind of result was not found in 24 m because we could detect the *Cry2* levels at ZT12 only in 24 m compared to control.

Bmal1: Daily rhythm was persisted in RIPD model and the maximum levels were observed at ZT0 and minimum at ZT12 whereas in control group levels were maximum at ZT18 and minimum at ZT6 that means we have observed approximately 6 h delay in RIPD group (Fig. 69; $p \leq 0.05$). Mean 24h levels and daily pulse was decreased by about 0.39 and 0.2 fold respectively in RIPD model compared to control (Fig. 70, Table 19; $p \leq 0.05$). The phase delay observed in RIPD model is not comparable with 24 m because we could detect the *Bmal1* levels at ZT12 only in 24 m compared to control. However similar kind of decrease was found in 24 m in case of mean 24 h levels in 24 m and RIPD model compared to control.

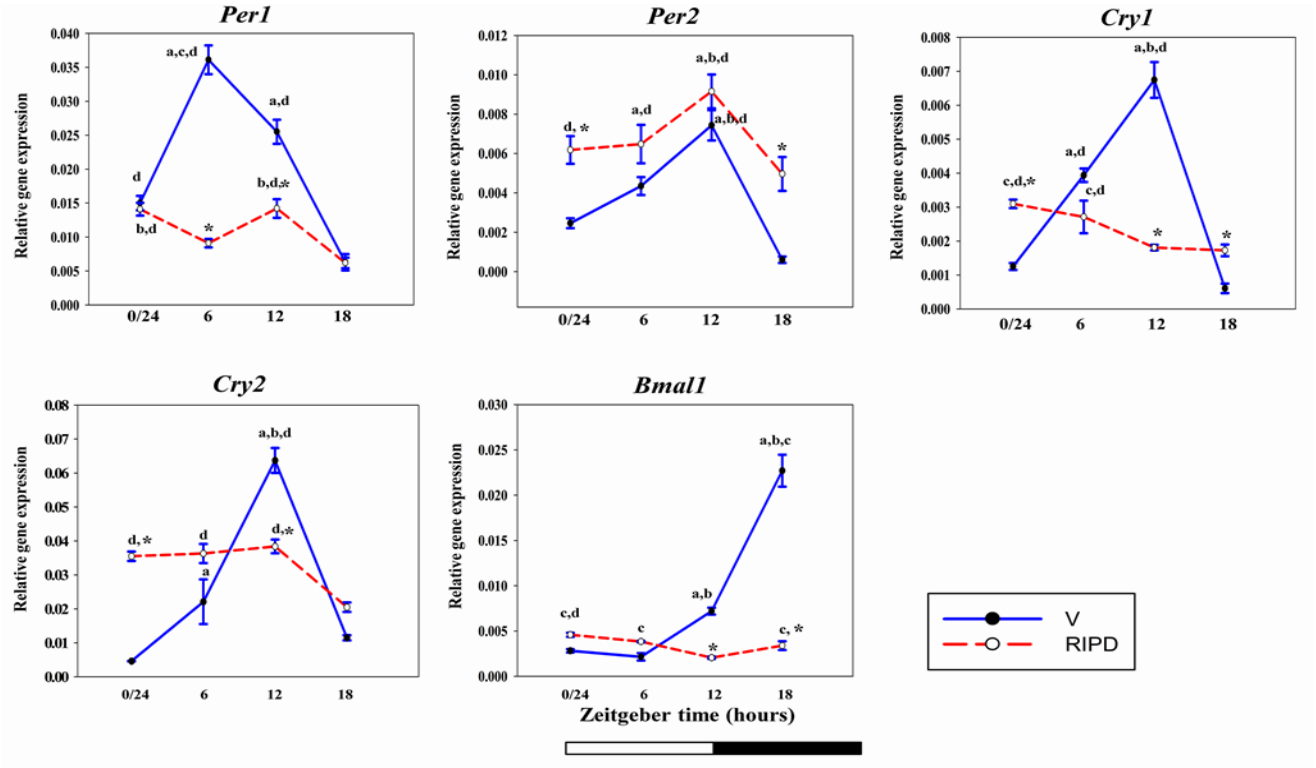

Fig. 69: Expression of various clock genes in SCN of RIPD rat model. Each value is mean ± SEM (n=4), $p \leq 0.05$ and expressed in relative gene expression. V - Vehicle and RIPD - Rotenone Induced PD rat model. $p_a \leq 0.05$; $p_b \leq 0.05$, $p_c \leq 0.05$ and $p_d \leq 0.05$ (where a, b, c and d refers to comparison with ZT0, ZT6, ZT12 and ZT18 respectively within the group). * refers to comparison of levels at same time point in vehicle group.

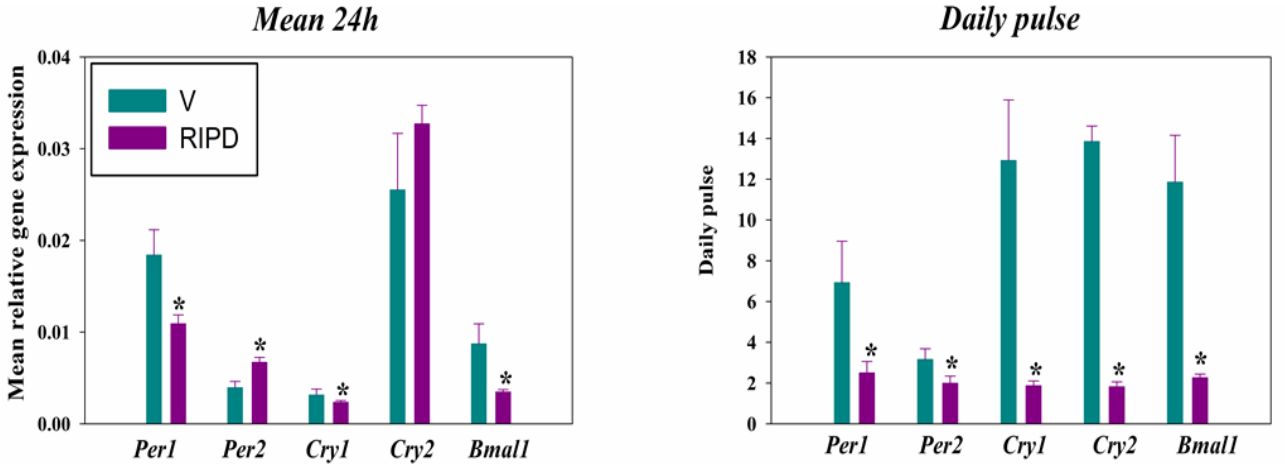

Fig. 70: Mean 24 h levels and daily pulse of various clock genes expression in SCN of RIPD rat model. $p_* \leq 0.05$ (where * refers to comparison with vehicle group).

Table 19. Clock gene expression in SCN of Vehicle (V) and Rotenone induced PD (RIPD) rat model

Gene	Experimental group	Levels (relative gene expression)*		Ratio *	Mean levels **
		Maximum	Minimum		
Per1	V	0.036 ± 0.002	0.006 ± 0.001 ^{q}	6.92 ± 2.04	0.02 ± 0.002
	RIPD	0.014 ± 0.001 ^{p}	0.006 ± 0.0007 ^{q}	2.49 ± 0.55 ^{p}	0.01 ± 0.0009 ^{p}
Per2	V	0.007 ± 0.0007	0.0006 ± 0.0001 ^{q}	3.15 ± 0.53	0.004 ± 0.0006
	RIPD	0.009 ± 0.0008 ^{p}	0.004 ± 0.0008 ^{q,p}	1.98 ± 0.34 ^{p}	0.007 ± 0.0005 ^{p}
Cry1	V	0.007 ± 0.0005	0.0006 ± 0.0001 ^{q}	12.96 ± 2.96	0.003 ± 0.0006
	RIPD	0.003 ± 0.0001 ^{p}	0.002 ± 0.0001 ^{q,p}	1.86 ± 0.23 ^{p}	0.002 ± 0.0001 ^{p}
Cry2	V	0.06 ± 0.003	0.004 ± 0.00006 ^{q}	13.84 ± 0.76	0.02 ± 0.006
	RIPD	0.04 ± 0.002 ^{p}	0.02 ± 0.001 ^{q,p}	1.82 ± 0.24 ^{p}	0.03 ± 0.002
Bmal1	V	0.023 ± 0.002	0.002 ± 0.0004 ^{q}	11.85 ± 2.3	0.009± 0.002
	RIPD	0.004 ± 0.0002 ^{p}	0.002 ± 0.0001 ^{q}	2.26 ± 0.18 ^{p}	0.003± 0.0002 ^{p}

* Each value is mean ± S.E. (n=4); **each value is mean ± S.E. (n=16, for Vehicle group and RIPD group); p refers to comparison between V and RIPD; q refers to comparison between maximum and minimum.

(e) Expression of various clock genes in the Pineal of rotenone induced PD model

No significant difference was found between 3 m control and vehicle group.

Per1: In RIPD model daily rhythm and pattern was persisted compared to control. In both control and RIPD group levels were maximum at ZT18 and minimum at ZT6 (Fig. 71; $p \leq 0.05$). Mean 24h levels and daily pulse was decreased by about 0.47 and 0.2 fold respectively in RIPD model compared to control (Fig. 72, Table 20; $p \leq 0.05$). The phase delay observed in 24 m has not observed in RIPD model.

Per2: Daily rhythm was persisted in RIPD model and the maximum levels were observed at ZT12 and minimum at ZT6 whereas in control group levels were maximum at ZT18 and

minimum at ZT6 that means we have observed approximately 6 h advance in RIPD group (Fig. 71; $p \leq 0.05$). Mean 24h levels and daily pulse was not altered in RIPD group compared to control (Fig. 72, Table 20; $p \leq 0.05$). The phase advance observed in RIPD model is not observed in 24 m.

Cry1: In RIPD model daily rhythm was persisted and maximum levels were observed at ZT12 and minimum at ZT6 whereas in control group levels were maximum at ZT18 and minimum at ZT6 that means we have observed approximately 6 h advance in RIPD group (Fig. 71; $p \leq 0.05$). Mean 24h levels and daily pulse was not altered in RIPD group compared to control (Fig. 72, Table 20; $p \leq 0.05$). In 24 m also we have observed similar type of daily rhythm pattern with approximately 6 h advance in phase of the daily rhythm which is comparable to RIPD model.

Cry2: Daily rhythm was persisted in RIPD model and maximum levels were observed at ZT18 and minimum at ZT6 whereas in control levels were maximum at ZT12 and minimum at ZT6 that means we have observed approximately 6 h advance in RIPD group (Fig. 71; $p \leq 0.05$). Mean 24h levels were not altered in RIPD group whereas daily pulse was increased by about 9 fold compared to control (Fig. 72, Table 20; $p \leq 0.05$). The phase advance observed in RIPD model is not observed in 24 m.

Bmal1: In RIPD model daily rhythm was persisted with maximum levels at ZT12 and minimum at ZT6 whereas in control levels were maximum at ZT18 and minimum at ZT0 that means we have observed approximately 6 h advance in RIPD group (Fig. 71; $p \leq 0.05$). Mean 24h levels was decreased and daily pulse was increased by about 0.63 and 180 fold respectively in RIPD model compared to control (Fig. 72, Table 20; $p \leq 0.05$). The phase advance observed in RIPD model is not observed in 24 m.

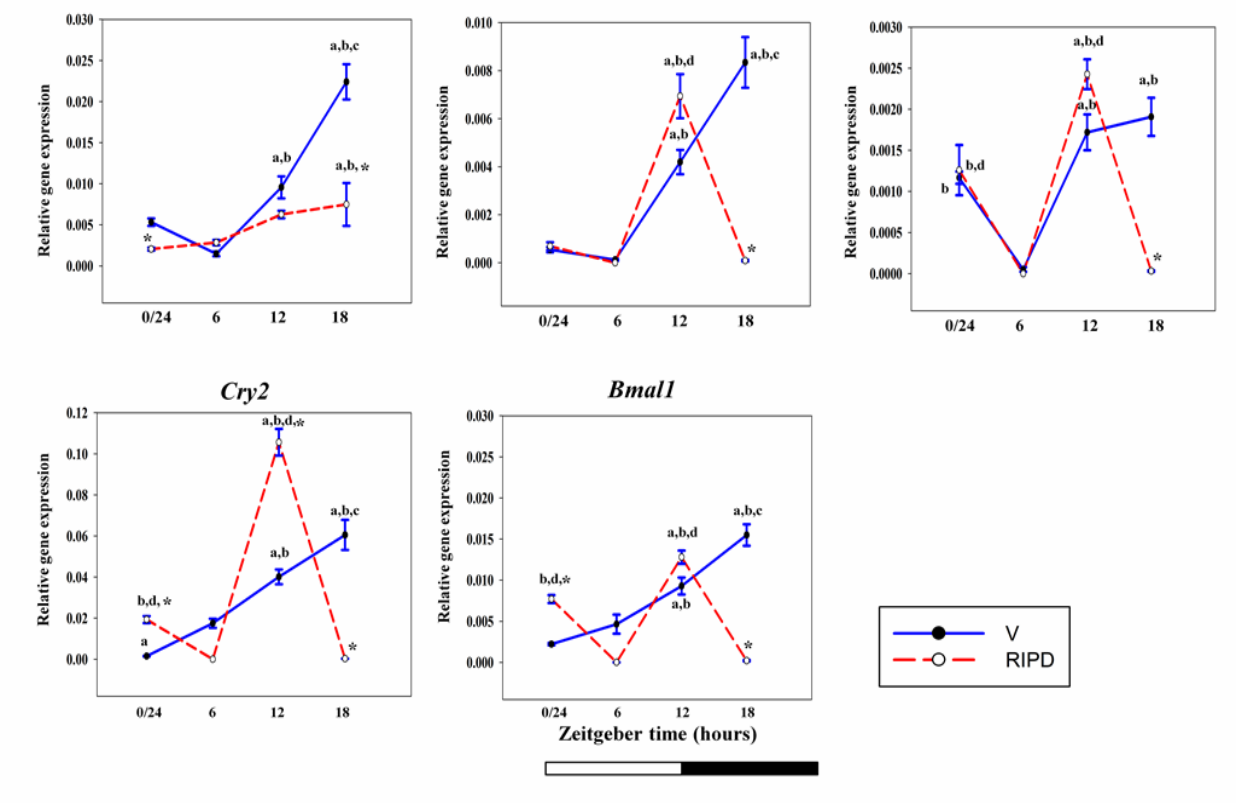

Fig. 71: Expression of various clock genes in Pineal of rotenone induced PD rat model. Each value is mean ± SEM (n=4), $p \leq 0.05$ and expressed in relative gene expression. V - Vehicle and RIPD - Rotenone Induced PD rat model. $p_a \leq 0.05$; $p_b \leq 0.05$, $p_c \leq 0.05$ and $p_d \leq 0.05$ (where a, b, c and d refers to comparison with ZT0, ZT6, ZT12 and ZT18 respectively within the group). * refers to comparison of levels at same time point in vehicle group.

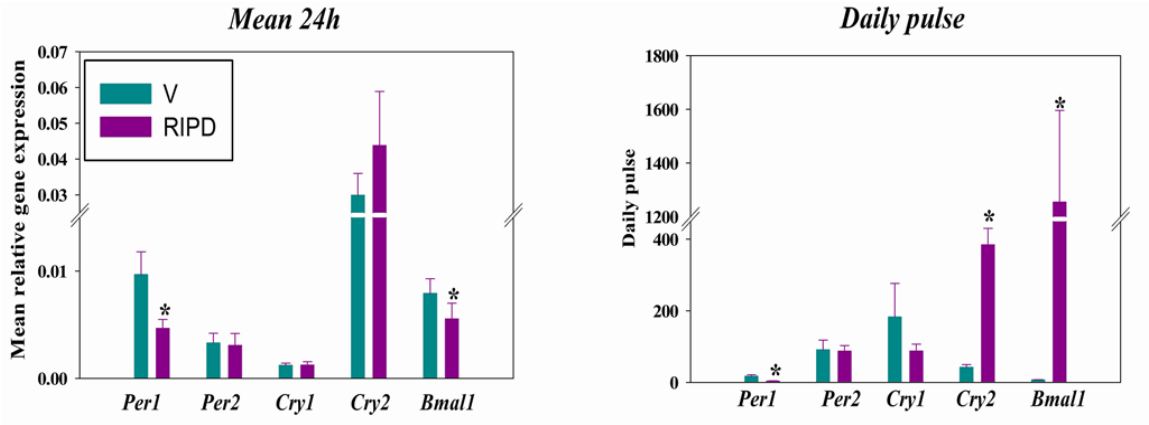

Fig. 72: Mean 24 h levels and daily pulse of various clock genes expression in Pineal of RIPD rat model. $p_* \leq 0.05$ (where * refers to comparison with vehicle group).

Table 20. Clock gene expression in Pineal of Vehicle (V) and Rotenone induced PD (RIPD) rat model

Gene	Experimental group	Levels (relative gene expression)*		Ratio *	Mean levels **
		Maximum	Minimum		
Per1	V	0.022 ± 0.002	0.001± 0.0002 ^{q}	17.39± 3.79	0.0096 ± 0.002
	RIPD	0.007 ± 0.002 ^{p}	0.002± 0.0001 $^{q, p}$	3.54 ± 1.12 ^{p}	0.004 ± 0.0008 ^{p}
Per2	V	0.008 ± 0.001	0.0001± 0.00003 ^{q}	91.01 ± 27.1	0.003 ± 0.0008
	RIPD	0.007 ± 0.0009	0.00009± 0.00003 $^{q, p}$	87.34 ± 15.3	0.003 ± 0.001
Cry1	V	0.0019 ± 0.0002	0.00005± 0.00002 ^{q}	182.63 ± 93.68	0.001 ± 0.0002
	RIPD	0.002 ± 0.0001 ^{p}	0.00003± 0.000009 ^{q}	87.63 ± 19.20	0.001 ± 0.0003
Cry2	V	0.06 ± 0.007	0.0014± 0.00013 ^{q}	42.04 ± 7.68	0.029 ± 0.006
	RIPD	0.1 ± 0.006 ^{p}	0.0003± 0.00003 $^{q, p}$	384.3 ± 46 ^{p}	0.044 ± 0.015
Bmal1	V	0.015 ± 0.001	0.002± 0.0001 ^{q}	6.93 ± 0.42	0.008 ± 0.001
	RIPD	0.013 ± 0.0008 ^{p}	0.00001± 0.000002 $^{q, p}$	1254 ± 341 ^{p}	0.005 ± 0.007 ^{p}

* Each value is mean ± S.E. (n=4); **each value is mean ± S.E. (n=16, for Vehicle group and RIPD group); p refers to comparison between V and RIPD; q refers to comparison between maximum and minimum

(f) Expression of various clock genes in the SN of rotenone induced PD model

No significant difference was found between 3 m control and vehicle group.

Per1: Daily rhythm of gene expression was persisted in RIPD model. The maximum and minimum of gene expression levels were ZT18 and ZT0 in control and ZT12 and ZT6 in RIPD model. The maximum expression level has shown approximately 6h advance when compared to control (Fig. 73; $p \leq 0.05$). Mean 24h levels and daily pulse was decreased by about 0.17 and 0.55 fold respectively in RIPD model compared to vehicle (Fig. 74, Table 21; $p \leq 0.05$). The phase advance observed in RIPD model is not observed in 24 m.

Per2: In RIPD model daily rhythm and pattern was not altered compared to control. Maximum levels were observed at ZT12 and minimum at ZT6 in both control and RIPD model (Fig. 73; $p \leq 0.05$). Mean 24h levels and daily pulse was decreased by about 0.53 and 0.2 fold respectively in RIPD model compared to vehicle (Fig. 74, Table 21; $p \leq 0.05$). In 24 m also we

have observed similar type of daily rhythm pattern with maximum levels at ZT12 which is comparable to RIPD model.

Cry1 and *Cry2:* In RIPD model daily rhythm and pattern of C*ry1* and *2* were not altered compared to control. Maximum levels were observed at ZT12 and minimum at ZT6 in both control and RIPD model (Fig. 73; $p \leq 0.05$). Mean 24h levels of *Cry1* and *2* was decreased by about 0.15 and 0.62 fold respectively and daily pulse of *Cry1* and *2* was decreased by about 0.08 and 0.002 fold respectively compared to control (Fig. 74, Table 21; $p \leq 0.05$).

Bmal1: Daily rhythm in RIPD model was persisted and expression levels were maximum at ZT12 and minimum at ZT6 whereas in control maximum levels were observed at ZT18 and minimum at ZT6 that means maximum levels in RIPD rat model shown approximately 6h advance compared to control (Fig. 73; $p \leq 0.05$). Mean 24h levels and daily pulse was decreased by about 0.17 and 0.19 fold respectively in RIPD model compared to control (Fig. 74, Table 21; $p \leq 0.05$).

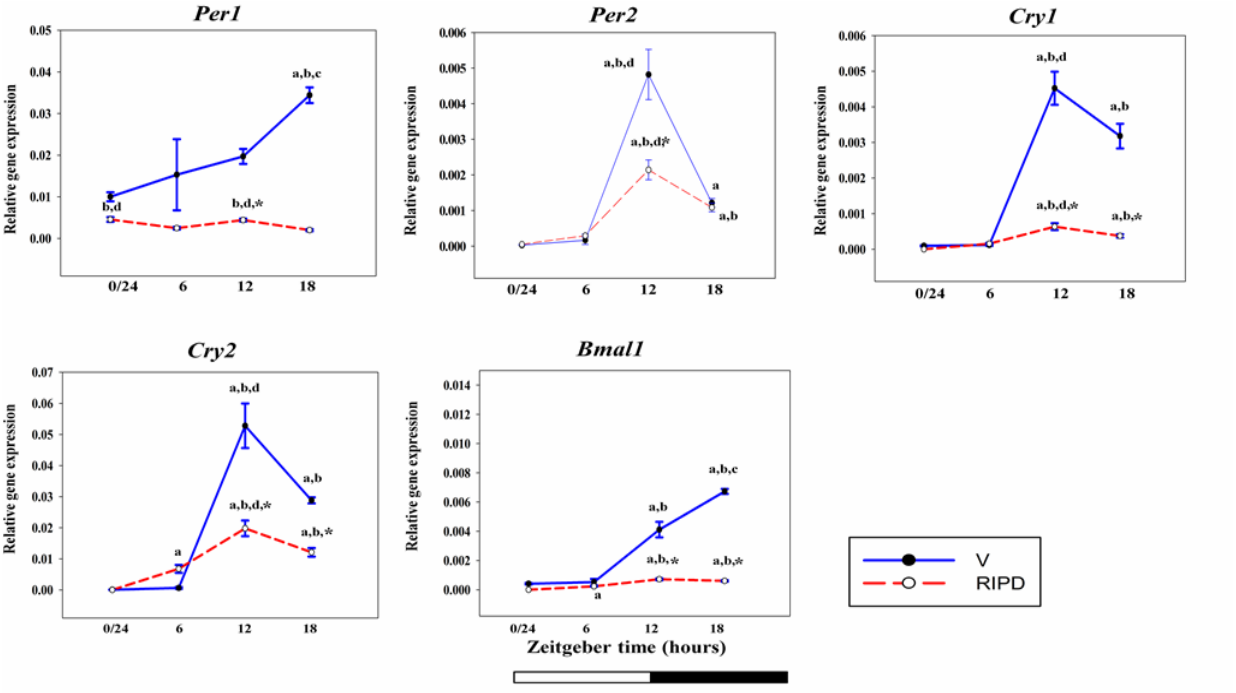

Fig. 73: Expression of various clock genes in SN of rotenone induced PD rat model. Each value is mean ± SEM (n=4), $p \leq 0.05$ and expressed in relative gene expression. V - Vehicle and RIPD - Rotenone Induced PD rat model. $p_a \leq 0.05$; $p_b \leq 0.05$, $p_c \leq 0.05$ and $p_d \leq 0.05$ (where a, b, c and d refers to comparison with ZT0, ZT6, ZT12 and ZT18 respectively within the group). * refers to comparison of levels at same time point in vehicle group.

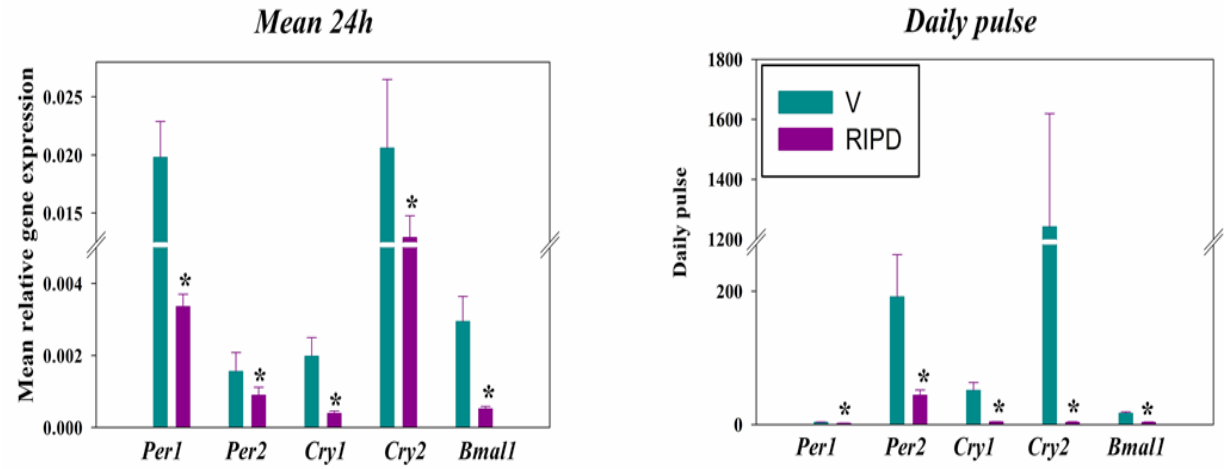

Fig. 74: Mean 24 h levels and daily pulse of various clock genes expression in Substantia nigra of RIPD rat model. $p_* \leq 0.05$ (where * refers to comparison with vehicle group).

Table 21. Clock gene expression in SN of Vehicle (V) and Rotenone induced PD (RIPD) rat model

Gene	Experimental group	Levels (relative gene expression)*		Ratio *	Mean levels **
		Maximum	Minimum		
Per1	V	0.034± 0.002	0.01 ± 0.001 [q]	3.52± 0.3	0.019± 0.003
	RIPD	0.002± 0.0002 [p]	0.004 ± 0.0005 [q, p]	1.95± 0.4 [p]	0.0033± 0.0003 [p]
Per2	V	0.005± 0.0007	0.00003 ± 0.000006 [q]	191± 63	0.001± 0.0005
	RIPD	0.002± 0.0003 [p]	0.00004 ± 0.000004 [q]	44 ± 1.74 [p]	0.0008 ± 0.0002 [p]
Cry1	V	0.004± 0.0004	0.00009± 0.00001 [q]	51.35 ± 11.88	0.002 ± 0.0005
	RIPD	0.0004 ± 0.00004 [p]	0.0001 ± 0.00002 [q, p]	4.14 ± 0.35 [p]	0.0004 ± 0.00006 [p]
Cry2	V	0.053± 0.007	0.00006 ± 0.00002 [q]	1241 ± 377	0.021 ± 0.005
	RIPD	0.019 ± 0.002 [p]	0.007 ± 0.001 [q, p]	3.38 ± 0.86 [p]	0.013 ± 0.002 [p]
Bmal1	V	0.007 ± 0.0002	0.0004 ± 0.00005 [q]	17.04 ± 1.9	0.003 ± 0.0006
	RIPD	0.0007± 0.00006 [p]	0.0002 ± 0.00002 [q, p]	3.29 ± 0.64 [p]	0.0005 ± 0.00006 [p]

* Each value is mean ± S.E. (n=4); **each value is mean ± S.E. (n=16, for Vehicle group and RIPD group); p refers to comparison between V and RIPD; q refers to comparison between maximum and minimum.

OBJECTIVE – V

5. Effect of melatonin administration on daily rhythms of various clock gene expressions in SCN, Pineal and SN upon aging and in RIPD rat model

No significant difference was found between the control and the vehicle control.

(a) Effect of melatonin administration on various clock gene expression levels and its rhythmicity in the aging SCN:

Per1: Maximum and minimum levels in 3 m Melatonin treated (MT) were at ZT6 and minimum at ZT0 respectively, same as that of 3 m vehicle group. In 12 m MT daily rhythm persisted and maximum levels were observed at ZT12 instead of ZT18 which has been observed in case of 12 m vehicle group, thus phase of the rhythm has been advanced by approximately 6h compared to 12 m vehicle group, leading to partial restoration of the phase of rhythm compared to 3m vehicle group. In 24 m MT daily rhythm persisted and maximum levels were observed at ZT6 instead of ZT0 which has been observed in case of 24 m vehicle group, thus phase of the rhythm has been delayed by approximately 6h compared to 24 m vehicle group, leading to restoration of the phase of rhythm compared to 3m vehicle group (Fig. 75; $p \leq 0.05$).Upon melatonin administration the mean 24h levels of were increased by 2.5 and 2.05 fold in 3m MT and 12m MT, compared to 3 and 12 m vehicle group respectively, whereas daily pulse has been restored in 12m MT compared to 12m vehicle group (Fig. 76, Table 22; $p \leq 0.05$).

Per2: In 3 m MT maximum levels were observed at ZT6 and minimum at ZT0, thus phase of the rhythm was advanced by approximately 6h compared to 3 m vehicle group. In 12 m MT daily rhythm persisted and maximum levels were observed at ZT12 instead of ZT18 which has been observed in case of 12 m vehicle group, thus phase of the rhythm has been advanced by approximately 6h compared to 12 m vehicle group, leading to restoration of the phase of rhythm compared to 3m vehicle group. In 24 m MT daily rhythm persisted and maximum levels were

observed at ZT12 and the levels at ZT12 were increased and restored compared to ZT12 in 24 and 3m vehicle group respectively (Fig. 75; $p \leq 0.05$). Upon melatonin administration the mean 24h levels were increased by 10.5, 3.42 and 39.33 fold in 3, 12 and 24m MT compared to 3, 12 and 24 m vehicle group respectively. However, daily pulse has been significantly decreased in 12 and 24m MT by about 0.63 and 0.27 fold compared to 12 and 24m vehicle group respectively (Fig. 76, Table 22; $p \leq 0.05$).

Cry1: Maximum and minimum levels in 3 m MT were observed at ZT6 and minimum at ZT0 respectively, thus phase of the rhythm was advanced by approximately 6h compared to 3 m vehicle group. In 12 m MT daily rhythm persisted and maximum levels were observed at ZT12 instead of ZT18 which has been observed in case of 12 m vehicle group, thus phase of the rhythm has been advanced by approximately 6h compared to 12 m vehicle group, leading to restoration of the phase of rhythm compared to 3m vehicle group. In 24 m MT daily rhythm restored compared to 24 m vehicle group, and its maximum levels were observed at ZT0 (Fig. 75; $p \leq 0.05$).Upon melatonin administration the mean 24h levels were significantly increased by 16.51, 2.15 and 8.09 fold in 3, 12 and 24m MT compared to 3, 12 and 24 m vehicle group respectively. However, daily pulse has significantly decreased in 3 and 12m MT by about 0.01 and 0.33 fold compared to 3 and 12m vehicle group respectively(Fig. 76, Table 22; $p \leq 0.05$).

Cry2: In 3 m MT maximum levels were observed at ZT6 and minimum at ZT0, thus phase of the rhythm was advanced by approximately 6h compared to 3 m vehicle group. In 12 m MT daily rhythm persisted and its maximum levels were observed at ZT12 instead of ZT18 which has been observed in case of 12 m vehicle group, thus phase of the rhythm has been advanced by approximately 6h compared to 12 m vehicle group, leading to restoration of the phase of rhythm compared to 3m vehicle group. In 24 m MT daily rhythm restored compared to 24 m vehicle group, and its maximum levels were observed at ZT0 (Fig. 75; $p \leq 0.05$).Upon melatonin administration the mean 24h levels were significantly increased by 9.73 and 4.5 fold in 3 and 24m MT, compared to 3 and 24 m vehicle group respectively. However, daily pulse has been significantly decreased in 3 and 12m-MT by about 0.01 and 0.36 fold compared to 3 and 12m vehicle group respectively(Fig. 76, Table 22; $p \leq 0.05$).

Bmal1: Maximum and minimum levels in 3 m MT were observed at ZT6 and minimum at ZT6 respectively, thus phase of the rhythm was advanced by approximately 12h compared to 3 m vehicle group. In 12 m MT daily rhythm persisted and maximum levels were observed at ZT18 instead of ZT6 which has been observed in case of 12 m vehicle group, thus phase of the rhythm has been advanced by approximately 12h compared to 12 m vehicle group, leading to restoration of the phase of rhythm compared to 3m vehicle group. In 24 m MT daily rhythm restored compared to 24 m vehicle group, and its maximum levels were observed at ZT0 (Fig. 75; $p \leq 0.05$).Upon melatonin administration the mean 24h levels were significantly increased by 3.86, 3.23 and 11.25 fold in 3, 12 and 24m MT compared to 3, 12 and 24 m vehicle group respectively. However, daily pulse is significantly decreased in 3 and 12m-MT by about 0.002 and 0.18 fold compared to 3 and 12m vehicle group respectively (Fig. 76, Table 22; $p \leq 0.05$).

In 3 m vehicle group light phase positive correlation between *Bmal1-Per2; Cry1-Bmal1; Cry2-Bmal1* has not observed in dark phase. There was no correlation between *Bmal1-Per1* in the light phase whereas they were correlated in dark phase. In light and dark phase of 3 m MT group positive correlation was observed between *Per1-Per2; Per1-Cry1; Per1-Cry2; Per2-Cry1; Per2-Cry2; Cry1-Cry2; Cry1-Bmal1; Cry2-Bmal1*. There was no correlation between *Bmal1-Per1* in the light phase whereas they were correlated in dark phase. In light and dark phase of 12 m vehicle group positive correlation was observed between *Per2-Cry1; Per2-Cry2; Cry1-Cry2; Cry1-Bmal1; Cry2-Bmal1; Per2-Bmal1*. Negative correlation between *Per1-Per2; Per1-Cry2* in the light phase has become positive in dark phase and light phase negative correlation between *Per1-Bmal1* has not observed in dark phase. In 12m MT group there was no correlation between *Bmal1-Cry1* in light phase whereas they were correlated in dark phase and correlation observed between *Per1-Bmal1; Per2-Bmal1* in the light phase has not been observed in the dark phase. In both light and dark phase positive correlation was observed between *Per1-Per2; Per1-Cry1; Per1-Cry2; Per2-Cry1; Per2-Cry2; Cry1-Cry2; Cry2-Bmal1*. In 24 m vehicle group light phase negative correlation between *Per1-Per2* has not been observed in dark phase. No correlation observed between remaining pair wise comparisons in 24 m vehicle group. In both light and dark phase of 24 m MT group positive correlation was observed between *Cry1-Cry2; Cry1-Bmal1; Cry2-Bmal1*. There was negative correlation between *Per1-Bmal1; Per1-Cry2; Per1-Cry1* in light phase whereas they were not correlated in dark phase (Fig. 77; $p \leq 0.05$).

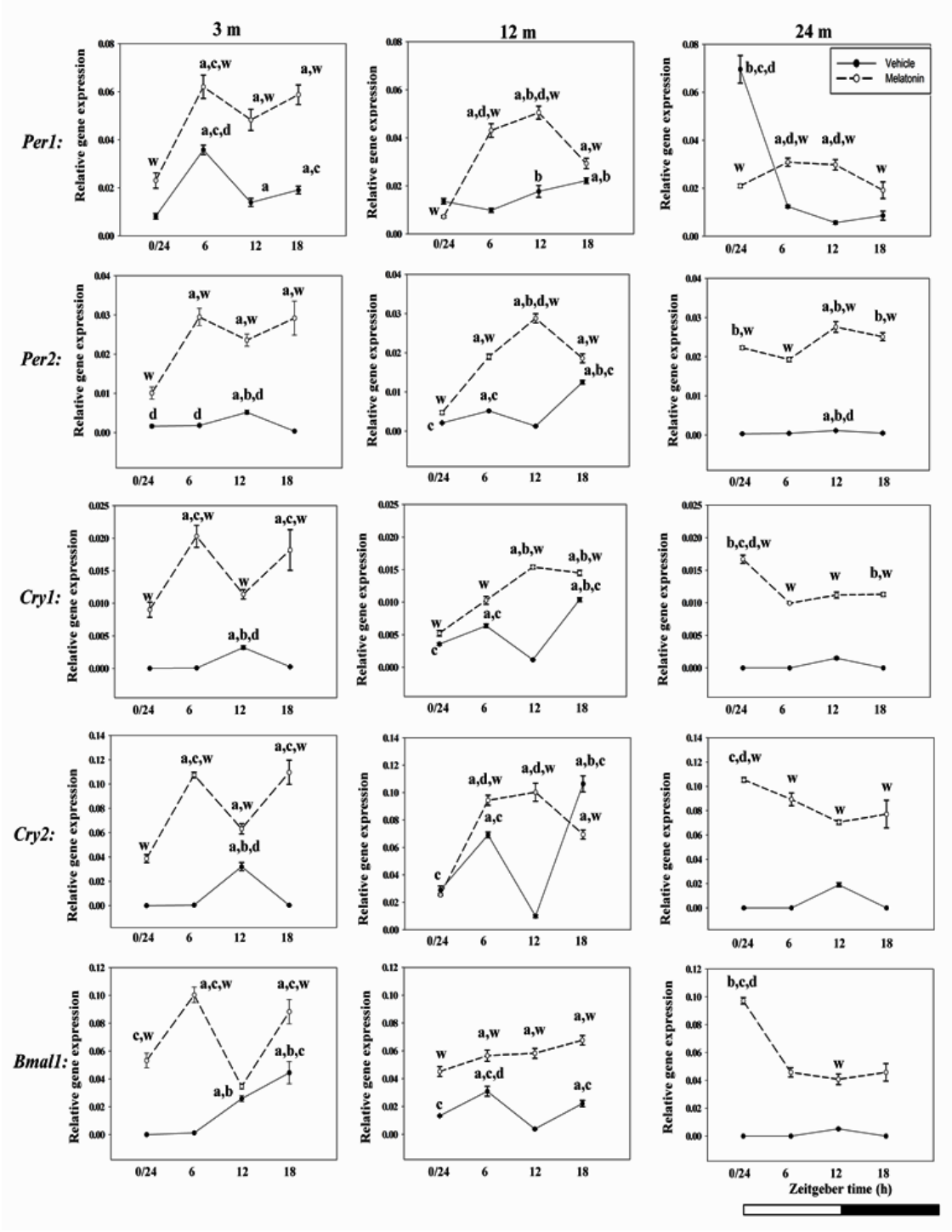

Fig. 75: Effect of melatonin administration on levels and rhythmicity of *Per1*, *Per2*, *Cry1*, *Cry2* and *Bmal1* genes in the aging rat SCN in 3, 12 and 24 months. Each value is mean ± SEM (n=4), $p \leq 0.05$ and expressed as relative gene expression. $p_a \leq 0.05$; $p_b \leq 0.05$, $p_c \leq 0.05$ and $p_d \leq 0.05$ (where a, b, c and d refers to comparison with ZT0, ZT6, ZT12 and ZT18 respectively within the group) $p_w \leq 0.05$ (where w refers to comparison of gene levels at same time point in vehicle group in same age group).

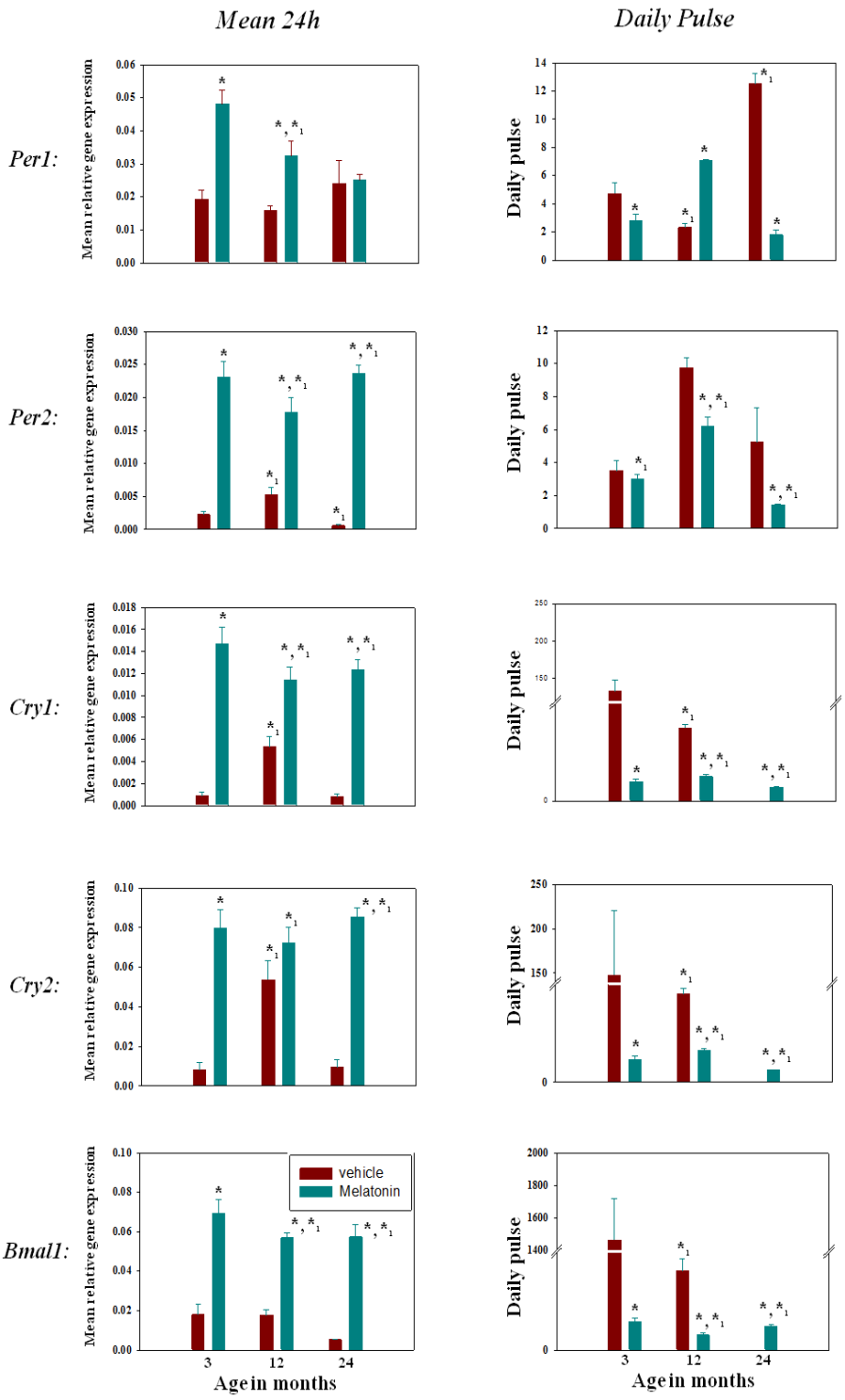

Fig. 76: Effect of melatonin administration on mean 24h levels and Daily Pulse of *Per1, Per2, Cry1, Cry2 and Bmal1* genes in the aging rat SCN in 3, 12 and 24 m. Each value is mean ± SEM $p \leq 0.05$ and expressed as mean relative gene expression. $p_{*} \leq 0.05$ (where * refers to comparison with vehicle group). $p_{*1} \leq 0.05$ (where $_{*1}$ refers to comparison with 3 m vehicle group).

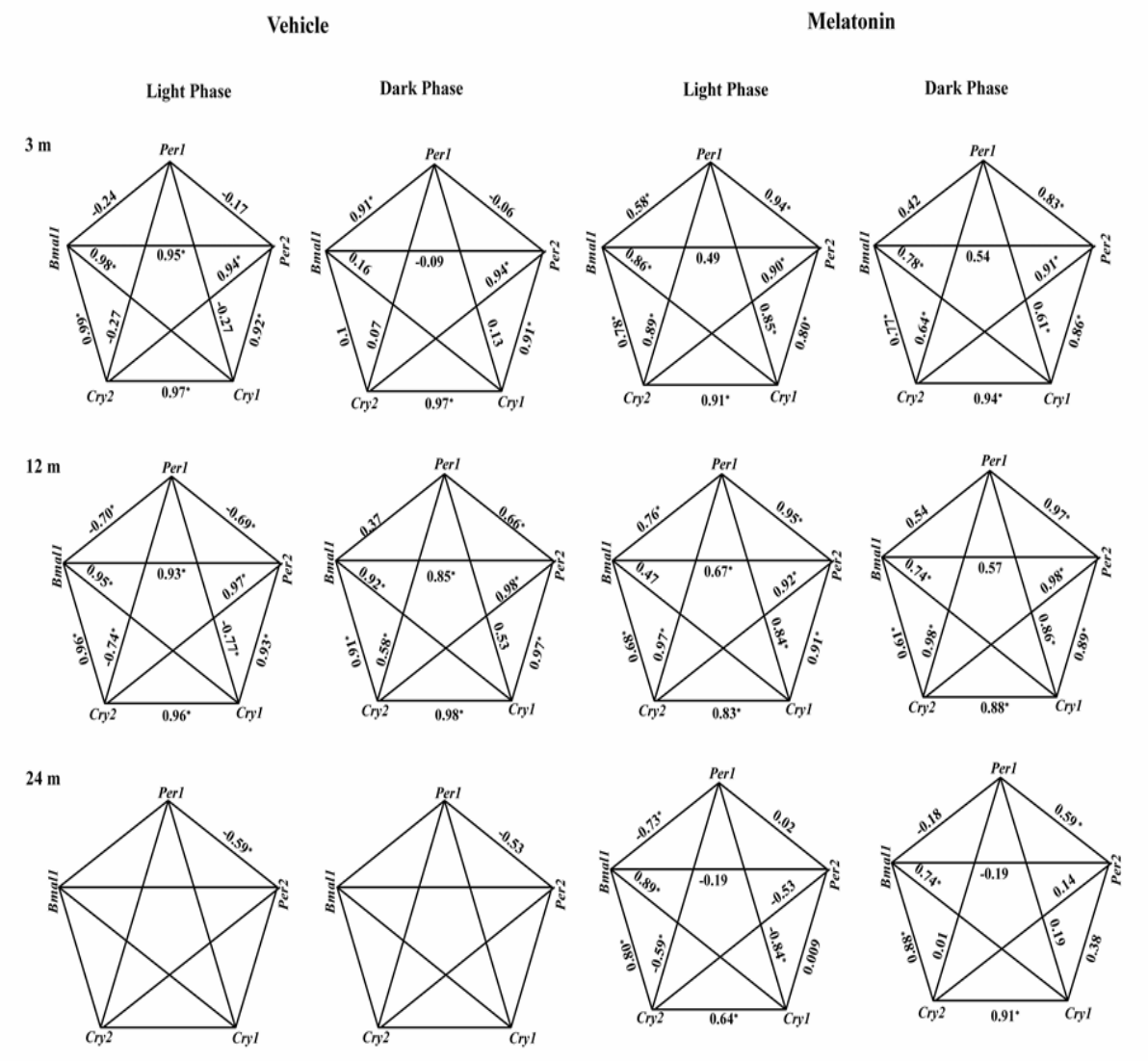

Fig. 77: Effect of melatonin administration on pair wise correlation between mean light (ZT 0, 6 and12) and mean dark (ZT 12,18 and 24/0) phase values of *Per1, Per2,Cry1, Cry2 and Bmal1* in various age groups 3, 12 and 24 m in rat SCN. Each value is correlation coefficient between the parameters. * indicates statistically significant value between parameters ($p \leq 0.05$). Negative value indicates negative correlation between parameters.

Table 22. Effect of melatonin on age induced changes in mean 24 h levels and daily pulse of various clock genes expression in SCN.

Genes	Age in Months (m)	Ratio maximum: minimum		Mean (24h) **	
		Vehicle	Melatonin	Vehicle	Melatonin
Per1	3	4.72±0.76	2.82±0.4 *	0.019±0.002	0.048±0.004 *
	12	2.32±0.28 x	7.05±0.1 *	0.016±0.001	0.032±0.004 *
	24	12.51±0.74 x, y	1.78±0.33 *	0.024±0.007	0.025±0.001
Per2	3	3.5±0.63	3.01±0.16	0.0022±0.0005	0.023±0.002 *
	12	9.75±0.58 x	6.21±0.56 *	0.005±0.001 x	0.018±0.002 *
	24	5.23±2.09 y	1.43±0.05 *	0.0006±0.00009 x, y	0.023±0.001 *
Cry1	3	132.98±15.26	2.35±0.3 *	0.0009±0.0003	0.015±0.001 *
	12	9.03±0.38 x	3±0.27 *	0.005±0.0009 x	0.011±0.001 *
	24	?	1.68±0.05 *	0.0015±0.0001 y	0.012±0.0009 *
Cry2	3	147.75±72.49	2.78±0.41 *	0.008±0.003	0.079±0.009 *
	12	10.89±0.63 x	3.93±0.23 *	0.054±0.009 x	0.072±0.008
	24	?	1.5±0.06 *	0.019±0.0016 x, y	0.085±0.004 *
Bmal1	3	1461±256	2.95±0.31 *	0.018±0.005	0.069±0.007 *
	12	8.15±1.22 x	1.54±0.20 *	0.017±0.003	0.057±0.002 *
	24	?	2.44±0.22 *	0.005±0.0002 x, y	0.057±0.006 *

Each value is Mean ± SE (n=4). **Mean (24 h) n=16 represented (with n=4 at ZT0, 6, 12 and 18) for relative gene expression of all the studied clock genes. $P_x \leq 0.05$, $P_y \leq 0.05$ and $P_z \leq 0.05$ (where x, y and z refers to comparison with 3, 12 and 24 m old rats respectively) and * refers to comparison with control and melatonin administered rats within same age groups ($P \leq 0.05$).

(b) Effect of melatonin administration on various clock gene expression levels and its rhythmicity in the aging Pineal:

Per1: In 3 m MT maximum levels were observed at ZT6 and minimum at ZT0, thus phase of the rhythm was advanced by approximately 12h compared to 3 m vehicle group. In 12 m MT daily rhythm persisted and maximum levels were observed at ZT0 instead of ZT18 which has been observed in case of 3m and 12 m vehicle group, thus phase of the rhythm has been delayed by approximately 6h compared with the same. In 24 m MT daily rhythm persisted and maximum levels were observed at ZT0 and minimum at ZT6 which has been observed in case of 24 m vehicle group, thus phase of the rhythm has not been restored by melatonin (Fig. 78; $p \leq 0.05$). Upon melatonin administration the mean 24h levels were decreased by 0.51 fold in 24m-MT compared to 24m vehicle group, whereas daily pulse in 3m-MT has been decreased by about 0.23fold compared 3m vehicle group (Fig. 79, Table 23; $p \leq 0.05$).

*Per2:*Maximum and minimum levels in 3 m MT were observed at ZT6 and minimum at ZT12 respectively, thus phase of the rhythm was advanced by approximately 12h compared to 3 m vehicle group. In 12 m MT daily rhythm persisted and maximum levels were observed at ZT6 minimum at ZT12 which has been observed in case of 12 m vehicle group, thus phase of the rhythm has not been restored by melatonin. In 24 m MT daily rhythm persisted and maximum levels were observed at ZT6 and minimum at ZT18 that means the phase has been advance by approximately 12h compared to 24 and 3m vehicle group (Fig. 78; $p \leq 0.05$). Upon melatonin administration the mean 24h levels were increased by 6.51 and 9.41 fold in 12 and 24m compared to 12 and 24m vehicle group. However, daily pulse has been decreased in 3m-MT by about 0.02 fold compared to 3m vehicle group (Fig. 79, Table 23; $p \leq 0.05$).

Cry1: In 3 m MT maximum levels were observed at ZT6 and minimum at ZT18, thus phase of the rhythm was advanced by approximately 12h compared to 3 m vehicle group. In 12 m MT daily rhythm persisted and its maximum levels were observed at ZT18 instead of ZT6 which has been observed in case of 12 m vehicle group, thus phase of the rhythm has been delayed by approximately 12h compared to 12 m vehicle group, leading to restoration of the phase of rhythm compared to 3m vehicle group. In 24 m MT daily rhythm persisted and its

maximum levels were observed at ZT0 and minimum at ZT18 that means the phase has been delayed by approximately 6h compared to 3m vehicle group and advanced by approximately 12h compared to 24m vehicle group (Fig. 78; $p \leq 0.05$). Upon melatonin administration the mean 24h levels were increased by 11.35 and 14.53 fold in 3 and 24m MT compared to 3 and 24 m vehicle group respectively. However, daily pulse has decreased in 3m-MT by about 0.009 fold compared to 3m vehicle group (Fig. 79, Table 23; $p \leq 0.05$).

*Cry2:*Maximum and minimum levels in 3 m MT were observed at ZT6 and minimum at ZT18 respectively, thus phase of the rhythm was advanced by approximately 12h compared to 3 m vehicle group. In 12 m MT daily rhythm persisted and its maximum levels were observed at ZT18 instead of ZT6 which has been observed in case of 12 m vehicle group, thus phase of the rhythm has been delayed by approximately 12h compared to 12 m vehicle group, leading to restoration of the phase of rhythm compared to 3m vehicle group. In 24 m MT daily rhythm persisted and its maximum levels were observed at ZT6 and minimum at ZT18 that means the phase has been advanced by approximately 12h compared to 3m vehicle group and delayed by approximately 6h compared to 24m vehicle group (Fig. 78; $p \leq 0.05$). Upon melatonin administration the mean 24h levels were increased by 8.33 and 34.69 fold in 3 and 24m MT, compared to 3 and 24 m vehicle group respectively. However, daily pulse has been decreased in 3m-MT and increased in 24m-MT by about 0.001 and 5.52 fold compared to 3 and 24m vehicle group respectively (Fig. 79, Table 23; $p \leq 0.05$).

Bmal1: In 3 m MT maximum levels were observed at ZT6 and minimum at ZT12, thus phase of the rhythm was advanced by approximately 12h compared to 3 m vehicle group. In 12 m MT daily rhythm persisted and its maximum levels were observed at ZT6, which has been observed in case of 12 m vehicle group, thus phase of the rhythm has not been restored by melatonin. In 24 m MT daily rhythm persisted and its maximum levels were observed at ZT0 and minimum at ZT18 that means the phase has been delayed by approximately 6h compared to 3and 12m vehicle group (Fig. 78; $p \leq 0.05$). Upon melatonin administration the mean 24h levels were increased by 6.72 and 6.91 fold in 3 and 24m MT, compared to 3 and 24 m vehicle group respectively. However, daily pulse has been decreased in 3 and 12m-MT by about 0.02 and 0.04

fold compared to 3 and 12m vehicle group respectively and increased in 24m-MT by about 3.81 fold compared to 24m vehicle group (Fig. 79, Table 23; $p \leq 0.05$).

There was no correlation between *Per2-Cry1; Per2-Cry2; Per2-Bmal1; Cry1-Cry2; Per1-Cry2; Cry2-Bmal1* in the light phase whereas they were correlated in dark phase in 3 m vehicle group. The *Per1-Per2* has shown positive correlation in both light and dark phase of 3 m vehicle group. In 3m MT group there was no correlation between *Per1-Per2; Per1-Cry1; Per1-Cry2; Per1-Bmal1; Per2-Cry1; Per2-Cry2; Per2-Bmal1; Cry1-Cry2; Cry2-Bmal1* in the dark phase whereas they were correlated in light phase. In light and dark phase of 12 m vehicle group positive correlation was observed between *Per2-Cry1; Cry2-Bmal1*. There was no correlation between *Per2-Cry1; Per2-Cry2; Per2-Bmal1; Cry1-Bmal1* in the dark phase whereas they were correlated in light phase. Negative correlation between *Per1-Bmal1; Per1-Cry2* in the dark phase has not observed in light phase. In 12m MT group there was no correlation between *Per1-Per2* in light phase whereas they were correlated in dark phase and correlation observed between *Per2-Bmal1; Per2-Cry1* in the light phase has not been observed in the dark phase. In both light and dark phase correlation was observed between *Cry1-Bmal1; Per2-Cry2; Cry1-Cry2; Cry2-Bmal1*. In 24 m vehicle group light phase correlation between *Per1-Cry2* has not been observed in dark phase and correlation between *Per2-Bmal1; Per2-Cry2* observed in dark phase is not observed in light phase. No correlation observed between remaining pair wise comparisons in 24 m vehicle group. In both light and dark phase of 24 m MT group positive correlation was observed between *Per1-Cry1; Per1-Bmal1; Cry2-Bmal1*. There was negative correlation between *Per1-Per2* in light phase whereas they were not correlated in dark phase (Fig. 80; $p \leq 0.05$).

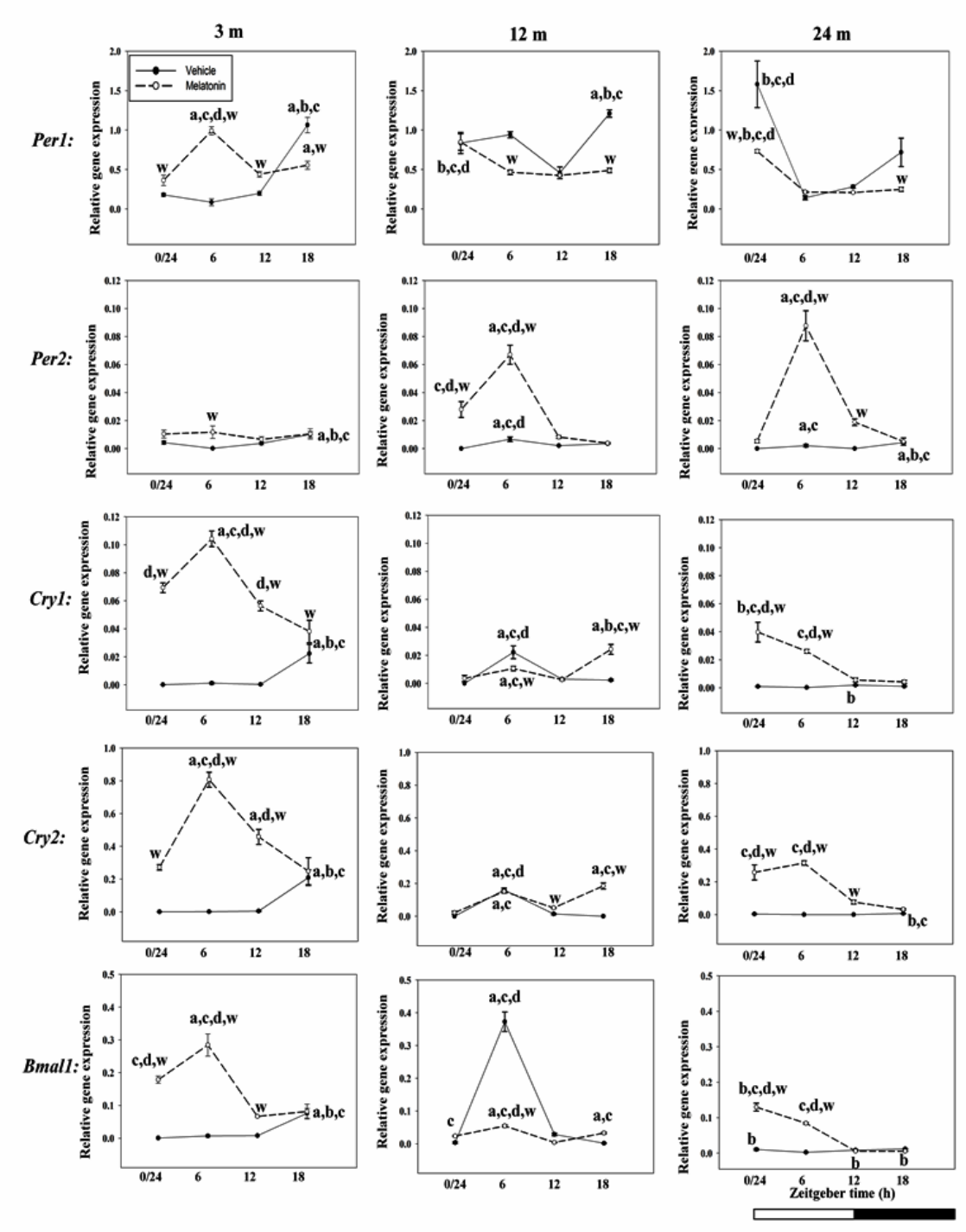

Fig. 78: Effect of melatonin administration on levels and rhythmicity of *Per1*, *Per2*, *Cry1*, *Cry2* and *Bmal1* genes in the aging rat Pineal in 3, 12 and 24 m. Each value is mean ± SEM (n=4), $p \leq 0.05$ and expressed as relative gene expression. $p_a \leq 0.05$; $p_b \leq 0.05$, $p_c \leq 0.05$ and $p_d \leq 0.05$ (where a, b, c and d refers to comparison with ZT0, ZT6, ZT12 and ZT18 respectively within the group) $p_w \leq 0.05$ (where w refers to comparison of gene levels at same time point in vehicle group in same age group).

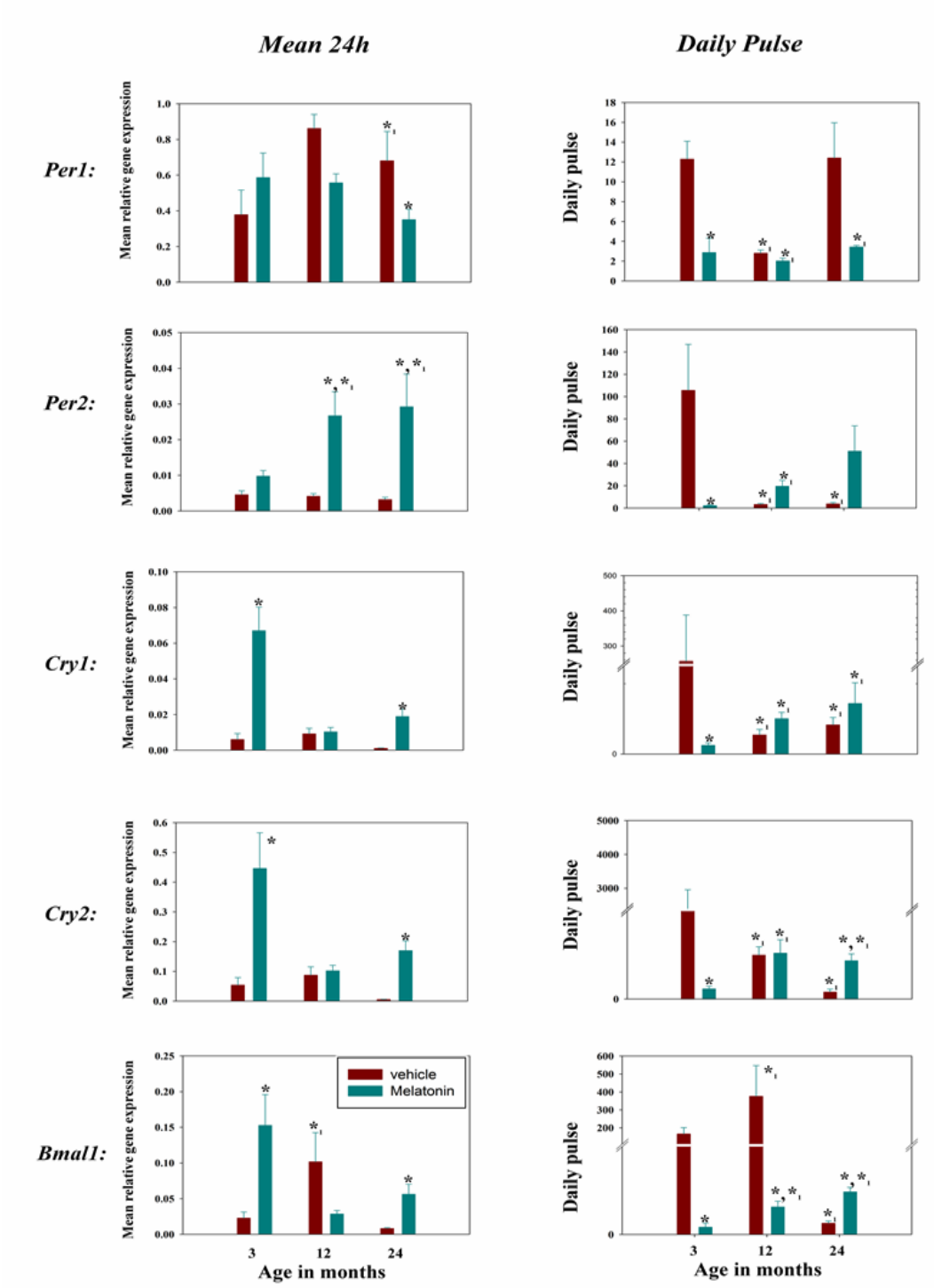

Fig. 79: Effect of melatonin administration on mean 24h levels and Daily Pulse of *Per1, Per2, Cry1, Cry2 and Bmal1* genes in the aging rat Pineal in 3, 12 and 24 m. Each value is mean ± SEM $p \leq 0.05$ and expressed as mean relative gene expression. $p_{*} \leq 0.05$ (where * refers to comparison with vehicle group). $p_{*1} \leq 0.05$ (where $_{*1}$ refers to comparison with 3 m vehicle group).

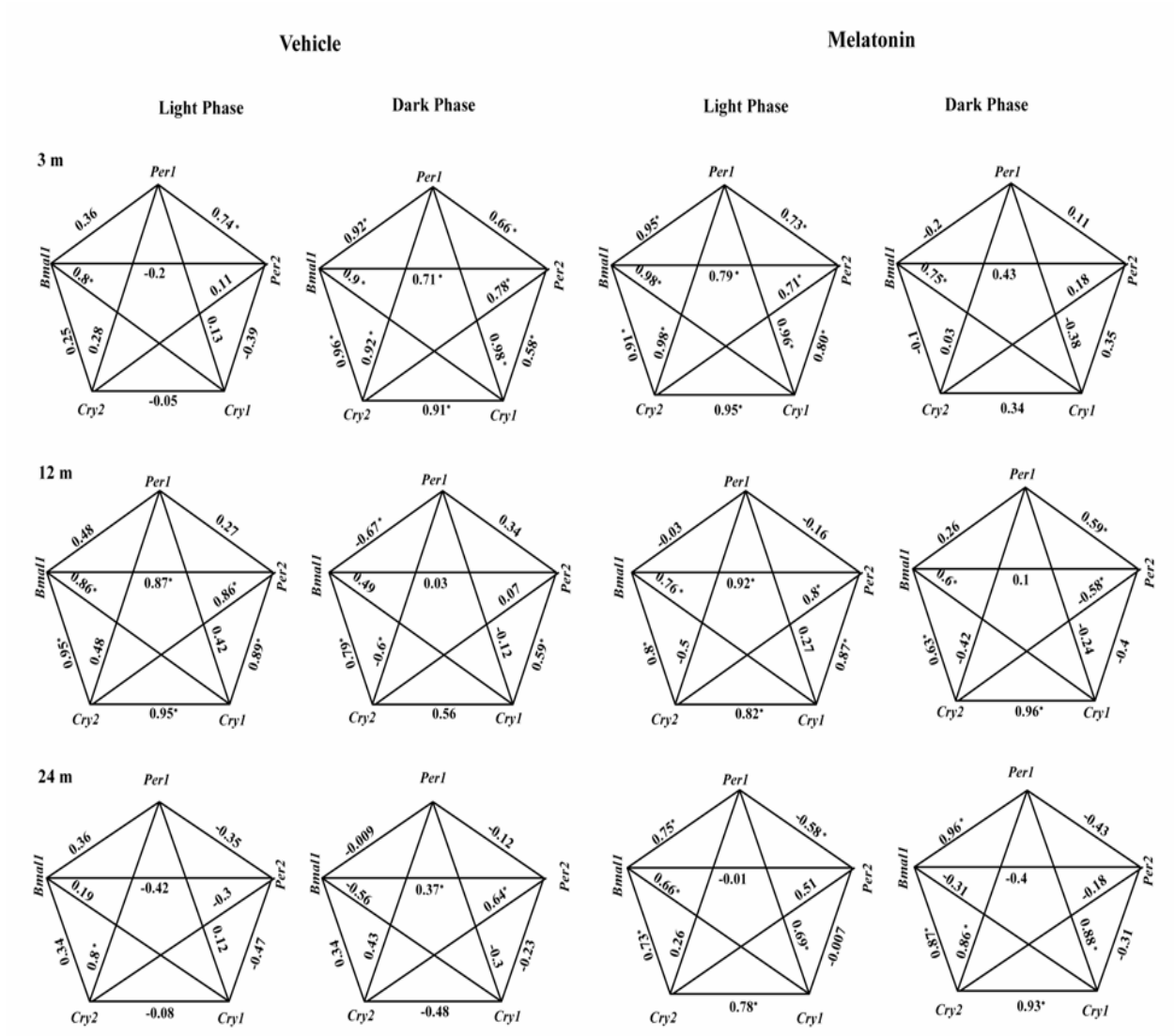

Fig. 80: Effect of melatonin administration on pair wise correlation between mean light (ZT 0, 6 and12) and mean dark (ZT 12,18 and 24/0) phase values of *Per1, Per2,Cry1, Cry2 and Bmal1* in various age groups 3, 12 and 24 m in rat Pineal. Each value is correlation coefficient values between the parameters. * indicates statistically significant value between parameters ($p \leq 0.05$). Negative value indicates negative correlation between parameters.

Table 23. Effect of melatonin on age induced changes in mean 24 h levels and daily pulse of various clock genes expression in Pineal.

Genes	Age in Months (m)	Ratio maximum: minimum		Mean (24h) **	
		Vehicle	Melatonin	Vehicle	Melatonin
Per1	3	12.29±1.81	2.87±1.45 *	0.38±0.14	0.58±0.14
	12	2.79±0.33 x	2.01±0.3	0.86±0.08 x	0.55±0.05
	24	12.39±3.56 y	3.43±0.15	0.68±0. 16 x	0.35±0.057 *
Per2	3	105.65±41.17	2.27±0.76 *	0.004±0.001	0.009±0.0015
	12	3.23±0.84 x	19.67±5.27	0.004±0.0007	0.0267±0.0067 *
	24	3.68±1.28 x	50.98±22.83	0.003±0.0006	0.0292±0.009 *
Cry1	3	256.54±131.53	2.49±0.71	0.006±0.003	0.07±0.013 *
	12	5.46±1.54 x	10.05±1.8 *	0.009±0.003 x	0.01±0.002
	24	8.32±2.08 x	14.39±5.89	0.001±0.0002 x, y	0.019±0.004 *
Cry2	3	2362.10±593.2	2.88±0.75 *	0.053±0.025	0.44±0.12 *
	12	12.48±2.34 x	13.05±3.8	0.087±0.028	0.1±0.02
	24	1.97±0.82 x	10.89±1.93	0.005±0.001 y	0.2±0.03 *
Bmal1	3	166.06±35.36	4.17±2.31	0.023±0.008	0.15±0.04 *
	12	376.13±170.88	15.59±3.32 *	0.1±0.04 x	0.028±0.005
	24	6.36±1.27 x	24.25±2.61	0.008±0.001 y	0.056±0.01 *

Each value is Mean ± SE (n=4). **Mean (24 h) n=16 represented (with n=4 at ZT0, 6, 12 and 18) for relative gene expression of all the studied clock genes. $P_x \leq 0.05$, $P_y \leq 0.05$ and $P_z \leq 0.05$ (where x, y and z refers to comparison with 3, 12 and 24 month old rats respectively) and * refers to comparison with control and melatonin administered rats within same age groups ($P \leq 0.05$).

(c) Effect of melatonin administration on various clock gene expression levels and its rhythmicity in the aging SN:

Per1: Maximum and minimum levels in 3 m MT were observed at ZT12 and minimum at ZT6 respectively, thus phase of the rhythm was advanced by approximately 6h compared to 3 m vehicle group. In 12 m MT daily rhythm persisted and maximum levels were observed at ZT0 instead of ZT6 which has been observed in case of 12 m vehicle group, thus phase of the rhythm has been advanced by approximately 6h compared to 12 m vehicle group and approximately 6h delay compared to 3m vehicle group. In 24 m MT daily rhythm persisted and maximum levels were observed at ZT12 instead of ZT0 which has been observed in case of 24 m vehicle group, thus phase of the rhythm has been delayed by approximately 12h compared to 24 m vehicle group and approximately 6h advance compared to 3m vehicle group (Fig. 81; $p \leq 0.05$). Upon melatonin administration the mean 24h levels were increased by 9 fold in 3m and decreased by 0.5 fold in 24 m compared to 3 and 24 m vehicle group respectively, whereas daily pulse has been decreased in 3m-MT by 0.09 fold compared to 3m vehicle group (Fig. 82, Table 24; $p \leq 0.05$).

Per2: In 3 m MT maximum levels were observed at ZT0 and minimum at ZT6, thus phase of the rhythm was advanced by approximately 12h compared to 3 m vehicle group. In 12 m MT daily rhythm persisted and maximum levels were observed at ZT18 instead of ZT0 which has been observed in case of 12 m vehicle group, thus phase of the rhythm has been advanced by approximately 6h compared to 12 m vehicle group and delayed by approximately 6h compared to 3m vehicle group. In 24 m MT daily rhythm persisted and maximum levels were observed at ZT6 instead of ZT12 which has been observed in case of 24m and 3m vehicle group, thus phase of the rhythm has been advanced by approximately 6h compared to 3and 24m vehicle group (Fig. 81; $p \leq 0.05$). Upon melatonin administration the mean 24h levels were decreased by 0.26, 0.22 and 0.13 fold in 3, 12 and 24m MT compared to 3, 12 and 24 m vehicle group respectively. However, daily pulse has been increased in 12m-MT by about 1.68 and 1.4 fold compared to 12 and 3m vehicle group respectively (Fig. 82, Table 24; $p \leq 0.05$).

Cry1: Maximum and minimum levels in 3 m MT were observed at ZT0 and minimum at ZT6, thus phase of the rhythm was delayed by approximately 6h compared to 3 m vehicle group. In 12 m MT daily rhythm persisted and maximum levels were observed at ZT18 instead of ZT0 which has been observed in case of 12 m vehicle group, thus phase of the rhythm has been advanced approximately 6h compared to 12 m vehicle group, leading to restoration of the phase of rhythm compared to 3m vehicle group. In 24 m MT daily rhythm persisted and maximum levels were observed at ZT0 instead of ZT12 which has been observed in case of 24m vehicle group, thus phase of the rhythm has been advanced by approximately 12h compared to 24m vehicle group and delayed by approximately 6h compared to 3m vehicle group (Fig. 81; $p \leq 0.05$). Upon melatonin administration the mean 24h levels were decreased by 0.33, 0.24 and 0.18 fold in 3, 12 and 24m MT compared to 3, 12and 24 m vehicle group respectively. However, daily pulse has decreased in 12m-MT by about 0.48 and increased in 24m-MT by about 2.44 fold compared to 12 and 24m vehicle group respectively (Fig. 82, Table 24; $p \leq 0.05$).

Cry2: In 3 m MT maximum levels were observed at ZT0 and minimum at ZT6, thus phase of the rhythm was advanced by approximately 12h compared to 3 m vehicle group. In 12 m MT daily rhythm persisted and maximum levels were observed at ZT18 instead of ZT0 which has been observed in case of 12 m vehicle group, thus phase of the rhythm has been advanced by approximately 6h compared to 12 m vehicle group and delayed by approximately 6h compared to 3m vehicle group. In 24 m MT daily rhythm persisted and maximum levels were observed at ZT0 instead of ZT18 which has been observed in case of 24m vehicle group, thus phase of the rhythm has been delayed by approximately 6h compared to 24m vehicle group and advanced by approximately 12h compared to 3m vehicle group (Fig. 81; $p \leq 0.05$). Upon melatonin administration the mean 24h levels were decreased by 0.3, 0.25 and 0.13 fold in 3, 12 and 24m MT compared to 3, 12 and 24 m vehicle group respectively. Daily pulse has been decreased in 12m-MT by about 0.24 fold compared to 12m vehicle group (Fig. 82, Table 24; $p \leq 0.05$).

*Bmal1:*Maximum and minimum levels in 3 m MT were observed at ZT0 and minimum at ZT6, thus phase of the rhythm was delayed by approximately 6h compared to 3 m vehicle group. In 12 m MT daily rhythm persisted and maximum levels were observed at ZT18 instead of ZT0

which has been observed in case of 12 m vehicle group, thus phase of the rhythm has been advanced by approximately 6h compared to 12 m vehicle group, leading to restoration of the phase of rhythm compared to 3m vehicle group. In 24 m MT daily rhythm restored compared to 24 m vehicle group, and its maximum levels were observed at ZT0 and delayed by approximately 6h compared to 3m vehicle group (Fig. 81; $p \leq 0.05$). Upon melatonin administration the mean 24h levels were decreased by 0.34, 0.27 and 0.25 fold in 3, 12 and 24m MT compared to 3, 12 and 24 m vehicle group respectively. However, daily pulse is increased in 24m-MT by about 3.43 and 3.28 fold compared to 24 and 3m vehicle group respectively (Fig. 82, Table 24; $p \leq 0.05$).

In 3 m vehicle group there was no correlation between *Per2-Bmal1; Cry1-Cry2* in the dark phase whereas they were correlated in light phase. The *Per1-Cry1; Per2-Cry1; Per2-Cry2; Cry1-Bmal1* has shown positive correlation in both light and dark phase of 3 m vehicle group. In 3m MT group there was no correlation between *Per1-Cry1; Per1-Cry2; Per1-Bmal1* in the dark phase whereas they were correlated in light phase. The *Per1-Per2; Per2-Cry1; Per2-Bmal1; Cry1-Cry2; Cry1-Bmal1* has shown positive correlation in both light and dark phase of 3 m MT group. In light and dark phase of 12 m vehicle group positive correlation was observed between *Per2-Cry1; Cry2-Bmal1; Per2-Cry2; Per2-Bmal1; Cry1-Cry2; Cry2-Bmal1*. There was no correlation between *Per1-Bmal1; Per1-Cry1; Per1-Cry2* in the dark phase whereas they were correlated in light phase. In 12m MT group there was no correlation between *Per2-Bmal1* in light phase whereas they were correlated in dark phase. In both light and dark phase, correlation was observed between *Per1-Per2; Per1-Cry1; Per1-Cry2; Per1-Bmal1; Per2-Cry1; Per2-Cry2; Cry1-Cry2; Cry1-Bmal1; Cry2-Bmal1*. In 24 m vehicle group light phase correlation between *Per1-Per2; Per2-Cry1; Per1-Cry2*has not been observed in dark phase. The *Per1-Bmal1; Per2-Cry2* has shown positive correlation in both light and dark phase of 24 m vehicle group. No correlation observed between remaining pair wise comparisons in 24 m vehicle group. In both light and dark phase of 24 m MT group positive correlation was observed between *Cry1-Bmal1*. There was negative correlation between *Per1-Bmal1; Per2-Bmal1; Per2-Cry1; Per1-Cry1* in light phase whereas they were not correlated in dark phase (Fig. 83; $p \leq 0.05$).

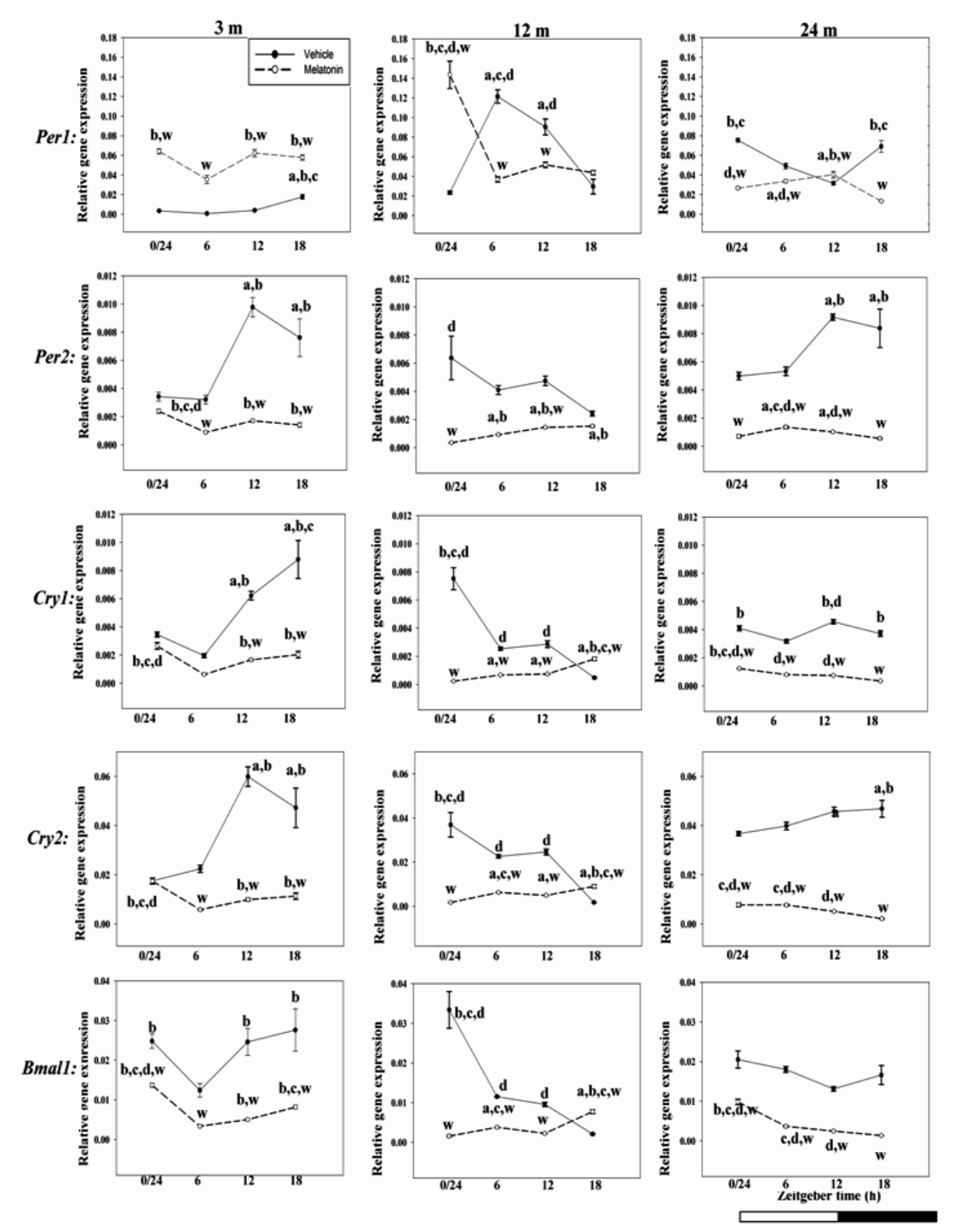

Fig. 81: Effect of melatonin administration on levels and rhythmicity of *Per1*, *Per2*, *Cry1*, *Cry2* and *Bmal1* genes in the aging rat SN in 3, 12 and 24 m. Each value is mean ± SEM (n=4), $p \leq 0.05$ and expressed as relative gene expression. $p_a \leq 0.05$; $p_b \leq 0.05$, $p_c \leq 0.05$ and $p_d \leq 0.05$ (where a, b, c and d refers to comparison with ZT0, ZT6, ZT12 and ZT18 respectively within the group) $p_w \leq 0.05$ (where w refers to comparison of gene levels at same time point in vehicle group in same age group).

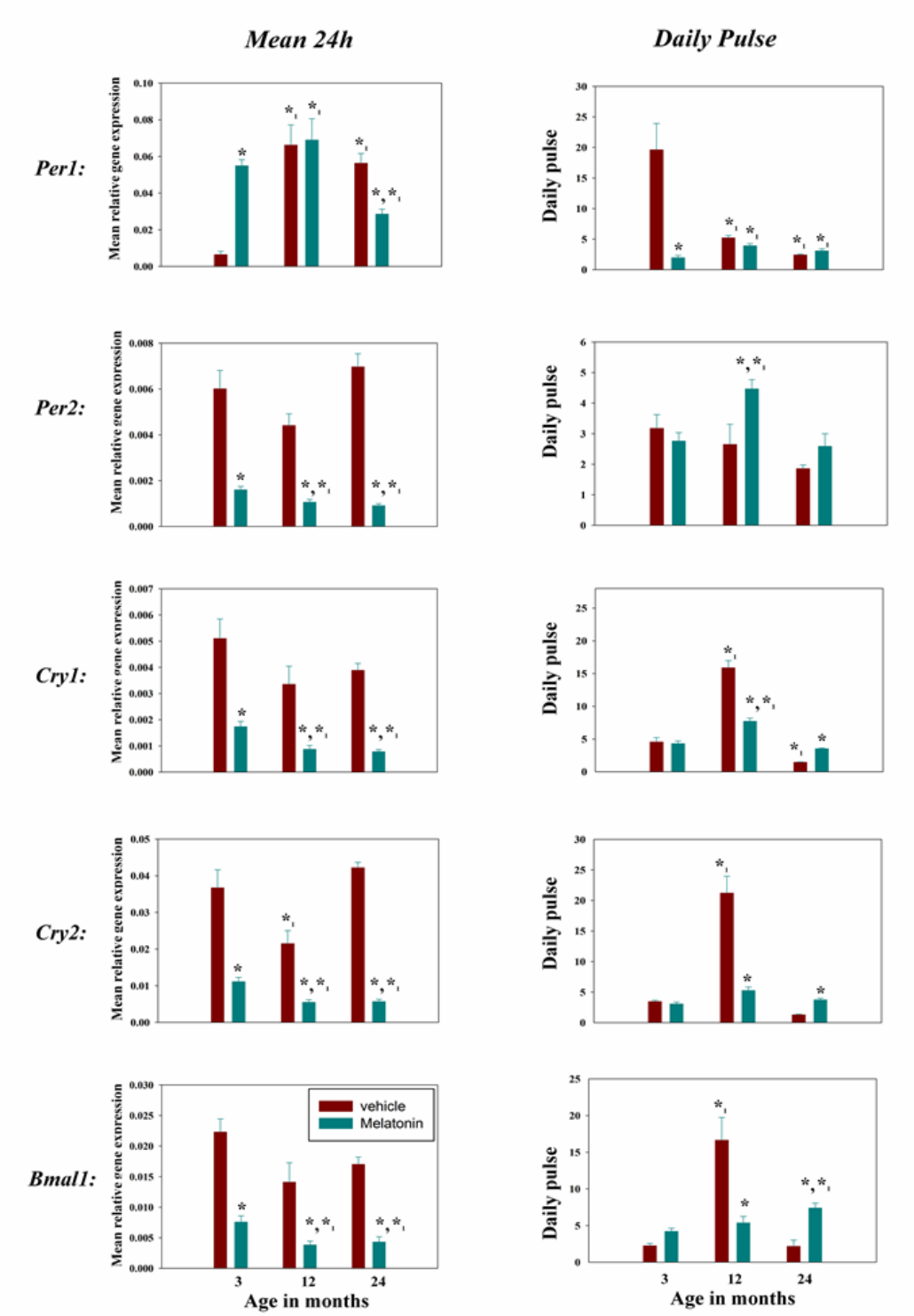

Fig. 82: Effect of melatonin administration on mean 24h levels and Daily Pulse of *Per1*, *Per2*, *Cry1*, *Cry2* and *Bmal1* genes in the aging rat SN in 3, 12 and 24 m. Each value is mean ± SEM $p \leq 0.05$ and expressed as mean relative gene expression. $p_{*} \leq 0.05$ (where * refers to comparison with vehicle group). $p_{*1} \leq 0.05$ (where $_{*1}$ refers to comparison with 3 m vehicle group).

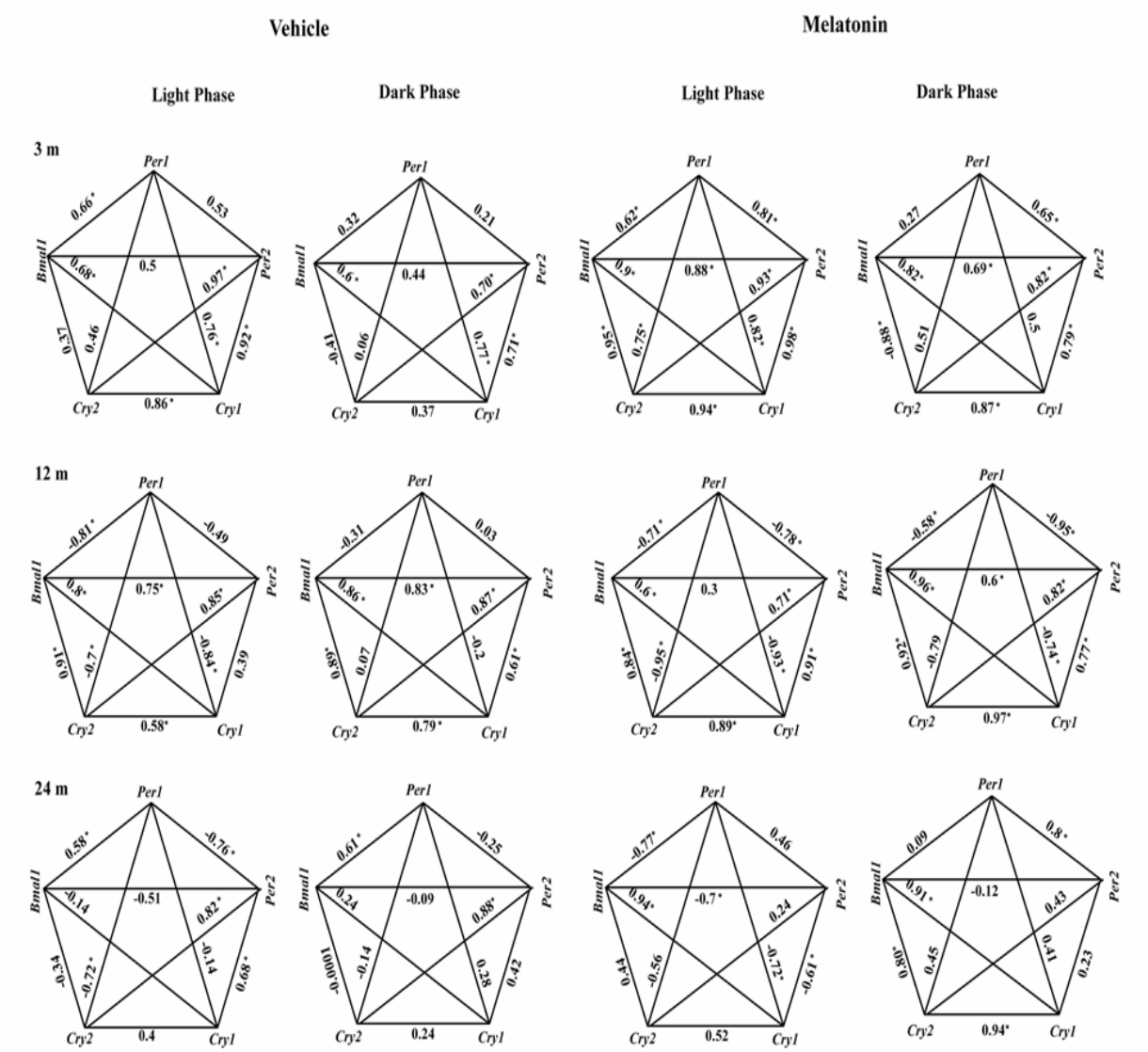

Fig. 83: Effect of melatonin administration on pair wise correlation between mean light (ZT 0, 6 and 12) and mean dark (ZT 12,18 and 24/0) phase values of *Per1, Per2,Cry1, Cry2 and Bmal1* in various age groups 3, 12 and 24 m in rat SN. Each value is correlation coefficient between the parameters. * indicates statistically significant value between parameters ($p < 0.05$). Negative value indicates negative correlation between parameters.

Table 24. Effect of melatonin on age induced changes in mean 24 h levels and daily pulse of various clock genes expression in SN.

Genes	Age in Months (m)	Ratio maximum: minimum		Mean (24h) **	
		Vehicle	Melatonin	Vehicle	Melatonin
Per1	3	19.62±4.3	1.94±0.37 *	0.006±0.002	0.05±0.003 *
	12	5.20±0.38 x	3.91±0.34	0.06±0.01 x	0.07±0.01
	24	2.41±0.14 x	3.07±0.36	0.05±0.0.005 x	0.03±0.003 *
Per2	3	3.17±0.45	2.76±0.27	0.006±0.0008	0.001±0.0001 *
	12	2.64±0.66	4.46±0.3 *	0.004±0.0005 x	0.001±0.0001 *
	24	1.85±0.12	2.58±0.41	0.007±0.0006 y	0.0009±0.00008 *
Cry1	3	4.55±0.68	4.29±0.4	0.005±0.0007	0.002±0.0002 *
	12	15.89±1.09 x	7.7±0.5 *	0.003±0.0007 x	0.0008±0.0001 *
	24	1.44±0.08 x, y	3.53±0.12 *	0.004±0.0002	0.0007±0.00008 *
Cry2	3	3.44±0.19	3.05±0.33	0.04±0.005	0.01±0.001 *
	12	21.22±2.73 x	5.26±0.56 *	0.02±0.35 x	0.005±0.0006 *
	24	1.28±0.11 y	3.73±0.27	0.04±0.001 y	0.005±0.0006 *
Bmal1	3	2.25±0.31	4.21±0.42	0.02±0.002	0.007±0.001 *
	12	16.63±3.09 x	5.36±0.87 *	0.014±0.003 x	0.004±0.0006 *
	24	2.15±0.87 y	7.38±0.68 *	0.02±0.001 x	0.004±0.0008 *

Each value is Mean ± SE (n=4). **Mean (24 h) n=16 represented (with n=4 at ZT0, 6, 12 and 18) for relative gene expression of all the studied clock genes. $P_x \leq 0.05$, $P_y \leq 0.05$ and $P_z \leq 0.05$ (where x, y and z refers to comparison with 3, 12 and 24 month old rats respectively) and * refers to comparison with control and melatonin administered rats within same age groups ($P \leq 0.05$).

(d) Effect of melatonin administration on various clock gene expression levels and its rhythmicity in SCN of RIPD rat model:

Per1: In RIPD MEL group, maximum levels were observed at ZT6 and minimum at ZT18 as in vehicle group, thus melatonin restored phase of the daily rhythm which has altered in RIPD rat model. In RT+MEL group, maximum levels were atZT12 as in RIPD group, thus melatonin administration along with rotenone could not stop the rotenone induced phase alteration in *Per1* daily rhythm (Fig. 84; $p \leq 0.05$). Mean 24h levels of *Per1* in both RIPD MEL and RT+MEL group has been increased by about 2.15 and 2.1 fold respectively compared to RIPD rat model, whereas daily pulse has not restored in both the groups compared to RIPD group(Fig. 85, Table 25; $p \leq 0.05$).

Per2: In RIPD MEL and RT+MEL group, maximum levels were observed at ZT12 and minimum at ZT0 as in vehicle and RIPD group (Fig. 84; $p \leq 0.05$). We observed increased mean 24h levels of *Per2* in RIPD, RIPD MEL and RT+MEL group by about 1.71, 1.43 and 1.43 fold respectively. Decreased daily pulse in RIPD group compared to vehicle has been restored in RT+MEL group but not in RIPD MEL group (Fig. 85, Table 25; $p \leq 0.05$).

Cry1: In RIPD MEL group, maximum levels were observed at ZT0 as in RIPD group but, in RT+MEL group maximum levels were at ZT12 as in vehicle group, thus melatonin has restored *Cry1* phase of the daily rhythm in RT+MEL group(Fig. 84; $p \leq 0.05$). Mean 24h levels were increased in both RIPD MEL and RT+MEL group by about 2.43 and 2 fold respectively compared to RIPD. Daily pulse has been restored by melatonin in both RIPD MEL and RT+MEL group (Fig. 85, Table 25; $p \leq 0.05$).

Cry2: In RIPD MEL and RT+MEL group, maximum levels were observed at ZT12 as in vehicle and RIPD group (Fig. 84; $p \leq 0.05$). We have not observed any significant difference in mean 24h levels among all the groups studied. Decreased daily pulse in RIPD group compared to vehicle has not been restored by melatonin in both RIPD MEL and RT+MEL group (Fig. 85, Table 25; $p \leq 0.05$).

Bmal1: In RIPD MEL and RT+MEL group, maximum levels were observed at ZT0 as in RIPD group (Fig. 84; $p \leq 0.05$). We observed increased mean 24h levels in both RIPD MEL and RT+MEL group by about 8.7 and 6.7 fold respectively compared to RIPD group. Decreased daily pulse in RIPD group compared to vehicle has not been restored by melatonin in both RIPD MEL and RT+MEL group (Fig. 85, Table 25; $p \leq 0.05$).

In vehicle group light phase positive correlation between *Bmal1-Per2* has become negative in dark phase. There was no correlation between *Bmal1-Per1; Per1-Per2; Per1-Cry2; Per1-Cry1* in the light phase whereas they were correlated in dark phase. In both light and dark *Per2-Cry1; Per2-Cry2* has shown positive correlation. Positive correlation between *Bmal1-Cry1* in light phase has not observed in dark phase. In RIPD group there was no correlation between *Per1-Per2; Per1-Cry2* in the light phase whereas they were correlated in dark phase. In both light and dark *Bmal1-Cry1; Per2-Cry2* has shown positive correlation. Negative correlation between *Bmal1-Per2* in light phase has not observed in dark phase. In RIPD MEL group we observed positive correlation between *Per1-Per2; Per2-Cry2; Cry1-Cry2; Cry1-Bmal1*in both light and dark phase. There was no correlation between *Per1-Cry2* in the light phase whereas they were correlated in dark phase. In RT+MEL group positive correlation was observed between *Per1-Per2; Per2-Cry2; Cry1-Cry2; Per1-Cry2* in both light and dark phase. There was no correlation between *Per1-Cry1*in the light phase whereas they were correlated in dark phase and light phase negative correlation between *Per2-Bmal* has not observed in dark phase (Fig. 86; $p \leq 0.05$).

In light phase there was no correlation between *Per1-Per2; Per1-Cry2* in vehicle and RIPD group but they were correlated in both RIPD MEL and RT+MEL group. Vehicle group positive correlation between *Cry1-Cry2* which has lost in RIPD group has been restored by melatonin in RIPD MEL and RT+MEL groups. Vehicle group positive correlation between *Per2-Cry1; Cry2-Bmal1* which has lost in RIPD group has not restored by melatonin in RIPD MEL and RT+MEL groups. In dark phase the correlation between *Per1-Bmal1; Per2-Cry1; Per2-Bmal1; Cry1-Cry2* has lost in RIPD compared to vehicle which has been restored by melatonin in RIPD MEL and RT+MEL groups. Vehicle group positive correlation between *Cry1-Cry2* which has lost in RIPD group has been restored by melatonin in RT+MEL group but not in RIPD MEL group (Fig. 86; $p \leq 0.05$).

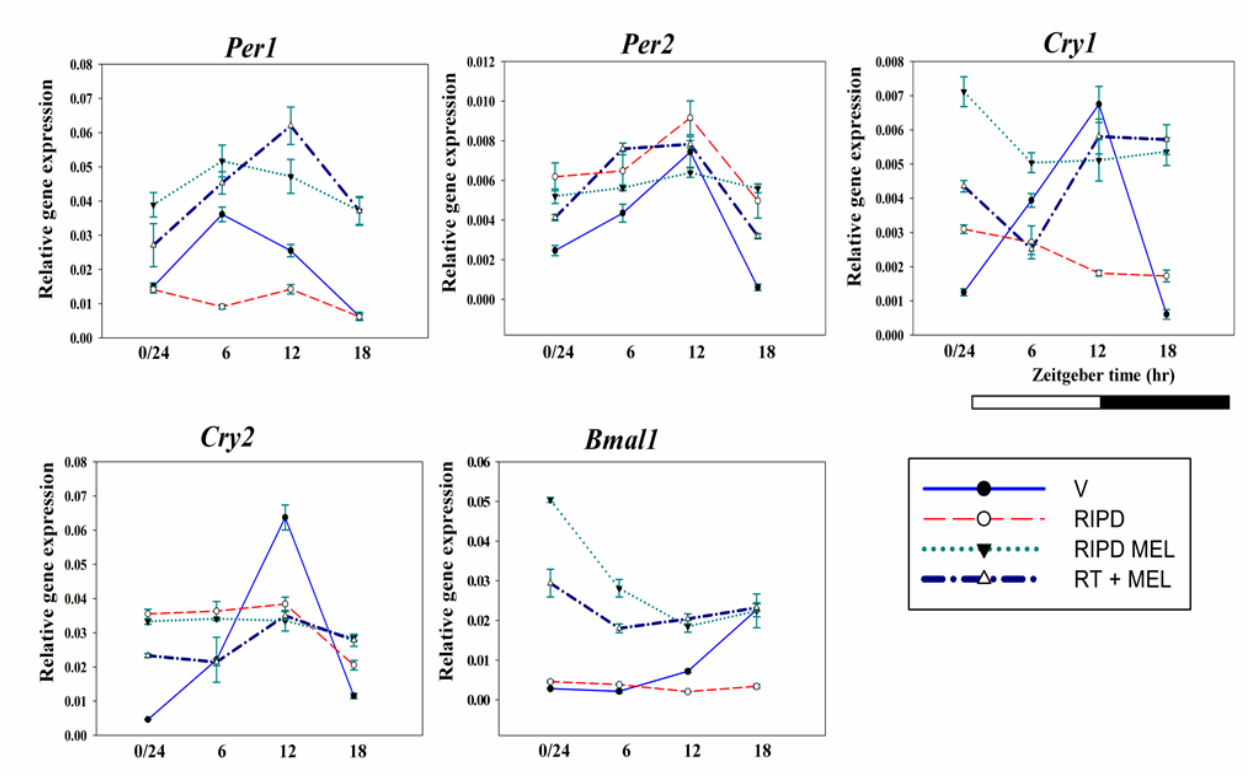

Fig. 84: Effect of melatonin administration on levels and rhythmicity of *Per1*, *Per2*, *Cry1*, *Cry2* and *Bmal1* genes in the SCN of RIPD rat model. Each value is mean ± SEM (n=4). V - Vehicle, RIPD - Rotenone induced PD, RIPD MEL - RIPD model received MEL for 11 days and RT + MEL - animals received both Rotenone and MEL for 48 days.

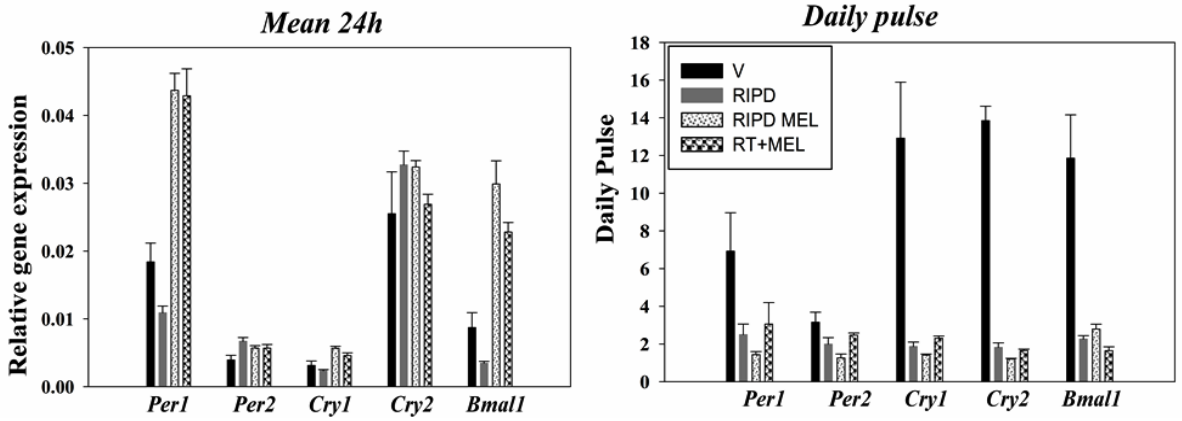

Fig. 85: Effect of melatonin administration on mean 24h levels and Daily Pulse of *Per1*, *Per2*, *Cry1*, *Cry2 and Bmal1* genes in the SCN of RIPD rat model. Each value is mean ± SEM (n=4). V - Vehicle, RIPD - Rotenone induced PD, RIPD MEL - RIPD model received MEL for 11 days and RT + MEL - animals received both Rotenone and MEL for 48 days.

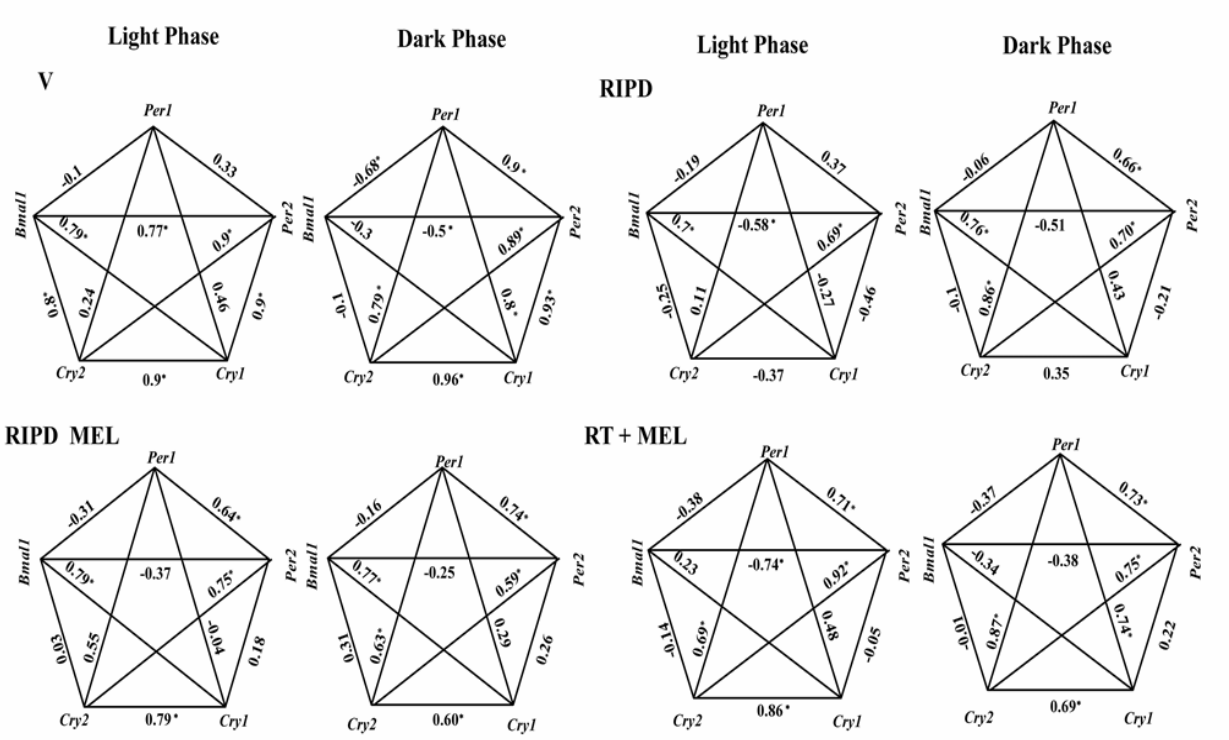

Fig. 86: Effect of melatonin administration on pair wise correlation between mean light (ZT 0, 6 and 12) and mean dark (ZT 12, 18 and 24/0) phase values of *Per1, Per2, Cry1, Cry2 and Bmal1* in the SCN of RIPD rat model. Each value is mean ± SEM (n=4). V - Vehicle, RIPD - Rotenone induced PD, RIPD MEL - RIPD model received MEL for 11 days and RT + MEL - animals received both Rotenone and MEL for 48 days. Each value is correlation coefficient values between the parameters. * indicates statistically significant value between parameters ($p \leq 0.05$). Negative value indicates negative correlation between parameters.

Table 25. Effect of melatonin on mean 24 h levels and daily pulse of various clock genes expression in SCN of Rotenone induced PD (RIPD) rat model.

Gene	Experimental Group	Zeitgeber time (h)				Ratio	Mean 24h
		0	6	12	18		
Per1	V	0.015 ± 0.001 [d]	0.036 ± 0.002 [a, c, d]	0.025 ± 0.001 [a, d]	0.006 ± 0.001	6.92 ± 2.04	0.02 ± 0.002
	RIPD	0.014 ± 0.0009 [b, d]	0.009 ± 0.0006	0.014 ± 0.001 [b, d]	0.006 ± 0.0007	2.49 ± 0.55 [r]	0.01 ± 0.0009 [r]
	RIPD MEL	0.04 ± 0.003 [b]	0.05 ± 0.004	0.047 ± 0.004	0.037 ± 0.004 [b]	1.43 ± 0.16 [r]	0.04 ± 0.002 [r, p]
	RT + MEL	0.027 ± 0.006	0.045 ± 0.003 [a]	0.06 ± 0.005 [a, b, d]	0.037 ± 0.004	3.06 ± 1.13 [r]	0.042 ± 0.003 [r, p]
Per2	V	0.002 ± 0.0002 [d]	0.004 ± 0.0004 [a, d]	0.007 ± 0.0007 [a, b, d]	0.0006 ± 0.0001	3.15 ± 0.53	0.004 ± 0.0006
	RIPD	0.006 ± 0.0007	0.006 ± 0.0009	0.009 ± 0.0008 [a, b, d]	0.004 ± 0.0008	1.98 ± 0.34 [r]	0.007 ± 0.0005 [r]
	RIPD MEL	0.005 ± 0.0003	0.0056 ± 0.0001	0.006 ± 0.0002 [a]	0.005 ± 0.0002	1.21 ± 0.2 [r]	0.0056 ± 0.0003 [r]
	RT + MEL	0.004 ± 0.0001 [d]	0.007 ± 0.0002 [a, d]	0.008 ± 0.0001 [a, d]	0.003 ± 0.0001	2.46 ± 0.11	0.0056 ± 0.0005 [r]
Cry1	V	0.001 ± 0.0001	0.004 ± 0.0001 [a, d]	0.007 ± 0.0005 [a, b, d]	0.0006 ± 0.0001	12.96 ± 2.96	0.0031 ± 0.0006
	RIPD	0.003 ± 0.0001 [c, d]	0.002 ± 0.0004 [c, d]	0.002 ± 0.00008	0.002 ± 0.0001	1.86 ± 0.23 [r]	0.002 ± 0.0001
	RIPD MEL	0.007 ± 0.0004 [b, c, d]	0.005 ± 0.0002	0.005 ± 0.0006	0.005 ± 0.0004	1.41 ± 0.05 [r]	0.0056 ± 0.0002 [r, p]
	RT + MEL	0.004 ± 0.0001 [b]	0.002 ± 0.0001	0.0058 ± 0.0005 [a, b]	0.0057 ± 0.0004 [a, b]	2.31 ± 0.11 [r]	0.0046 ± 0.0003 [r, p]
Cry2	V	0.0046 ± 0.00006	0.02 ± 0.0006 [a]	0.063 ± 0.003 [a, b, d]	0.011 ± 0.0007	13.84 ± 0.76	0.025 ± 0.006
	RIPD	0.035 ± 0.001 [d]	0.036 ± 0.002 [d]	0.038 ± 0.002 [d]	0.02 ± 0.0013	1.82 ± 0.24 [r]	0.032 ± 0.002
	RIPD MEL	0.033 ± 0.0008	0.033 ± 0.0001	0.034 ± 0.0003	0.028 ± 0.0007 [c]	1.2 ± 0.035 [r]	0.032 ± 0.0009
	RT + MEL	0.023 ± 0.0005	0.021 ± 0.001	0.035 ± 0.001 [a, b, d]	0.027 ± 0.0017 [a, b]	1.64 ± 0.078 [r]	0.026 ± 0.001
Bmal1	V	0.0028 ± 0.0002	0.0021 ± 0.0004	0.0072 ± 0.0003 [a, b]	0.023 ± 0.0017 [a, b, c]	11.85 ± 2.3	0.0087± 0.0021
	RIPD	0.0045 ± 0.00022 [c, d]	0.0038 ± 0.00007 [c]	0.0020 ± 0.0001	0.0033 ± 0.0004 [c]	2.26± 0.18 [r]	0.0034± 0.0002 [r]
	RIPD MEL	0.50 ± 0.0006 [b, c, d]	0.028± 0.0021 [c]	0.018 ± 0.0014	0.022 ± 0.0042	2.78± 0.258 [r]	0.03± 0.0033 [r, p]
	RT + MEL	0.029 ± 0.0035 [b, c, d]	0.018 ± 0.0011	0.02 ± 0.0012	0.023 ± 0.0009	1.64± 0.20 [r]	0.023± 0.0014 [r, p]

Each value is Mean ± SE (n=4) and expressed in relative genes expression. V - Vehicle, RIPD - Rotenone induced PD, RIPD MEL - RIPD model received MEL for 11 days and RT + MEL - animals received both Rotenone and MEL for 48 days. $p_a \leq 0.05$; $p_b \leq 0.05$, $p_c \leq 0.05$ and $p_d \leq 0.05$ (where a, b, c and d refers to comparison with ZT0, ZT6, ZT12 and ZT18 respectively within the group) *);* r - refers to comparison with vehicle and p - refers to comparison with RIPD.

(e) Effect of melatonin administration on various clock gene expression levels and its rhythmicity in Pineal of RIPD rat model:

Per1: In RIPD MEL group, maximum levels were observed at ZT6 and minimum at ZT0 which is showing approximately 6h advance to vehicle and approximately 12h advance to RIPD group. In RT+MEL group, maximum levels were observed at ZT18as in RIPD group thus melatonin administration along with rotenone could not stop the rotenone induced phase alteration in *Per1* daily rhythm (Fig. 87; $p \leq 0.05$). Mean 24h levels of *Per1* in both RIPD MEL and RT+MEL group has been increased by about 8 and 20 fold respectively compared to RIPD rat model, whereas daily pulse has not restored in both the groups compared to RIPD group (Fig. 88, Table 26; $p \leq 0.05$).

Per2: In RT+MEL group, maximum levels were observed at ZT0 which is showing approximately 6h delay to vehicle and approximately 12h advance to RIPD group. In RIPD MEL group, maximum levels were observed at ZT12 as in RIPD group thus melatonin administration could not restore the rotenone induced phase alteration in *Per2* daily rhythm (Fig. 87; $p \leq 0.05$). We observed increased mean 24h levels of *Per2* in RT+MEL group by about 8.7 fold compared to both vehicle and RIPD but not in RIPD MEL group. Daily pulse has not been restored by melatonin in both RIPD MEL and RT+MEL group (Fig. 88, Table 26; $p \leq 0.05$).

Cry1: In RIPD MEL and RT+MEL group, maximum levels were at ZT18 as in Vehicle group, thus melatonin administration could restore rotenone induced phase alteration in *Cry1* daily rhythm (Fig. 87; $p \leq 0.05$). Mean 24h levels were increased in both RIPD MEL and RT+MEL group by about 51 and 68 fold respectively compared to Vehicle and RIPD group. Daily pulse has not been restored by melatonin in both RIPD MEL and RT+MEL group (Fig. 88, Table 26; $p \leq 0.05$).

Cry2: In RIPD MEL group, maximum levels were at ZT12 as in RIPD group, thus melatonin administration could not restore rotenone induced phase alteration in *Cry1* daily rhythm. In RT+MEL group, maximum levels were observed at ZT18 as in vehicle group, thus melatonin administration along with rotenone could stop the rotenone induced phase alteration in

Cry1 daily rhythm (Fig. 87; $p \leq 0.05$). We observed increased mean 24h levels of *Cry2* in both RIPD MEL and RT+MEL group by about 9.4 and 18 fold respectively compared to RIPD group. Daily pulse has not been restored by melatonin in both RIPD MEL and RT+MEL group (Fig. 88, Table 26; $p \leq 0.05$).

Bmal1: In RIPD MEL group, maximum levels were observed at ZT18 and minimum at ZT0 as in vehicle group, thus melatonin restored phase of the daily rhythm which has altered in RIPD. In RT+MEL group, maximum levels were at ZT12 as in RIPD group, thus melatonin administration along with rotenone could not stop the rotenone induced phase alteration in *Bmal1* daily rhythm (Fig. 87; $p \leq 0.05$). Mean 24h levels of *Bmal1* in both RIPD MEL and RT+MEL group has been increased by about 53 and 35 fold respectively compared to RIPD rat model, whereas daily pulse has not restored in both the groups compared to RIPD group (Fig. 88, Table 26; $p \leq 0.05$).

In vehicle group there was no correlation between *Bmal1-Per1; Bmal1-Cry1; Cry1-Cry2* in the light phase whereas they were correlated in dark phase. In both light and dark phase *Per1-Per2; Per1-Cry1; Per1-Cry2; Per2-Cry1; Per2-Cry2; Per2-Bmal1; Cry2-Bmal1* has shown positive correlation. In RIPD group light phase positive correlation observed between *Per1-Per2; Per1-Cry1; Per1-Cry2; Per1-Bmal1*is not observed in dark phase. In both light and dark phase *Per2-Cry1; Per2-Cry2; Per2-Bmal1; Cry1-Cry2; Cry1-Bmal1; Cry2-Bmal1* has shown positive correlation. In RIPD MEL group we observed positive correlation between *Per1-Per2; Per2-Cry2; Cry1-Cry2; Per1-Cry1; Per1-Cry2; Per2-Cry1*in both light and dark phase. There was no correlation between *Cry1-Bmal1* in the light phase whereas they were correlated in dark phase. In RT+MEL group positive correlation was observed between *Per1-Per2; Per2-Cry2; Cry1-Cry2; Per1-Cry1; Per1-Cry2; Per2-Cry1; Cry2-Bmal1*in both light and dark phase. There was no correlation between *Per2-Bmal1* in the light phase whereas they were correlated in dark phase (Fig. 89; $p \leq 0.05$).

In light phase there was no significant difference in pair wise correlation of all the clock genes studied between Vehicle, RIPD, RIPD MEL and RT+MEL group. In dark phase the correlation between *Per1-Per2; Per1-Cry1; Per1-Cry2* has lost in RIPD compared to vehicle which has been restored by melatonin in both RIPD MEL and RT+MEL groups. Vehicle group positive correlation between *Per1-Bmal1*which has lost in RIPD group has not been restored by melatonin in both RIPD MEL and RT+MEL groups (Fig. 89; $p \leq 0.05$).

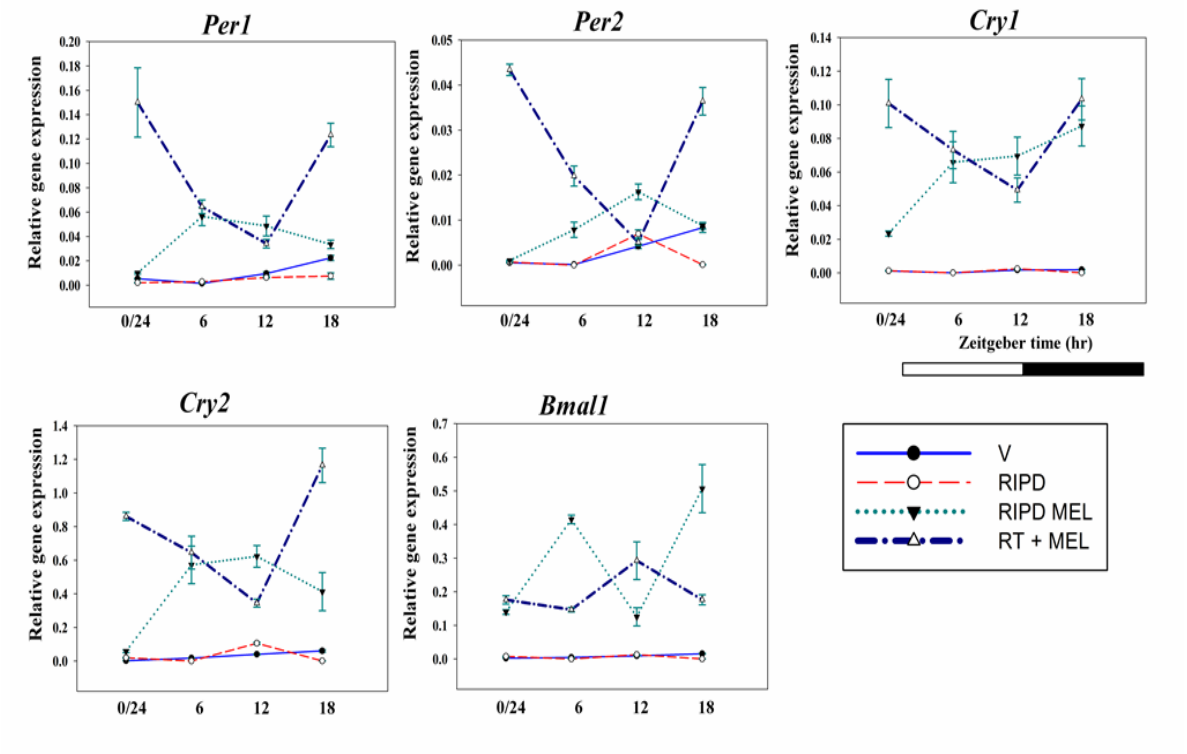

Fig. 87: Effect of melatonin administration on levels and rhythmicity of *Per1, Per2, Cry1, Cry2* and *Bmal1* genes in the Pineal of RIPD rat model. Each value is mean ± SEM (n=4). V - Vehicle, RIPD - Rotenone induced PD, RIPD MEL - RIPD model received MEL for 11 days and RT + MEL - animals received both Rotenone and MEL for 48 days.

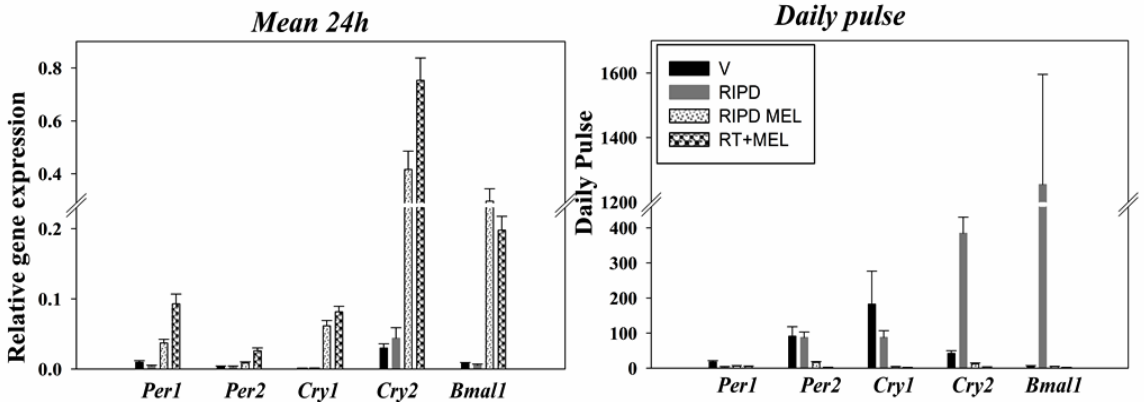

Fig. 88: Effect of melatonin administration on mean 24h levels and Daily Pulse of *Per1, Per2, Cry1, Cry2 and Bmal1* genes in the Pineal of RIPD rat model. Each value is mean ± SEM (n=4). V - Vehicle, RIPD - Rotenone induced PD, RIPD MEL - RIPD model received MEL for 11 days and RT + MEL - animals received both Rotenone and MEL for 48 days.

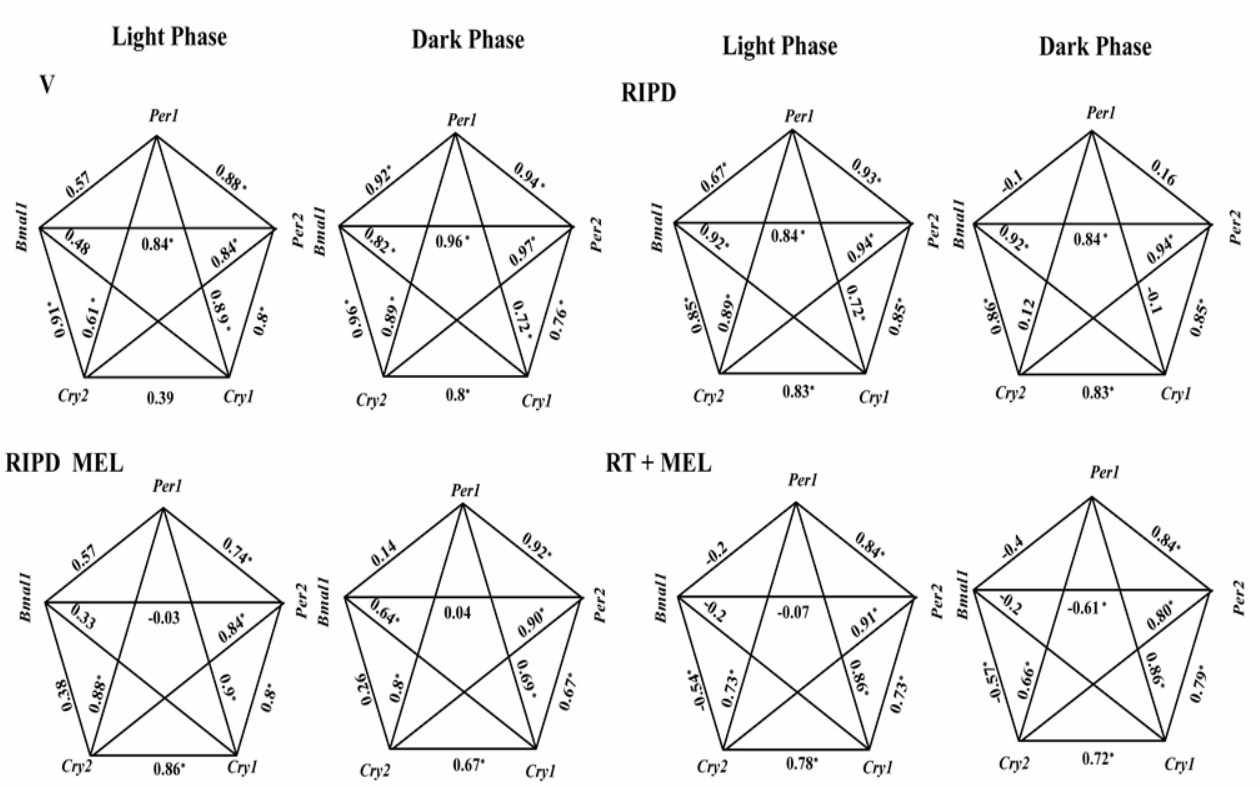

Fig. 89: Effect of melatonin administration on pair wise correlation between mean light (ZT 0, 6 and 12) and mean dark (ZT 12, 18 and 24/0) phase values of *Per1, Per2, Cry1, Cry2 and Bmal1* in the Pineal of RIPD rat model. Each value is mean ± SEM (n=4). V - Vehicle, RIPD - Rotenone induced PD, RIPD MEL - RIPD model received MEL for 11 days and RT + MEL - animals received both Rotenone and MEL for 48 days. Each value is correlation coefficient values between the parameters. * indicates statistically significant value between parameters ($p \leq 0.05$). Negative value indicates negative correlation between parameters.

Table 26. Effect of melatonin on mean 24 h levels and daily pulse of various clock genes expression in Pineal of Rotenone induced PD (RIPD) rat model.

Gene	Experimental Group	Zeitgeber time (h)				Ratio	Mean 24h
		0	6	12	18		
Per1	V	0.0053± 0.0004	0.0014± 0.0002	0.0095± 0.0013 a, b	0.022± 0.0021 a, b, c	17.39± 3.79	0.0096± 0.0021
	RIPD	0.002± 0.0001	0.0028± 0.0003	0.0062± 0.0004	0.0074± 0.0026 a, b	3.54± 1.12 r	0.0046± 0.0008 r
	RIPD MEL	0.01± 0.0008	0.056± 0.0007 a, d	0.048± 0.003 a	0.033± 0.003 a	5.97 ± 1.35	0.037± 0.005 r, p
	RT + MEL	0.115± 0.026 b, c	0.064± 0.005	0.034± 0.003	0.123± 0.009 b, c	4.72± 1.17	0.093± 0.014 r, p
Per2	V	0.0005± 0.0001	0.00012± 0.00003	0.0041± 0.0005 a, b	0.0083± 0.001 a, b, c	91.013± 27.1	0.0033± 0.0008
	RIPD	0.00069± 0.0001	undet	0.0069± 0.0009 a, d	0.00009± 0.00003	87.34± 15.3	0.003± 0.001
	RIPD MEL	0.00103± 0.00008	0.0078± 0.0017 a	0.016± 0.0017 a, b, d	0.009± 0.0007	16.33± 2.24 r, p	0.0085± 0.0016
	RT + MEL	0.043± 0.0012 b, c, d	0.02± 0.0022	0.0050± 0.0006	0.036± 0.003 b, c	2.275± 0.238 r, p	0.026± 0.0039 r, p
Cry1	V	0.0011± 0.00007 b	0.00005± 0.00002	0.0017± 0.0002 a, b	0.0019± 0.0002 a, b	182.63± 93.68	0.0012± 0.0002
	RIPD	0.0012± 0.0003 d	undet	0.0024± 0.0001 a, d	0.00003± 0.000009	87.63± 19.20	0.0012± 0.0003
	RIPD MEL	0.023± 0.0015	0.065± 0.012 a	0.07± 0.0113 a	0.087± 0.012 a	3.86± 0.73 r	0.061± 0.0075 r, p
	RT + MEL	0.101± 0.0143 c	0.073± 0.011	0.049± 0.0071	0.103± 0.012 c	2.157± 0.231 r	0.081± 0.0076 r, p
Cry2	V	0.0014± 0.00013 a	0.0175± 0.0022	0.0401± 0.0035 a, b	0.065± 0.0073 a, b, c	42.04± 7.68	0.03± 0.0060
	RIPD	0.019± 0.0017 d	undet	0.105± 0.0064 a, d	0.00028± 0.00003	384.30± 46 r	0.044± 0.0151
	RIPD MEL	0.058± 0.0083	0.57± 0.11 a	0.62± 0.064 a	0.41± 0.113 a	11.86± 2.81 p	0.416± 0.069 r, p
	RT + MEL	0.86± 0.024 c	0.64± 0.09 c	0.34± 0.024	1.16± 0.102 a, b, c	3.38± 0.17 p	0.75± 0.084 r, p
Bmal1	V	0.0022± 0.0001	0.0046± 0.0011	0.0093± 0.001 a, b	0.015± 0.0013 a, b, c	6.93± 0.43	0.0079± 0.0013
	RIPD	0.0077± 0.0004 b, d	0.000012± 0.000002	0.013± 0.0008 a, b, d	0.00021± 0.00007	1254.29± 341 r	0.0055± 0.0074 r
	RIPD MEL	0.14± 0.0071	0.41± 0.013 a, c	0.125± 0.027	0.51± 0.072 a, c	4.59± 0.95 p	0.297± 0.046 r, p
	RT + MEL	0.176± 0.0122	0.147± 0.0066	0.292± 0.056 a, b, d	0.176± 0.0149	1.981± 0.32 p	0.198± 0.002 r, p

Each value is Mean ± SE (n=4) and expressed in relative genes expression. V - Vehicle, RIPD - Rotenone induced PD, RIPD MEL - RIPD model received MEL for 11 days and RT + MEL - animals received both Rotenone and MEL for 48 days. $p_a \leq 0.05$; $p_b \leq 0.05$, $p_c \leq 0.05$ and $p_d \leq 0.05$ (where a, b, c and d refers to comparison with ZT0, ZT6, ZT12 and ZT18 respectively within the group); r - refers to comparison with vehicle and p - refers to comparison with RIPD.

(f) Effect of melatonin administration on various clock gene expression levels and its rhythmicity in SN of RIPD rat model:

Per1: In RIPD MEL group, maximum levels were observed at ZT6 which is showing approximately 12h advance to vehicle and approximately 6h delay to RIPD group. In RT+MEL group, maximum levels were observed at ZT12 which is showing approximately 6h advance to vehicle and approximately 12h delay to RIPD group (Fig. 90; $p \leq 0.05$). Mean 24h levels of *Per1* in both RIPD MEL and RT+MEL group has been increased by about 52 and 48 fold respectively compared to RIPD rat model, whereas daily pulse has not been restored in both the groups compared to RIPD group(Fig. 91, Table 27; $p \leq 0.05$).

Per2: In RT+MEL group, maximum levels were observed at ZT12as observed in RIPD group and Vehicle. In RIPD MEL group, maximum levels were observed at ZT18which is showing approximately 6h delay compared to vehicle and RIPD group (Fig. 90; $p \leq 0.05$). We observed increased mean 24h levels of *Per2* in both RIPD MEL and RT+MEL group by about 10 and 14 fold respectively compared to RIPD. Daily pulse has not been restored by melatonin in both RIPD MEL and RT+MEL group (Fig. 91, Table 27; $p \leq 0.05$).

Cry1: In RIPD MEL group, maximum levels were observed at ZT18 which is showing approximately 6h delay compared to vehicle and RIPD group. In RT+MEL group, maximum levels were observed at ZT0 which is showing approximately 12h advance to vehicle and RIPD group (Fig. 90; $p \leq 0.05$). Mean 24h levels were increased in both RIPD MEL and RT+MEL group by about 429 and 356 fold respectively compared to RIPD group. Daily pulse has not been restored by melatonin in both RIPD MEL and RT+MEL group (Fig. 91, Table 27; $p \leq 0.05$).

Cry2: In RIPD MEL and RT+MEL group, maximum levels were at ZT6which is showing approximately 6h advance to vehicle and RIPD group (Fig 90; $p \leq 0.05$). We observed increased mean 24h levels of *Cry2* in both RIPD MEL and RT+MEL group by about 4.5 and 5 fold respectively compared to RIPD group. Daily pulse has not been restored by melatonin in both RIPD MEL and RT+MEL group (Fig. 91, Table 27; $p \leq 0.05$).

Bmal1: In RIPD MEL group, maximum levels were observed at ZT12 as in RIPD group. In RT+MEL group, maximum levels were at ZT0which is showing approximately 6h delay compared to vehicle approximately 12 h advances to RIPD group (Fig. 90; $p \leq 0.05$). Mean 24h levels of *Bmal1* in both RIPD MEL and RT+MEL group has been increased by about 96 and 93 fold respectively compared to RIPD, whereas daily pulse has not restored in both the groups compared to RIPD group (Fig. 91, Table 27; $p \leq 0.05$).

In vehicle group there was no correlation between *Bmal1-Per1; Per1-Cry1* in the light phase whereas they were correlated in dark phase. In both light and dark phase *Cry1-Cry2; Per2-Cry1; Per2-Cry2; Cry1-Bmal1; Cry2-Bmal1* has shown positive correlation. Positive correlation between *Per2-Bmal1* in light phase has not observed in dark phase. In RIPD group both light and dark phase *Per2-Cry1; Per2-Cry2; Per2-Bmal1; Cry1-Cry2; Cry1-Bmal1; Cry2-Bmal1* has shown positive correlation. In RIPD MEL group we observed positive correlation between *Per1-Per2; Per2-Cry2; Cry1-Cry2; Per2-Cry1* in both light and dark phase. There was no correlation between *Per1-Cry1; Per1-Cry2; Per2-Bmal1* in the light phase whereas they were correlated in dark phase. In RT+MEL group correlation was observed between *Per1-Per2; Per1-Bmal1*in both light and dark phase. There was no correlation between *Per1-Cry2; Cry1-Cry2* in the light phase whereas they were correlated in dark phase (Fig. 92; $p \leq 0.05$).

In light phase there was no significant difference in pair wise correlation of all the clock genes studied between Vehicle, RIPD, RIPD MEL and RT+MEL group. In dark phase the correlation between *Per1-Cry1* has lost in RIPD compared to vehicle which has been restored by melatonin in RIPD MEL but not in RT+MEL group. Vehicle group positive correlation between *Per1-Bmal1* which has lost in RIPD group has not been restored by melatonin in both RIPD MEL and RT+MEL groups (Fig. 92; $p \leq 0.05$).

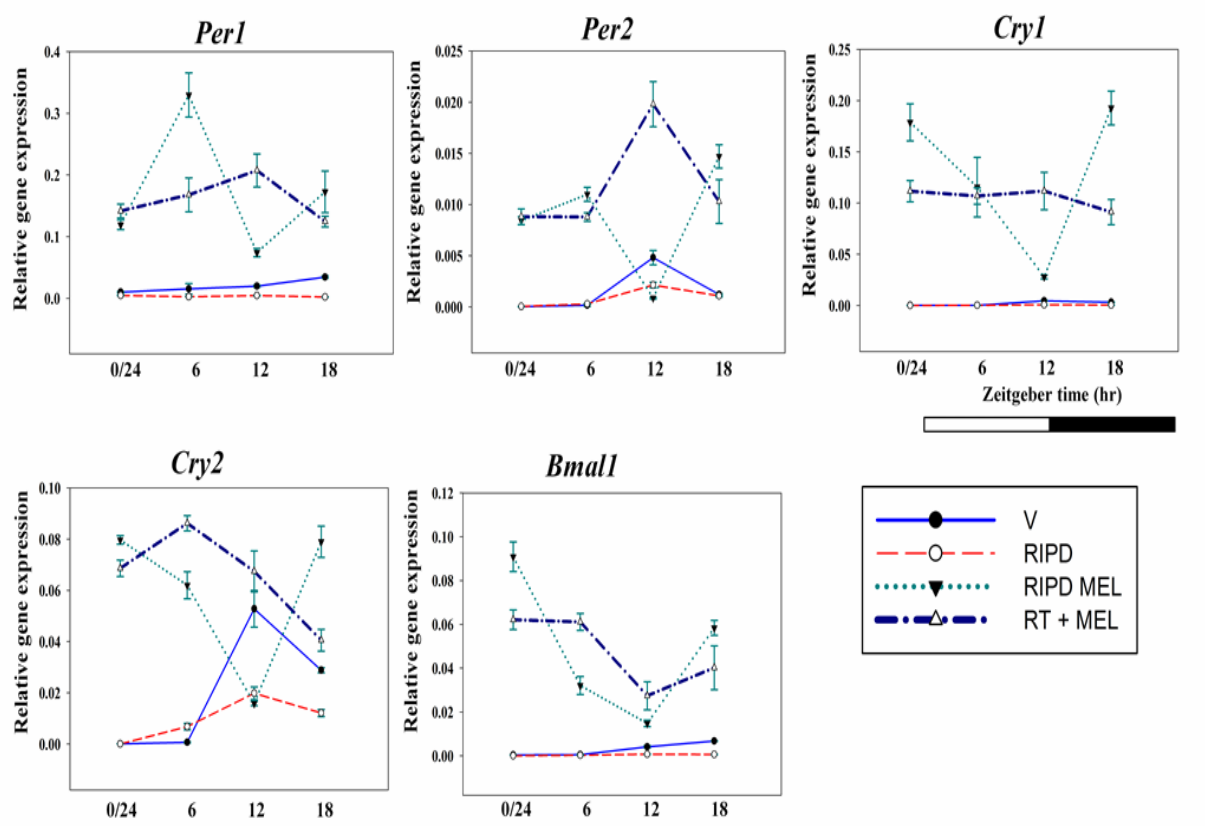

Fig. 90: Effect of melatonin administration on levels and rhythmicity of *Per1*, *Per2*, *Cry1*, *Cry2* and *Bmal1* genes in the SN of RIPD rat model. Each value is mean ± SEM (n=4). V - Vehicle, RIPD - Rotenone induced PD, RIPD MEL - RIPD model received MEL for 11 days and RT + MEL - animals received both Rotenone and MEL for 48 days.

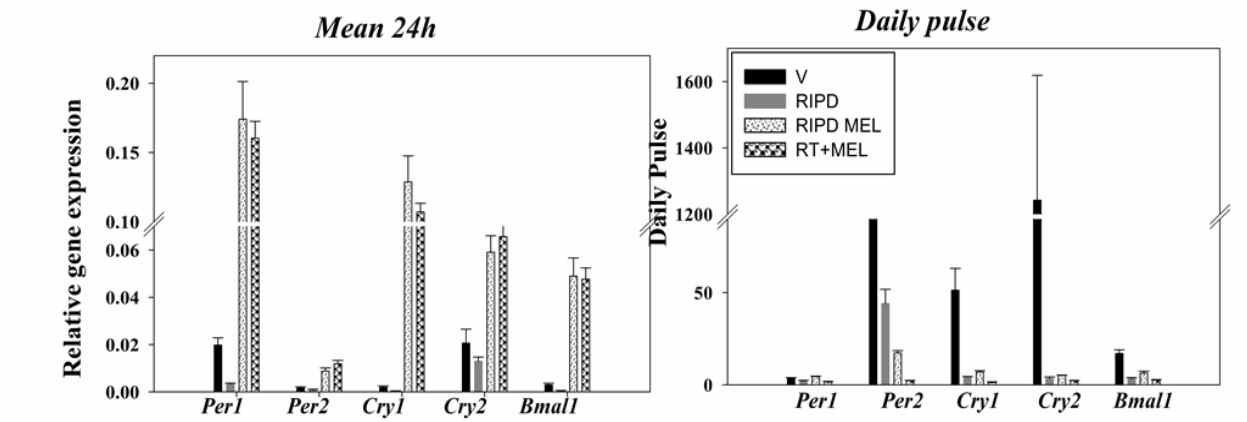

Fig. 91: Effect of melatonin administration on mean 24h levels and Daily Pulse of *Per1*, *Per2*, *Cry1*, *Cry2 and Bmal1* genes in the SN of RIPD rat model. Each value is mean ± SEM (n=4). V - Vehicle, RIPD - Rotenone induced PD, RIPD MEL - RIPD model received MEL for 11 days and RT + MEL - animals received both Rotenone and MEL for 48 days.

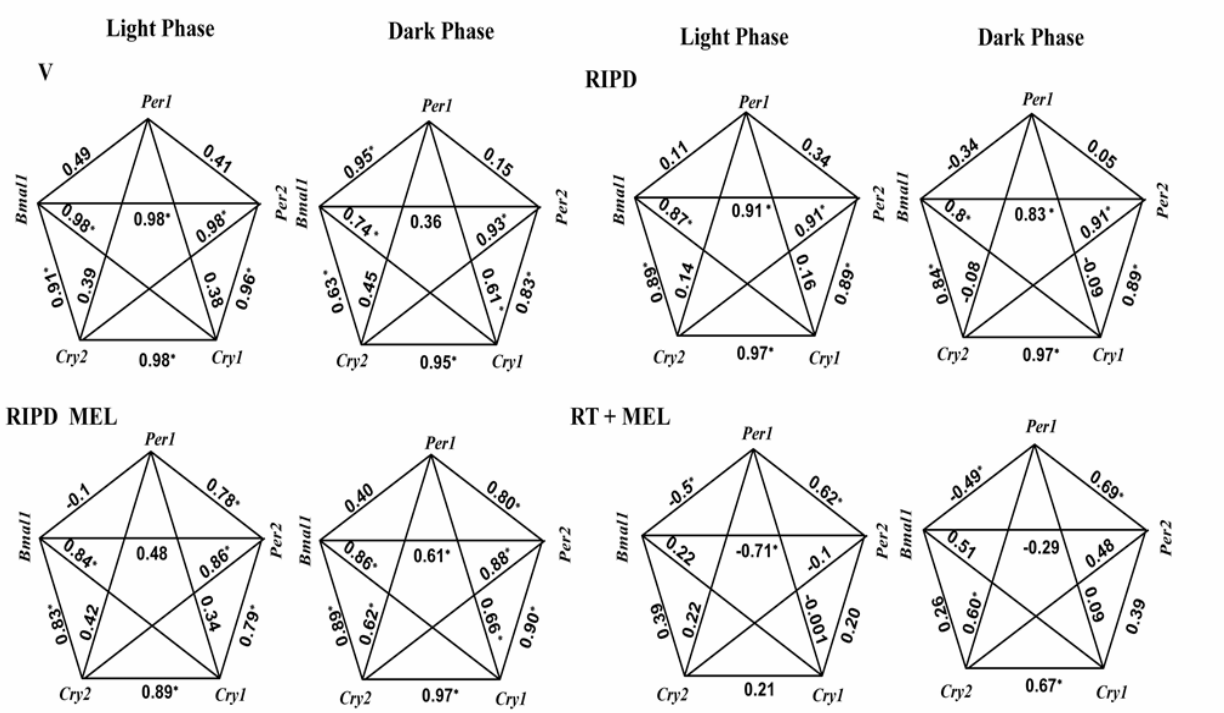

Fig. 92: Effect of melatonin administration on pair wise correlation between mean light (ZT 0, 6 and 12) and mean dark (ZT 12, 18 and 24/0) phase values of *Per1, Per2, Cry1, Cry2 and Bmal1* in the SN of RIPD rat model. Each value is mean ± SEM (n=4). V - Vehicle, RIPD - Rotenone induced PD, RIPD MEL - RIPD model received MEL for 11 days and RT + MEL - animals received both Rotenone and MEL for 48 days. Each value is correlation coefficient values between the parameters. * indicates statistically significant value between parameters ($p \leq 0.05$). Negative value indicates negative correlation between parameters.

Table 27. Effect of melatonin on mean 24 h levels and daily pulse of various clock genes expression in SN of Rotenone induced PD (RIPD) rat model.

Gene	Experimental Group	Zeitgeber time (h)				Ratio	Mean 24h
		0	6	12	18		
Per1	V	0.01± 0.0011	0.015± 0.0085	0.02± 0.0018	0.034± 0.0018 [a, b, c]	3.52± 0.306	0.02± 0.0030
	RIPD	0.0045± 0.0005 [b, d]	0.0024± 0.0003	0.0044± 0.0003 [b, d]	0.0019± 0.0002	1.95± 0.406	0.0033± 0.0003 [r]
	RIPD MEL	0.12± 0.0077	0.33± 0.036 [a, c, d]	0.074± 0.0067	0.173± 0.034 [c]	4.45± 0.272 [p]	0.174± 0.027 [r, p]
	RT + MEL	0.142± 0.011	0.17± 0.027	0.207± 0.027 [d]	0.125± 0.0087	1.68± 0.206	0.160± 0.012 [r, p]
Per2	V	0.00003± 0.000006	0.00016± 0.00012	0.0048± 0.0007 [a, b, d]	0.00122± 0.00012 [a]	191.58± 633	0.0015± 0.0005
	RIPD	0.00004± 0.000004	0.00029± 0.00004	0.0021± 0.00027 [a, b, d]	0.00109± 0.00012 [a, b]	44.11± 1.74 [r]	0.0008± 0.0002 [r]
	RIPD MEL	0.0084± 0.0003 [c]	0.01± 0.0006 [a, c]	0.00086± 0.00007	0.015± 0.0011 [a, b, c]	17.245± 1.27	0.0087± 0.0013 [r, p]
	RT + MEL	0.0082± 0.00076	0.0087± 0.0004	0.02± 0.0022 [a, b, d]	0.010± 0.0021	2.238± 0.1726	0.012± 0.0013 [r, p]
Cry1	V	0.00009± 0.00001	0.000119± 0.00002	0.0045± 0.00046 [a, b, d]	0.0031± 0.0003 [a, b]	51.35± 11.88	0.0019± 0.0005
	RIPD	undet	0.00015± 0.00002	0.00063± 0.00009 [b, d]	0.00037± 0.00004 [b]	4.137± 0.35 [r]	0.00038± 0.00006 [r]
	RIPD MEL	0.18± 0.018 [b, c]	0.116± 0.029 [c]	0.028± 0.002	0.193± 0.016 [b, c]	6.969± 0.679	0.129± 0.019 [r, p]
	RT + MEL	0.112± 0.0104 [d]	0.107± 0.008	0.112± 0.018	0.091± 0.012	1.29± 0.28	0.107± 0.0067 [r, p]
Cry2	V	0.00006± 0.00002	0.00064± 0.0003	0.053± 0.0071 [a, b, d]	0.029± 0.00098 [a, b]	1241± 377	0.0206± 0.005
	RIPD	undet	0.0067± 0.001	0.02± 0.0025 [b, d]	0.012± 0.0013 [b]	3.38± 0.86 [r]	0.013± 0.0018 [r]
	RIPD MEL	0.08± 0.0016 [b, c]	0.62± 0.0053 [c]	0.016± 0.0008	0.08± 0.006 [b, c]	5.089± 0.202 [r]	0.059± 0.007 [r, p]
	RT + MEL	0.068± 0.0032	0.086± 0.003 [a, c, d]	0.067± 0.008 [d]	0.040± 0.004 [d]	2.202± 0.25 [r]	0.066± 0.004 [r, p]
Bmal1	V	0.0004± 0.00005	0.0005± 0.0002	0.0041± 0.0005 [a, b]	0.0067± 0.00017 [a, b, c]	17.043± 1.907	0.0029± 0.0006
	RIPD	undet	0.0002± 0.00002	0.0007± 0.00006 [b]	0.0006± 0.00005 [b]	3.29± 0.64 [r]	0.00051± 0.00006
	RIPD MEL	0.091± 0.0067 [b, c, d]	0.032± 0.0041 [c]	0.15 ± 0.0014	0.058± 0.0034 [b, c]	6.414± 0.99 [r]	0.049± 0.0076 [r, p]
	RT + MEL	0.063± 0.004 [c, d]	0.061± 0.0038 [c, d]	0.027± 0.0064	0.0402± 0.01	2.506± 0.367 [r]	0.048± 0.0048 [r, p]

Each value is Mean ± SE (n=4) and expressed in relative gene expression. V - Vehicle, RIPD - Rotenone induced PD, RIPD MEL - RIPD model received MEL for 11 days and RT + MEL - animals received both Rotenone and MEL for 48 days. $p_a \leq 0.05$; $p_b \leq 0.05$, $p_c \leq 0.05$ and $p_d \leq 0.05$ (where a, b, c and d refers to comparison with ZT0, ZT6, ZT12 and ZT18 respectively within the group) *);* r - refers to comparison with vehicle and p - refers to comparison with RIPD.

Discussion

1. Characterization of rotenone induced Parkinson's disease (RIPD) rat model

Weight loss was observed in the rotenone treated animals. Decreased TH positive neurons in the present study indicate the decrease in the Dopamine synthesis which is a major clinical symptom of Parkinson's disease (Cannon *et al*., 2009). The increase in levels of α-Synuclein which is a major protein in Lewy body in the present study could be due to its accumulation in the Dopaminergic neurons of SNpC, a process triggered by Rotenone (Betarbet *et al*., 2000). Thus, Rotenone treated PD rat model was successfully developed (Alam and Schmidt, 2002).

2. Studies of chronomics of serotonin metabolism in SCN, Pineal and SN in PD

Tryptophan is transported from blood across blood brain barrier (BBB) by a competitive transport carrier which is also shared by other large neutral amino acids (LNAA) such as threonine and tyrosine (Ruddick *et al*., 2006). ATP depletion due to oxidative stress induced by rotenone leads to reduced transport of tryptophan from blood across BBB and this could be the reason for the decreased tryptophan levels observed in the SCN and SN of RIPD rat model. Pineal gland is not covered with BBB (Ruddick *et al*., 2006), so tryptophan transport is not affected by oxidative stress and this could be the reason for unaltered tryptophan levels observed in the pineal of RIPD rat model.

Apart from cardinal symptoms, non motor symptoms like circadian dysfunction is also commonly observed in PD and many are traced to serotonin neuronal deficits. In the biosynthesis of serotonin, tryptophan hydroxylase (TPH) is the major rate limiting enzyme (Kema *et al*., 2000) and it is known to be extremely labile to oxidation (Kuhn *et al*., 2011). 50-80% reduction in the activity of TPH was also observed in the hypothalamus, pallidum, raphe nucleus and SN of PD patients (Sawada *et al*., 1985). Decreased mean 24 h levels of 5-HT, 5-HTP, NAS and MEL observed in the present study could be due to decreased activity of TPH upon oxidative attack in RIPD rat model. Decreased levels of serotonin in SCN, Pineal and SN and its abolished daily rhythm in SCN and SN of RIPD rat model in the present study can be correlated to the loss of serotonin neuronal functions in PD and the emergence of non-motor (psychiatric) symptoms (Kuhn *et al*., 2011).

Decreased mean levels of 5-HTP, 5-HT, NAS and MEL in the SCN, Pineal and SN of RIPD rat model are also in agreement with the changes in the levels of these metabolites observed in SCN and Pineal of aged male wistar rats (Reddy, 2010). Degeneration of human serotonergic axons in neurodegenerative conditions has been reported by some workers (Azmitia and Nixon, 2008). These results are in agreement with an elevated TRP degradation and decreased TRP and 5-HT levels observed in the serum, CSF and caudate nuclei of PD patients (Iacono *et al*., 1997; Sparks and Slevin, 1984). Plasma melatonin levels were also reported to be significantly reduced in PD patients (Catala *et al*., 1997). There was no significant difference in 5-HIAA levels, neither in CSF of PD patients (Sparks and Slevin, 1984; Iacono *et al*., 1997) nor in the striatum of 6-hydroxydopamine induced PD rat model (Aguiar *et al*., 2005). In our studies, there was no significant difference in mean levels of 5-HIAA in SCN, Pineal and SN of RIPD rat model.

No change in the activity of MAO was reported in the hypothalamus, pallidum, raphe nucleus and SN of PD patients (Sawada *et al*., 1985). Significant increase in mean levels of 5-HTOH and 5-MTOH in the present study could be possibly due to decreased activity of Tryptophan hydroxylase and unaltered Monoamine Oxidase (MAO) activity. Increased NAT levels observed in the present study could be an indicative of conversion of more TRP into Tryptamine rather than into 5-HTP.

Decreased ratio of 5-HT-5-HIAA, 5-HT-5-MIAA and 5-HT-5-MTOH in SCN and SN of RIPD model suggests the elevated catabolism of 5-HT into 5-HIAA and 5-HTOH. Decreased synthesis of 5-HT from TRP is evident from decreased ratio of 5-HT-TRP and 5-HT-5-HTP in the SN of RIPD model and this could be due to reduced tryptophan hydroxylase activity under oxidative stress (Kuhn *et al*., 2011). Increased ratio of 5-HT-MEL and 5-HT-NAS in the SCN and pineal of RIPD model infers decreased synthesis of NAS and MEL from 5-HT. However in the SN of RIPD model even though 5-HT-NAS ratio is decreased we have observed increased ratio of 5-HT-MEL which indicates less conversion of NAS into MEL. N-acetyl Serotonin (NAS) being an equally potent antioxidant like melatonin, it is getting utilized in the SN because of the presence of high levels of free radicals which could be generated by rotenone and as well as cellular processes used to break down dopamine. This could be the reason for the reduced conversion of NAS in to MEL even though more 5-HT is converted into NAS. Reduced ratio of 5-HT-NAT in the SCN, Pineal and SN of RIPD model compared to control group indicates

enhanced conversion of TRP into NAT rather getting converted into 5-HTP. This is in correlation with an increased TRP degradation in PD patients (Iacono *et al*., 1997).

We have observed abolished daily rhythm in case of 5-HTP, 5-MIAA and MEL rhythmicity in the SCN of RIPD rat model which is in agreement with abolished daily rhythm of MEL in the brain of other neurodegenerative disorder like Alzhiemers disease and in aged persons (Skene *et al*., 1990). No change in the MEL rhythms however have been reported in blood samples of naive PD patients (Patients without taking L-DOPA therapy) (Fertl *et al*., 1993).

Vehicle group negative correlation between 5-HT-NAS, 5-HT-MEL in the light phase of SCN, 5-HT-5-HIAA in the dark phase of SCN, 5-HT-5-MIAA, 5-HT-5-MTOH, 5-HT-MEL, 5-HT-NAT in the light phase of pineal, 5-HT-5-MIAA, 5-HT-5-MTOH, 5-HT-MEL in the dark phase of pineal and 5-HT-5-HTOH in the dark phase of SN has become positive in RIPD model. The correlation observed between 5-HT-5-HTP in the dark phase of SCN and light phase of pineal, 5-HT-NAT in the dark phase of pineal, 5-HT-NAS, 5-HT-NAT in the light phase of SN and 5-HT-5-HIAA, 5-HT-5-MIAA in the dark phase of the SN in the vehicle group has lost in RIPD model. Given the importance of correlation between the metabolites in a metabolic pathway in maintaining the stoichiometry of each reaction in the pathway, altered and lost correlation between the metabolites in RIPD model could be responsible for metabolite phase alterations observed in the present study.

Hence, serotonin metabolism is altered as seen in altered amplitude and rhythmicity of Serotonin, its precursor and various metabolites in RIPD rat model, these altered compounds may contribute to circadian disorders of Parkinsonism.

3. Studies of daily rhythms of protein profile in SCN, Pineal and SN upon Aging and in rotenone induced PD rat model

We have analyzed the difference in the number of matched protein spots across the age groups at ZT6 and ZT18, keeping the 3 m group as reference. In both SCN and Pineal, at ZT6 the number of spots showed reduction in 12 and 24 m. The fold reduction observed was 0.82 and 0.35 in 12 and 24 m respectively in the SCN. Between the 12 and 24 m the spots had reduced by 0.42 folds in this tissue. In pineal the spots were reduced by 0.78 folds both in 12 as well as 24

m. Though in the SN, the number of protein spots were reduced by 0.77 fold in the 24 m, a 1.28 fold increase was observed in 12 m. There was an increase in the number of matched spots at ZT18 in the SCN of 12 m; where a 2.14 fold increase was observed and in 24 m; where the fold change was 1.59. In the pineal matched protein spots were increased by 1.17 fold in 24 m, whereas it was reduced by 0.45 fold in 12 m. A 2.6 fold increase in the number of spots was observed between the pineal of 12 and 24 m rats. The SN protein spots showed a decrease of 0.69 and 0.57 folds respectively in the 12 and 24 m against the 3 m. The RIPD protein data was also compared with 3 m control group at both ZT6 and ZT18. In the SN, at both time points there was a reduction in the number of matched protein spots. At ZT6, the fold reduction was 0.76 whereas at ZT18 it was 0.58. In the SCN of RIPD model at ZT6, the number of matched spots was reduced by 0.59 fold but it was increased by 2.3 fold at ZT18.

Any variation in the number of protein spots between ZT6 and ZT18 samples in all the age groups was analyzed. In the SCN a distinct variation was observed in the 3 m, and this variation was reduced in 12 and 24 m. Considerable variation persisted between these two time points in the pineal as well as in SN of both 3 and 12 m. When in the 24 m pineal this difference had been drastically reduced, in the SN it was completely lost. The number of spots expressed at ZT6 and ZT18 in both SCN and SN of RIPD model were similar.

The number of protein spots showing daily rhythm has been decreased upon aging in both SCN and SN, but in case of pineal the number has been decreased from 3 to 12 m and then increased in 24 m. Interestingly we found similarity between 24 m and RIPD model in the number of spots showing daily rhythm in case of SCN and SN.

In the SCN the number of unregulated protein spots was high at ZT6 than at ZT18. Both 12 and 24 m retained this pattern. Up regulated protein spots were more at ZT18 than at ZT6 in 3 as well as 24 m old pineal and in 3 m old SN. This pattern was found to be reversed in 12 m SN whereas it was lost in 12 m pineal and 24 m SN. We observed a drastic decrease in the number of up regulated proteins at both time points in the SCN of RIPD model, no specific pattern in this parameter could be found between ZT6 and ZT18. In the SN of RIPD model no difference in the number of up regulated proteins was observed between the time points.

The protein spots showing robust changes in daily pulse and mean 24 h levels within a day between the age groups and in RIPD rat model will be analyzed and then characterized by

mass spectroscopy followed by MALDI TOF/TOF analysis. This would help in identifying specific markers for aging and also for the rat model of rotenone induced Parkinsonism.

4. Studies of daily rhythms of various clock gene expressions in SCN, Pineal and SN upon Aging and in rotenone induced PD rat model

The daily rhythm pattern of circadian clock genes (*Per1, Per2, Cry1, Cry2 and Bmal1*) in 3 m SCN of vehicle group observed in the present study is in agreement with previous findings (Abe *et al*., 1998; Yan *et al*., 1999; Park and Kang, 2004), that is *Per1, Per2, Cry1* and *Cry2* peaking in light phase and *Bmal1* peaking at dark phase in the SCN. As *Bmal1* showed maximum values of its rhythmic expression during the subjective night at ZT18 and is thus phase opposed to *Per1, Per2, Cry1* and *Cry2* mRNA expression. These data of 3 m vehicle group primarily used as control, with which other age groups would be compared with, also validate our experimental procedures.

The levels of *Per1* were not altered in 12 and 24 m SCN, this is in agreement with unaltered *Per1* levels observed in aging hamsters (Asai *et al*., 2001; Kolker *et al*., 2003), Phase advancement in *Per1* daily rhythm in 24 m of SCN and SN observed in the present study can be correlated with phase advancement observed in circadian activity/rest cycle in aged mice (Weinert *et al*., 2001), however the phase advance effect is not seen in case of 24 m pineal. Daily rhythm of *Per2* has shown diminished amplitude in 24 m SCN, Pineal and SN but not *Per1* daily rhythm; this is in agreement with similar changes observed in *per2* and *per1* expression and daily rhythm in aged mice (Weinert *et al*., 2001). Age dependent difference found in case of *Per2* mRNA expression, with the maximum levels at ZT12 in 3 and 24 m SCN, significantly decreased in 24 m is in agreement with the earlier report of *mPer2* expression in aged mice (Weinert *et al*., 2001).

Bmal1 knockout animals are arrhythmic (Bunger *et al*., 2000) and have been reported to have reduced lifespan and develop a number of age related pathologies (kondrotov *et al*., 2006). Reduced mean levels and altered expression profile of *Bmal1* in 12 and 24 m SCN, Pineal and SN observed in the present study is in agreement with its lower and altered expression profile reported in aged hamsters (Kolker *et al*., 2003; Wyse and coogan, 2010). Given the importance of *Bmal1*, arrhythmicity of *Bmal1* in 24 m SCN and SN observed in the present study could be responsible for age-related pathologies observed in old age.

In the present study *Per1, Per2, Cry1, Cry2* and *Bmal1* phase of the daily rhythm was altered in 12 m SCN, Pineal and SN however; daily rhythmicity of the same persisted. But, in 24 m daily rhythm of *Per1, Per2* in the SCN and *Per1, Per2, Cry1* and *Cry2* in the SN persisted and *Cry1, Cry2* and *Bmal1* daily rhythm was abolished in the SCN and *Bmal1* daily rhythms was abolished in SN. Upon aging, the alterations in the daily rhythm pattern and levels of clock genes observed in the present study could be responsible for the age related phase desynchronization at the network level, electrophysiological arrhythmia at the single cell level in the SCN (Farajnia *et al*., 2012) and changes in sleep and circadian timing of SCN (Biello, 2009).

Although PD is characterized by the cardinal motor symptoms, non-motor symptoms such as circadian dysfunction markedly impair the quality of life. Recently several studies have suggested disruption of circadian clock in PD (Bruguerolle and Simon, 2002; Cai *et al*., 2010; Kudo *et al*., 2011); however, the changes in the daily rhythms of molecular clock were unclear. In this study, we report the molecular clock alterations in the RIPD rat model. We observed significant reduction in mean levels as well as a 6 h phase delay in circadian oscillation of *Bmal1* in the SCN of rotenone induced PD model, similar observations were reported with *hbmal1* in the total leukocytes of PD patients (Cai *et al*., 2010), however we observed 6 h phase advance in case of pineal and SN of RIPD rat model. BMAL1 controls antioxidant defense by regulating the expression of major antioxidant enzymes (Kondratov *et al*., 2009), low mean levels of *Bmal1* together with its altered circadian profile could be contributing to the decreased antioxidant defense and increased oxidative stress in the RIPD rat model. In the RIPD model, *Per2* daily rhythmicity persisted in SCN, pineal and SN. Similar observations were found in the SCN of 6-hydroxydopamine induced PD model (Gravotta *et al*., 2011), however striatal *Per2* rhythms of a 6-hydroxydopamine induced PD rat model has shown abolished daily rhythm (Hood *et al*., 2010). Arrhythmic expression of *hper1* in serum has been reported with Alzheimer's disease (Ying-Hui *et al*., 2006).

The positive loop of CLOCK-BMAL1 is recurrently counterbalanced by a core inhibitory loop formed by the PER and CRY heterodimer that translocate into the nucleus from cytosol (Ko and Takahashi, 2006). There are no reports on *Cry* rhythms in association with Parkinson's disease; however *hcry1* rhythmicity was reported abolished in the serum of Alzheimer's patients (Ying-Hui, *et al*., 2006). RIPD model in the present study has shown 12h phase advance in *Cry1*

and *Cry2* rhythms of the SCN which would further augment the physiological and behavioral anomalies associated with circadian dysfunction in PD.

RIPD model in the present study has shown 12h phase advance in *Cry1* rhythms of the SCN and 6h phase advance in *Cry1* rhythms in Pineal which would further increase the physiological and behavioral abnormalities associated with circadian dysfunction in PD. These results indicate that rhythms of molecular clock components of SCN, Pineal and SN are altered in RIPD model, which could be responsible for circadian disorders observed in PD.

Daily rhythm and phase of *Per2* has not been altered in SCN and SN of RIPD model and 24 m animals, however its daily pulse and mean 24 h levels were decreased. We have observed reduced mean 24 h levels of *Bmal1* expression in SCN of both RIPD and 24 m group animals. In case of pineal, maximum expression of *Cry1* has shown approximately 6 h phase advancement both in RIPD and 24 m group animals.

5. Effect of melatonin administration on daily rhythms of various clock gene expressions in SCN, Pineal and SN upon Aging and in rotenone induced PD rat model

The circadian pacemaker system has diminished amplitude with the age as indexed by a decrease in circulating melatonin levels (Coevorden *et al*., 1991). Increase in the amplitude of the daily rhythms of clock genes upon melatonin administration observed in the present study could be due to increased amplitude of the circadian pacemaker system by melatonin through feedback regulation (Armstrong and Redman, 1991). Daily rhythm and phase restoration effect of melatonin observed in the present study are attributed to its known action on MT1 and MT2 melatonin receptors abundantly present in the SCN (Reppert *et al*., 1994; Reppert *et al*., 1995; Srinivasan *et al*., 2009). Melatonin has two distinct effects on the SCN: phase shifting and acute inhibition of SCN electrical activity (Liu *et al*., 1997, Jin *et al*., 2003) and it has been shown that effect of melatonin on circadian free-running period is genetically determined in mice (Shimomura *et al*., 2010). Melatonin can also affect *Rev-erbα*, *Bmal1* and nuclear orphan receptor gene expression in the adult rat SCN (Poirel *et al*., 2003; Agez *et al*., 2007; Agez *et al*., 2009). Phase shifting of the circadian rhythm by melatonin in the SCN is mediated through PKC activation (Dubocovich and Markowska 2005). Resetting of circadian rhythms is through PKC mediated phosphorylation of CLOCK (Shim et al. 2007) and PK-Cα has been shown to interact

with BMAL1 in a circadian manner. CLOCK and BMAL are ultimately affected by melatonin induced activation of PKC (Robles *et al*., 2010) and thus in turn regulating the expression of *Per, Cry, Clock, Bmal1* and *Ccg.*

Reduced amplitude in the activity-rest rhythm and decreased sleep quality was observed in aged ring doves in comparison to young ones which were improved after melatonin administration (Garau *et al*., 2006). Administration of single melatonin injection in the late subjective day (CT11.5) is able to inhibit the SCN metabolic activity (Cassone *et al*., 1987), phase shifting the clock *in vivo* (Warren *et al*., 1993) and phase advancing the light induced expression of c-fos in the adult SCN (Sumova and Illnerova, 1996). SCN circadian neuronal activity was phase advanced after the application of melatonin on SCN slices *in vitro* (McArthur *et al*., 1991; Gillette and McArthur, 1996). We have observed increase in mean 24h levels of all the studied clock genes upon melatonin administration in 3 m melatonin treated SCN and pineal this is in agreement with significant increase in *bmal1* and AVP mRNA expression by 14.6 % and 14.8 % respectively during the whole circadian period in adult SCN after melatonin injection (Poirel *et al*., 2003), whereas decreased levels of *Per2, Cry1, Cry2* and *Bmal1* were observed in SN by melatonin in all the age groups. Increased mean 24h levels of all the clock gene expression in 12 and 24 m of melatonin treated SCN and pineal observed in the present study could be due to same effect of melatonin on aged SCN as seen on young SCN (Poirel *et al*., 2003).

Phase advancement in the daily rhythm pattern of *Per2, Cry1* and *Bmal1* upon melatonin administration in 3 m old SCN and Pineal compared to 3 m vehicle group observed in the present study could be correlated with known phase advancement effect of exogenously administered melatonin on SCN circadian neuronal activity (McArthur *et al*., 1991; Gillette and McArthur, 1996). However, single melatonin injection at CT11 has no immediate effect on clock gene expression (Poirel *et al*., 2003; Yasuo *et al*., 2002) and it has been reported that clock gene transcriptional regulation occurs 24h after the melatonin application (Poirel *et al*., 2003). Interestingly, the response of clock genes in 12 and 24 m melatonin treated SCN observed in the present study is similar to the behavioral effect (locomotor activity rhythm), *c-fos* rhythm (Sumova and Illnerova, 1996), as for all these parameters melatonin administration induces phase shift (Sharma *et al*., 1999) which helped in the restoration of phase of the daily rhythm of *Per2, Cry1, Cry2* and *Bmal1* expression in 12 m SCN, *Cry1* and *Cry2* in 12 m Pineal, *Cry1* and

Bmal1 in 12 m SN but not in 24m, which is correlating with restoration of daily rhythms of Serotonin in SCN (Jagota and Kalyani, 2010) and lipid peroxidation and antioxidants (Manikonda and Jagota, 2012) and this could be correlated with reduced sensitivity of SCN to melatonin in aged SCN (Gall and Weaver, 2008) and restoration of daily rhythm of *Cry1, Cry2* and *Bmal1* in 24 m SCN and *Bmal1* in 24 m SN.

Pair wise correlation analysis revealed that there was decrease and loss of correlation between the levels of clock genes in the SCN, Pineal and SN of 24 m old animals. This decreased and lost correlation has been restored by melatonin. Correlation observed between the various clock genes studied in light and dark phase of 3 and 12 m is lost in 24 m SCN and restored by melatonin. Melatonin could restore the lost correlation in 24 m between *Cry2-Bmal1*; *Cry1-Cry2; Per1-Cry1; Cry1-Bmal1* in case of pineal and *Per1-Cry2; Cry1-Cry2; Cry1-Bmal1* in case of SN.

In the present study melatonin has been observed to help in restoration of phase only in case of *Per1, Cry1* in SCN, *Cry1, Cry2* in Pineal and *Cry1* alone in SN of RIPD rat model, no restoration in daily pulse has been observed in all the tissues studied and this could be due to reduced melatonin receptors in Parkinson's disease (Adi *et al*., 2010). The observed mean level restoration in case of *Per1* and *Bmal1* in the SCN, *Per1, Per2, Cry1, Cry2* and *Bmal1* in case of Pineal and SN of RIPD rat model by melatonin could be due to non genomic action of melatonin (Jagota, 2012).

The lost correlation between *Cry1-Cry2; Per2-Cry1; Per2-Bmal1; Cry1-Cry2* in case of SCN, *Per1-Per2; Per1-Cry1; Per1-Cry2* in case of pineal of RIPD model compared to control has been restored by melatonin in both RIPD MEL and RIPD+MEL groups. Melatonin could restore the correlation between *Per1-Cry1* only in SN of RIPD MEL group but not in SN of RIPD+MEL group. Correlation between *Per1-Bmal1* in SCN and SN of dark phase of control group is lost in RIPD model. Melatonin could restore this correlation only in SCN but not in SN of RIPD MEL and RIPD+MEL group.

Reduced mean 24 h levels of *Per2* has been restored by melatonin in case of SCN but not in SN of 24 m old animals whereas in case of RIPD melatonin has restored the *Per2* levels in SN but not in SCN. Melatonin could not restore the decreased daily pulse of *Per2* in both 24 m old animals and RIPD model. Decreased mean 24 h levels of *Bmal1* expression in the SCN of RIPD

model and in 24 m old animals has been restored by melatonin. Phase of the daily rhythm of *Cry1* has been restored by melatonin only in pineal RIPD model but not in 24 m old animals.

Summary and Conclusion

The present study has focused on neurodegeneration in rat brain aging and RIPD model by studying chronomics of serotonin metabolism, protein profile and clock gene expression. We have observed that 5-HTP daily rhythm was found to be abolished in SCN, Pineal as well as in SN of RIPD model. 5-HT daily rhythm was abolished in the SN. These three brain regions also had a significant reduction in the mean 24 h levels of 5-HTP, 5-HT and MEL. While both NAS and TRP levels were reduced in the SCN, only the NAS levels had declined in pineal, whereas the TRP mean levels had dropped in SN. The SCN of RIPD model also showed significant increase in mean 24 h levels of 5-HTOH, 5-MTOH and NAT. With the proteomics data we had observed that the number of protein spots that showed a rhythmic pattern in occurrence, between ZT6 and ZT18 has decreased with age in SCN and SN. When compared to their respective controls the SCN and SN of RIPD model also showed a reduction in the number of rhythmically expressed spots which were similar to 24 m. Aging and RIPD has significantly affected the expression profile of clock genes in all the three brain regions studied. Abolished *Cry2* rhythm and decrease in the amplitude of *per1* and *per2* rhythm were seen in SCN of aged animals. Phase alteration of *Per1* and *Cry1* and reduction in the daily pulse of *Cry2* and *Bmal1* was seen in both aged SN as well as in the RIPD-SN. Aging had also resulted in *Bmal1* rhythm abolishment and *Cry2* phase alteration in SN. Alteration in the phase of *Bmal1* rhythm was also seen in the SN of RIPD model. Aging in pineal was marked by phase altered *Per1, Cry1* and *Bmal1* daily rhythm. Phase advancement of 6 h in the daily rhythms of *Per2, Cry1, Cry2* and *Bmal1* was observed in the pineal of RIPD model. The daily rhythmic pattern of *Per2* expression was not altered upon aging or RIPD in any of the three brain regions studied.

We have studied the effect of melatonin administration on 12 and 24 m animals as well as on RIPD rats, with respect to clock gene expression. Upon melatonin administration the phase of *Cry1* rhythm in 12 m could be restored in SCN, Pineal and SN. In both SCN and Pineal of this age group melatonin could restore the phase of *Cry2* rhythm, whereas restoration of *Bmal1* phase was seen in SCN and SN. Phase restoration of *Cry1, Cry2* and *Bmal1* daily rhythm could be seen in 24 m SCN. In the RIPD model melatonin significantly affected the phase and the levels of clock gene expression. *Per1* and *Bmal1* levels were restored in SCN, Pineal and SN. *Per2* and *Cry1* levels were restored in both pineal and SN whereas restoration of *Cry2* levels was seen in SN. Melatonin had restored the phase of *Cry1* rhythm in SN and SCN; melatonin also had phase restorative effects on *Cry2* rhythm in the pineal (Fig. 93).

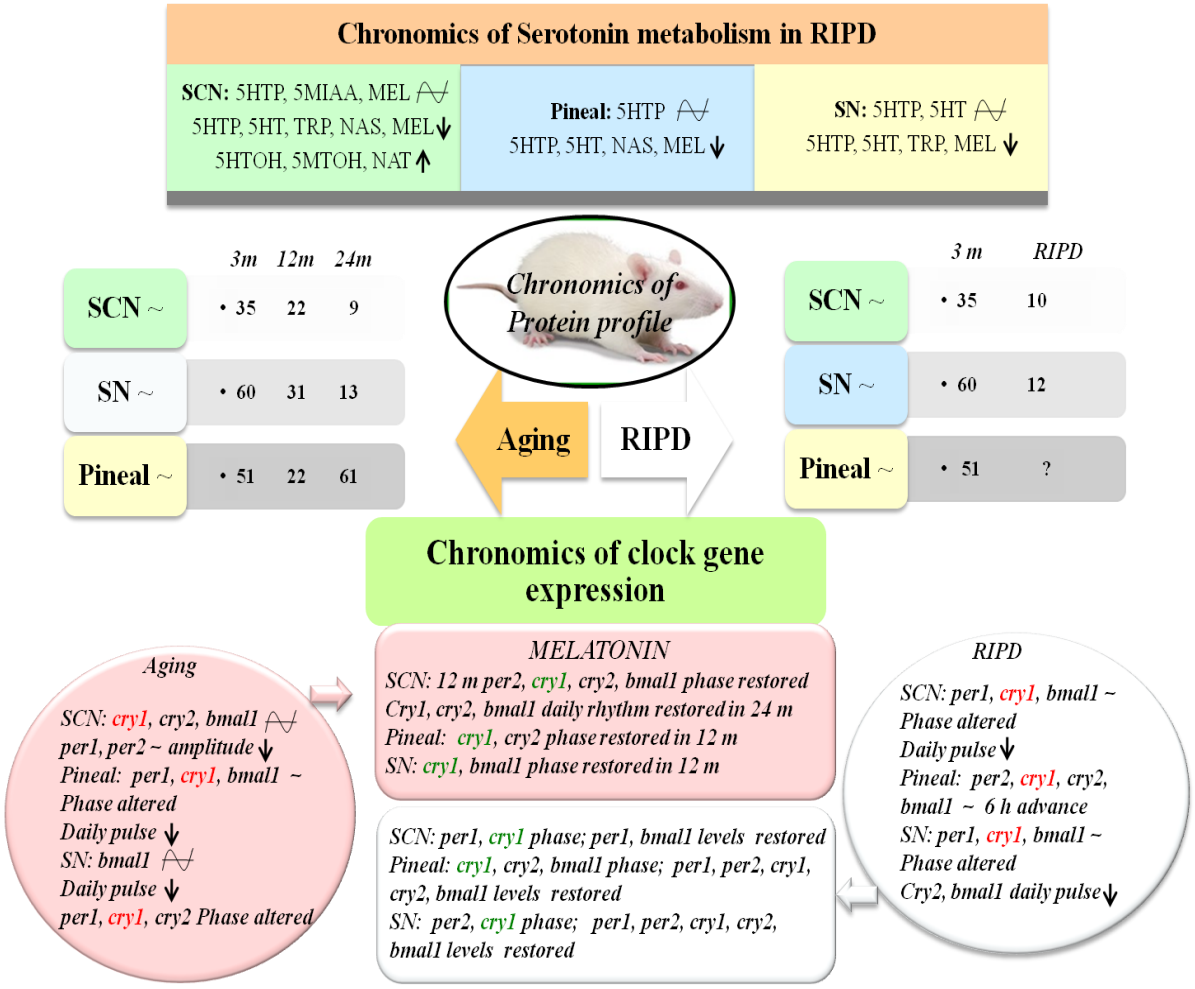

Fig. 93: A diagrammatic summary showing the alterations in chronomics of serotonin metabolism in RIPD model, influence of aging and rotenone induced Parkinson's disease (RIPD) on proteome and clock gene expression and effect of exogenous melatonin administration on clock genes expression in aging and RIPD.

Hence Serotonin metabolism was disturbed as indicated by the altered amplitude and rhythmicity of various components of serotonin metabolism in RIPD model. Proteomic studies showed a robust decrease in daily rhythm showing protein spots in aging and in RIPD rat model. Clock genes expression profile was also affected both in aging and in RIPD model. The exogenous melatonin administration restored the phase of clock gene daily rhythm in 12 m SCN, Pineal and SN but not in 24 m. Decreased daily pulse of clock gene expression in RIPD model could not be restored by melatonin administration.

References

Abe H, Honma S, Namihira M, Tanahashi Y, Ikeda M, Honma K (1998) Circadian rhythm and light responsiveness of BMAL1 expression, a partner of mammalian clock gene Clock, in the suprachiasmatic nucleus of rats. Neurosci Lett. 258:93-96.

Adi N, Mash DC, Ali Y, Singer C, Shehadeh L, Papapetropoulos S (2010) Melatonin MT1 and MT2 receptor expression in Parkinson's disease. Med Sci Monit. 16:61-67.

Agez L, Laurent V, Guerrero YH, Pevet P, Masson-Pevet M, Gauer F (2009) Endogenous melatonin provides an effective circadian message to both the suprachiasmatic nuclei pars tuberalis of the rat. J Pineal Res. 46:95-105.

Agez L, Laurent V, Pevet P, Masson-Pevet M, Gauer F (2007) Melatonin affects nuclear orphan receptors mRNA in the rat suprachiasmatic nuclei. Neuroscience. 144:522-530.

Aguiar ML, Macedo SD, de Freitas MR, Oliveira AA, Vasconcelos MMS, de Sousa C, Viana BSG (2005) Protective effects of N-acetylserotonin against 6-hydroxydopamine-induced neurotoxicity Life Sci. 76:2193-2202.

Alam M, Schmidt WJ (2002) Rotenone destroys dopaminergic neurons and induces parkinsonian symptoms in rats. Behav Brain Res. 136:317-324.

Arendt J (2005) Melatonin: characteristics, concerns, and prospects. J Biol Rhythms. 20:291-303.

Armstrong SM, Redman JR (1991) Melatonin: a chronobiotic with anti-aging properties? Med Hypotheses. 34:300-309.

Asai M, Yoshinobu Y, Kaneko S, Mori A, Nikaido T, Moriya T, Akiyama M, Shibata S (2001) Circadian Profile of *Per* Gene mRNA Expression in the Suprachiasmatic Nucleus, Paraventricular Nucleus, and Pineal Body of Aged Rats. J Neurosci Res. 66:1133-1139.

Aujard F, Herzog ED, Block GD (2001) Circadian rhythms in firing rate of individual suprachiasmatic nucleus neurons from adult and middle aged mice. Neuroscience. 106:255-261.

Azmitia EC, Nixon R (2008) Dystrophic serotonergic axons in neurodegerative diseases. Brain Res. 1217:185-194.

Beal MF (2001) Experimental models of Parkinson’s disease. Nat Rev Neurosci. 2:325-334.

Berger M, Gray JA, Roth BL (2009) The expanded biology of serotonin. Annu Rev Med. 60:355-360.

Betarbet R, Sherer BT, MacKenzie G, Garcia-Osuna M, Panov VA (2000) Chronic systemic pesticide exposure reproduces features of Parkinson's disease. Nat Neurosci. 3:1301-1306.

Biello MS (2009) Circadian clock resetting in the mouse changes with age. AGE. 31:293-303.

Bradford MM (1975) A Rapid Sensitive Method for the Quantitization of Microgram Quantities of Protein Utilizing the Principle Protein-Dye Binding. Anal Biochem. 72:248-254.

Bruguerolle B, Simon N (2002) Biologic Rhythms and Parkinson's Disease: A Chronopharmacologic Approach to Considering Fluctuations in Function. Clin Neuropharmacol. 25:194-201.

Bunger MK, Wilsbacher LD, Moran SM, Clendenin C, Radcliffe LA, Hogenesch JB, Simon MC, Takahashi JS, Bradfield CA (2000) Mop3 is an essential component of the master circadian pacemaker in mammals. Cell. 103:1009-1017.

Cabezas R, Avila MF, Torrente D, El-Bachá RS, Morales L, Gonzalez J, Barreto GE (2013) "Astrocytes Role in Parkinson: A Double-Edged Sword" in "Neurodegenerative diseases". pp 491-517.

Caboni P, Sherer TB, Zhang N, Taylor G, Na HM, Greenamyre JT, Casida JE (2004) Rotenone, deguelin, their metabolites, and the rat model of Parkinson's disease. Chem Res Toxicol. 17:1540-1548.

Cai Y, Liu S, Sothern BR, Xu S, Chan P (2010) Expression of clock genes Per1 and Bmal1 in total leukocytes in health and Parkinson's disease. Eur J Neurol. 17:550-554.

Cannon JR, Tapias MV, Na HM, Honick SA, Drolet RE, and Greenamyre JT (2009) A highly reproducible rotenone model of Parkinson's disease. Neurobiol Dis. 34:279-290.

Cardinali DP, Pagano ES, Scacchi Bernasconi PA, Reynoso R, Scacchi P (2013) Melatonin and mitochondrial dysfunction in the central nervous system. Horm Behav. 63:322-330.

Cardinali DP, Srinivasan V, Brzezinski A, Brown GM (2012) Melatonin and its analogs in insomnia and depression. J Pineal Res. 52:365-375.

Cassone MV, Roberts HM, Moore YR (1987) Melatonin inhibits metabolic activity in the rat suprachiasmatic nuclei. Neurosci Lett. 81:29-34.

Cassone VM, Chesworth MJ, Armstrong SM (1986) Entrainment of rat circadian rhythms by daily injection of melatonin depends upon the hypothalamic suprachiasmatic nuclei. Physiol Behav. 36:1111-1121.

Catalá MD, Cañete-Nicolás C, Iradi A, Tarazona PJ, Tormos JM, Pascual-Leone A (1997) Melatonin levels in Parkinson's disease: drug therapy versus electrical stimulation of the internal globus pallidus. Exp Gerontol. 32:553-558.

Chaudhuri KR, Healy DG, Schapira AH (2006) Non-motor symptoms of Parkinson's disease: diagnosis and management. Lancet Neurol. 5:235-245.

Chaudhuri KR, Schapira AH (2009) Non-motor symptoms of Parkinson's disease: dopaminergic pathophysiology and treatment. Lancet Neurol. 8:464-474.

Chen ST, Chuang JI, Hong MH, Li EI-C (2002) Melatonin attenuates MPP^+-induced neurodegeneration and glutathione impairment in the nigrostriatal dopaminergic pathway. J Pineal Res. 32:262-269.

Chomczynski P, Sacchi N (2006) Single-step method of RNA isolation by acid guanidinium thiocyanatephenol-chloroform extraction: Twenty-something years on. Nat Protoc. 1:581-585.

Coevorden VA, Mockel J, Laurent E, Kerkhofs M, L'Hermite-Balériaux M, Decoster C, Nève P, Van Cauter E (1991) Neuroendocrine rhythms and sleep in aging men. Am J Physiol. 260:651-661.

Cookson MR (2005) The biochemistry of Parkinson's disease. Annu Rev Biochem. 74:29-52.

Dauer W, Przedborski S (2003) Parkinson's Disease: Mechanisms and Models. Neuron. 39:889-909.

Davie CA (2008) A review of Parkinson's disease. Br Med Bull. 86:109-127.

De Blas LA, Cherwinski MH (1983) Detection of antigens on nitrocellulose paper immunoblots with monoclonal antibodies. Anal Biochem. 133:214-219.

Di Monte DA (2003) The environment and Parkinson's disease: is the nigrostriatal system preferentially targeted by neurotoxins? Lancet Neurol. 2:531-8.

Dibner C, Schibler U, Albrecht U (2010) The Mammalian Circadian Timing System: Organization and Coordination of Central and Peripheral Clocks. Annu Rev Physiol. 72:517-549.

Donaldson ZR, Nautiyal KM, Ahmari SE, Hen R(2013) Genetic approaches for understanding the role of serotonin receptors in mood and behavior. Curr Opin Neurobiol. 23:399-406.

Dubocovich ML, Markowska M (2005) Functional MT1 and MT2 melatonin receptors in mammals. Endocrine. 27:101-110.

Dunlap JC (1999) Molecular bases for circadian clocks. Cell. 96:271-290.

Esposti DM (1998) Inhibitors of NADH-ubiquinone reductase: an overview. Biochem Biophys Acta. 1364:222-235.

Farajnia S, Michel S, Deboer T, Vanderleest HT, Houben T, Rohling JH, Ramkisoensing A, Yasenkov R, Meijer JH (2012) Evidence for neuronal desynchrony in the aged suprachiasmatic nucleus clock. J Neurosci. 32:5891-5899.

Fertl E, Auff E, Doppelbauer IA, Waldhauser F (1993) Circadian secretion pattern of melatonin in de novo Parkinsonian patients: evidence for phase-shifting properties of l-dopa. J Neural Transm Park Dis Dement Sect. 5:227-234.

Forno LS, Langston JW, DeLanney LE, Irwin I, Ricaurte GA (1996) Locus ceruleus lesions and eosinophilic inclusions in MPTP-treated monkeys. Ann Neurol. 20:449-455.

Francesca C, Nicolas L, Antoine RT, Martine SP, Lincoln J, Brooks WF and Robert EG (2005) Systemic exposure to paraquat and maneb models early Parkinson's disease in young adult rats. Neurobiol Dis. 20:360-371.

Gall CV, Weaver DR (2008) Loss of responsiveness to melatonin in the aging mouse suprachiasmatic nucleus. Neurobiol Aging. 29:464-470.

Garattini S, Valzelli L (1965) "Metabolism of serotonin in vivo" in "Serotonin". Elsevier Publishing Company, Amsterdam. pp:9-73.

Garau C, Aparicio S, Rial VR, Nicolau CM, Esteban S (2006) Age related changes in the activity-rest circadian rhythms and c-fos expression of ring doves with aging. Effects of tryptophan intake. Exp Gerontol. 41:430-438.

Giasson BI, Murray, Troanowski JQ, Lee VM (2001) A hydrophobic stretch of 12 amino acid residues in the middle of alpha-synuclein is essential for filament assembly. J Biol Chem. 276:2380-2386.

Gillette UM, McArthur JA (1996) Circadian actions of melatonin at the suprachiasmatic nucleus. Behav Brain Res. 73:135-139.

Granados-Fuentes D, Herzog ED (2013) The clock shop: Coupled circadian oscillators. Exp Neurol. 243:21-27.

Gravotta L, Gavrila AM, Hood S, Amir S (2011) Global Depletion of Dopamine Using Intracerebroventricular 6-Hydroxydopamine Injection Disrupts Normal Circadian Wheel-Running Patterns and PERIOD2 Expression in the Rat Forebrain. J Mol Neurosci. 45:162-171.

Grivennikova VG, Maklashina EO, Gavrikova EV, Vinogradov AV (1997) Interaction of the mitochondrial NADH-ubiquinone reductase with rotenone as related to the enzyme active/inactive transition. Biochim Biophys Acta. 1319:223-232.

Hardeland R (2012) Melatonin in Aging and Disease - Multiple Consequences of Reduced Secretion, Options and Limits of Treatment. Aging Dis. 3:194-225.

Hardeland R, Cardinali DP, Srinivasan V (2011) Melatonin - a pleiotropic, orchestrating regulator molecule. Prog Neurobiol. 93:350-384.

Hardeland R, Madrid JA, Tan D, Reiter RJ (2012) Melatonin, the circadian multioscillator system and health: the need for detailed analyses of peripheral melatonin signaling. J Pineal Res. 52:139-166.

He Y, Imam ZS, Dong Z, Jankovic J, Ali FS, Appel HS, Le W (2003) Role of nitric oxide in rotenone-induced nigro-strital injury. J Neurochem. 86:1338-1345.

Heffner TG, Hartman JA, Seiden LS (1980) A Rapid Method for the Regional Dissection of the Rat Brain. Pharmacol Biochem Behav.13:453-456.

Hofman MA, Swaab DF (2006) Living by the clock: the circadian pacemaker in older people. Ageing Res Rev. 5:33-51.

Hood S, Cassidy P, Cossette M, Weigl Y, Verwey M, Robinson B, Stewart J, Amir S (2010) Endogenous Dopamine Regulates the Rhythm of Expression of the Clock Protein PER2 in the Rat Dorsal Striatum via Daily Activation of D2 Dopamine Receptors. J Neurosci. 30:14046-14058.

Iacono PR, Kuniyoshi MS, Ahlman RJ, Zimmerman JG, Maeda G, Pearlstein DR (1997) Concentrations of indoleamine metabolic intermediates in the ventricular cerebrospinal fluid of advanced Parkinson's patients with severe postural instability and gait disorders. J Neural Transm. 104:451-459.

Imbesi M, Yildiz S, Dirim Arslan A, Sharma R, Manev H, Uz T (2009) Dopamine receptor-mediated regulation of neuronal "clock" gene expression. Neuroscience. 158:537-544.

Inden M, Kondo J, Kitamura Y (2003). Differences in rotational asymmetry in rats caused by single intranigral injections of 6-hydroxydopamine, 1-methyl-4-phenylpyridinium ion and rotenone. Biogenic amines. 17:281-291.

Jagota A (2005) Aging and sleep disorders. Indian J gerontol. 19:415-424.

Jagota A (2006) Suprachiasmatic Nucleus: The Center for Circadian Timing System in Mammals. Proc Indian Natl Sci Acad. 71:275-288.

Jagota A (2012) "Age- Induced Alterations in Biological Clock: Therapeutic Effects of Melatonin" in "Brain Aging and Therapeutic Interventions". Springer Netherlands publishing group. London. pp 111-129.

Jagota A, de la Iglesia HO, Schwartz WJ (2000) Morning and evening circadian oscillations in the suprachiasmatic nucleus in vitro. Nat Neurosci. 3:372-376.

Jagota A, Kalyani D (2010) Effect of melatonin on age induced changes in daily serotonin rhythms in suprachiasmatic nucleus of male wistar rat. Biogerontol. 11:299-308.

Jagota A, Reddy MY (2007) The effect of Curcumin on ethanol induced changes in Suprachiasmatic nucleus (SCN) and Pineal. Cellular Molecular Neurobiol. 27:997-1006.

Jenner P (2003) Oxidative stress in Parkinson's disease. Ann Neurol. 53:S26-S38.

Jin X, von Gall C, Pieschl RL, Gribkoff VK, Stehle JH, Reppert SM, Weaver DR (2003) Targeted disruption of the mouse Mel(1b) melatonin receptor. Mol Cell Biol. 23:1054-1060.

Karasek M (2004) Melatonin, human aging, and age-related diseases. Exp Gerontol. 39:1723-1729.

Kema IP, Elisabeth G.E. de Vries, Muskiet FAJ (2000) Clinical chemistry of serotonin and metabolites. J Chromatogr B Biomed Sci Appl. 747:33-48.

Khaldy H, León J, Escames G, Bikjdaouene L, García JJ, Acuña-Castroviejo D (2002) Circadian Rhythms of Dopamine and Dihydroxyphenyl Acetic Acid in the Mouse Striatum: Effects of Pinealectomy and of Melatonin Treatment. Neuroendocrinology. 75:201-208.

Kitada T, Asakawa S, Hattori N (1998) Mutations in the parkin gene cause autosomal recessive juvenile parkinsonism. Nature. 392:605-608.

Klein DC, Moore RY, Reppert SM (1991) Suprachiasmatic Nucleus: The Mind's Clock. Oxford University Press, New York.

Ko HC, Takahashi SJ (2006) Molecular components of circadian clock. Hum Mol Genet. 15:271-277.

Kolker DE, Fukuyama H, Huang DS, Takahashi JS, Horton TH, Turek FW (2003) Aging alters circadian and light-induced expression of clock genes in golden hamsters. J Biol Rhythms. 18:159-169.

Kolker DE, Olson SL, Dutton-Boilek J, Bennett KM, Wallen EP (2002) Feeding melatonin enhances the phase shifting response to triazolam in both young and old golden hamsters. Am J Physiol. 282:1382-1388.

Kondratov VR (2007) A role of the circadian system and circadian proteins in aging (2007). Ageing Res Rev. 6:12-27.

Kondratov VR, Vykhovanets O, Kondratova AA, Antoch PM (2009) Antioxidant N-acetyl-L-cysteine ameliorates symptoms of premature aging associated with the deficiency of the circadian protein BMAL1. Aging. 1:979-987.

Kondratova AA, Kondratov RV (2012) The circadian clock and pathology of the ageing brain. Nat Rev Neurosci. 13:325-335.

Kondrotov RV, Kondrotova AA, Gorbacheva VY, Vychovanets OV, Antoch MP (2006) Early aging and age related pathologies in mice deficient in BMAL1, the core component of the circadian clock. Genes Dev. 20:1868-1873.

Kudo T, Loh DH, Truong D, Wu Y, Colwell CS (2011) Circadian dysfunction in a mouse model of Parkinson's disease. Exp Neurol. 232:66-75.

Kuhn MD, Sykes EC, Geddes JT, Bishop CK (2011) Tryptophan hydroxylase 2 aggregates through disulphide cross-linking upon oxidation: possible link to serotonin deficits and non-motor symptoms in Parkinson's disease. J Neurochem. 116:426-437.

Kunieda T, Minamino T, Katsuno T, Tateno K, Nishi J, Miyauchi H, Orimo M, Okada S, Komuro I (2006) Cellular senescence impairs circadian expression of clock genes in vitro and in vivo. Circ Res. 3:532-539.

Lambert AJ, Brand MD (2004) Inhibitors of the quinine-binding site allow rapid superoxide production from mitochondrial NADH: ubiquinone oxidoreductase (complex I). J Biol Chem. 279:39414-39420.

Lamelli UK (1970) Cleavage of Structural Proteins during the Assembly of the Head of Bacteriophage T4. Nature. 227:680-685.

Lezoualc'h F, Sparapani M, Behl C (1998) N-acetyl-serotonin (normelatonin) and melatonin protect neurons against oxidative challenges and suppress the activity of the transcription factor NF-kB. J Pineal Res. 24:168-178.

Lin C, Huang J, Ching C, Chuang J (2008) Melatonin reduces the neuronal loss, downregulation of dopamine transporter, and upregulation of D2 receptor in rotenone-induced parkinsonian rats. J. Pineal Res. 44:205-213.

Liu C, Weaver DR, Jin X, Shearman LP, Pieschl RL, Gribkoff VK, Reppert SM (1997) Molecular dissection of two distinct actions of melatonin on the suprachiasmatic circadian clock. Neuron. 19:91-102.

Livak KJ, Schmittgen TD (2001) Analysis of relative gene expression data using real-time quantitative PCR and the $2^{-\Delta\Delta Ct}$ Method. Methods. 25:402-408.

Lucas G, De Deurwaerdère P, Caccia S, Umberto Spampinato (2000) The effect of serotonergic agents on haloperidol-induced striatal dopamine release in vivo: opposite role of 5-HT(2A) and 5-HT(2C) receptor subtypes and significance of the haloperidol dose used. Neuropharmacology. 39:1053-1063.

Mammen AP, Jagota A (2011) Immunocytochemical evidence for different patterns in daily rhythms of VIP and AVP peptides in the suprachiasmatic nucleus of diurnal Funambulus palmarum. Brain Res. 1373: 39-47.

Manikonda PK and Jagota A (2012) Melatonin administration differentially affects age-induced alterations in daily rhythms of lipid peroxidation and antioxidant enzymes in male rat liver. Biogerentology. 13:511-524.

Matteo DV, Di Giovanni G, Pierucci M, Esposito E (2008) Serotonin control of central dopaminergic function: focus on in vivo microdialysis studies. Prog Brain Res. 172:7-44.

Mattson MP, Duan W, Wan R, Guo Z (2004) Prophylactic activation of neuroprotective stress response pathways by dietary and behavioral manipulations. NeuroRx. 1:111-116.

McArthur JA, Gillette UM, Prosser AR (1991) Melatonin directly resets the rat suprachiasmatic circadian clock in vitro. Brain Res. 565:158-161.

Miguez JM, Recio J, Sanchez-Barcelo E, Aldegunde M (1998) Changes with age in daytime and nighttime contents of melatonin and indoleamines, and catecholamines in the pineal gland: a comparative study in rats and Syrian hamster. J Pineal Res. 25:106-115.

Mistlberger RE, Antle MC, Glass JD, Miller JD (2000) Behavioral and serotonergic regulation of circadian rhythms. Biol Rhythms Res. 31:240-283.

Mohawk JA, Green CB, Takahashi JS (2012) Central and peripheral circadian clocks in mammals. Annu Rev Neurosci. 35:445-462.

Moore RY, Halaris AE, Jones BE (1978) Serotonin neurons of the midbrain raphe: Ascending projections. J Comp Neurol. 180:417-438.

Mortz E, Krogh TN, Vorum H, Görg A (2001) Improved silver staining protocols for high sensitivity protein identification using matrix-assisted laser desorption/ionization-time of flight analysis. Proteomics.1:1359-63.

Nakamura JT, Nakamura W, Yamazaki S, Kudo T, Cutler T, Colwell CS, Block GD (2011) Age-Related Decline in Circadian Output. J Neurosci. 31:10201-10205.

Nicola S, Micaela M and Anna RC (2007) The 6-Hydroxydopamine Model of Parkinson's Disease. Neurotoxic Research. 11:151-167.

Oikawa TS, Hiraku Y, Kawanishi M, Kawanishi S (2003) Mechanism for generation of hydrogen peroxide and change of mitochondrial membrane potential during rotenone-induced apoptosis. Life Sci. 73:3277-3288.

Ono O, Mochizukib H, Ikedaa T, Nihirac T, Takasakia J, Teplowd DB, Yamada M (2012) Effect of melatonin on α-synuclein self-assembly and cytotoxicity. Neurobiol Aging. 33:2172-2185.

Paisán-Ruíz C, Jain S, Evans EW, Gilks WP, Simón J, van der Brug M, López de Munain A, Aparicio S, Gil AM, Khan N, Johnson J, Martinez JR, Nicholl D, Carrera IM, Pena AS, de Silva R, Lees A, Martí-Massó JF, Pérez-Tur J, Wood NW, Singleton AB (2004) Cloning of the gene containing mutations that cause PARK8-linked Parkinson's disease. Neuron. 44:595-600.

Palomba M, Nygard M, Florenzano F, Bertini G, Kristenssion K, Bentivoglio M (2008) Decline of the presynaptic network, including GABAergic terminals, in the aging suprachiasmatic nucleus of the mouse. J Biol Rhythms. 23:220-231.

Pandi-Perumal SR, BaHammam AS, Brown GM, Spence DW, Bharti VK, Kaur C, Hardeland R, Cardinali DP (2013) Melatonin Antioxidative Defense: Therapeutical Implications for Aging and Neurodegenerative Processes. Neurotox Res. 23:267-300.

Pandi-Perumal SR, Trakht I, Spence DW, Srinivasan V, Dagan Y, Cardinali DP (2008) The roles of melatonin and light in the pathophysiology and treatment of circadian rhythm sleep disorders. Nat Clin Pract Neurol. 4:436-447.

Park K, Kang MH (2004) Cloning and Circadian Expression of Rat Cry1. Mol Cells. 18:256-260.

Poeggeler B (2005) Melatonin, aging, and age-related diseases: perspectives for prevention, intervention, and therapy. Endocrine. 27:201-212.

Poirel VJ, Boggio V, Dardente H, Pevet P, Masson-Pevet M, Gauer F (2003) Contrary to other non-photic cues, acute melatonin injection does not induce immediate change of clock gene mRNA expression in the rat suprachiasmatic nuclei. Neuroscience. 120:745-755.

Reddy YM (2010) Effect of Curcumin on Ethanol Induced Changes in Daily Serotonin Chronometabolomics and Gene Expression in SCN and Pineal: Locomotor Rhythms. Ph.D thesis with Jagota A, University of Hyderabad, India.

Reghunandanan V, Reghunandanan R (2006) Neurotransmitters of the suprachiasmatic nuclei. J Circadian Rhythms. 4:2-22.

Reiter RJ, Paredes SD, Manchester LC, Tan DX (2009) Reducing oxidative/nitrosative stress: a newly-discovered genre for melatonin. Crit Rev Biochem Mol Biol. 44:175-200.

Reiter RJ, Tan DX, Broto LF (2010) Melatonin: a multitasking molecule. Prog Brain Res. 181:127-151

Reppert SM, Weaver DR, Ebisawa T (1994) Cloning and characterization of a mammalian melatonin receptor that mediates reproductive and circadian responses. Neuron. 13:1177-1185.

Reppert SM, Godson C, Mahle CD, Weaver DR, Slaugenhaupt SA, Gusella JF (1995) Molecular characterization of a second melatonin receptor expressed in human retina and brain: The Mel1b melatonin receptor. Proc Natl Acad Sci. 92:8734-8738.

Revell VL, Burgess HJ, Gazda CJ, Smith MR, Fogg LF, Eastman CI (2006) Advancing human circadian rhythms with afternoon melatonin and morning intermittent bright light. J Clin Endocrinol Metab. 91:54-59.

Robles MS, Boyault C, Knutti D, Padmanabhan K, Weitz CJ (2010) Identification of RACK1 and protein kinase c alpha as integral components of the mammalian circadian clock. Science. 327:463-466.

Ruddick JP, Evans AK, Nutt DJ, Lightman SL, Rook GA, Lowry CA (2006) Tryptophan metabolism in the central nervous system: medical implications. Expert Rev Mol Med. 8:1-27.

Sack RL, Lewy AJ, Hughes RJ (1998) Use of melatonin for sleep and circadian rhythm disorders. Ann Med. 30:115-121.

Saper CB, Lu J, Chou TC, Gooley J (2005) The hypothalamic integrator for circadian rhythms. Trends Neurosci. 28:152-157.

Saudou F, Hen R (1994) 5-Hydroxytryptamine receptor subtypes in vertebrates and invertebrates. Neurochem Int. 25:503-32.

Sawada M, Nagatsu T, Nagatsu I, Ito K, Iizukas R, Kondo T, Narabayashi H (1985) Tryptophan Hydroxylase Activity in the Brains of Controls and Parkinsonian Patients. J Neural Transm. 62:107-115.

Schaffner W, Weissmann C (1973) A rapid, sensitive, and specific method for the determination of protein in dilute solution. Anal Biochem. 56:502-514.

Sharma VK, Singaravel M, Subbaraj R, Chandrashekaran KM (1999) Timely Administration of Melatonin Accelerates Reentrainment to Phase-Shifted Light-Dark Cycles in the Field Mouse Mus Booduga. Chronobiol Int. 16:163-170.

Shim HS, Kim H, Lee J, Son GH, Cho S, Oh TH, Kang SH, Seen DS, Lee KH, Kim K (2007) Rapid activation of CLOCK by $Ca2^{+}$-dependent protein kinase C mediates resetting of the mammalian circadian clock. EMBO Rep. 8:366-371.

Shimomura K, Lowrey LP, Vitaterna HM, Buhr DE, Kumar V, Hanna P, Omura C, Izumo M, Low SS, Barrett KR, LaRue IS, Green BC, Takahashi SJ (2010) Genetic suppression of the circadian clock mutation by the melatonin biosynthesis pathway. Proc Natl Acad Sci. 107:8399-8403.

Singhal NK, Srivastava G, Agrawal S, Jain SK, Singh MP (2012) Melatonin as a Neuroprotective Agent in the Rodent Models of Parkinson's Disease: Is it All Set to Irrefutable Clinical Translation? Mol Neurobiol. 45:186-199.

Skene JD, Vivien-Roels B, Sparks LD, Hunsaker CJ, Pevet P, Ravid D, Swaab FD (1990) Daily variation in the concentration of melatonin and 5-methoxytryptophol in the human pineal gland: effect of age and Alzheimer's disease. Brain Res. 528:170-174.

Smith RG, Betancourt L, Sun Y (2005) Molecular Endocrinology and Physiology of the Aging Central Nervous System. Endoc Rev. 26:203-250.

Sousa SC, Castilho RF (2005) Protective effect of melatonin on rotenone plus Ca2+-induced mitochondrial oxidative stress and PC12 cell death. Antioxid Redox Signal. 7:1110-1116.

Sparks LD, Slevin JT (1984) Determination of Tyrosine, Tryptophan and their metabolic derivatives by Liquid chromatography-Electrochemical detection: Application to post mortem samples from patients with Parkinson's and Alzheimer's disease. Life Sci. 36:449-457.

Spillantini MG, Crowther RA, Jakes R, Hasegawa M, Goedert M (1998) α-Synuclein in filamentous inclusions of Lewy bodies from Parkinson's disease and dementia with Lewy bodies. Proc Natl Acad Sci U S A. 99:6469-6473.

Srinivasan V, Pandi-Perumal SR, Trahkt , Spence DW, Poeggeler B, Hardeland R, Cardinali DP (2009) Melatonin and melatonergic drugs on sleep: possible mechanisms of action. Int J Neurosci. 119:821-846.

Sumova A, Illnerova H (1996) Melatonin instantaneously resets intrinsic circadian rhythmicity in the rat suprachiasmatic nucleus. Neurosci Lett. 218:181-184.

Toh LK (2008) Basic Science Review on Circadian Rhythm Biology and Circadian Sleep Disorders. Ann Acad Med Singapore. 37:662-668.

Uversky NV (2004) Neurotoxicant –induced animal modes of Parkinson's disease: understanding the role of rotenone, maneb and paraquat in neurodegeneration. Cell Tissue Res. 318:225-241.

Wang J, Zhao H, Zhang Q, Cai H, Wang P (2013) Application of a metal–insulator–semiconductor (MIS) sensor for extracellular redox potential detection. Sensors and Actuators B 182:538-545.

Warren SW, Hodges BD, Cassone MV (1993) Pinealectomized rats entrain and phase-shift to melatonin injections in a dose-dependent manner. J Biol Rhythms. 8:233-245.

Weber M, Lauterburga T, Toblerb I, Burgunder M (2004) Circadian patterns of neurotransmitter related gene expression in motor regions of the rat brain. Neurosci Lett. 358:17-20.

Weckwerth W (2003) Metabolomics in systems biology. Annu Rev Plant Biol. 54:669-89.

Weinert D (2010) Circadian temperature variation and aging. Ageing Res Rev. 9:51-60.

Weinert H, Weinert D, Schurov I, Maywood ES, Hastings MH (2001) Impaired expression of the mPer2 circadian clock gene in the suprachiasmatic nuclei of aging mice. Chronobiol Int. 18:559-565.

Welsh KD, Takahashi SJ, Kay AS (2010) Suprachiasmatic Nucleus: Cell Autonomy and Network Properties. Annu Rev Physiol. 72:551-577.

Wilking M, Ndiaye M, Mukhtar H, Ahmad N (2013) Circadian Rhythm Connections to Oxidative Stress: Implications for Human Health. Antioxid Redox Signal. 19:192-208.

Willem K, Cailotto C, Dijk F, Bergen A and Buijs RM (2005) Circadian expression of clock genes and clock-controlled genes in the rat retina. Biochem Biophys Res Commun. 330:18-26

Willis GL, Robertson AD (2004) Recovery of experimental Parkinson's disease with the melatonin analogues ML-23 and S-20928 in a chronic, bilateral 6-OHDA model: a new mechanism involving antagonism of the melatonin receptor. Pharmacol Biochem Behav. 79:413-29.

Wu Y, Swaab FD (2005) The human pineal gland and melatonin in aging and Alzheimer's disease. J Pineal Res. 38:145-152.

Wyse AC, Coogan NA (2010) Impact of aging on diurnal expression patterns of CLOCK and BMAL1 in the mouse brain. Brain Res. 1337:21-31.

Yan ST, Shigeyoshi YT, Okamura H (1999) Per1 and Per2 gene expression in the rat suprachiasmatic nucleus: circadian profile and the compartment-specific response to light. Neuroscience. 94:141-150.

Yasuo S, Yoshimura T, Bartell AP, Iigo M, Makino E, Okabayashi N, Ebihara S (2002) Effect of melatonin administration on *qPer2*, *qPer3*, and *qClock* gene expression in the suprachiasmatic nucleus of Japanese quail. Eur J Neurosci. 16:1541-1546.

Ying-Hui W, Fischer DF, Kalsbeek A, Garidou-Boof M, Vlietm J, Heijningen C, Liu R, Zhou J, Swaab DF (2006) Pineal clock gene oscillation is disturbed in Alzheimer's disease, due to functional disconnection from the "master clock". FASEB J. 20:1874-6.

Yuan H, Zheng J, Liu P, Zhang S, Xu J, Bai L (2007) Pathogenesis of Parkinson's disease: Oxidative stress, environmental impact factors and inflammatory processes. Neurosci Bull. 23:125-130.

Yujnovsky I, Hirayama J, Doi M, Borrelli E, Sassone-Corsi P (2006) Signaling mediated by the dopamine D2 receptor potentiates circadian regulation by CLOCK:BMAL1. Proc Natl Acad Sci U S A. 103: 6386-6391.

Appendix I

List of Tables

Table 1: Characteristics of animal models of Parkinson's disease.

Table 2: Rhythmic alterations in the serotonin metabolism in the SCN of Rotenone induced Parkinson's disease (RIPD) rat model.

Table 3: Rhythmic alterations in the serotonin metabolism in the Pineal of Rotenone induced Parkinson's disease (RIPD) rat model.

Table 4: Rhythmic alterations in the serotonin metabolism in the SN of Rotenone induced Parkinson's disease (RIPD) rat model.

Table 5: Daily rhythms of protein profiles in 3 month SCN.

Table 6: Daily rhythms of Protein Profiles in 12 month SCN.

Table 7: Daily rhythms of Protein Profiles in 24 month SCN.

Table 8: Daily rhythms of Protein Profiles in 3 month Pineal.

Table 9: Daily rhythms of Protein Profiles in 12 month Pineal.

Table 10: Daily rhythms of Protein Profiles in 24 month Pineal

Table 11: Daily rhythms of Protein Profiles in 24 month Pineal.

Table 12: Daily rhythms of Protein Profiles in 3 month SN.

Table 13: Daily rhythms of Protein Profiles in 12 month SN.

Table 14: Daily rhythms of Protein Profiles in 24 month SN.

Table 15: Daily rhythms of Protein Profiles in aging and RIPD rat model.

Table 16: Clock gene expression in 3, 12 and 24 m SCN.

Table 17: Clock gene expression in 3, 12 and 24 m Pineal.

Table 18: Clock gene expression in 3, 12 and 24 m SN.

Table 19: Clock gene expression in SCN of Vehicle (V) and Rotenone induced PD (RIPD) rat model.

Table 20: Clock gene expression in Pineal of Vehicle (V) and Rotenone induced PD (RIPD) rat model.

Table 21: Clock gene expression in SN of Vehicle (V) and Rotenone induced PD (RIPD) rat model.

Table 22: Effect of melatonin on age induced changes in mean 24 h levels and daily pulse of various clock genes expression in SCN.

Table 23: Effect of melatonin on age induced changes in mean 24 h levels and daily pulse of various clock genes expression in Pineal.

Table 24: Effect of melatonin on age induced changes in mean 24 h levels and daily pulse of various clock genes expression in SN.

Table 25: Effect of melatonin on mean 24 h levels and daily pulse of various clock genes expression in SCN of Rotenone induced PD (RIPD) rat model.

Table 26: Effect of melatonin on mean 24 h levels and daily pulse of various clock genes expression in Pineal of Rotenone induced PD (RIPD) rat model.

Table 27: Effect of melatonin on mean 24 h levels and daily pulse of various clock genes expression in SN of Rotenone induced PD (RIPD) rat model.

Appendix II

List of Figures

Figure 1: Suprachiasmatic nucleus

Figure 2: Afferent and efferent pathways of the SCN. (i) Afferent to the SCN involves RHT - retinohypothalamic tract; GHT - geniculohypothalamic tract via intergeniculate nucleus (IGL); RRP -retino raphe pathway from median and dorsal raphe (ii) Efferent's of the SCN involves neural and humoral signals (Jagota, 2006).

Figure 3: Mammalian circadian timing system: Glutamate and PACAP which act on Cam K and PKA via NMDA and PAC2 receptors respectively to increase P-CREB thus entraining and regulating clock gene expression and clock proteins in SCN. The time information from SCN through GABA reaches PVN and then to SCG via ILCC. Then during the night the time information travels from SCG by NE to β-adrenergic receptors at pineal, stimulating AC resulting in increased cAMP which activate PKA and hence increased P-CREB activating AANAT resulting in melatonin synthesis. Both blood and CSF melatonin acts on SCN via MT1 and MT2 receptors, for resetting the circadian pacemaker (Jagota, 2012).

Figure 4: Skeletal structure of Serotonin (5-Hydroxy tryptamine).

Figure 5: Serotonin (5-HT) receptors and their effector systems. 5-HT1 receptor subtypes (5-HT1A, 5-HT1B, 5-HT1D, 5-HT1E and 5-HT1F) belongs to the family of Gi/o which is a pertusis toxin-sensitive G protein and inhibits Adenylyl cyclase (AC), 5-HT2 receptor subtypes (5-HT2A, 5-HT2B and 5-HT2C) belongs to the family of Gq (pertusis toxin insensitive) activates phospholipase C (PLC), 5-HT3 is a sodium (Na+) – Potassium (K+) ion channel and 5-HT4, 5-HT6 and 5-HT7 belongs to Gs (G stimulatory) and activates AC. cAMP. 3', 5'-adenosine monophosphate, DAG. 1, 2-diacylglycerol, IP3. inositol 1,4,5-triphosphate, ER. Endoplasmic reticulum (Saudou and Hen, 1994).

Figure 6: Neural regulation of Pineal by SCN. Synthesis of Melatonin (MEL) from tryptophan (TRP) in pinealocyte. TPH - tryptophan hydroxylase; 5-TRP - 5-hydroxytryptophan; AADD - L-amino acid decarboxylase; 5-HT - serotonin, AANAT - arylalkylamine N-acetyltransferase; NAS - N-acetylserotonin; HlOMT - hydroxyindole-Omethyltransferase (Reiter *et al*., 2010).

Figure 7: Skeletal structure of Melatonin (*N*-[2-(5-methoxy-1*H*-indol-3-yl) ethyl] acetamide)

Figure 8: Major signaling pathways of melatonin through membrane receptors MT1 and MT2. Diagrammatic representation of combined pathways. Every target cell may not have all these pathways collectively. Activation of MT1/MT2 leads to decrease in intra-cellular cAMP levels finally ends in decreased expression of gene with CRE-containing promoters. Another pathway

which gets activated by MT1/MT2 is Cam Kinase and MAP kinase pathway. CaM-calmodulin, cAMP-cyclic adenosine monophosphate, DAG-diacyl glycerol, ERK-extracellular signal-regulated kinase, IP3-inositol 1,4,5-tris-phosphate, Kir3.1/2 subtypes 3. MAP-mitogen-activated protein kinase, MEK MAP ERK kinase, pCREB- phosphorylated cAMP/Ca2? Response element-binding protein, PI3K-phosphoinositide 3-kinase, PLC-phospholipase C, PK-protein kinase, Raf homolog of retroviral kinase, the product of oncogene v-raf, upregulation or rise, downregulation or decrease (Pandi-Perumal *et al*., 2013).

Figure 9: Many free radicals are generated due to chemical reduction of molecular oxygen (O_2). Many of the free radicals are scavenged by melatonin. Apart from detoxifying free radicals melatonin activates many antioxidant enzymes (as indicated by ↑) and inhibiting pro-oxidant enzymes (as indicated by ↓). CAT, catalase; CuZnSOD, copper/zinc superoxide dismutase; MnSOD, magnesium superoxide dismutase; GCL, glutamylcysteine ligase; GPx, glutathione peroxidase; GRd, glutathione reductase; MPO, myeloperoxidase; $^1O_2$, singlet oxygen; $O^{2\bullet-}$, superoxide anion radical; H_2O_2, hydrogen peroxide, HOCl, hypochlorous acid; GSH, reduced glutathione; GSSG, oxidized glutathione; e^-, electron (Reiter, 2010).

Figure 10: Antioxidant cascade of melatonin occurs due to detoxification of free radicals by melatonin. Detoxification of $^{\bullet}OH$ by melatonin leads to the formation of cyclic 3-hydroxymelatonin, further cyclic 3-hydroxymelatonin also neutralizes free radicals and generates *N*-acetyl-*N*-formyl-5-methoxykynuramine (AFMK) or melatonin can directly forms AFMK by reacting with H_2O_2. AFMK also acts as free radical scavenger and generates *N*-acetyl-5-methoxykynuramine (AMK). As its precursors AMK also an antioxidant whose products are not yet identified (Reiter, 2010).

Figure 11: Diagrammatic representation of role of melatonin in biological clock system (Hardeland *et al*., 2012).

Figure 12: Network of metabolite feedback pathways regulates transcription and translation. Alterations in the metabolome are the ultimate answer of an organism to genetic alterations, disease, or environmental influences (Weckwerth, 2003).

Figure 13: Serotonin biosynthesis and catabolism. Tryptophan hydroxylase converts tryptophan (TRP) into to 5-hydroxytryptophan (5-HTP) and then 5-HTP is converted to Serotonin (5-HT) by an enzyme L- aromatic amino acid decarboxylase. TRP is converted to N-acetyl tryptamine (NAT) by decarboxylase and acetylase enzymes respectively. 5-HT has two important pathways: (i) N-acetylase enzyme converts 5-HT into N-acetyl serotonin (NAS) and then to melatonin (MEL) by hydroxyl indole-O-methyl transferase (HIOMT) enzyme. (ii) Monoamine oxidase (MAO) converts 5-HT into 5-hydroxyindole acetaldehyde and then is converted to 5-hydroxyindoleacetic acid (5-HIAA) and 5-hydroxy tryptophol (5-HTOH) by aldehyde

dehydrogenase and aldehyde reductase respectively. 5-HIAA is converted to 5- methoxyindole acetic acid (5-MIAA) and 5-HTOH is converted to 5-methoxy indole acetic acid (5-MTOH) by HIOMT enzyme; (Garattini and Valzelli, 1965).

Figure 14: Mammalian circadian clock molecular mechanism. SCN rhythmicity is regulated by the interactions of clock genes and their protein product characterized by feedback loops. C*lock*, *Bmal1*and *Ror α* are positive regulators. CLOCK and BMAL1 - forms heterodimers and promotes expression of *Per*, *Cry, Ror α, Rev-erb α* and *Ccg* genes. *Per, Cry* and *Rev-erbα* are negative regulators. PER/CRY complex inhibits the transcription of their own genes and as well as *Ccg's.* PER and CRY stability is determined by its phosphorylation states by CK1 and AMPK (Mohawk *et al*., 2012).

Figure 15: Schematic diagram showing various sleep disorders associated with disturbances of the circadian system. The open bars represent intervals during which wakefulness typically occurs, black bars correspond to usual sleep times in normal and pathological conditions and vertical rectangle represents desired sleep time. Individuals with advanced sleep phase syndrome (ASPS), sleep at earlier than desired time whereas individuals with irregular sleep-wake patterns such as sleep disordered breathing (SDB), periodic leg movements in sleep (PLMS) and rapid eye movement (REM) behavior disorder (RBD) etc. may have disturbed sleep at other than desired times also (Jagota, 2005).

Figure 16: Parkinson's disease neuropathology. (A) Schematic representation of the normal nigrostriatal pathway (in red). (B) Schematic representation of the nigrostriatal pathway in Parkinson's disease (in red). (C) Intraneuronal inclusions, termed Lewy bodies, in a SNpc dopaminergic neuron (Dauer and Przedborski, 2003).

Figure 17: Mechanisms of Neurodegeneration in Parkinson's disease. Accumulation of misfolded proteins, pathogenic mutations which lead to abnormal protein conformations, damage to cellular machinery which detect and degrade misfolded proteins. Oxidative damage resulting from mitochondrial dysfunction and abnormal dopamine metabolism plays a key role in PD neurodegeneration (Dauer and Przedborski, 2003).

Figure 18: Circadian clock-dependent regulation of neurodegeneration. Metabolism, reactive oxygen species (ROS) homeostasis, DNA repair and, probably, autophagy (systems and pathways controlled by the circadian clock are shown in green) are regulated by circadian clock. Compromise in the activities of these systems occurs with circadian disruption, which leads to oxidative stress (shown in red) and accumulation of intracellular and extracellular aggregates in the brain. This, in turn, leads to brain cell death and degeneration of brain structures (shown in yellow) (Kondratova and Kondratov, 2012).

Figure 19: Picture showing localization of human and rat substantia nigra (SN) in coronal sections of human and rat brain respectively.

Figure 20: Serotonin-dopamine interaction in the nigrostriatal dopaminergic system. Serotonin-containing cell bodies of the raphe nuclei send projections to dopaminergic cells in both the ventral tegmental area (VTA, A10) and the substantia nigra (SN, A9), and to their terminal fields in the nucleus accumbens, prefrontal cortex and striatum (Matteo *et al.*, 2008).

Figure 21: Mode of action of various toxins used in the development of experimental models of Parkinson's disease. MPTP, 6-hydroxydopamine and paraquat gets entry into dopaminergic neurons through dopamine transporter whereas rotenone readily diffuses across the lipid bilayer and get enter into dopaminergic neurons. Pathology induced by these toxins is activation of programmed cell death via the release of cytochrome C and accumulation of misfolded proteins (Cabezas *et al*., 2013).

Figure 22: Skeletal structure of Rotenone - (2*R*,6a*S*,12a*S*)-1,2,6,6a,12,12a-hexahydro-2-isopropenyl-8,9-dimethoxychromeno[3,4-*b*]furo(2,3-h)chromen-6-one.

Figure 23: Binding site of Rotenone to complex I of electron transport chain. This leads to inhibition of electron flow from complex I to ubiquinone binding site in the mitochondria during oxidative phosphorylation (Wang *et al*., 2013).

Figure 24: Daily rhythmic profiles of serum melatonin concentrations at various ages; grey area - darkness (Karasek, 2004).

Figure 25: Therapeutic effects of antioxidant melatonin in restoration of circadian functions. Exogenous administration of antioxidants leads to restoration of circadian function and decrease in the severity of neurological, physiological and sleep disorders which leads to increase in quality of life (Jagota, 2012).

Figure 26: Mitochondrial pathophysiology and Melatonin. Reactive oxygen species (ROS) production is mediated, partly via cardiolipin (CL) peroxidation which makes detachment of cytochrome c from the inner mitochondrial membrane and changes in mitochondrial permeability transition (mPT) leads to mitochondrial swelling and the release of cytochrome c and other pro-apoptotic proteins. Activation of caspase cascade in the cytoplasm results in apoptosis leading to cell death. Melatonin prevents this cascade by as scavenging ROS and preventing apoptosis and inhibiting the change in mPT (Cardinali *et al*., 2013).

Figure 27: Mode of neuroprotection by melatonin at various steps of toxin induced neurodegeneration. Melatonin inhibits Oxidative stress, lipid peroxidation, microglial activation,

inflammatory cytokines, caspase 9, apoptosis and decreases ROS (CI, CII, CIII and CIV - mitochondrial complexes I, II, III, and IV; ROS - reactive oxygen species; LPO - lipid peroxidation; DA - dopamine; Cyt -cytochrome; ETS - electron transport system; MAO-B monoamine oxidase-B enzyme) (Singhal *et al*., 2012).

Figure 28: Flow diagram showing plan of administration of (i) Rotenone and (ii) Melatonin.

Figure 29: Standard representative peaks of HPLC for Serotonin and its related compounds. (A) 10%methanol; 0.1N Sodium acetate; 0.1N citric acid, 50mg/L EDTA was used for detection of compounds- 5-HTP, 5-HT, 5-HIAA, NAS, TRP and 5-HTOH. (B) 25%methanol; 0.1N Sodium acetate; 0.1N citric acid, 50 mg/L EDTA was used for detection of compounds- 5-MIAA, 5-MTOH, MEL and NAT. nA refers to nanoampere (Unit of strength of electric current).

Figure 30: (A) Agarose gel electrophoresis of PCR generated amplicons of various clock genes generated after 40 amplification cycles length of the PCR products in rat SCN. (B) Representative dissociation curves for *β-actin, Per1, Per2, Cry1, Cry2* and *Bmal1*genes.

Figure 31: Representative picture of vehicle and rotenone treated rats.

Figure 32: Each value is mean ± SEM (n=10), $p \leq 0.05$ C - control, VT - vehicle treated and RT - Rotenone treated. * refers to comparison between VT and RT.

Figure 33: Tyrosin hydroxylase (TH) and α- Synuclein immunoreactivity in Rat Substantia nigra (SN). A (i and ii) TH immunoblot and densitometry analysis. B (i and ii) α- Synuclein immunoblot and densitometry analysis. C. TH-immunoreactivity (TH-ir) in coronal SN brain sections of VT and RT. M- Molecular weight marker, C-Control, VT- Vehicle treated, RT-Rotenone treated, SNpC- Substantia nigra pars compacta, SNpR- Substantia nigra pars reticulata. Data were expressed as mean ± SEM. $P \leq 0.05$, * refers to comparison between VT and RT.

Figure 34: Rhythmic alterations in the serotonin metabolism in the SCN of Rotenone induced Parkinson's disease (RIPD) rat model. Each value is mean ± SEM (n=6), $p \leq 0.05$ and expressed in µmol/g protein. V - Vehicle. $p_a \leq 0.05$; $p_b \leq 0.05$, $p_c \leq 0.05$ and $p_d \leq 0.05$ (where a, b, c and d refers to comparison with ZT-0, ZT-6, ZT-12 and ZT-18 respectively within the group). * refers to comparison of levels at same time point in vehicle group.

Figure 35: Various parameters studied in serotonin metabolism components. (i) Mean 24h levels, (ii) Daily Pulse i.e. ratio between maximum and minimum and (iii) Ratio between 5-HT and other Serotonin metabolism components studied in SCN of Vehicle (V) and Rotenone induced PD rat model (RIPD). Each value is mean ± SEM; $p_* \leq 0.05$ (where * refers to comparison with vehicle group.

Figure 36: Diagrammatic representation of mean 24 h alterations in the serotonin metabolism in the SCN of Rotenone induced Parkinson's disease (RIPD) rat model compared to vehicle.

Figure 37: Pair wise correlation between mean light (ZT 0, 6 and 12) and mean dark (ZT 12, 18 and 24/0) phase values of various components of serotonin metabolism in the SCN of vehicle (V) and Rotenone induced Parkinson's disease (RIPD) rat model. Each value is correlation coefficient values between the parameters. * indicates statistically significant value between parameters ($p \leq 0.05$). Negative value indicates negative correlation between parameters.

Figure 38: Rhythmic alterations in the serotonin metabolism in the Pineal of Rotenone induced Parkinson's disease (RIPD) rat model. Each value is mean ± SEM (n=6), $p \leq 0.05$ and expressed in µmol/g protein. V - Vehicle. $p_a \leq 0.05$; $p_b \leq 0.05$, $p_c \leq 0.05$ and $p_d \leq 0.05$ (where a, b, c and d refers to comparison with ZT-0, ZT-6, ZT-12 and ZT-18 respectively within the group). * refers to comparison of levels at same time point in vehicle group.

Figure 39: Various parameters studied in serotonin metabolism components. (i) Mean 24h levels, (ii) Daily Pulse i.e. ratio between maximum and minimum and (iii) Ratio between 5-HT and other Serotonin metabolism components studied in Pineal of Vehicle (V) and Rotenone induced PD rat model (RIPD). Each value is mean ± SEM; $p_* \leq 0.05$ (where * refers to comparison with vehicle group.

Figure 40: Diagrammatic representation of mean 24 h alterations in the serotonin metabolism in the Pineal of Rotenone induced Parkinson's disease (RIPD) rat model compared to vehicle.

Figure 41: Pair wise correlation between mean light (ZT 0, 6 and 12) and mean dark (ZT 12,18 and 24/0) phase values of various components of serotonin metabolism in the Pineal of vehicle (V) and Rotenone induced Parkinson's disease (RIPD) rat model. Each value is correlation coefficient values between the parameters. * indicates statistically significant value between parameters ($p \leq 0.05$). Negative value indicates negative correlation between parameters.

Figure 42: Rhythmic alterations in the serotonin metabolism in the Substantia nigra of Rotenone induced Parkinson's disease (RIPD) rat model. Each value is mean ± SEM (n=6), $p \leq 0.05$ and expressed in µmol/g protein. V - Vehicle. $p_a \leq 0.05$; $p_b \leq 0.05$, $p_c \leq 0.05$ and $p_d \leq 0.05$ (where a, b, c and d refers to comparison with ZT-0, ZT-6, ZT-12 and ZT-18 respectively within the group). * refers to comparison of levels at same time point in vehicle group.

Figure 43: Various parameters studied in serotonin metabolism components. (i) Mean 24h levels, (ii) Daily Pulse i.e. ratio between maximum and minimum and (iii) Ratio between 5-HT and other Serotonin metabolism components studied in SN of Vehicle (V) and Rotenone induced PD rat model (RIPD). Each value is mean ± SEM; $p_* \leq 0.05$ (where * refers to comparison with vehicle group.

Figure 44: Diagrammatic representation of mean 24 h alterations in the serotonin metabolism in the SN of Rotenone induced Parkinson's disease (RIPD) rat model compared to vehicle.

Figure 45: Pair wise correlation between mean light (ZT 0, 6 and 12) and mean dark (ZT 12, 18 and 24/0) phase values of various components of serotonin metabolism in the SN of vehicle (V) and Rotenone induced Parkinson's disease (RIPD) rat model. Each value is correlation coefficient values between the parameters. * indicates statistically significant value between parameters ($p \leq 0.05$). Negative value indicates negative correlation between parameters

Figure 46: Age induced alteration in protein profiles in variable age groups. (A) 3, (B) 12 and (C) 24 m SCN at (i) ZT6 and (ii) ZT18 with n=2. Protein spots which were differentially expressed between ZT6 and ZT18 of SCN are highlighted with green.

Figure 47: Age induced alteration in protein profiles in SCN of variable age groups at ZT6 (i and ii) and ZT18 (i and ii) with n=2. Protein spots which were differentially expressed between 3, 12 and 24 m SCN at ZT6 and ZT18 were highlighted.

Figure 48: Age induced alteration in protein profiles in variable age groups. Protein spots which were differentially expressed daily in 3, 12 and 24 m SCN were highlighted.

Figure 49: Daily rhythms of Protein Profiles in SCN of Control and Rotenone induced Parkinson's disease (RIPD) rat model. Protein spots which were differentially expressed between ZT6 and ZT18 of control A (i) and (ii) and RIPD B (i) and (ii) were highlighted with green.

Figure 50: Daily rhythms of Protein Profiles in SCN at ZT6 (i) and ZT18 (ii) of Control and Rotenone induced Parkinson's disease (RIPD) rat model.

Figure 51: Daily rhythms of Protein Profiles in SCN of Control and Rotenone induced Parkinson's disease (RIPD) rat model. Protein spots which were differentially expressed daily in SCN of control and RIPD rat model were highlighted.

Figure 52: Age induced alteration in protein profiles in variable age groups. (A) 3, (B) 12 and (C) 24 m Pineal at (i) ZT6 and (ii) ZT18 with n=2. Protein spots which were differentially expressed between ZT6 and ZT18 of Pineal are highlighted with green.

Figure 53: Age induced alteration in protein profiles in pineal of variable age groups at ZT6 (i and ii) and ZT18 (i and ii) with n=2. Protein spots which were differentially expressed between 3, 12 and 24 m pineal at ZT6 and ZT18 were highlighted.

Figure 54: Age induced alteration in protein profiles in variable age groups. Protein spots which were differentially expressed daily in 3, 12 and 24 m Pineal were highlighted.

Figure 55: Age induced alteration in protein profiles in variable age groups. (A) 3, (B) 12 and (C) 24 m SN at (i) ZT6 and (ii) ZT18 with n=2. Protein spots which were differentially expressed between ZT6 and ZT18 of SN are highlighted with green.

Figure 56: Age induced alteration in protein profiles in SN of variable age groups at ZT6 (i and ii) and ZT18 (i and ii) with n=2. Protein spots which were differentially expressed between 3, 12 and 24 m SN at ZT6 and ZT18 were highlighted.

Figure 57: Age induced alteration in protein profiles in variable age groups. Protein spots which were differentially expressed daily in 3, 12 and 24 m SN were highlighted.

Figure 58: Daily rhythms of Protein Profiles in SN of Control and Rotenone induced Parkinson's disease (RIPD) rat model. Protein spots which were differentially expressed between ZT6 and ZT18 of Control A (i) and (ii) and RIPD B (i) and (ii) were highlighted with green.

Figure 59: Daily rhythms of Protein Profiles in SN at ZT6 (i) and ZT18 (ii) of Control and Rotenone induced Parkinson's disease (RIPD) rat model.

Figure 60: Daily rhythms of Protein Profiles in SN of Control and Rotenone induced Parkinson's disease (RIPD) rat model. Protein spots which were differentially expressed daily in SN of control and RIPD rat model were highlighted.

Figure 61: Alterations in the number of protein spots which were differentially expressed daily in SCN, Pineal and SN. 3 month (m), 12 m, 24 m and rotenone induced Parkinson's disease (RIPD) rat model.

Figure 62: Age induced alterations in the number of protein spots which were differentially expressed in (i) variable age groups and (ii) Rotenone induced Parkinson's disease (RIPD) rat model at ZT6 and ZT18.

Figure 63: Effect of aging on expression of *Per1, Per2, Cry1, Cry2* and *Bmal1* genes in the SCN of male wistar rat. Each value is mean ± SEM (n=4), $p \leq 0.05$ and expressed in relative gene expression. 3, 12 and 24 m. $p_a \leq 0.05$; $p_b \leq 0.05$, $p_c \leq 0.05$ and $p_d \leq 0.05$ (where a, b, c and d refers to comparison with ZT-0, ZT-6, ZT-12 and ZT-18 respectively within the group).

Figure 64: Effect of aging on mean 24 h levels and daily pulse of various clock genes expression in SCN of male wistar rat.

Figure 65: Effect of aging on expression of *Per1, Per2, Cry1, Cry2* and *Bmal1* genes in the Pineal of male wistar rat. Each value is mean ± SEM (n=4), $p \leq 0.05$ and expressed in relative gene expression. 3, 12 and 24 m. $p_a \leq 0.05$; $p_b \leq 0.05$, $p_c \leq 0.05$ and $p_d \leq 0.05$ (where a, b, c and d refers to comparison with ZT-0, ZT-6, ZT-12 and ZT-18 respectively within the group).

Figure 66: Effect of aging on mean 24 h levels and daily pulse of various clock genes expression in Pineal of male wistar rat

Figure 67: Effect of aging on expression of *Per1, Per2, Cry1, Cry2* and *Bmal1* in the SN of male wistar rat. Each value is mean ± SEM (n=4), $p \leq 0.05$ and expressed in relative gene expression.

3, 12 and 24 m. $p_a \leq 0.05$; $p_b \leq 0.05$, $p_c \leq 0.05$ and $p_d \leq 0.05$ (where a, b, c and d refers to comparison with ZT-0, ZT-6, ZT-12 and ZT-18 respectively within the group).

Figure 68: Effect of aging on mean 24 h levels and daily pulse of various clock genes expression in Substantia nigra of male wistar rat.

Figure 69: Expression of various clock genes in SCN of RIPD rat model. Each value is mean ± SEM (n=4), $p \leq 0.05$ and expressed in relative gene expression. V - Vehicle and RIPD - Rotenone Induced PD rat model. $p_a \leq 0.05$; $p_b \leq 0.05$, $p_c \leq 0.05$ and $p_d \leq 0.05$ (where a, b, c and d refers to comparison with ZT-0, ZT-6, ZT-12 and ZT-18 respectively within the group). * refers to comparison of levels at same time point in vehicle group.

Figure 70: Mean 24 h levels and daily pulse of various clock genes expression in SCN of RIPD rat model. $p_* \leq 0.05$ (where * refers to comparison with vehicle group.

Figure 71: Expression of various clock genes in Pineal of rotenone induced PD rat model. Each value is mean ± SEM (n=4), $p \leq 0.05$ and expressed in relative gene expression. V - Vehicle and RIPD - Rotenone Induced PD rat model. $p_a \leq 0.05$; $p_b \leq 0.05$, $p_c \leq 0.05$ and $p_d \leq 0.05$ (where a, b, c and d refers to comparison with ZT-0, ZT-6, ZT-12 and ZT-18 respectively within the group). * refers to comparison of levels at same time point in vehicle group.

Figure 72: Mean 24 h levels and daily pulse of various clock genes expression in Pineal of RIPD rat model. $p_* \leq 0.05$ (where * refers to comparison with vehicle group.

Figure 73: Expression of various clock genes in SN of rotenone induced PD rat model. Each value is mean ± SEM (n=4), $p \leq 0.05$ and expressed in relative gene expression. V - Vehicle and RIPD - Rotenone Induced PD rat model. $p_a \leq 0.05$; $p_b \leq 0.05$, $p_c \leq 0.05$ and $p_d \leq 0.05$ (where a, b, c and d refers to comparison with ZT-0, ZT-6, ZT-12 and ZT-18 respectively within the group). * refers to comparison of levels at same time point in vehicle group.

Figure 74: Mean 24 h levels and daily pulse of various clock genes expression in Substantia nigra of RIPD rat model. $p_* \leq 0.05$ (where * refers to comparison with vehicle group.

Figure 75: Effect of melatonin administration on levels and rhythmicity of *Per1, Per2, Cry1, Cry2* and *Bmal1* genes in the aging rat SCN in 3, 12 and 24 months. Each value is mean ± SEM (n=4), $p \leq 0.05$ and expressed as relative gene expression. $p_a \leq 0.05$; $p_b \leq 0.05$, $p_c \leq 0.05$ and $p_d \leq 0.05$ (where a, b, c and d refers to comparison with ZT-0, ZT-6, ZT-12 and ZT-18 respectively within the group) $p_w \leq 0.05$ (where w refers to comparison of gene levels at same time point in vehicle group in same age group).

Figure 76: Effect of melatonin administration on mean 24h levels and Daily Pulse of *Per1, Per2, Cry1, Cry2 and Bmal1* genes in the aging rat SCN in 3, 12 and 24 m. Each value is mean ± SEM $p \leq 0.05$ and expressed as mean relative gene expression. $p_* \leq 0.05$ (where * refers to comparison with vehicle group). $p_{*\,1} \leq 0.05$ (where $_{*\,1}$ refers to comparison with 3 m vehicle group).

Figure 77: Effect of melatonin administration on pair wise correlation between mean light (ZT 0, 6 and12) and mean dark (ZT 12,18 and 24/0) phase values of *Per1, Per2, Cry1, Cry2 and Bmal1* in various age groups 3, 12 and 24 m in rat SCN. Each value is correlation coefficient values between the parameters. * indicates statistically significant value between parameters ($p \leq 0.05$). Negative value indicates negative correlation between parameters.

Figure 78: Effect of melatonin administration on levels and rhythmicity of *Per1, Per2, Cry1, Cry2* and *Bmal1* genes in the aging rat Pineal in 3, 12 and 24 m. Each value is mean ± SEM (n=4), $p \leq 0.05$ and expressed as relative gene expression. $p_a \leq 0.05$; $p_b \leq 0.05$, $p_c \leq 0.05$ and $p_d \leq 0.05$ (where a, b, c and d refers to comparison with ZT-0, ZT-6, ZT-12 and ZT-18 respectively within the group) $p_w \leq 0.05$ (where w refers to comparison of gene levels at same time point in vehicle group in same age group).

Figure 79: Effect of melatonin administration on mean 24h levels and Daily Pulse of *Per1, Per2, Cry1, Cry2 and Bmal1* genes in the aging rat Pineal in 3, 12 and 24 m. Each value is mean ± SEM $p \leq 0.05$ and expressed as mean relative gene expression. $p_* \leq 0.05$ (where * refers to comparison with vehicle group). $p_{*\ 1} \leq 0.05$ (where $_{*\ 1}$ refers to comparison with 3 m vehicle group).

Figure 80: Effect of melatonin administration on pair wise correlation between mean light (ZT 0, 6 and12) and mean dark (ZT 12, 18 and 24/0) phase values of *Per1, Per2, Cry1, Cry2 and Bmal1* in various age groups 3, 12 and 24 m in rat Pineal. Each value is correlation coefficient values between the parameters. * indicates statistically significant value between parameters ($p \leq 0.05$). Negative value indicates negative correlation between parameters.

Figure 81: Effect of melatonin administration on levels and rhythmicity of *Per1, Per2, Cry1, Cry2* and *Bmal1* genes in the aging rat SN in 3, 12 and 24 m. Each value is mean ± SEM (n=4), $p \leq 0.05$ and expressed as relative gene expression. $p_a \leq 0.05$; $p_b \leq 0.05$, $p_c \leq 0.05$ and $p_d \leq 0.05$ (where a, b, c and d refers to comparison with ZT-0, ZT-6, ZT-12 and ZT-18 respectively within the group) $p_w \leq 0.05$ (where w refers to comparison of gene levels at same time point in vehicle group in same age group).

Figure 82: Effect of melatonin administration on mean 24h levels and Daily Pulse of *Per1, Per2, Cry1, Cry2* and *Bmal1* genes in the aging rat SN in 3, 12 and 24 m. Each value is mean ± SEM $p \leq 0.05$ and expressed as mean relative gene expression. $p_* \leq 0.05$ (where * refers to comparison with vehicle group). $p_{*\ 1} \leq 0.05$ (where $_{*\ 1}$ refers to comparison with 3 m vehicle group).

Figure 83: Effect of melatonin administration on pair wise correlation between mean light (ZT 0, 6 and 12) and mean dark (ZT 12,18 and 24/0) phase values of *Per1, Per2, Cry1, Cry2 and Bmal1* in various age groups 3, 12 and 24 m in rat SN. Each value is correlation coefficient values between the parameters. * indicates statistically significant value between parameters ($p < 0.05$). Negative value indicates negative correlation between parameters.

Figure 84: Effect of melatonin administration on levels and rhythmicity of *Per1, Per2, Cry1, Cry2* and *Bmal1* genes in the SCN of RIPD rat model. Each value is mean ± SEM (n=4). V - Vehicle, RIPD - Rotenone induced PD, RIPD MEL - RIPD model received MEL for 11 days and RT + MEL - animals received both Rotenone and MEL for 48 days.

Figure 85: Effect of melatonin administration on mean 24h levels and Daily Pulse of *Per1, Per2, Cry1, Cry2 and Bmal1* genes in the SCN of RIPD rat model. Each value is mean ± SEM (n=4). V - Vehicle, RIPD - Rotenone induced PD, RIPD MEL - RIPD model received MEL for 11 days and RT + MEL - animals received both Rotenone and MEL for 48 days.

Figure 86: Effect of melatonin administration on pair wise correlation between mean light (ZT 0, 6 and 12) and mean dark (ZT 12, 18 and 24/0) phase values of *Per1, Per2, Cry1, Cry2 and Bmal1* in the SCN of RIPD rat model. Each value is mean ± SEM (n=4). V - Vehicle, RIPD - Rotenone induced PD, RIPD MEL - RIPD model received MEL for 11 days and RT + MEL - animals received both Rotenone and MEL for 48 days. Each value is correlation coefficient values between the parameters. * indicates statistically significant value between parameters ($p \leq 0.05$). Negative value indicates negative correlation between parameters.

Figure 87: Effect of melatonin administration on levels and rhythmicity of *Per1, Per2, Cry1, Cry2* and *Bmal1* genes in the Pineal of RIPD rat model. Each value is mean ± SEM (n=4). V - Vehicle, RIPD - Rotenone induced PD, RIPD MEL - RIPD model received MEL for 11 days and RT + MEL - animals received both Rotenone and MEL for 48 days.

Figure 88: Effect of melatonin administration on mean 24h levels and Daily Pulse of *Per1, Per2, Cry1, Cry2 and Bmal1* genes in the Pineal of RIPD rat model. Each value is mean ± SEM (n=4). V - Vehicle, RIPD - Rotenone induced PD, RIPD MEL - RIPD model received MEL for 11 days and RT + MEL - animals received both Rotenone and MEL for 48 days.

Figure 89: Effect of melatonin administration on pair wise correlation between mean light (ZT 0, 6 and 12) and mean dark (ZT 12, 18 and 24/0) phase values of *Per1, Per2, Cry1, Cry2 and Bmal1* in the Pineal of RIPD rat model. Each value is mean ± SEM (n=4). V - Vehicle, RIPD - Rotenone induced PD, RIPD MEL - RIPD model received MEL for 11 days and RT + MEL - animals received both Rotenone and MEL for 48 days. Each value is correlation coefficient values between the parameters. * indicates statistically significant value between parameters ($p \leq 0.05$). Negative value indicates negative correlation between parameters.

Figure 90: Effect of melatonin administration on levels and rhythmicity of *Per1, Per2, Cry1, Cry2* and *Bmal1* genes in the SN of RIPD rat model. Each value is mean ± SEM (n=4). V - Vehicle, RIPD - Rotenone induced PD, RIPD MEL - RIPD model received MEL for 11 days and RT + MEL - animals received both Rotenone and MEL for 48 days.

Figure 91: Effect of melatonin administration on mean 24h levels and Daily Pulse of *Per1, Per2, Cry1, Cry2 and Bmal1* genes in the SN of RIPD rat model. Each value is mean ± SEM (n=4). V - Vehicle, RIPD - Rotenone induced PD, RIPD MEL - RIPD model received MEL for 11 days and RT + MEL - animals received both Rotenone and MEL for 48 days.

Figure 92: Effect of melatonin administration on pair wise correlation between mean light (ZT 0, 6 and 12) and mean dark (ZT 12, 18 and 24/0) phase values of *Per1, Per2, Cry1, Cry2 and Bmal1* in the SN of RIPD rat model. Each value is mean ± SEM (n=4). V - Vehicle, RIPD - Rotenone induced PD, RIPD MEL - RIPD model received MEL for 11 days and RT + MEL - animals received both Rotenone and MEL for 48 days. Each value is correlation coefficient values between the parameters. * indicates statistically significant value between parameters ($p \leq 0.05$). Negative value indicates negative correlation between parameters.

Fig. 93: A diagrammatic summary showing the alterations in chronomics of serotonin metabolism in RIPD model, influence of aging and rotenone induced Parkinson's disease (RIPD) on proteome and clock gene expression and effect of exogenous melatonin administration on clock genes expression in aging and RIPD.

Appendix III

Abbreviations

^{o}C	:	degree centigrade/ degree Celsius
$^{1}O_2$	:	Singlet oxygen
5-HIAA	:	5-Hydroxy indole acetic acid
5-HT	:	5-Hydroxytryptamine
5-HTOH	:	5-Hydroxy tryptophol
5-MIAA	:	5-Methoxy indole acetic acid
5-MTOH	:	5-Methoxy indole acetic acid
AA-NAT	:	Arylalkylamine N-acetyl transferase
AANAT	:	Arylalkylamine N-acetyl transferase
AC	:	Adenylyl cyclase
AFMK	:	N-acetyl- N-formyl-5-methoxy kynuramine
AMK	:	N-acetyl-5-methoxy kynuramine
ANOVA	:	Analysis of Variance
ASPS	:	Advanced Sleep Phase Syndrome
ATP	:	Adenosine-tri-phospate
AVP	:	Arginine vasopressin
BBB	:	Blood brain barrier
bHLH	:	basic helix-loop-helix
Bmal1	:	Brain and muscle arnt like protein 1
BSA	:	Bovine serum albumin
CaM	:	Calmodulin
cAMP	:	Cyclic Adenosine Mono Phosphate
CAT	:	Catalase
CCG	:	Clock controlled genes
cDNA	:	Complentary DNA
CkIε	:	Casein kinase Iε
CL	:	Cardiolipin
Clock	:	Circadian locomotor output cycles kaput
CREB	:	cAMP response element binding protein
Cry	:	Cryptochrome
CSF	:	Cerebrospinal fluid
Ct	:	Cycle threshold
CTS	:	Circadian timing system
CuZnSOD	:	Copper/zink superoxide dismutase
DAG	:	1,2 Diacyl glycerol
DNA	:	deoxy-ribo nucleic acid
DSPS	:	Delayed Sleep Phase Syndrome
e^{-}	:	Electron
ECD	:	Electrochemical detection
EDTA	:	Ethylene di-amine tetra acetic acid

ER	:	Endoplasmic reticulum
ETC	:	Electron transport chain
GABA	:	Gamma amino butyric acid
GHT	:	Geniculo hypothalamic tract
Gi	:	G Inhibitory
GPCRs	:	G protein-coupled receptors
GRd	:	Glutathione reductase
Gs	:	G stimulatory
GSH	:	Reduced glutathione
GSSG	:	Oxidized glutathione
H_2O_2	:	Hydrogen peroxide
HIOMT	:	Hydroxy indole -o-methyl transferase
IEF	:	Iso electric focussing
IGL	:	Intergeniculate nucleus
IHC	:	Immunohistochemistry
IP_3	:	Inositol Phosphate 3
LB	:	Lewy bodies
LD	:	Light Dark cycle
LGICs	:	Ligand-gated ion channels
LN	:	Lewy neuritis
LNAA	:	Large neutral aminoacids
LSD	:	Lysergic Acid Diethylamide
MAO	:	Monoamine oxidase
MAPK	:	Mitogen activated protein kinase
MEK	:	Map ERK kinase
MEL	:	Melatonin
mg	:	milligram
ml	:	milliliter
mM	:	milli molar
MnSOD	:	Magnesium superoxide dismutase
mPT	:	Mitochondrial permeability transition
mRNA	:	messenger ribonucleic acid
MT	:	Melatonin treatment
MT1	:	Melatonin receptor subtype1
NAD	:	Nicotinamide adenine dinucleotide
NAS	:	N-acetyl serotonin
NAT	:	N- Acetyl tryptamine
NE	:	Norepinephrine
NPY	:	Neuropeptide Y
$O2^{\cdot -}$	:	Superoxide anion radical
PACAP	:	Pitutary adenylyl cyclase actvating peptide
PAS	:	Period-Arnt-single minded
PCD	:	Programmed cell death
PD	:	Parkinson’s disease
Per	:	Period
PI3K	:	Phospho ionositol -3 kinase

PK2	:	Prokineticin 2
PKA	:	Protein kinase A
PKC	:	Protein kinase C
PLC	:	Phospholipase C
PLMS	:	periodic leg movements in sleep
pM	:	Pico mole
qRT-PCR	:	Quantitative reverse transcriptase polymerase chain reaction
RHT	:	Retino hypothalamic tract
RIPD	:	Rotenone induced Parkinson disease
RNA	:	Ribonucleic acid
ROR	:	Retinoic-acid related orphan nuclear receptors
RORE	:	Retinoic acid related orphan receptor response elements
ROS	:	Reactive oxygen species
RP-HPLC	:	Reverse phase high pressure liquid chromatography
RRP	:	Retinoraphe pathway
SCG	:	Superior cervical ganglion
SCN	:	Suprachiasmatic nucleus
SDB	:	Sleep disorder breathing
SN	:	Substantia nigra
SNpC	:	Substantia nigra pars compacta
SNpR	:	Substantia nigra pars reticulata
TH	:	Tyrosine hydroxylase
TPH	:	Tryptophan hydroxylase
TRP	:	Tryptophan
UPS	:	Ubiquitin proteasomal system
VIP	:	Vasoactive intestinal peptide
VTA	:	Ventral tagmental area
ZT	:	Zeitgeber time
μM	:	micro molar